JPL Publication 96-7

Science Results from the Spaceborne Imaging Radar-C/X-Band Synthetic Aperture Radar (SIR-C/X-SAR): Progress Report

Diane L. Evans
Jeffrey J. Plaut
Editors

April 1996

National Aeronautics and
Space Administration

Jet Propulsion Laboratory
California Institute of Technology
Pasadena, California

JPL Publication 96-7

Science Results from the Spaceborne Imaging Radar-C/X-Band Synthetic Aperture Radar (SIR-C/X-SAR): Progress Report

Diane L. Evans
Jeffrey J. Plaut
Editors

April 1996

National Aeronautics and
Space Administration

Jet Propulsion Laboratory
California Institute of Technology
Pasadena, California

This publication was prepared by the Jet Propulsion Laboratory, California Institute of Technology, under a contract with the National Aeronautics and Space Administration.

ABSTRACT

The Spaceborne Imaging Radar-C/X-band Synthetic Aperture Radar (SIR-C/X-SAR) is the most advanced imaging radar system to fly in Earth orbit. Carried in the cargo bay of the Space Shuttle Endeavour in April and October of 1994, SIR-C/X-SAR simultaneously recorded SAR data at three wavelengths (L-, C-, and X-bands; 23.5, 5.8, and 3.1 cm, respectively).

The SIR-C/X-SAR Science Team consists of 52 investigator teams from more than a dozen countries. Science investigations were undertaken in the fields of ecology, hydrology, geology, and oceanography. This report contains 44 investigator team reports and several additional reports from co-investigators and other researchers.

Page intentionally left blank

Contents

ADDITIONAL REPORTS

FOREWORD

The Spaceborne Imaging Radar-C/X-band Synthetic Aperture Radar (SIR-C/X-SAR) is the most advanced imaging radar system to have flown in Earth orbit. Carried in the cargo bay of the Space Shuttle Endeavour in April and October, 1994, SIR-C/X-SAR simultaneously recorded SAR data at three wavelengths (L-, C-, and X-bands; 23.5, 5.8 and 3.1 cm, respectively). In addition, the full polarimetric scattering matrix was obtained by the SIR-C instrument at L- and C-band over a variety of terrain and vegetation types. The integrated system is steerable in look angle (electronically in the case of SIR-C, mechanically in the case of X-SAR) to obtain data in the angular range of 15°-60°. Imaging resolution varies from about 10 to 50 meters, depending on the geometry and data taking configuration. Over the two flights, a total of 143 hours (93 terabits) of SAR data were digitally recorded on tape for subsequent processing in the U.S., Germany, and Italy. During the October 1994 flight of SIR-C/X-SAR, over one million square kilometers of repeat-pass SAR interferometry data were also obtained.

SIR-C/X-SAR is a cooperative experiment between the National Aeronautics and Space Administration (NASA), the German space agency, Deutsche Agentur für Raumfahrtangelegenheiten (DARA), and the Italian Space Agency, Agenzia Spaziale Italiana (ASI). SIR-C was developed by NASA's Jet Propulsion Laboratory. X-SAR was developed by the Dornier and Alenia Spazio companies, with the Deutsche Forschungsanstalt für Luft- und Raumfahrt (DLR), the major partner in science, operations, and data processing. The experiment provides an evolutionary step in NASA's Spaceborne Imaging Radar (SIR) program that began with the Seasat SAR in 1978, and continued with SIR-A in 1981 and SIR-B in 1984. It also represents a continuation of Germany's imaging radar program which started with the Microwave Remote Sensing Experiment (MRSE) flown aboard the Shuttle on the first SPACELAB mission in 1983.

The SIR-C/X-SAR Science Team consisting of 52 investigator teams from more than a dozen countries are using SIR-C/X-SAR data in studies of geology, hydrology, ecology, oceanography. Other investigations are focused on topics in SAR calibration and electromagnetic theory. In addition, interferometric data from SIR-C/X-SAR are being used for topographic mapping, and surface change monitoring connected with tectonism, volcanism and glacier ice motion.

SIR-C/X-SAR data provide unique information for studying the health of the planet and its biodiversity, as well as critical data for natural hazards and resource assessments. The following papers summarize science results from the two flights of SIR-C/X-SAR. This report contains 44 investigator team reports and several additional reports from co-investigators and other researchers. At the time of this writing, processing and analysis of SIR-C/X-SAR data are continuing. Since the SIR-C/X-SAR flights in 1994, hundreds of additional investigators have accessed SIR-C/X-SAR data for studies as diverse as archeology, land-use, and resource management indicating that new findings and discoveries can be expected from this rich and varied data set for many years to come.

This document can be found at the following World Wide Web site:

http://southport.jpl.nasa.gov

D. L. Evans
J. J. Plaut, editors

PRINCIPAL INVESTIGATORS

Dr. Werner Alpers
Institute of Oceanography
Troplowitzstr. 7
University of Hamburg
D-22529, Hamburg
Germany

Co-Investigators:
H. Masuko Radio Research Laboratory
P. Trivero Istituto di Cosmogeofisica

Comparison of SIR-C Simulated and Measured SIR-C SAR Image Spectra with Ocean Wave Spectra Derived from Buoys and Wave Production Models in the North Sea

OBJECTIVES

Carry out measurements of two-dimensional ocean wave spectra by a pitch and roll buoy from the Forschungsplatform Nordsee (Germany Research Platform North Sea) and from a ship of the German Hydrographic Office in the North Sea. Collaborate with North Sea oil rig operators to obtain wave spectra from these sites.

A third generation wave prediction model (WAMODEL) will be applied to forecast and hindcast the wave fields in the North Sea from the measured wind history during the SIR-C overflight. The WAMODEL has a resolution of 0.5 degree longitude and 0.25 degree latitude. This model (Komen and Zambreski, 1986; Bauer et al. 1988) seems to be accurate in predicting two-dimensional ocean wave spectra in the North Sea and will be refined for the SIR-C mission.

PROGRESS

During both shuttle missions, experimenters at the University of Hamburg performed experiments in the German Bight of the North Sea, off the island of Sylt. The aim of these experiments was to investigate the radar signatures which are caused by different surface films, i.e., by different monomolecular slicks consisting of artificial biogenic substances and, on the other hand, by different mineral oils, i.e., heavy and light (Diesel) fuel. The SIR-C/X-SAR data from both experiments were acquired and processed in different ways, i.e., performing different statistical analyses, during the last months. In addition to the experiments in the German Bight, Japanese scientists under the leadership of Dr. H. Masuko performed similar surface film experiments off the Japanese coast. Here, a certain substance was deployed several times to get a reliable set of SAR images with radar signatures for intercomparison and polarimetric studies. X-SAR quicklook processor data tapes provided by DLR, as well as the quicklook data on CD ROM provided by JPL (L- or C-band), and I-PAF (X-band) after both shuttle missions have been checked for features which could be of interest for oceanographic studies. It turned out that in several parts of the world's oceans the water surface was covered with surface films during the shuttle flights. However, only a few data takes showing oil spills have been found (e.g., one large oil spill in the Baltic Sea during the first shuttle mission). Therefore, a collection of interesting scenes taken in different SAR modes (i.e., only like-polarization or full polarization mode) have been ordered and are to be processed in the near future.

Another aim of the participation of the University of Hamburg in the shuttle missions was to compare wave spectra obtained from the SAR images at different radar bands and polarizations with in-situ data from buoy measurements and spectra obtained from a wave prediction model (WAM) provided by the European Center for Medium Range Weather

Forecast (ECMWF). For this purpose, SAR images from the North Sea test site have been acquired and processed. A SAR image taken during the first shuttle mission over the northeast (NE) Atlantic shows a broad, dark band crossing the SAR track. After watching the videotape of this data take (96.3), scientists first thought that this dark band was due to a mineral oil spill. However, it turned out that a strong atmospheric (rain) front was responsible for this signature. The SAR images of this topic have been ordered and processed. Other data takes of the NE Atlantic (adjacent in space and time) have been checked for this front, however, such strong signatures have not been found. Furthermore, bright signatures caused by strong rain cells have been found on SAR images of the Tropical Pacific, the Mexican Gulf, and the Central Atlantic. They will be processed and studied during the next months.

SIGNIFICANT RESULTS

The two slick experiments in the German Bight took place under different weather conditions: During the first mission, on April 18, the weather was fine with a wind speed of 5 m/s, but during the second mission, on October 6, the weather was stormy, and the wind speed raised up to values of more than 10 m/s. Under these strong wind conditions, surface slicks remain on the water surface only for a short time, because they are rapidly washed down. However, most of the deployed surface films have been recognized as dark patches on the SAR images taken at this test site. It turned out that the surface wave damping behavior of one substance (oleyl alcohol), which was used for both experiments, was different for the unlike wind conditions: Under strong winds the measured reduction of the radar backscatter was lower and was comparable to one of the other substances, especially mineral oil (one has to admit that, for environmental reasons, the amount of mineral oil was kept very small, so that this oil spill obviously showed a damping behavior similar to that of the monomolecular surface films). Significant differences between the surface films resulting from various statistical processing have therefore not been found. On the other hand, under low to moderate wind conditions, the monomolecular slick deployed during the first experiment showed a different damping behavior from a mineral oil spill that was found on a SAR image of the Baltic Sea. A characteristic damping maximum at C-band has been found which can be explained by the Marangoni damping theory (which is applicable to monomolecular surface films). This result is in agreement with the results obtained from the Japanese scientists during their experiments (Masuko and Alpers, 1995). The mineral oil spill in the Baltic Sea showed a strong inhomogeneity, because of a drifting of the upper oil layer, due to wind and surface currents. However, on the thick (windward) edge of the spill, in particular, a different damping behavior was found, i.e., no damping maximum at C-band, but an increasing radar contrast with increasing radar wave number (Gade and Alpers 1995a) (Gade and Alpers 1995b). Recent polarimetric studies of slick-free and slick-covered water surfaces have shown that there are differences in the polarization signatures with respect to incidence angle, wind (i.e., surface roughness), and slick coverage. In all cases, Bragg scattering seems to be the dominant scattering mechanism, where the fraction of spatial scattering varies with incidence and slick coverage. The processing of SAR image spectra, which was extensively done with the JPL airborne SAR (AIRSAR) images taken in 1991, was extended to SIR-C/X-SAR data taken over the North Sea and showed distinct wave systems. The two-dimensional image spectra processed from these SAR images show unimodal wave systems and reproduce very well the spectra obtained using the WAM model, with respect to peak wavelength and direction. This can be explained by the weak nonlinearity of the imaging of these ocean waves, except for the cases of shallow water close to the coastline. Further image spectra, which were calculated on both sides of the atmospheric front over the Atlantic Ocean, showed strong differences, although taken at a distance of only 25 km from each other: The obtained spectra were

rotated, which was most pronounced for X-band and less for L-band. This effect can be explained by the different dependence of the ocean wave-radar modulation transfer function (MTF) on wind speed, which results in a different imaging of the wave fields. This could be proved by simulations of wave spectra for both sides of the front (Alpers et al. 1995a).

FUTURE PLANS

The results on radar signatures of different ocean surface films are not yet sufficient for any definitive statement on whether or not active radar techniques are capable of discriminating between natural (biogenic) slicks and (manmade) mineral oil spills. Therefore, more SAR scenes showing surface slicks or mineral oil spills (e.g., oil spills around oil drilling fields in the Arabian Sea west of Bombay) are to be studied in the future. Special attention will be focused on polarimetric studies of these SAR scenes. New chemical insights into the morphology of monomolecular surface films will be gained from laboratory experiments. Results will be presented at the next International Geoscience and Remote Sensing Symposium (IGARSS) (Alpers et al. 1996) and in a Ph.D. thesis (Gade 1996).

Theoretical studies of the classification of SAR image spectra, i.e., a new method of the best fit between simulated and measured image spectra, will be published soon in a Ph.D. thesis (Schmidt 1995).

Taking advantage of the polarimetric capabilities of the SIR-C radar system, more studies regarding the backscattering mechanism of the water surface (theoretical as well as experimental) shall be done. For this purpose, some additional SAR scenes may be ordered. For studies of radar signatures of rain cells over the world's oceans, more SAR scenes shall be ordered to get reliable statistical results out of the huge amount of such data. First results coming out of these studies will be presented at the IGARSS '96 Symposium (Alpers et al. 1996). The results may be extended by laboratory experiments. Several SAR images were taken over the Wadden Sea in the German Bight showing distinct dark and bright structures corresponding to underwater bottom topography or dry-fallen sandbanks. This interesting data set is worth being studied, and the results will be compared with those obtained from ERS-1 SAR images and with theoretical models for surface convergence (and the resulting radar backscatter).

PUBLICATIONS

Alpers, W., and B. Holt, Imaging of ocean features by SIR-C/X-SAR: An overview, *Proceedings of the International Geoscience and Remote Sensing Symposium (IGARSS '95)*, Florence, Italy, 1588-1590, 1995.

Alpers, W., C. Melsheimer, C. Brnning, and R. Schmidt, Imaging of ocean waves by SIR-C/X-SAR over the North Sea and North Atlantic, *Proceedings of the International Geoscience and Remote Sensing Symposium (IGARSS '95)*, Florence, Italy, 1317-1319, 1995a.

Alpers, W., A. Schmidt, R. Schmidt, and C. Brnning, A comparison of ocean wave-radar modulation transfer functions at different radar frequencies and polarizations determined from tower and aircraft measurements, *Proceedings of the International Geoscience and Remote Sensing Symposium (IGARSS '95)*, Florence, Italy, 1087-1089, 1995b.

Alpers, W. et al., several papers about different results obtained from SIR-C/X-SAR data, presented at *IGARSS '96*, 1996.

Bao, M., C. Brnning, and W. Alpers, On the nonlinear imaging of two-dimensional ocean surface wave fields by interferometric SAR, *Proceedings of the International Geoscience and Remote Sensing Symposium (IGARSS '95)*, Florence, Italy, 775-777, 1995.

Gade, M., and W. Alpers, The German surface film experiments during the two SIR-C/X-SAR missions, *EARSel Newsletters 3/95*, 1995a.

Gade, M., and W. Alpers, First results from the German surface film experiments during the two SIR-C/X-SAR missions, *Proceedings of the 15th EARSeL Symposium*, Basel, Switzerland, 1995b (in press).

Gade, M., Ph.D. thesis about the damping behavior of different surface films with respect to the energy flux on the water surface, 1996.

Huehnerfuss, H., W. Alpers, H. Dannhauer, M. Gade, P. A. Lange, V. and V. Wismann, Natural and man-made sea slicks in the North Sea investigated by a helicopter-borne 5-frequency radar scatterometer, *Int. J. Remote Sens.*, 1995 (in press).

Mango, S., S. Chubb, F. Askari, J. Lee, G. Valenzuela, R. W. Jansen, R. A. Fusina, B. Holt, R. M. Goldstein, W. Alpers, T. F. Donato, M. R. Grunes, H. H. Shih, J. Verdi, J. C. Church, and L. K. Shay, Remote sensing of current-wave interactions with SIR-C/X-SAR during SRL-1 and SRL-2 at the Gulf Stream supersite, *Proceedings of the International Geoscience and Remote Sensing Symposium (IGARSS '95)*, Florence, Italy, 1325-1327, 1995.

Masuko, H. and W. Alpers, Observation of artificial slicks with SIR-C/X-SAR around Japan, *Proceedings of the International Geoscience and Remote Sensing Symposium (IGARSS '95)*, Florence, Italy, 227-229, 1995.

Schmidt, R., Ph.D. thesis about a new method of classification of SAR image spectra, 1995.

Mr. Robert C. Beal
The Johns Hopkins University
Applied Physics Laboratory (APL)
Johns Hopkins Road
Laurel, MD 20707-6099

Co-Investigators:
Frank M. Monaldo (APL)
Thomas Gerling (APL)

Global Wave Forecasting in the Southern Ocean

OBJECTIVES

The goal of this project is to demonstrate the potential value of spaceborne Synthetic Aperture Radar (SAR) for operational ocean wave monitoring and forecasting.

This project complements the Space Radar Laboratory (SRL) investigation "Optimization of SAR Parameters for Wave Spectra" (PI: F. Monaldo, CI: R. Beal), with somewhat overlapping tasks and similar goals, that is, the understanding and application of spaceborne SAR to operational ocean wave monitoring and forecasting.

PROGRESS

Using the APL real-time SAR processor with both the SRL-1 and SRL-2 missions, we have acquired a SAR wave imaging and comparison data set more than two orders of magnitude greater than in any previous U.S. SAR mission. This SRL data set is all the more unique and valuable, since it was acquired at both a low altitude and a low off-nadir angle. Both of these are necessary conditions for any future free flyer dedicated to global ocean wave monitoring. The data set for our SRL investigation consists of:

1) Over 100,000 SAR Image Spectra over the Southern Ocean from the real-time APL SAR Processor: 45,000 from April, and 55,000 from October.

2) Eighteen precision, high resolution SAR imagery data-takes correlated by JPL, both over the Southern Ocean and over the North Atlantic.

3) Numerical wave model (WAM) nowcasts for the periods covering both April and October missions, from both the U.S. Navy Fleet Numerical and Meteorological Center (Monterey) and the European Centre for Medium Range Forecasting (ECMWF) (Reading).

4) European Remote Sensing Satellite (ERS-1) SAR derived wave spectra from the Max Planck Institute covering the entire globe for the time intervals of both the April and October missions.

APL Processor SAR Data

Aboard Endeavour, an APL-built processor correlated SAR imagery from the SIR-C C-band HH-polarization signal and produced image spectra which were transmitted to the ground in real time. More than 100,000 image spectra from the APL-processor were stored from 120 data takes in SRL-1 and 126 data takes in SRL-2. The wave spectra cover most of the Southern Ocean from 45S to 60S. The data set includes measurements where the ocean significant wave height (SWH) varied from near zero to over 12 m, spanning nearly the full range of naturally occurring sea states.

WAM Nowcasts

During SRL-1 and SRL-2, the Navy's Fleet Numerical Meteorology and Oceanography Center (FNMOC) retained the nowcast spectra made from their version of the operational WAM forecast model. An analogous comparison model data set is also available from ECMWF through collaborators at the Max Planck Institute (Hamburg).

ERS-1 SAR Imagery

Given the broad geographical coverage of data from the APL processor, there are at least 30 times in the Southern Ocean during each mission when ERS-1 wave spectra and APL-processor image spectra were located less than 50 km apart and acquired within one hour of one another. Loosening the colocation criteria only slightly will produce more than 100 such comparisons sets.

SIGNIFICANT RESULTS

Using real-time APL-processor data received at Johnson Space Center, we merged SAR wave vector estimates over the Southern Ocean with wave vector forecasts from FNMOC, and daily placed the combined products on a World Wide Web site. During the mission, the site was visited more than 150 times by investigators from as far away as South Africa and Australia. This effort demonstrated the potential of providing wave information from spaceborne SAR quickly enough to be usefully assimilated into wave forecast models. The site

ftp://fermi.jhuapl.edu/sirc/sirc.html

currently shows recent data and analyses from the SRL missions. In the past year, we have processed image spectra with only a simple SAR modulation transfer function. Even these results show quality retrievals of wave direction and wavelength. In the future, we will employ more sophisticated retrieval schemes that may permit the accurate measurement of ocean SWH as well.

FUTURE PLANS

Given the totality of the SIR-C image spectra, ERS-1 SAR spectra, and WAM model estimates, we intend to 1) make a definitive determination of what ocean wave parameters can be extracted from spaceborne SARs and with what accuracy; 2) specify the SAR satellite configuration that optimizes this retrieval; and 3) demonstrate, with a statistically significant data set, the value of SAR for improved global wave forecasting.

We are currently collaborating with William Plant who, while a visiting scientist at the Max Planck Institute this last year, applied nonlinear retrieval algorithms to estimate wave spectra from coincident SIR-C and ERS-1 data. We expect to submit a joint paper in the upcoming year, documenting the comparison of ERS-1 and SIR-C-derived image spectra.

We intend to make a systematic comparison, wave system by wave system, to ascertain systematic differences between WAM model wave estimates and SIR-C measurements for the entire Southern Ocean data set. We will then determine whether these differences are due to input wind field errors, model problems, and/or SAR wave imaging

limitations. We expect the results to form the major scientific and operational justification for a low altitude wave monitoring SAR satellite. Such a satellite would easily fit into the NASA "Lightsat" category, and would also be a candidate for the "New Millennium" spacecraft announcement of opportunity. Both the U.S. Navy and National Oceanic and Atmospheric Administration (NOAA) have strong interests in the improvement of operational wave forecast products that would be possible with such a dedicated low altitude free-flyer. Moreover, NASA should have an equally strong interest in the demonstration of the advanced technology necessary to do the SAR on-board processing and the real-time global dissemination of data to a worldwide user network.

PUBLICATIONS

Beal, R. C., S. F. Oden, J. L. MacArthur, and F. M. Monaldo, Real Time Ocean Wave Monitoring from Space: A Thirty-Year Quest Achieved, *Johns Hopkins APL Technical Digest*, vol. 15, No. 3, pp. 237-241.

Gerling, T. G and P. A. Wittmann, Comparison of SAR-estimated Wave Spectra with WAM Model Estimates During the SRL Southern Ocean Experiment, *Proc. 1995 International Geoscience and Remote Sensing Symposium*, Florence, Italy, July 1995.

Monaldo, F. M. and R. C. Beal, SRL Real-Time Wave Forecasting in the Southern Ocean, *Proc. 1995 International Geoscience and Remote Sensing Symposium Florence*, Italy, July 1995.

Monaldo, F. M. and R. C. Beal, Real-Time Observations of Southern Ocean Waves Fields from the Shuttle Imaging Radar, *IEEE Transactions on Geoscience and Remote Sensing*, vol. 33, No. 4, pp. 942-949, 1995.

Plant, W., S. Hasselmann, C. Bruning, R. Beal, and F. Monaldo, Comparison of Ocean Wave Spectra from a Nonlinear SAR Inversion Scheme using ERS-1 and SIR-C Data Sets, *Proc. 1995 International Geoscience and Remote Sensing Symposium*, Florence, Italy, July 1995.

Wittmann, P. A., R. M. Clancy, and R. C. Beal, FNMOC Supports Wave Modeling Around the World and into Space, *Naval Meteorology and Oceanography News,* July 1995.

In addition, the following formal presentations have been given:

Beal, R. C., *The SRL Real Time Wave Forecasting Experiment and its Implications for a Future Satellite Design*, invited seminar to NOAA/NESDIS, 15 December 1994.

Beal, R. C., *The SIR-C Real-Time Southern Ocean Experiment*, invited seminar to the Max Planck Institute for Meteorology, 6 July 1995.

Beal, R. C., *Ocean Applications of Spaceborne SAR*, invited presentation at the US-ROC Oceanic Microwave Remote Sensing Workshop, U. Delaware, 16 August 1995.

Dr. R. J. Brown
Applications Division
Canada Centre for Remote Sensing
588 Booth Street
Ottawa, Ontario K1A 0Y7
Canada

Co-Investigators:
H. Gwyn University of Sherbrooke
T. J. Pultz Canada Ctr. for Remote Sensing

Canada Centre for Remote Sensing Altona, Manitoba test site

OBJECTIVES

The overall objectives of the experiment were to evaluate the capabilities of multidate, multiparameter SAR data to estimate soil moisture in an agricultural environment for a variety of soil types in the spring and fall, develop models which provide a better understanding on the relationships between soil moisture and texture, surface roughness and radar frequency, polarization and incidence angle, evaluate the use of a change detection approach for soil moisture monitoring and to gain a better understanding of the information content of polarimetric data.

PROGRESS

Temporal changes in SIR-C, C- and L-band radar backscatter over the Altona site in relation to changing environmental conditions such as frost, rain and soil moisture have been evaluated. In addition, the soil moisture model developed by J. C. Shi has been applied to the data.

SIGNIFICANT RESULTS

The results indicate that environmental events such as frost and rain can be monitored. However, care must be taken as some soil targets at high moisture contents may behave as specular reflectors at longer wavelengths, such as L-band at large incidence angles which will mask soil moisture effects. The strongest correlation (rho=.84) with soil moisture was obtained for the 0-2.5 cm soil profile at HH polarizations and was approximately the same at C- and L-band. All polarizations displayed a decrease in soil moisture correlation with increasing soil profile depths. It was observed that soil texture effects on the estimation of soil moisture from radar backscatter are relatively small and can be neglected. Although the sensitivity to surface roughness is greater at HV and VV than at HH polarization, it is possible that roughness could be neglected when measuring soil moisture over relatively short periods of time at a given site without significantly reducing the sensitivity of the relationship between radar backscatter and soil moisture. The L-band soil moisture model produced estimated values which were in good agreement with the observed conditions.

FUTURE PLANS

Evaluation of existing soil moisture models and extension of results to RADARSAT data.

PUBLICATIONS

Boisvert, J. B., T. J. Pultz, Y. Crevier, R. J. Brown, B. Eilers, 1995. "Potential of Multi-date Imagery for Soil Moisture, Texture and Drainage Classification: Preliminary Results." 17th Canadian Symposium on Remote Sensing, Saskatoon, Saskatchewan, June 13-15, pp. 511-515.

Crevier, Y., T. J. Pultz , T. Toutin, 1995. "The Influence of Data Integration Methodology on Multi-Source SAR Image Radiometry and Soil Moisture Estimation." 17th Canadian Symposium on Remote Sensing, Saskatoon, Saskatchewan, June 13-15, pp. 448-453.

Crevier, Y., T. J. Pultz, R. J. Brown. Towards the Use of Multi-Beam RADARSAT Data for Soil Moisture Estimation: Results from the CCRS SIR-C/X-SAR Experiment. Submitted to 26th International Symposium on Remote Sensing of Environment/18th Canadian Symposium on Remote Sensing.

Pultz, T. J., R. J. Brown, J. Boisvert, Y. Crevier, R. Duncan, H. McNairn, D. Mullins, D. Randall, D. Wood, P. Vincent 1994. "The CCRS SIR-C/X SAR Soil Moisture Experiment." In G. W. Kite, A. Pietroniro and T. J. Pultz (ed.), Application of Remote Sensing in Hydrology, Second International Workshop, Saskatoon, Saskatchewan, 18-20, October 1994, NHRI Symposium No. 14, pp. 34-42.

Pultz, T. J., R. J. Brown, J. Boisvert, H. Gwyn, R. Protz. "SIR-C/X-SAR Observations of Soil Moisture over The CCRS Altona. Manitoba Test Site." *IGARSS '95,* July 10-14, Florence, Italy, pp. 990-993.

Dr. Ralph Cordey
Marconi Research Centre
GEC Research Limited
West Hanningfield Road
Great Baddow
Essex, CM2 8HN
United Kingdom

Co-Investigators:
G. E. Keye DRA, Farnborough
J. R. Baker British National Space Centre
S. Quegan University of Sheffield
G. M. Foody University of Swansea
N. J. Veck National Remote Sensing Centre
A. Wielogorska Hunting Technical Services

A Study of the Potential of Multicomponent SAR Imagery for Agricultural and Forestry Studies

OBJECTIVES

Develop the methods to fully exploit multicomponent SAR data sets of agricultural and forestry areas.

Determine the radiometric information content of multicomponent SAR imagery of agricultural and forested areas by developing backscatter models.

Develop techniques for the derivation of specific target information from a multicomponent data set, and consequently determine the optimum set of measurement parameters for use in specifying future SAR missions.

Develop improved image processing techniques for the extraction of specific image attributes from these images.

PROGRESS

To date, the analysis team have received more than 50 SIR-C or X-SAR image products. They cover three sites:

Feltwell/Thetford in England
Tapajos in Brazil
Manaus CSAP in Brazil

Generally, the data have been of a very high quality. However, some problems have been noted with SIR-C antenna pattern corrections over Tapajos, and other artifacts (e.g., nadir ambiguities and interference in certain data). Feedback on these has been given to JPL.

The English data takes encompass agricultural and forestry research sites, while the Brazilian sites cover areas of tropical forest and regeneration.

Analysis is being conducted by GEC-Marconi Research Centre, primarily on the agricultural site at Feltwell, by RSADU on Thetford Forest, Tapajos and Manaus, by the University of Sheffield on Tapajos and Feltwell, and by the University of Swansea on Manaus.

At GEC-Marconi Research Centre, imagery of the agricultural test site from both missions has been ingested into a database. Field-averaged mean backscatter levels have been investigated to date, with particular attention given to examining differences between SIR-C/X-SAR observations early and late in the growing season, with previous

results from AIRSAR campaigns in 1989 and 1991 in the middle of the growing season. Essentially the aim here has been to provide a clearer indication of the radar channels, whether polarimetric or multifrequency, which are necessary for effective crop identification. A preliminary investigation has also been undertaken of the accuracy of soil moisture retrieval using the algorithm of Pascale Dubois.

At RSADU, Thetford Forest imagery from both missions are being entered into a long-standing database which also contains various AIRSAR, ERS-1, and JERS-1 images of the forest. Comparisons are being made of the relationships between backscatter cross sections as a function of forest biomass between the different sensors. Over Tapajos, only SIR-C imagery from the October mission is currently being analyzed, because of the calibration problems with the April acquisition. The October data have been added to a Tapajos database containing JERS-1, ERS-1 satellite images, and images from the Canadian SAREX experiment. Biomass change is, again, the focus of analysis, with field data having been gathered in 1994 as part of a joint Brazil/UK ground experiment. The Tapajos analysis is also being related to work on the Manaus CSAP site. Along with ground measurements for sample plots in the Manaus region made in 1993 and 1995, an April scene is being used to validate the relationships between biomass and microwave backscatter derived at Tapajos. The Sheffield team have started examining multipolarized image segmentation, using the agricultural Feltwell area as a test site. They also have an interest in sites at Tapajos, although these were not ideally imaged by the selected Tapajos swath.

Field work at Manaus has continued. This year, the team from Swansea undertook a further field campaign and collected data from 22 forests of different ages. A preliminary analysis of Manaus imagery has been undertaken.

SIGNIFICANT RESULTS

Feltwell Agriculture

The agricultural experiments at somewhat unconventional times of the growing season have yielded some very clear and fascinating results. With relatively little ground cover by crops, we found the L-band channels of limited effectiveness in discriminating crop types. This compares markedly with observations at the height of the growing season made with the AIRSAR. Rather, we see polarimetric C-band observations as the main source of discrimination. Information contained in the HH-to-VV correlation was of most apparent value. The L- and C-band results have been backed up by simulations using a second-order radiative transfer backscatter model. It was also observed that, under these conditions, C-VV and X-VV backscatter measurements were very highly correlated.

Initial attempts at using Dubois' algorithm for soil moisture retrieval have not proved successful. However, there is probably a need for more careful consideration of the calibration status of the data before more firm conclusions are drawn.

No open-literature publications have yet been made. An account of the agricultural discrimination work has been prepared for the British National Space Centre (GEC-Marconi Research Centre Report MTR 95/51 by P. Wright et al.), and of the soil moisture retrievals for the European Space Agency ("SAR Retrieval Algorithms for Land Applications" MTR 95/36, by R. Cordey et al).

Thetford Forest

The SIR-C L-HH data over Thetford Forest support the conclusions already reached from JERS-1 and AIRSAR data and show a monotonic rise in backscatter with biomass density up to 50-80 tonnes per hectare, with saturation being reached thereafter. The behavior of SIR-C L-HV is currently being investigated to determine its dynamic range and saturation point.

Manaus

Early results from the Swansea team are currently being written up for a letter in the International Journal of Remote Sensing.

FUTURE PLANS

Across the various test sites, there remains a considerable program of work to be undertaken. The priority for the agricultural analysis is to find an appropriate route to publication. Presentation at PIERS (Innsbruck) is anticipated. Elsewhere, analysis programs are to be pursued. Joint analysis of tropical forest biomass estimation between the Tapajos and Manaus sites is planned at RSADU, while the Swansea team are to begin bringing optical data (Landsat) into their analyses. The Sheffield group plan to continue their studies with more detailed statistical analyses of the agricultural imagery over Feltwell.

Generally, SIR-C/X-SAR data have attracted much attention as a multiparameter satellite data set and it is anticipated that the interest in the UK will continue to broaden beyond the confines of the specific agricultural and forestry experiments reported here.

Dr. Abdallah E. Dabbagh
Research Institute
King Fahd University of
Petroleum and Minerals
Dhahran 31261
Saudi Arabia

Co-Investigators:
Khattab G. Al-Hinai — King Fahd Univ.
Weston C. Gardner
M. Asif Khan — King Fahd Univ.
Mohammed A. Tawfiq — Ministry of Petroleum and Minerals

Geologic and Hydrologic Studies of Saudi Arabia Under the Spaceborne Imaging Radar-C (SIR-C) Science Plan

OBJECTIVES

Use Synthetic Aperture Radar (SAR) imagery to detect lithological boundaries, distinguish tectonic features, map fluvial geomorphology, and elucidate hydrologic systems within larger areas of Saudi Arabia having a thin sand cover.

Establish the Pleistocene paleodrainage system of Saudi Arabia with implications for the hydrology of the country and possibly for archeological geology.

Assess the effects of sand terrain diversities on backscatter intensity as a function of radar parameters.

PROGRESS

During each of the Space Shuttle Endeavor missions in April and October 1994, fourteen data takes were acquired by the Space Radar Laboratory-1 and -2 (SRL-1 and SRL-2) over the Arabian Peninsula (Figure 1). The SIR-C/X-SAR L-band data from both the missions on CD-ROMs have been received. These data have been processed, analyzed, and interpreted to assess their significance for mapping geological and hydrological features in the Arabian Peninsula.

The main objectives of this study are: 1) assess the sand penetration capability of L- band radar in an eolian environment, 2) conduct digital image processing experiments on the multiparameter data sets and merge radar data with Landsat images, and 3) detect lithological boundaries, distinguish tectonic features, and map hydrological systems (surface and subsurface).

The L-band survey mode data (50-meter resolution) have been processed and printed at a 1:500,000 scale. The geological interpretation of all fourteen data takes over the Arabian Peninsula from SRL-1 have been completed, and the interpretation of SRL-2 data is in progress. The general interpretation of the radar data has revealed several previously unmapped geologic structures which are being further investigated (see results). Detailed evaluation of radar subsurface penetration and eolian sand deposit mapping is also in progress.

SIGNIFICANT RESULTS

The interpretation of SRL-1 and SRL-2 data has indicated instances of L-band penetration in loose dry sand. Stream drainage patterns which are either on the surface or covered by a thin layer of sand were visible on the radar images. Several faults, folds, and joints which are not visible on optical remote sensing images and are not shown on existing geologic maps, were identifiable on the radar images. These findings are described for four designated sites, viz. Test sites 1 through 4 (Figure 2), in the subsequent sections.

Sand Penetration of L-Band

Test site 1 was selected to investigate the L-band sand penetration capability. Figure 3 shows Landsat TM coverage of this site. The area consists of a coastline, sabkhas, sand dunes, and sand sheets. The sand sheet and sand dune areas, designated as A and B in the image, have sand thicknesses of 2-3 meters. As can be seen from Figures 4 (C-band) and 5 (L-band), the sand cover disappears on the L-band images, whereas it is visible on C-band at both designated areas A and B, indicating L-band penetration of the sand cover. For further verification of L-band sand penetration capability, one of the corner reflectors was buried under 2 meters of sand to be imaged during the SRL-2 mission, but unfortunately, the site was not imaged. Ground data collection for penetration verification is in progress.

Mapping Of Paleo-Drainage Channels

The paleo-drainage mapping capability of L-band radar has been investigated at two sites, one in Nafud Al-Mazhur, Test site 2 (Figure 2), and the other in Southern Rubal Khali, Test site 3 (Figure 2). Both of these sites have drainage systems, parts of which are either filled or covered with sand and, hence, are suitable for the assessment of radar data to detect both exposed and buried drainage channels.

Landsat MSS and L-band radar images of Nafud Al Mazhur, test site 2, comprising bedrock, sand sheets, and drainage channels are shown in Figures 6 and 7. In Figure 6 which is an MSS near IR image, there is little contrast between drainage channel beds and the adjacent bedrock and, hence, the drainage channels are not pronounced. The dry channels which are either floored or filled with layers of wind-blown silt and sand produce very low radar returns and appear dark gray on the L-band radar image (Figure 7). The adjacent bedrock has rough angular surfaces that produce strong radar returns and appear bright on the radar image. The contrast between drainage channels and the adjacent bedrock surfaces strongly enhances the drainage pattern seen in Figure 7, the L-band radar image. The medium gray tones in the middle of the image (Figure 7), represent a thin cover of sand sheet. In the Landsat MSS image (Figure 6) one of the major channels is barely visible where it crosses the sand sheet in the middle of the image. However, the same channel can be traced further on the radar image, suggesting penetration of radar signals through the sand. Since the radar images used in this analysis are low resolution survey mode
data, improved results are expected from the interpretation of the full resolution data, which is currently being acquired from NASA JPL.

For Test site 3 (Figure 2), the southern margin of Rubal Khali, Landsat MSS IR band and L-band radar images, are shown in Figures 8 and 9. This area comprises barchan, longitudinal, and dome dunes, as well as interdune areas. The rectangle in the Landsat MSS IR band (Figure 8) shows the area covered by L-band radar images (Figure 9). Comparison of Figures 8 and 9 reveals some large channels (shown by black arrows) meandering between sand dunes that are visible on the L-band radar and totally missing on Landsat MSS image. This is possible because of L-band radar penetration in the dry loose sand. These channels may be old river beds buried under a thin cover of sand. Field verification is planned to validate these findings.

Digital image processing experiments were conducted to enhance the radar data, and merge it with other remote sensing data. Figure 10 shows a color composite of test site 2 which was produced by speckle removal of L-band data and arithmetically merging it with Landsat MSS bands 2,4, and 7. As can be seen from Figure 10, the merged data retain the benefits of both the data sets, and can significantly aid the interpretation of the radar data.

Figure 11 shows a Pleistocene drainage map of the Arabian Peninsula, compiled from a variety of published maps as well as interpretation of Landsat images. The green dotted lines on this map

represent possible extensions of drainage systems which need to be validated. The improved radar L-band detection of paleo-drainage channels, at the two sites, demonstrates its ability to define paleo-drainage channels under thin sand cover, and should help in updating existing understanding of the hydrology and paleo-climate of the Arabian Peninsula.

Mapping Of Geologic Structures

The SIR-C/X-SAR data strips traversing some 50,000 km cross the land area of the Arabian Peninsula (Figure 1), provide a unique, synoptic view of the geology of this largely remote and barren desert terrain. Interpretation of these data, with the aid of Landsat MSS images and geologic maps, have revealed faults, joints, folds, and formation contacts which are not clearly visible on Landsat images or on published maps.

An exciting example of thin sand cover penetration and enhancement of a major fault is present along Wadi Sahba, Test site 4 (Figure 2). The L-band radar image, and its geologic interpretation, are shown in Figures 12a and 12b. This radar image extends across a section of Wadi Sahba where the lower Tertiary strata of the Umm Er Radhuma limestone are largely covered by Ad Dhana sand. To the north of the Wadi Sahba fault, the drainage pattern and karst terrain, incised in the bedrock below the dune sand, are clearly visible on the radar image (Figure 12a), but are not apparent south of the Wadi Sahba fault. The fault is clearly shown here by its linear character, but can only be inferred from other types of remote sensing images or geologic maps. Immediately to the south of the fault, that is the topographically low side, dark tone is the result of low radar return from thick sand dunes and alluvium, thus providing the strong contrast which defines the fault trace. Further southward, thick sand yields to thin sand below which the karstified Tertiary limestone and marl is once again revealed. On maps and Landsat images this is all shown as Ad Dahna sand dunes with scattered small outcrops. This is an excellent example of sand penetration by the SIR-C/X-SAR L-band radar exposing geologic structure which is not apparent from other geologic data.

Detailed field investigation of the new evidence provided by the SIR-C/X-SAR data for the extension of the Nisah-Sahba fault, a major fault zone in the vicinity of the oil rich Khurais and Ghawar anticlines, is being conducted and results are anticipated to be published in an international journal.

The overall results of geologic interpretation of the L-band image strips indicate that the radar images complement and enhance other remote sensing data and provide a new and unique view of the geologic structures.

FUTURE PLANS

Interpretation of the remaining SRL-2 L-band image strips over the Arabian Peninsula from survey data products at a scale of 1:500,000. Interpretation and mapping of fourteen image strips from SRL-1 and six data takes from SRL-2 have already been completed.

Acquisition of full resolution data, all bands, for 10 sites that showed promising results in the initial interpretation.

Compare SRL-1 and SRL-2 data for changes of radar backscatter caused by seasonal variations.

Field verification of paleo-drainage channels and geologic features identified on SRL-1 and SRL-2 data.

PUBLICATIONS

Al-Hinai K. G., 1995. A look at earth through the eyes of shuttle imaging radar, Al-Kafila, Saudi Aramco Oil Company Magazine, March.

Al-Hinai K. G., A. E. Dabbagh, W. C. Gardner, and M. Asif Khan, 1996. Geological Interpretation of Shuttle Imaging Radar SIR-C/X-SAR Data of Saudi Arabia, The Middle East Geoscience Conference and Exhibition, Manama, Bahrain, April 15-17, (Submitted).

Al-Hinai K. G., M. Asif Khan, and A. E. Dabbagh, 1996. Evaluation of Space Radar Laboratory (SRL) data for Sand Dune Mapping, Conference on Desert Development in the Arabian Gulf Countries, State of Kuwait, 23-26 March, (Submitted).

Dabbagh A. E., Khattab G. Al-Hinai, and M. Asif Khan, 1994, An overview of the shuttle imaging radar (SIR-C/X- SAR) experiment and preliminary analysis of the early data products, Symposium on Desert Studies in the Kingdom of Saudi Arabia, Center for Desert Studies, King Saud University, Riyadh, 2-4 October.

Dabbagh A. E., Khattab G. Al-Hinai, and M. Asif Khan, 1995. Evaluation of the Shuttle Imaging Radar (SIR-C/X- SAR) Data for Mapping Paleo-Drainage Systems in the Kingdom of Saudi Arabia, International Conference on Quaternary and Climatic Change, United Arab Emirates, Al-Ain, December 9-11.

We plan to publish a book on the application of radar remote sensing with an emphasis on the Saudi Arabian experience.

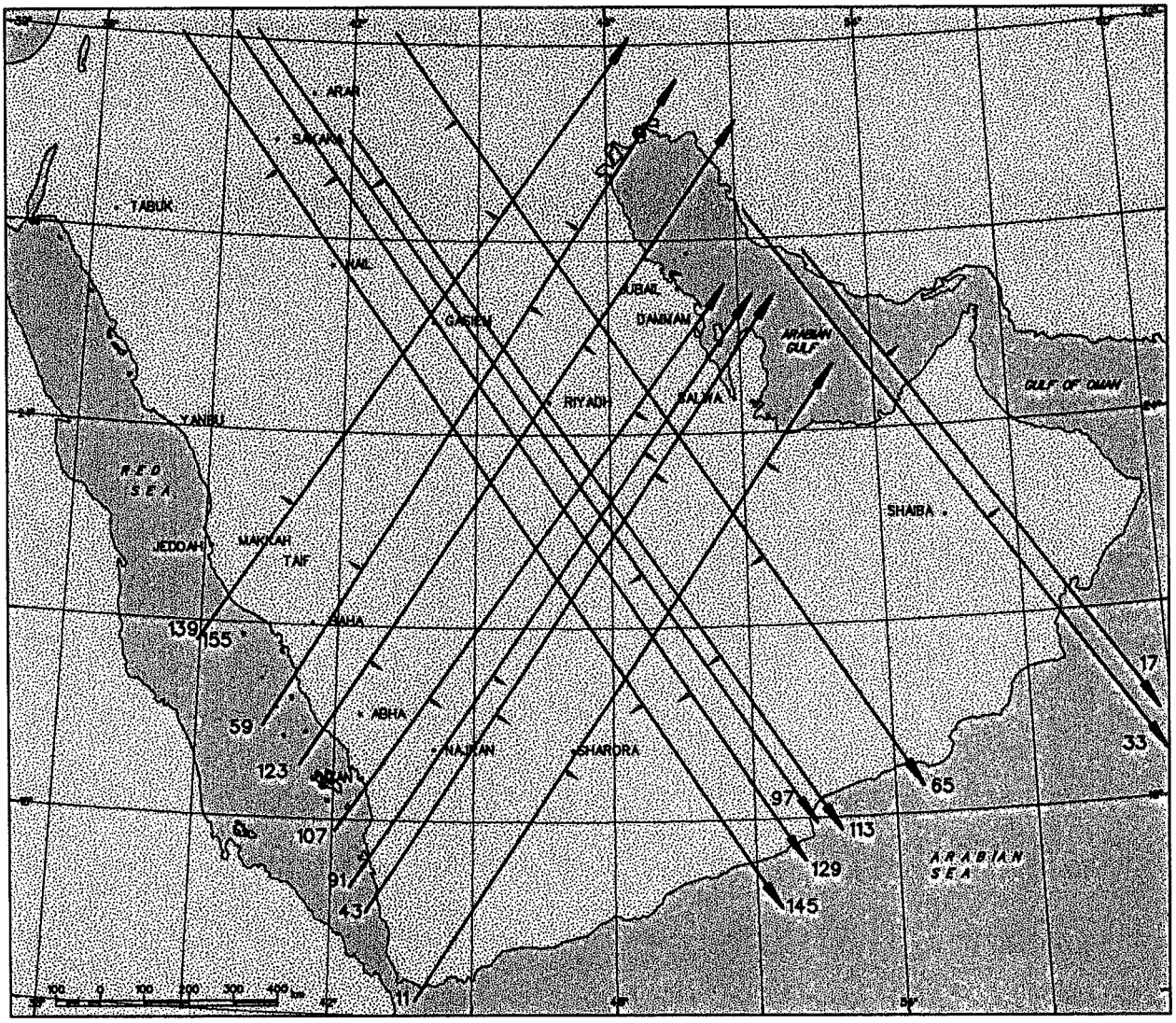

Figure 1. SIR-C/X-SAR data takes flown over the Arabian Peninsula.

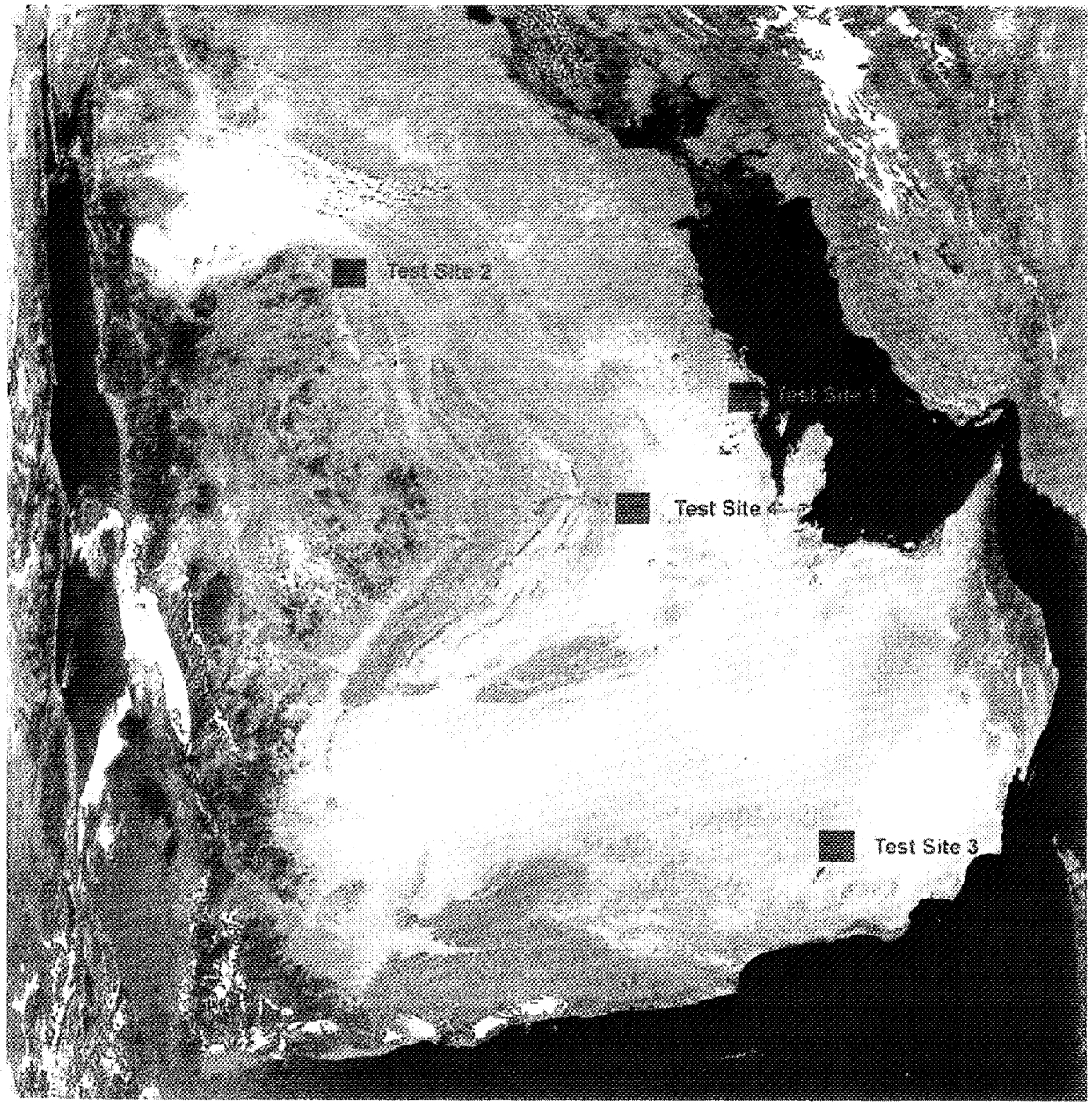

Figure 2. Location of the four test sites.

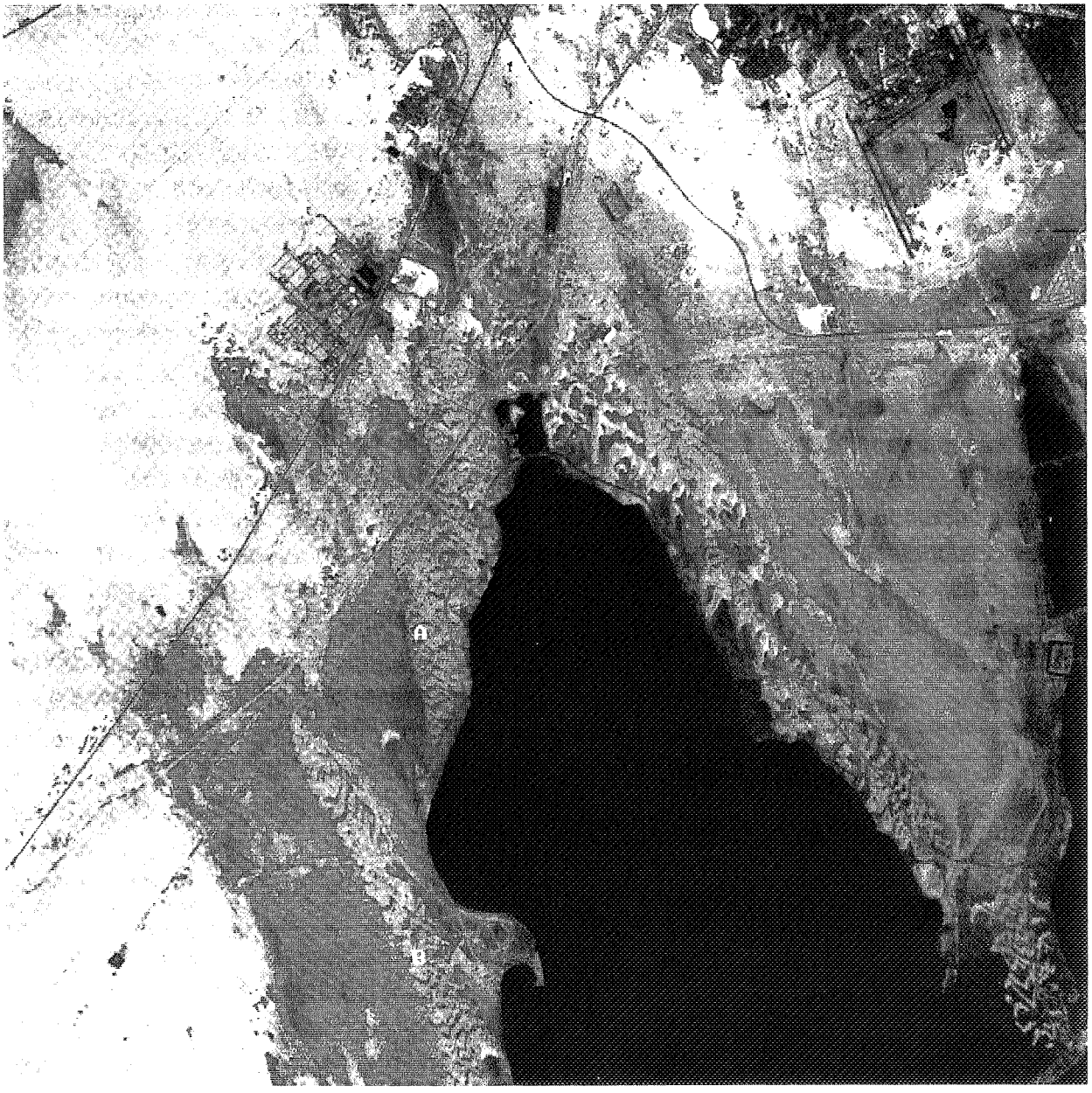

Figure 3. Landsat MSS band 7 of test site 1.

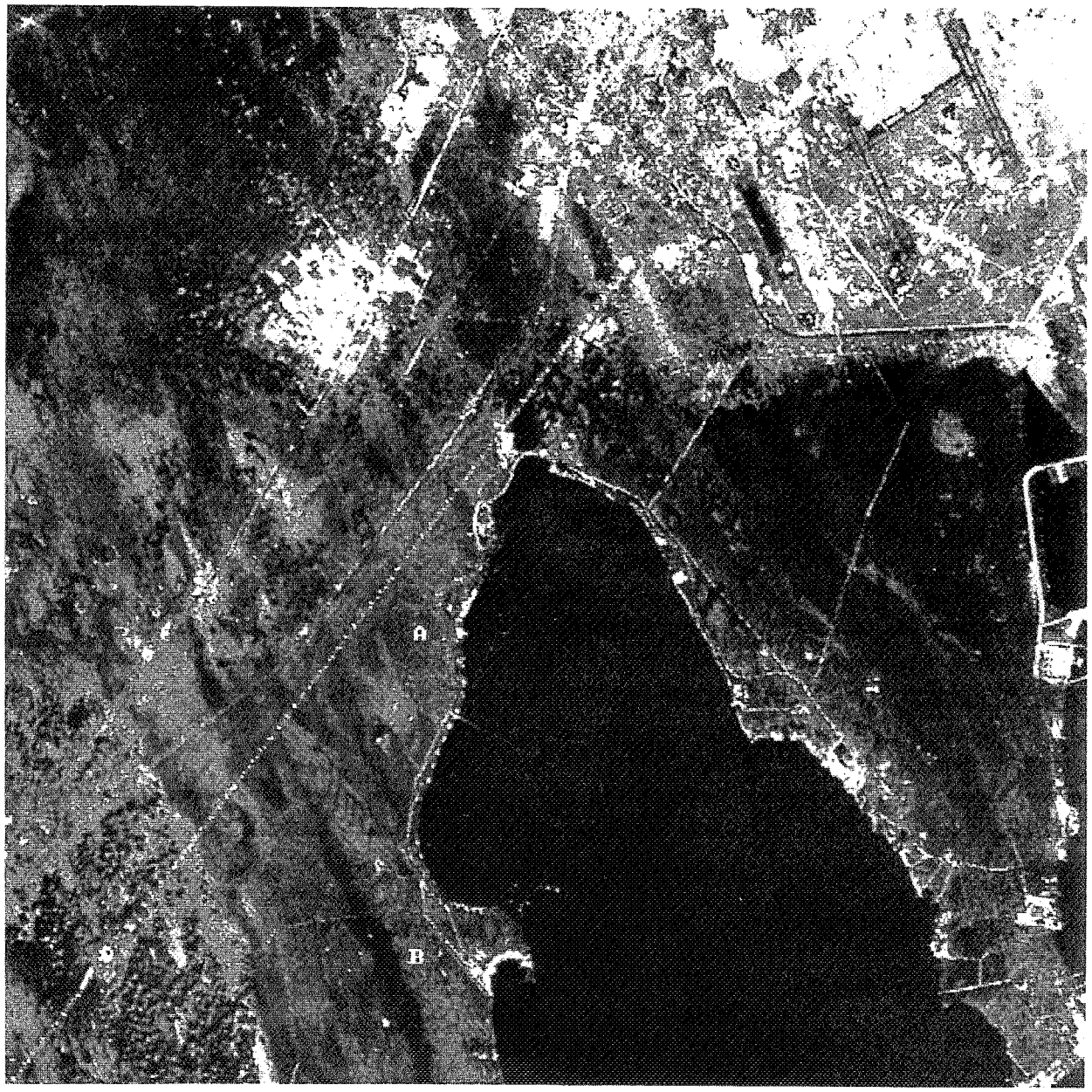

Figure 4. SIR-C/X-SAR C-band of test site 1.

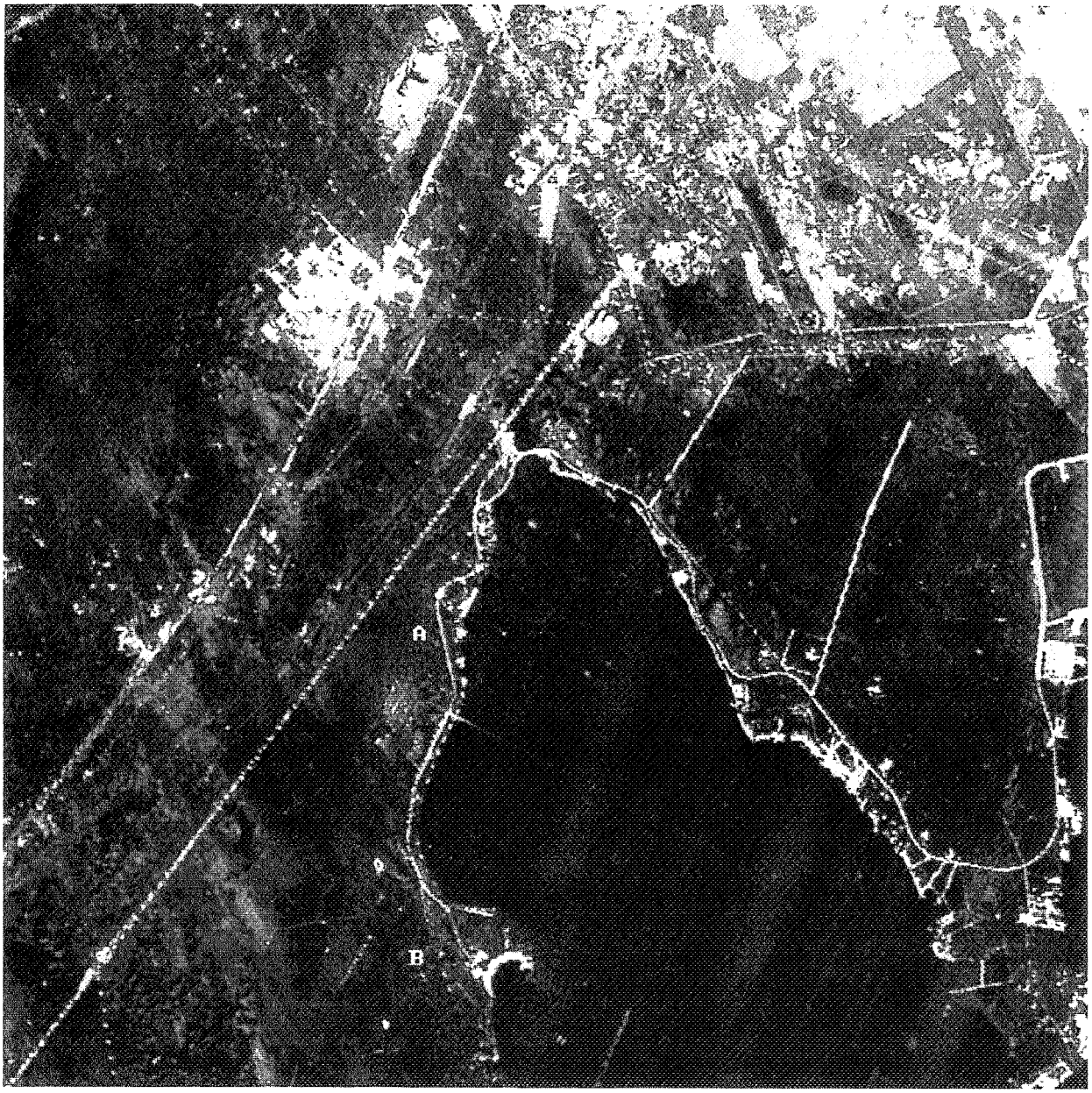

Figure 5. SIR-C/X-SAR L-band of test site 1.

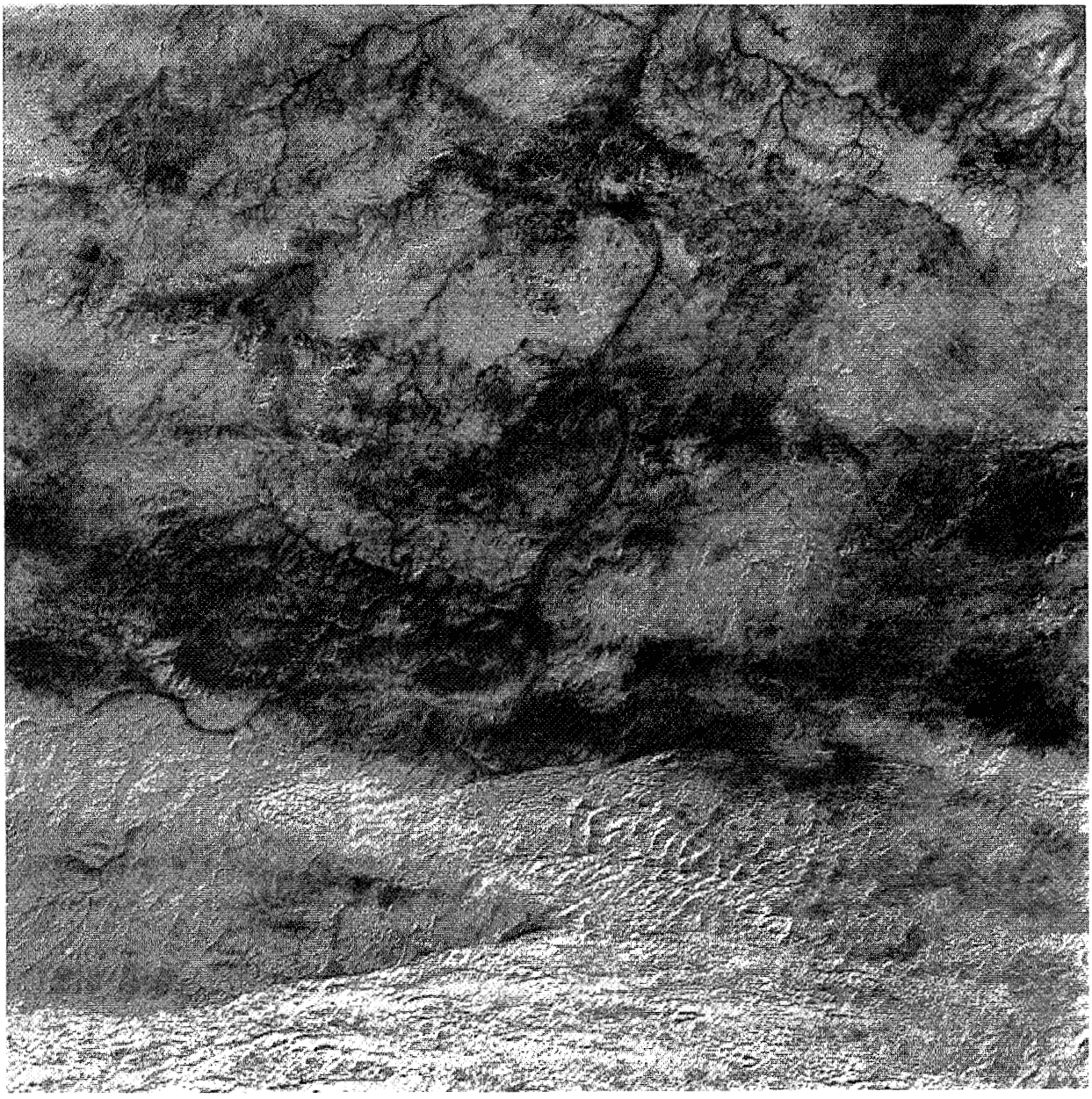

Figure 6. Landsat MSS band 7 of test site 2.

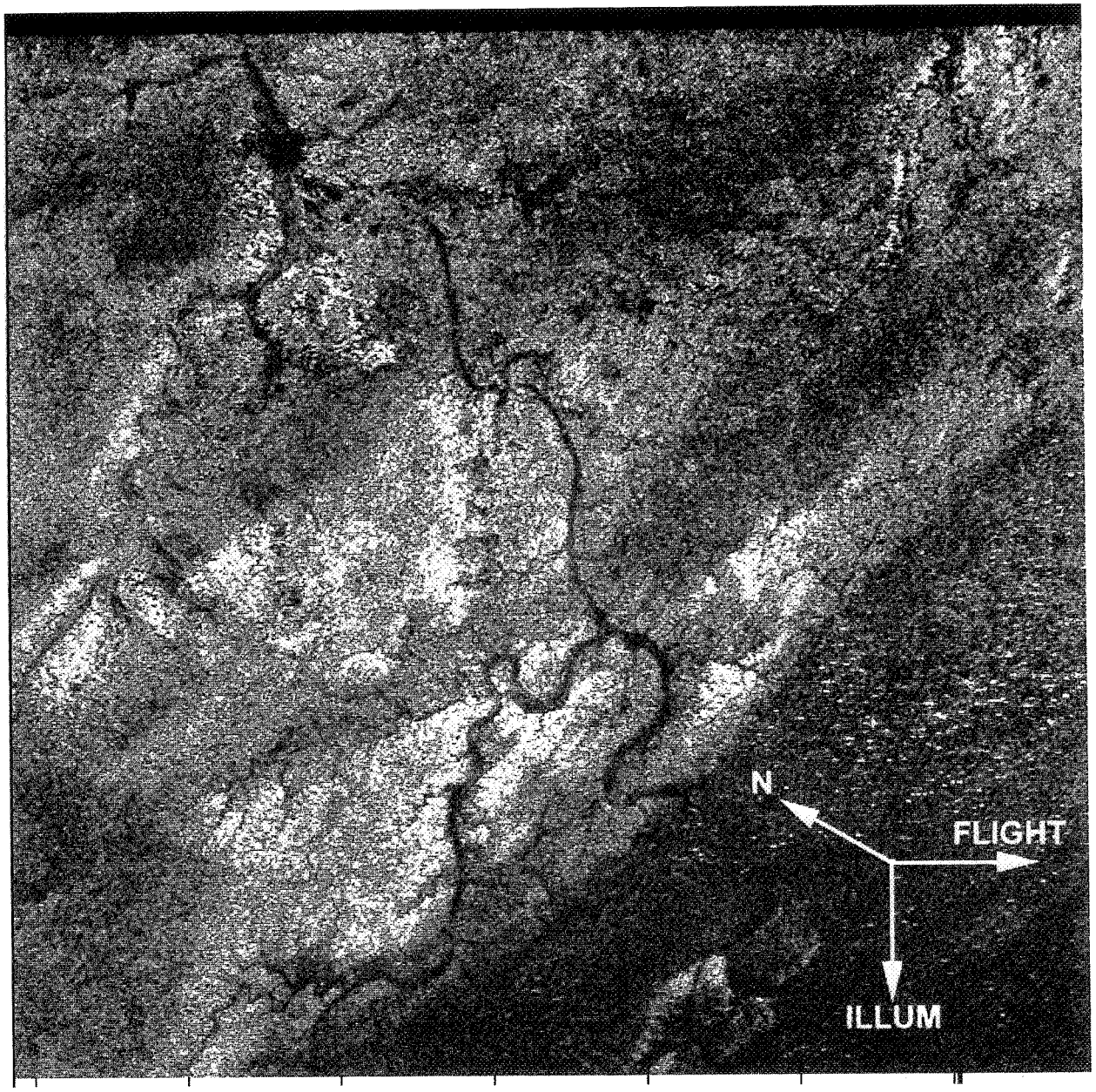

Figure 7. SIR-C/X-SAR L-band of test site 2.

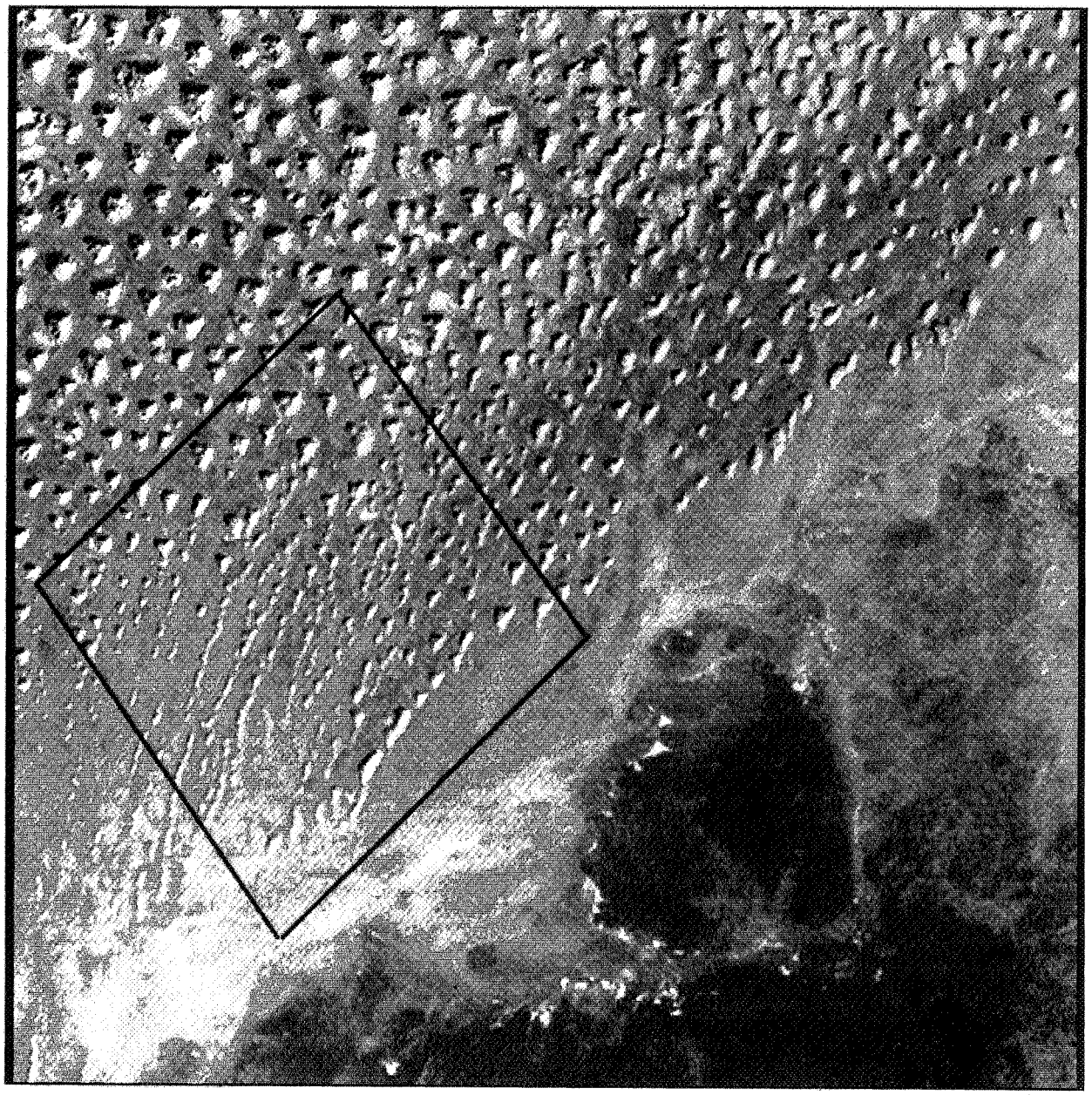

Figure 8. Landsat MSS band 7 of test site 3

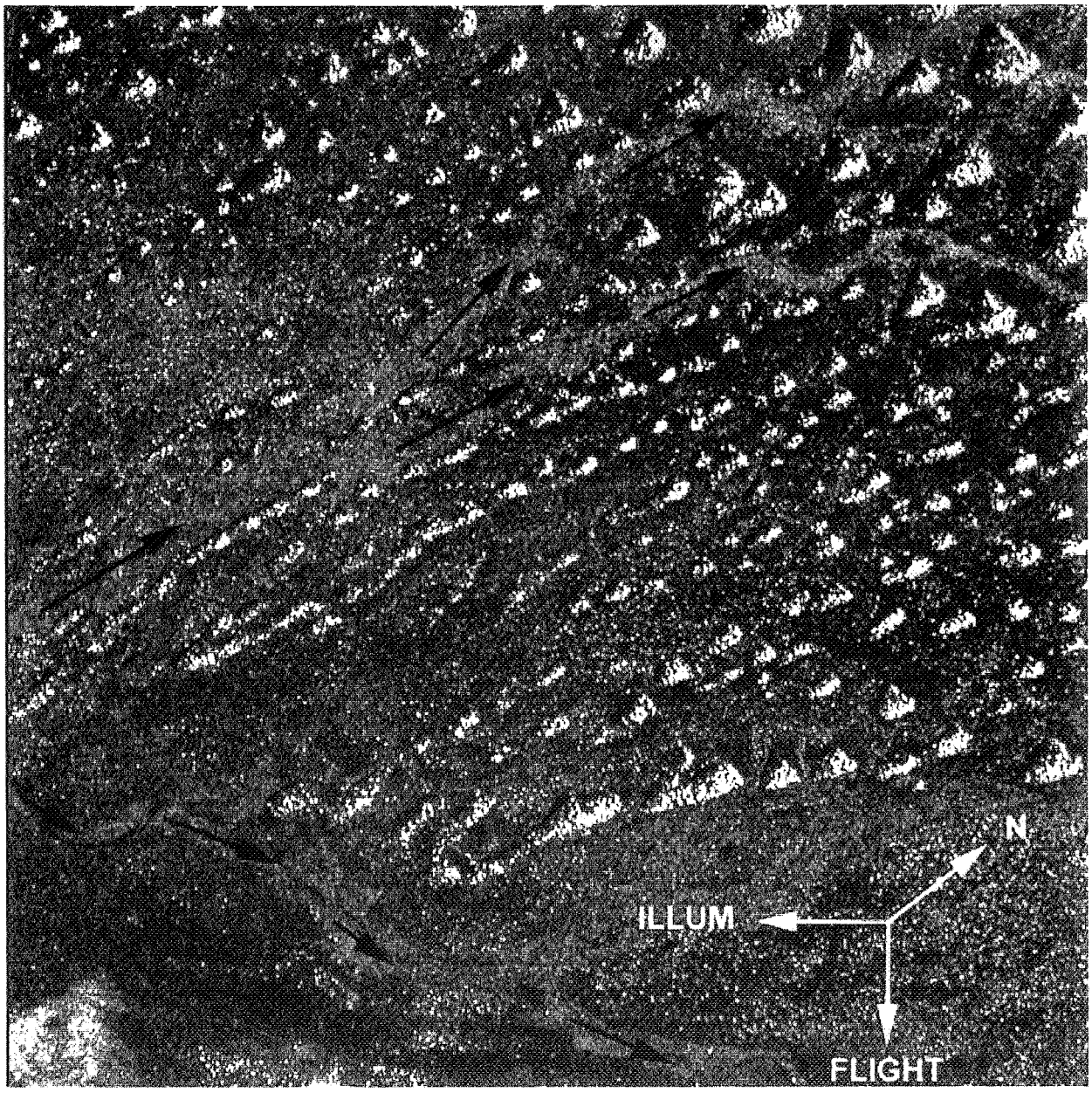

Figure 9. SIR-C/X-SAR C-band of test site 3.

Figure 10. Originally a color composite for test site 2 produced by merging L-band and LANDSAT MSS bands 4, 5, and 7.

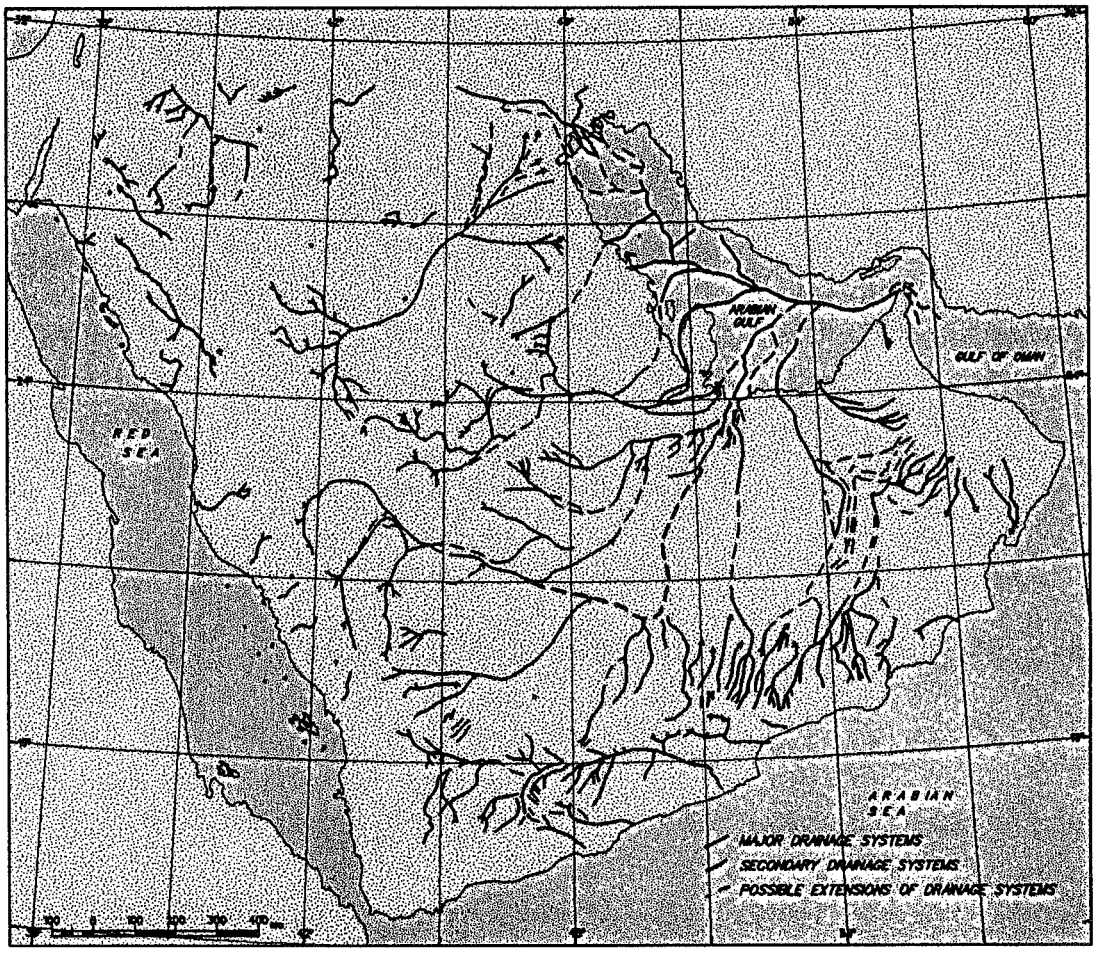

Figure 11. PLEISTOCENE DRAINAGE OF ARABIAN PENINSULA

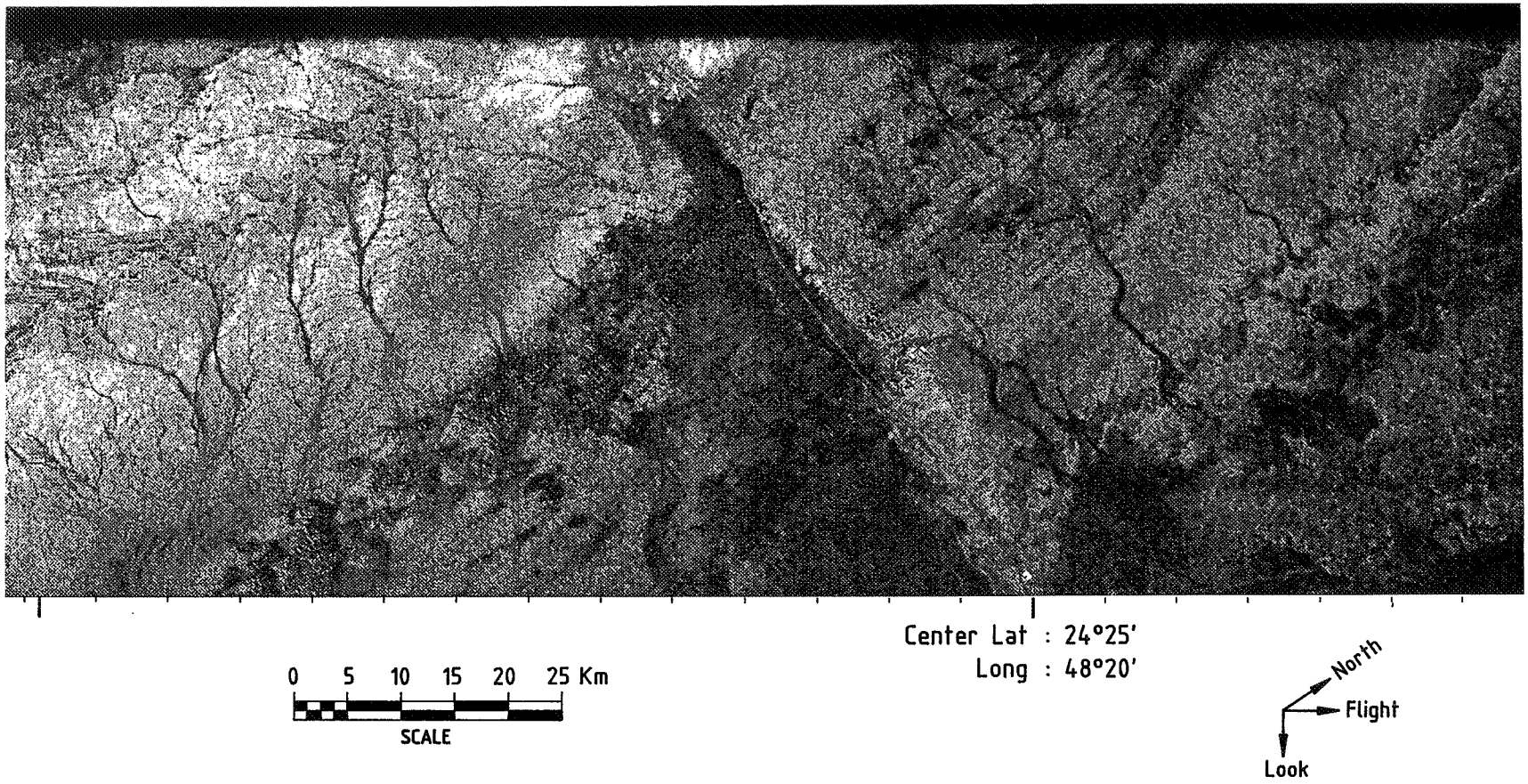

Figure 12a. SIR-C L-Band Strip 107.30 SRL-1 Wadi Sahba Area.

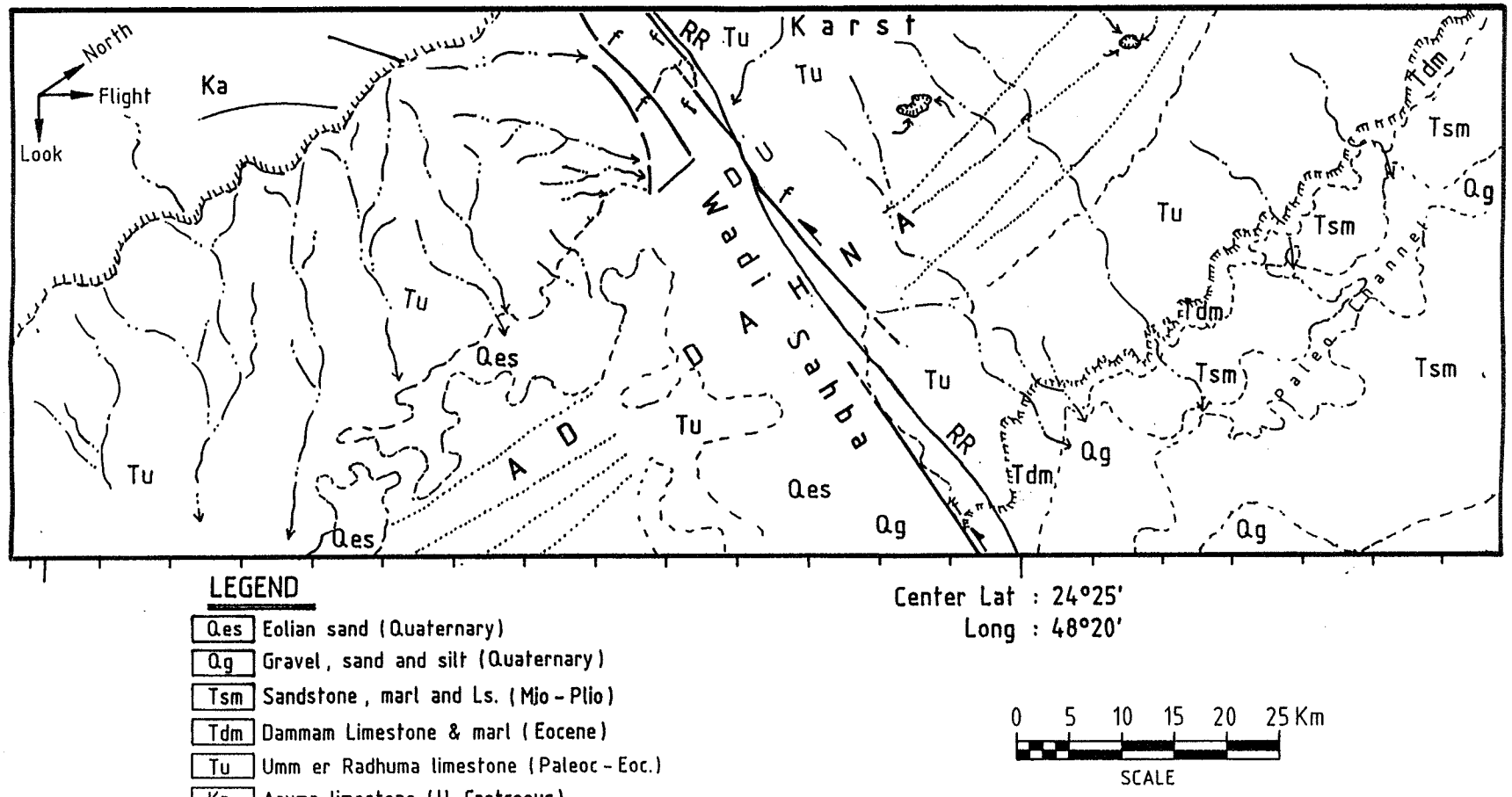

Figure 12b. Geological Map of Wadi Sahba Area.

Dr. Frank W. Davis
Center for Remote Sensing
and Environmental Optics
University of California
Santa Barbara, CA 93106

Co-Investigators:
John M. Melack Univ. of Calif., Santa Barbara (UCSB)

Biomass Modeling of the Ponderosa Pine Forests of Western North America with SIR-C/X-SAR for Input to Ecosystem Models

OBJECTIVES

Integrate existing forest biophysical measurements with field measurements and calibrated aircraft SAR and calibrated SIR-C/X-SAR images to form a spatially registered data set for model development and testing. Extend our L-band radar forest model to X- and C-band and four polarizations.

Determine the major backscattering components from a forest using aircraft SAR and SIR-C/X-SAR.

Develop and evaluate an inversion procedure through which the above-ground forest biomass, partitioning, patchiness, and spatial and height distributions within a stand can be estimated from SAR images.

PROGRESS

Our SIR-C/X-SAR research has focused on forest backscatter modeling and SIR-C data analysis for Loblolly pine forests at the Duke Forest Supersite. In support of the modeling and analysis, UCSB graduate students conducted a field study in Duke Forest during the SRL-1 mission. We are working in close collaboration with Eric Kasischke at Duke University who has provided forest stand data.

Data Acquisition/Analysis

Single-look calibrated SIR-C data for the ten available Duke Forest scenes have been ordered and received at UCSB. Four of the scenes are from the April mission, a time of rapid leafing-out of trees and shrubs in Duke Forest, during which it rained on three occasions. Six scenes are from October, at which time the leaves had not yet fallen, and ground conditions were much drier than in April. X-SAR data has also been ordered and received for nine scenes.

The following data processing has been completed for all ten SIR-C scenes: Sub-images of the Durham Division of the forest (the region for which stand data are the most complete) have been processed into sigma-0 images (L- and C-bands, polarizations). The sub-images have been imported into Arc-Info Grid. An Arc-Info stand map (supplied by ERIM) has been registered to each scene. Backscatter statistics for approximately 70 stands have been extracted and summarized for each data take. In our initial analysis of the Duke SIR-C data, we examined the backscatter statistics and trends in the data series that might be explained by variations in incidence angle or changes in forest conditions from day to day and season to season. Other graphical analyses done include comparisons of backscatter to stand age (and biomass) and comparisons of backscatter from pairs of same-incidence angle data takes from SRL-1 and SRL-2. An analysis of

model predictions versus observed backscatter changes resulting from soil moisture changes is in progress.

A study is under way on forest backscattering mechanisms, based on the radar target decomposition method (Cloude, 1992; Van Zyl, 1994). This study is presently based on AIRSAR data from floodplain swamp forest (Altamaha River, Georgia) and Ponderosa pine forest (Mt. Shasta, California). It may be extended to include SIR-C data from Duke Forest and Brazil.

Although the Shasta data set is not as rich as the Duke set, there are six scenes (including one of Mode 16) that include the Shasta site. Therefore, we plan an analysis of stand structure versus backscatter, utilizing our Shasta forest stand data. One Mt. Shasta scene has been ordered and received at UCSB and a second scene was ordered recently.

Forest Backscatter Modeling/Analysis

The Santa Barbara microwave canopy backscatter model underwent continuing evolution during 1994-95, with several improvements in coding and function. Notably, the discontinuous and continuous canopy models were integrated into a single program, and surface scattering models recently published by Oh et al. (1992, 1994) and Fung et al. (1992) were incorporated. Two modeling studies have been completed since 1994. In the first, Loblolly pine stands ranging from <1 to 14 kg/m^2 were modeled and the simulated backscatter was compared to AIRSAR data. In the second study, Loblolly stands ranging from 8 to 60 years of age were modeled. Sensitivity of backscatter from these stands to variations in surface roughness and soil moisture was evaluated by means of simulation. Response of SIR-C backscatter to soil moisture changes is presently being compared with the simulation results.

Field Work

During the April SIR-C mission, a study of the forest floor in six Loblolly stands in Duke Forest was carried out by UCSB graduate students. We were assisted by local high school students, in coordination with Eric Kasischke's soil moisture study. We measured surface roughness, soil moisture, and L-band dielectric constant, and litter depth, density, and volumetric moisture content. Some tree dielectric measurements and observations of forest state were made near the time of shuttle overflights.

SIGNIFICANT RESULTS

We validated a canopy backscatter model for Loblolly pine forest stands at the Duke Forest, North Carolina, by comparing the observed and modeled SAR backscatter from the stands. Given the SAR backscatter data calibration uncertainty, the model made good predictions (Wang et al. 1995) of C-HH, C-HV, L-HH, L-HV, L-VV, P-HH, and P-HV backscatter for most of 25 stands studied. The mode overestimated C-VV backscatter for several stands, and largely overestimated P-VV backscatter for most of the stands. Using the collected SAR backscatter and ground data, and the backscatter model, we studied the influences of changes in biomass on SAR backscatter as a function of radar frequency and polarization, and evaluated the feasibility of deriving the biomass from the backscatter. This study showed that C-HH, C-HV, C-VV, L-VV, and P-VV SAR backscatter may be insensitive to the biomass change. L-HH, L-HV, P-HH, and P-HV SAR backscatter changed more than 5 dB as the biomass varied. This study also showed that the L-HH and P-HH backscatter or L-HV and P-HV backscatter may be used to

develop algorithms to retrieve trunk biomass or canopy biomass of the Loblolly pine forests.

For young (< 15 years old) Loblolly pine stands at Duke Forest (North Carolina, USA), when the ground was wet, the observed ERS-1 SAR backscatter from short-grass fields of 0.05 kg/m^2 biomass was equal to the backscatter from the stands, and there was no significant correlation between the backscatter and biomass ($r^2 = 0.19$). Under dry soil conditions, the backscatter increased about 2 to 3 dB as the biomass (Wang et al. 1994) increased from 0.05 kg/m^2 to about 0.5-1.5 kg/m^2, and the backscatter may be saturated near a 0.5-1.5 kg/m^2 biomass level. The correlation coefficient between the backscatter and biomass was $r^2 = 0.46$. When the Santa Barbara microwave canopy backscatter model was applied to simulate the ERS-1 SAR backscatter from the stands over dry ground, modeled and observed backscatter had similar trends with increasing biomass. For these stands, sensitivity analyses using the model showed that as the surface-soil moisture increased, the major contributor to the total backscatter was changed from canopy volume scattering to surface backscatter between 0.4 and about 1 kg/m^2. Signal saturating at low standing biomass, and high sensitivity to soil moisture conditions limits the value of a short-wave (C-band) and steep local incidence angle (23 deg.) microwave sensor such as the ERS-1 SAR for forest monitoring.

Measurements of forest floor surface roughness were made in Duke Forest Loblolly pine stands in April 1994 in connection with the NASA Shuttle Imaging Radar (SIR-C) mission. A simple, inexpensive, and field-worthy surface roughness gauge (SRG) was built for this field study. The problem of how to define the "surface" within the layered forest floor system was addressed. A practical approach to forest floor roughness measurement tailored for the modeling of forest floor scattering was proposed. We estimated rms height and correlation length of the soil surface for 56 transects. Overall mean rms height is 2.2 cm and mean correlation length is 29 cm. Within-stand sampling variance is large, but stand means are similar. There is no evidence to indicate that surface roughness varies as a function of stand age or transect orientation. The data collected can be used to parameterize forest floor surface scattering models for Duke Forest and possibly other similar forests.

The Santa Barbara microwave canopy backscattering model was used to investigate the sensitivity of forest backscatter to soil roughness and moisture. Surface scattering was simulated using the empirical model of Oh et al. (1992, 1994, Salita, 1995). Values for surface roughness and soil moisture parameters were based on the ranges measured in Duke Forest during SRL-1 and SRL-2. The simulations indicate the following: At C-band, co-polarized backscatter was moderately sensitive to surface conditions at 20-30 degree incidence angles for a young (8 yr.) stand and at 20 degrees for a mid-aged (25 yr.) stand. C-HV was moderately sensitive only to the young stand at 20 degrees. C-band was insensitive to surface conditions at shallower incidence angles and in more mature forests. L-HH was moderately sensitive in mature stands and strongly sensitive in young and mid-aged stands in the range of surface conditions simulated. L-VV had moderate sensitivity only for one mid-aged stand at all incidence angles. L-HV was insensitive for all stands and angles. The insensitivity of L-HV to surface conditions is one likely cause the for relatively strong correlations observed between L-HV backscatter and biomass. Initial analyses of the Duke SIR-C data do not demonstrate the response of backscatter to soil moisture predicted by the modeling. Further work is needed to isolate the effects of soil moisture from other factors affecting SIR-C backscatter.

The radar target decomposition method was verified using SAR images containing dihedral corner reflectors. The method was applied to decompose multifrequency JPL

AIRSAR backscatter from two types of forests to analyze and understand scattering mechanisms in forested environments. For the Ponderosa pine forest (Mt. Shasta, Calif.), as SAR wavelength increased from C-band to P-band, scattering with an odd number of reflections decreased, scattering with an even number of reflections increased, and diffuse scattering showed no clear trend. For the floodplain swamp forest (Altamaha River, Georgia), scattering with an odd number of reflections dominated at C-band. Scattering with an even number of reflections was strong at L-band and stronger at P-band. Diffuse scattering from both marsh and swamp forest was <20% of total scattering at C-band and <15% at L-band and P-band. This study may be expanded to include SIR-C data from Duke Forest and Brazil.

Preliminary findings based on Duke Forest SIR-C data analysis

1) SIR-C backscatter from our site is exponentially distributed as expected for dense forest canopies that satisfy Rayleigh fading assumptions (Ulaby and Dobson, 1989). Because the fading statistics are well described, we can place confidence bounds around forest stand backscatter estimates. For the Duke Loblolly stands, 90% confidence intervals are in the range of +/- 0.3 to +/- 0.7 dB, depending on stand size.

2) Sigma-0 of the forest increases as incidence angle decreases. The trend is stronger than expected from modeling or previous data. The cause of the trend and whether or not it is statistically significant have not yet been determined.

3) As anticipated from previous studies, the relationship between backscatter and stand age (or biomass) is weak. Only L-HV appears to correlate directly with forest biomass. (The indirect biomass retrieval method discussed below may overcome this apparent limitation.)

4) In most cases, variations in backscatter between different dates (for data takes having the same incidence angle) are on the order of 0-3 dB for individual stands and <2 dB for averages of the stands. We cannot be sure whether the observed variations are due to calibration error or to known or unidentified differences in forest conditions. The variations are of the same magnitude as stand-to-stand sigma-0 differences attributable to biomass. Within-scene relative calibration is being considered to remove the systematic variations.

5) With the exception of one rainy morning during SRL-1, backscatter was not higher for wet soil than dry soil conditions, even at small incidence angles. This apparent contradiction to model-based expectations is under scrutiny and may lead to better understanding of sources of forest backscatter uncertainty.

FUTURE PLANS

Biomass separability under varying conditions

Our first priority is to investigate the separability of forest stands of differing structure and biomass under different environmental conditions for a range of incidence angles. The main emphasis will be on Duke Loblolly stands, however, Mt. Shasta data will also be evaluated. Our approach is outlined in the following questions: Under what conditions (incidence angle, moisture, season) do multiple regressions of SIR-C backscatter give the strongest predictions for total stand biomass, for crown biomass, for basal area, or for tree height? For the same conditions, how effective is the L-HV/C-HV ratio in predicting

biomass? This research will extend well into 1996. Some of the results will be utilized in the indirect biomass retrieval study (below).

Indirect Biomass Retrieval

It has become increasingly clear over the past three years that the direct regression approach for estimating forest biomass from backscatter is not very powerful, except in fairly low biomass forests. The use of cross-polarization ratios, as proposed by Ranson and Sun (1994), raises the biomass level at which the signal saturates, but it remains to be seen how applicable the technique will be for diverse forest structural types of moderate to high biomass. Dobson et al. (1995) speak to this issue very plainly. In that paper the authors observe that much of the data scatter seen in regressions of backscatter versus biomass is due to variations in forest structure. For example, a few large trees may have a total biomass equivalent to that of many small trees but the former produce higher backscatter.

Dobson et al. advocate an indirect method for estimating biomass. In the first step, regressions against backscatter are developed to predict crown biomass, basal area, and height of each forest structural class. Second, estimates of trunk biomass are derived from basal area and height using allometric equations. Finally, total biomass for each class is the sum of crown biomass plus trunk biomass. Instead of regressions on the aggregate forest system, the regressions are on individual structural components that are more like what microwaves actually interact with.

We plan to apply Dobson's indirect method to improve biomass estimates in the Duke Loblolly stands. Apart from the question of extensibility of this approach to the Loblolly forest, an equally important question needs to be addressed and will be investigated in this study: how consistent are results from pass to pass, for varying calibration and incidence angle, and under changeable forest conditions? The usefulness of the indirect biomass retrieval method will depend on whether it is broadly applicable and repeatable under different SAR and forest conditions.

Texture

A parallel study is planned utilizing texture measures to complement backscatter intensity in the estimation of biomass. There is much evidence that for many forests structural evolution accompanies biomass change over time. This is certainly true in the "old field" Loblolly stands at Duke. Furthermore, several papers demonstrate improved discrimination of forest types in SAR images when texture is used to augment tone. Differences in biomass, sensed indirectly through differences in forest structure, may be estimated more robustly through image texture than is possible using backscatter alone. Preliminary work has begun with a literature search and application of texture algorithms to Mt. Shasta data. At present, we view this study's primary goal as generating an independent channel of SIR-C information to feed into biomass estimation procedures.

PUBLICATIONS

Saleta, J., 1995, *Stand Discrimination in a Western Coniferous Forest Using AIRSAR Data*, M. A. thesis, Dept. of Geography, UCSB.

Wang, Y., F. W. Davis, J. M. Melack, E. S. Kasischke, and N. L. Christensen, 1995, The effects of changes in forest biomass on radar backscatter from tree canopies, *Int. J. Remote Sensing*, vol. 16, no. 3, pp. 503-513.

Wang, Y., E. S. Kasischke, J. M. Melack, F. W. Davis, and N. L. Christensen, Jr., 1994, The effects of changes in Loblolly pine biomass and soil moisture on ERS-1 SAR backscatter, *Remote Sens. Environ.,* vol. 48, pp. 1-25.

REFERENCES

Cloude, S. R., 1992, Uniqueness of target decomposition theorems in radar polarimetry, in *Direct and Inverse Methods in Radar Polarimetry, Part I,* (ed. by W. M. Boerner et al.) Kluwer Academic Publishers, Dordrecht, The Netherlands.

Dobson, M. C., F. T Ulaby, L. E. Pierce, T. L. Sharik, K. M. Bergen, J. Kellndorfer, J. R. Kendra, E. Li, Y. C Lin, A. Nashashibi, K. Sarabandi, and P. Siqueira, 1995, Estimation of forest biophysical characteristics in Northern Michigan with SIR-C/X-SAR, *IEEE Trans. Geosci. Remote Sensing*, in press.

Fung, A. K., Z. Li, and K. S. Chen, 1992, Backscattering from a randomly rough dielectric surface, *IEEE Trans. Geosci. Remote Sensing*, vol. 30, no. 2, pp. 356-369.

Oh, Y., K. Sarabandi, and F. T. Ulaby, 1992, An empirical model and an inversion technique for radar scattering from bare soil surfaces, *IEEE Trans. Geosci. Remote Sensing*, vol. 30, no. 2, pp. 370-381.

Oh, Y., K. Sarabandi, and F. T. Ulaby, 1994, An inversion algorithm for retrieving soil moisture and surface roughness from polarimetric radar observation, *Proceedings of IGARSS '94*, pp. 1582-1584.

Ranson, K. J., and G. Sun, 1994, Mapping biomass of a northern forest using multifrequency SAR data, *IEEE Trans. Geosci. Remote Sensing*, vol. 32, no. 2, pp. 388-396.

Ulaby, F. T. and Dobson, M. C., 1989, *Handbook of Radar Scattering Statistics for Terrain*, Artech House, Norwood, MA.

Van Zyl, J. J., 1994, Application of Cloude's target decomposition theorem to polarimetric imaging radar data, *Proceedings of the Third Spaceborne Imaging Radar Symposium*, held at Jet Propulsion Laboratory Pasadena, CA, Jan. 18-21, 1994, pp. 207-216.

Dr. Jeff Dozier
Computer Systems Laboratory
Center for Remote Sensing and
Environmental Optics
University of California
Santa Barbara, CA 93106

Co-Investigator:
J. Shi University of Calif., Santa Barbara

SIR-C Investigations of Snow Properties in Alpine Terrain

OBJECTIVES

Estimate snow-covered area and distribution of snow water equivalence over alpine drainage basins. Surface material may be trees that are taller than the snow depth, brush, or grass that will be covered by the snow, soil, scree, talus, or bedrock, or glacier ice.

Estimate spectral albedo of snow cover.

Model spatial distribution of snow surface energy exchange, melt rate, and snow metamorphism intensively during two-to-four-week periods around SIR-C/X-SAR flights, and less intensively during the rest of the snow season.

PROGRESS

Our recent studies, using SIR-C/X-SAR and AIRSAR data, have shown a significant improvement in understanding and modeling backscattering and polarization properties as a function of snow parameters. Maps of snow-covered areas derived from SIR-C/X-SAR and AIRSAR now compare well with those derived from visible images, which require clear weather and daylight. A better than 80% accuracy for both dry and wet snow covers can be achieved when compared with TM classification results. We have developed an accurate algorithm to retrieve snow-wetness, which indicates where and at what rate snow is melting. The tested results using C-band SIR-C and JPL AIRSAR data indicated that an accuracy of 2.5% can be achieved at 95% confidence interval. We have developed an algorithm to estimate snow density and depth. The initial test showed very promising results. Thus, accurate information about the spatial and temporal distributions of snow water equivalency and melting status of snow cover can be provided by SIR-C/X-SAR for hydrological and climatic investigations and operations.

Field Measurements

During the first and second SIR-C/X-SAR missions in April and October 1994, we carried out near-simultaneous field campaigns at three test sites: Mammoth Mountain in the Sierra Nevada, California, the Ürümqi River basin in the Tien Shan, China, and the Echaurren basin in the Andes, Chile.

At the Mammoth site, three corner reflectors were used for calibration. We selected three test sites near Mammoth Mountain based on SIR-C/X-SAR passes. For each data-take we measured two snow-pits for the vertical profile of snow properties at each site: temperature, snow density, grain size and size distribution, free liquid water content, and stratification. In addition, we measured snow properties along two transects that cross each site for information about spatial distribution. Those measurements included snow depth, density, wetness, and surface roughness.

At the Tien Shan site, five corner reflectors were used for calibration. Snow properties measurements included snow temperature, depth, and density. At the Echaurren site, we measured snow temperature, depth, density, particle size, and surface roughness.

Microwave Modeling and Backscattering Response to Snow Parameters

The main problem in estimating snow properties from remote sensing data is understanding the links between the electromagnetic interactions in different parts of the spectrum and the physical properties of the snow. Modeling microwave backscattering from snowpacks requires knowledge of snow characteristics and their dynamics to select an appropriate model. Both theory and field data show that microwave backscattering coefficients are sensitive to parameters describing snow microstructure.

Stereological methods, applied to images of sections cut from undisturbed snow, are used to obtain accurate, unbiased estimates of snow microstructure parameters for discrete scatterer modeling. Our recent studies have found that the ice particle size distribution in seasonal snow can be characterized as a log-normal distribution function. The required parameters (the geometric mean diameter and standard deviation of particle diameters) for fully describing the particle size variation and distribution can be directly measured by stereological variables. The results show that in addition to snow density and ice particle size, the particle size variation affects extinction properties of dry snow. The optically equivalent ice particle size for Rayleigh scattering in a snowpack with grain size variations can be determined from the stereological data.

We have developed a polarimetric model that includes both surface and volume scattering as well as the interaction terms between surface and volume. Radiative transfer models for dense media and the random media were used for the volume scattering. The surface scattering models (IEM, SPM, POM, and GOM) were introduced to the radiative transfer equations in order to evaluate the importance of the interactions between the surface and volume scattering signals.

Through SAR data analyses and model simulations, we found that backscattering measurements from dry snow are affected by three sets of parameters: (1) sensor parameters, (2) snowpack parameters, and (3) ground parameters. The relationships between backscattering signals and snow water equivalence can be either positive or negative, depending on the snow physical parameters, ground surface parameters, and incidence angle. In addition to snow density and ice particle size, size variation, snowpack stratification, and underlying ground conditions affect the interpretation of the observed backscattering signals. When the scattering signal from the snowpack is greater than the signal from the ground (attenuated by the overlying snow), a positive correlation is expected. Otherwise, the correlation is negative.

We also found that the relationship between the co-polarization signals at C-band and snow wetness is controlled by the scattering mechanisms. In addition to the snow properties, the surface roughness and local incidence angle play an important role in the relationships between the co-polarization signals and snow wetness. This relationship can be either positive or negative, depending on the snow properties, surface roughness, and incidence angle.

Snow Mapping

Previously, snow in alpine regions has been mapped with conventional SAR imagery by comparing a geocoded SAR image with a simulated image. This method requires a

compatible digital elevation model (DEM) for generation of the simulated image, and that the DEM and SAR data be coregistered. The capability of a single-polarization SAR in mapping snow-cover is limited to wet snow condition. Single polarization SARs operating at 5.3 GHz (C-band) can map wet snow and ice-free surfaces, but they poorly separate glacier ice from snow and rock.

Through evaluation of the characteristics of the backscattering and polarization response of snow, we found that mapping snow in remote alpine regions by using intensity measurements requires topographic information to obtain correct radiometric measurements and to reduce angular dependence for discrimination. Because the measurements of polarization properties and of the ratios between different frequencies provided by SIR-C/X-SAR do not require topographic correction, an appropriable selection of these measurements through evaluating the incidence angle dependence and separability between different targets within the scene makes it possible to map snow covers without requiring topographic information in remote alpine regions. Using this technique, we compared the coregistered TM classification results with SIR-C/X-SAR classification results. Accuracies better than 80% for wet snow-covered from pixel-by-pixel comparison can be obtained for binary classification. The major difference between TM and SIR-C/X-SAR binary classification results are due to the mixed pixel problem. In addition, we have found that SIR-C/X-SAR can map dry snow cover when multifrequency and multipolarization data with DEM are used. This is in contrast with single-polarization SARs which are limited only to mapping wet snow cover. A similar accuracy can also be obtained. Currently, we are evaluating the possibility of mapping dry snow cover without requiring topographic information. Thus, SIR-C/X-SAR has comparable capability with the visible and near-infrared sensors to map both dry and wet snow covers.

Snow Wetness

From a verified backscattering model, we have developed an algorithm for retrieving snow wetness using C-band polarimetric SAR imagery. Our algorithm is based on a first-order scattering model, with consideration of both surface and volume scattering. At the regional scale, the inferred spatial distribution of snow wetness from two SIR-C data-takes showed clear characteristics. Higher snow wetness was estimated on the south slope than on the north slope, and the elevation dependence of snow wetness was inferred. This agrees well with our knowledge of the characteristics of spatial distribution of free liquid water content in snow. The comparison of SAR-derived snow wetness with ground measurements indicated that the absolute error at 95% confidence interval was 2.5%. Both regional and point measurement indicate that the inversion algorithm performs well using C-band SIR-C/X-SAR data and will prove useful for routine and large-area snow wetness measurements if a multi-parameter spaceborne SAR becomes available.

Snow Water Equivalency

Based on the numerical simulations of our polarimetric model for dry snow covered conditions, we have developed a physical-based algorithm to estimate snow water equivalency and the snowpack equivalent particle size. This algorithm is based on the first-order backscattering model so that it should have less effect on the site-specific problems. It uses L-band co-polarization measurements to estimate snow density and the underlaying surface dielectric and roughness properties. Then, the backscattering signals from the snow-ground interface at C- and X-band can be decomposed from the total backscattering signals by estimation of the surface backscattering components from the underlaying surface dielectric and roughness properties. Finally, the snow depths and snowpack equivalent particle sizes can be estimated from C- and X-band measurements.

This algorithm does not require a background image (without snow cover) so that the problems due to mis-coregistration and the surface roughness properties change can be avoided. The current test results from two SIR-C/X-SAR data takes over our Mammoth test site showed the accuracies of 62 kg/m3, 38.1 cm and 19.8 cm for snow density, depth, and water equivalence, respectively. Currently, we are testing this algorithm over all data takes for dry snow cover at the Mammoth site.

PUBLICATIONS

O'Neill, P. E., A. Hsu, and J. Shi, Soil Moisture Estimation Using Time-Series Radar Measurements of Bare and Vegetated Fields in Washita '92, *Proceedings IGARSS '95*, volume I, pp. 498-500, IEEE No. 95CH35770, 1995.

Shi, J. and J. Dozier, Inferring Snow Wetness Using SIR-C C-Band Polarimetric Synthetic Aperture Radar, *IEEE Transactions on Geoscience and Remote Sensing*, July, 1995.

Shi, J. and J. Dozier, SIR-C/X-SAR Investigations of Snow Properties in Alpine Regions, *Proceedings IGARSS '95*, volume II, pp. 1582-1584, IEEE No. 95CH35770, 1995.

Shi, J. and J. Dozier, SIR-C/X-SAR Mapping Snow in Alpine Regions, *Proceedings IGARSS '95*, volume II, pp. 1508-1510, IEEE No. 95CH35770, 1995.

Shi, J., J. Wang, A. Hsu, P. O'Neill and E. T. Engman, Estimation of Soil Moisture and Surface Roughness Parameters Using L-band SAR Measurements, *Proceedings IGARSS '95*, volume I, pp. 507-509, IEEE No. 95CH35770, 1995.

Shi, J. and J. Dozier, Measurement of C-band SAR Response to Wet Snow: From Modeling to Observation, *Proceedings PIERS '95*, pp. 218-1041, 1995.

Shi, J. and J. Dozier, Estimation of Snow Water Equivalence Using SIR-C/X-SAR Image Data, *Proceedings PIERS '95*, p. 1041, 1995.

Shi, J., J. Wang, A. Hsu, P. O'Neill and E. T. Engman, Estimation of Soil Moisture and Surface Roughness Parameters Using SIR-C's and AIRSAR's L-band Measurements, to be submitted to the special issue of *IGARSS '95*, in preparation.

Shi, J. and J. Dozier, Estimation of Snow Water Equivalence Using SIR-C/X-SAR Image Data, Journal to be submitted to *IEEE Transactions on Geoscience and Remote Sensing*, in preparation.

Shi, J. and J. Dozier, SIR-C/X-SAR Mapping Snow in Alpine Regions, to be submitted to *Remote Sensing of Environment,* in preparation.

Shi, J., J. Dozier and H. Rott, Snow and glacier mapping in alpine regions using polarimetric SAR, *IEEE Transactions on Geoscience and Remote Sensing*, 32, pp. 152-158, 1994.

Shi, J., J. Dozier and H. Rott, Active microwave measurements of snow cover-Progress in polarimetric SAR, *Proceedings IGARSS '94*, pp. 1922-1924, IEEE No. 94CH3378-7, 1994.

Shi, J. and J. Dozier, Estimating snow particle size using TM band-4, *Proceedings IGARSS '94*, pp. 1747-1749, IEEE No. 94CH3378-7, 1994.

Shi, J., P. O'Neill, A. Hsu, J. van Zyl and M. Seifried, Estimating soil moisture and surface roughness parameters using L-band SAR measurements, *Proceedings SPIE '94*, 1994.

Shi, J., J. Wang, P. O'Neill, A. Hsu and T. Engman, Application of IEM model on Estimations soil moisture and surface roughness, *Fifth Annual JPL Airborne Earth Science Workshop*, 1994.

Wang, J., P. E. O'Neill, E. T. Engman, R. Pardipuram, J. Shi and A. Hsu, Estimating Surface Soil Moisture from SIR-C Measurements over the Little Washita Watershed, *Proceedings IGARSS '95*, volume III, pp. 1982-1984, IEEE No. 95CH35770, 1995.

Dr. Edwin T. Engman
Hydrological Sciences Branch
NASA/Goddard Space Flight Center
Greenbelt, MD 20771

Co-Investigators:
Peggy O'Neill — Goddard Space Flight Ctr.
Eric Wood — Princeton University

Contributors:
Valentine Pauwels — Princeton University
Ann Hsu — NASA/GSFC
Tom Jackson — USDA-ARS

Visiting Scientists:
J. C. Shi — University of California Santa Barbara
Corinna Prietzsch — ZALF, Muncheberg, Germany

Application of SIR-C SAR to Hydrology

OBJECTIVES

Determine and compare soil moisture patterns within one or more humid watersheds using SAR data, ground-based measurements, and hydrologic modeling.

Use radar data to characterize the hydrologic regime within a catchment and to identify the runoff producing characteristics of humid zone watersheds.

Use radar data as the basis for scaling up from small scale, near-point process models to larger scale water balance models necessary to define and quantify the land phase of GCMs.

PROGRESS

During the time since the SIR-C/X-SAR missions, this project has received 13 processed SIR-C images from SRL-1 (April 11-18, 1994) of the primary hydrology supersite in Chickasha, Oklahoma, as well as 10 X-SAR images On three days, long strips (either 98 or 200 km) of the data takes covering the Washita watershed were also processed. We have just now begun to receive processed scenes from the SRL-2 mission in October, with a total of 9 images logged in so far which cover a primary sampling site within the Little Washita watershed.

Data have also been received for the back up super site at Mahantango, PA. We have received the two scenes for April and three uncalibrated interferometric scenes from the October mission.

During both missions, and the week of the aborted August shuttle flight, extensive ground data and aircraft data were collected at both the primary and secondary supersites. The types and quantities of data collected at the two sites varied from mission to mission but included extensive ground truth data (soil moisture, roughness, vegetation, etc.), flux stations, radiosondes, weather stations, stream flow, and aircraft measurements (C-130 ESTAR, NS001, TIMS, JPL AIRSAR, USDA vis-nir, and thermal).

During the SRL-1 field experiment (April 6-16, 1994), field conditions were initially dry, became wet as a result of a heavy rainstorm on the afternoon of 4/10/94 and morning of 4/11/94, and then gradually dried down throughout the remainder of the experimental period (a change in volumetric

soil moisture of 15-20%). In contrast, during the SRL-2 experiment (October 1-6, 1994), most of the watershed remained dry except for localized rainfall in the northwest part of the watershed on the evening of 10/3/94 and in the northern part of the watershed on the evening of 10/4/94.

Conditions at Mahantango in April were very wet with little change in soil moisture between the two data takes. During October, conditions were quite a bit better. The area was initially dry for the first data take, followed by rain and a dry down for the next standard data take and the consecutive days of the interferometric data takes.

Estimation of soil moisture. Initially we have focused on data collected on April 11, 12, and 15th. After registering the images, we made a land cover classification that was needed for both the radar inversion models and the hydrological models. The land cover classification combined the algorithm with classifications of urban, tall vegetation, short vegetation and bare soil and the NDVI estimation from a Thematic Mapper image acquired April 1994. The NDVI allows us to distinguish between active short crops (like winter wheat) and pasture that is still in senescence.

Following the classification, two estimation procedures were applied: an empirical, regression similar to that described in Lin et al. (1994) and the inversion model of Dubois et al. (1995). In addition, a distributed hydrological model was also used to estimate soil moisture within the Little Washita for the April SIR-C mission period.

We also cooperated with J. C. Shi of the University of California at Santa Barbara (UCSB) to retrieve soil moisture from SIR-C data. Shi's approach is a combination of the Integral Equation Model (IEM) and a statistical technique. Due to the complexity of the IEM, Shi adopted the assumption that the random surface height is small and used the Small Perturbation model to approximate IEM. The results from Shi's model for an almost bare surface (a field with emerging corn and row structure) were quite good, except for overestimates on two dry days, which may be attributed to the calibration accuracy of SIR-C, i.e., within 2 dB. However, for the short vegetated fields, the model tends to overestimate on dry days and underestimate on wet days. This may be related to the Small Perturbation approximation of the model or to a vegetation attenuation effect, although theoretical studies show that the attenuation is small at L band.

Scaling of soil moisture. This research has been initially carried out with remotely sensed soil moisture collected during the Washita '92 field experiment. Results published in Dubayah et al. (1995) indicate that the soil moisture exhibits multiscaling properties, namely log-log linearity of statistical moments as a function of scale, and nonlinear dependence of scaling exponents with order moment.

Truck radar experiments. To complement the Shuttle radar data and provide an accurate means of comparison of microwave data acquired at different spatial scales from different platforms, NASA/GSFC's three-frequency, truck-mounted radar was deployed to the hydrology supersite near Chickasha during SRL-1. Designed and operated in conjunction with George Washington University, the truck radar consists of L-, C-, and X-band radars (1.6, 4.75, and 10 GHz) which approximate the L-, C-, and X-band radars on SIR-C and the L- and C-radars on NASA/JPL's airborne AIRSAR system. On each of eight days of actual data collection the truck radar took measurements at three frequencies (L, C, X), four polarizations (HH, HV, VV, VH), and three angles (30, 40, 50 degrees) for four test fields which each represented a typical surface cover found in the watershed (pasture, alfalfa, new corn/bare, winter wheat). Calibrated field averages of truck radar backscatter for each of these test fields have been compiled for L- and C-band and are available for distribution; most of the X-band data were considered to be marginal due to noise floor problems. Comparisons of truck radar, SIR-C, and AIRSAR L-band data indicate that for certain fields the three sensors were responding almost identically to the soil moisture dry down (agreement generally to within 1 dB). In other fields, there might be agreement in some channels

but not in others (like vs. cross polarization, for example). These differences are currently under investigation in light of surface scattering, cross calibration, and viewing geometry considerations.

SIGNIFICANT RESULTS

Cross-comparison of radar sensor response between the truck, AIRSAR, SIR-C, and ERS-1 radars indicates a general agreement on the order of 1 dB for certain fields at L-band (CVV for ERS-1). For other fields and data channels there is a poorer match in sensor response which is currently under investigation.

For a primary pasture test site measured by both SIR-C and the truck radar, an LHH radar sensitivity to soil moisture of 5-6 dB change in backscatter for a 11-12% change in volumetric soil moisture was recorded.

A soil moisture inversion procedure simplified from the Integral Equation Model produced estimation errors of 2.8% volumetric soil moisture when applied to L-band AIRSAR and SIR-C data of the Little Washita watershed.

An empirical algorithm based on scatterometer data has been developed for retrieving soil moisture and the RMS surface roughness. The model has been tested using AIRSAR and SIR-C data and the RMS error in the soil moisture estimate was less than 3.5%.

FUTURE PLANS

Estimation of soil moisture. We will continue to explore the role of radar data for the estimation of soil moisture. Specifically, we plan to do the following research:

(i) Extend the range of conditions for which SIR-C data has been investigated to date. This will be done by applying the same procedures used in Pauwels et al. (1995) to the October 1994 field data. In addition, we have been collaborating with other SIR-C soil moisture researchers in Italy and Belgium and anticipate a joint paper summarizing SIR-C soil estimation across a number of areas.

(ii) Test additional inversion algorithms, specifically J. C. Shi's and A. K. Fung's, to the data collected at Chickasha. This work would be done in collaboration with GSFC and will provide important insights into the range of estimates provided by radar inversion models.

(iii) In conjunction with JPL (J. van Zyl), we will continue to explore the usefulness of SIR-C data for estimation of soil moisture at regional scales. JPL has extracted an 800 km strip from the April 12 Chickasha ascending scene. We plan to do inter comparisons between this radar data and rain radar data (to identify wet areas) and with hydrological model derived soil moisture.

(iv) The effect of moisture and surface roughness to surface scattering is nonlinear. Instead of the current statistical approach of using polarization ratios to invert soil moisture from SIR-C data, we will test a combination of neural network and IEM, a technique currently under development by A. K. Fung's group that we learned when we attended IGARSS in July. We will cooperate with A. K. Fung's students, K. S. Chen and Y. C. Tseng, who now work at the Center for Space and Remote Sensing Research, National Central University, Taiwan.

Scaling soil moisture. We plan to carry out similar scaling analyses with the SIR-C backscatter data and with derived soil moisture data. The objective of this work is to determine a resolution appropriate for regional soil moisture estimation. Extension of soil moisture estimation procedures from the scale of individual fields to the scale of the entire watershed will be pursued in different

ways including use of a hydrological model for the watershed and comparison with SSM/I satellite microwave data. Processing of any SCANSAR data takes over the Little Washita watershed will be requested in this regard.

Active-Passive synergism. Future research will include continuing development of soil moisture inversion models utilizing SIR-C data alone and also radar data in combination with ESTAR passive microwave data and other remote sensing and meteorological measurements. Cross-calibration of sensor response for all mission conditions will be a preliminary focus.

Soil properties. We also intend to try to use the SIR-C and AIRSAR data sets to extract information about the physical properties of the soils. For this work, the relative rate of change in soil moisture (drying) can be associated with the percents of sand, silt, and clay, and the two-day drying with the saturated hydraulic conductivity.

Vegetation effects. Based on our current work, one of our research plans for the coming two years is to improve soil moisture retrieval algorithms with the goal of removing vegetation effects. This includes the following steps:

(i) We will extend the IEM term beyond the Small Perturbation approximation. With the application of neural networks, we hope it will improve the estimation of moisture for sparse and short vegetated surfaces. A second approach will be to apply a Rayleigh model to account for the attenuation effect of sparse and short vegetation when generating a training data set for a neural network.

(ii) For dense and tall crops such as corn and fully grown winter wheat, the interactions between the ground surface and the canopy should be accounted for when providing a training data set to the neural network; existing vegetation scattering models will be modified for this purpose.

(iii) A comparison of truck radar and SIR-C results at C-band with radar data from ERS-1 over the Little Washita area on 4/12/94 (wet day) and 4/15/94 (dry day) will be examined along with the L-band response to quantify vegetation effects through a multifrequency approach.

(iv) The truck radar data will be used to extend a vegetation scattering model to winter wheat canopies in order to quantify vegetation effects in a soil moisture retrieval procedure utilizing ESTAR brightness temperature data.

Aircraft experiments. There are plans being developed to add a significant soil moisture component to the intensive field campaigns for the GCIP program. The emphasis of these campaigns will be the spatial variability of soil moisture within a mesoscale grid cell (40 km) and the regional variability between grid cells (1000 km).

PUBLICATIONS

Dubois, P., J. van Zyl and E. Engman, "Measuring Soil Moisture with Imaging Radars," *IEEE Trans. Geosc and Rem. Sens.*, 33, 1995, pp. 915-926.

Dubayah, R., E. F. Wood and D. Lavallee, "The Spatial Scaling Properties of Remotely Sensed and Modeled Near-surface Soil Moisture State for the Little Washita Basin," in Quatrocchi and M. Goodchild, (editors), *Scaling of Remote Sensing Data for GIS*, 1995 submitted.

Lin, D. S., S. Saatchi and K. Beven, "Soil Moisture Estimation Over Grass-Covered Areas Using AIRSAR," *International Journal of Remote Sensing*, 15 (11), 1994, pp. 2323-2343.

O'Neill, P. E., N. S. Chauhan, and T.J. Jackson, "Use of Active and Passive Microwave Remote Sensing for Soil Moisture Estimation Through Corn," *International Journal of Remote Sensing*, 1995, in review.

O'Neill, P. E., N. S. Chauhan, and R. Lang, "Ground-Based Radar Measurements During the Washita '92 Hydrology Experiment," AGU Spring Meeting, *EOS Supplement*, Baltimore, MD, May 24-28, 1993, p. S132.

O'Neill, P. E., N.S. Chauhan, T.J. Jackson, D.M. LeVine, and R.H. Lang, "Microwave Soil Moisture Prediction Through Corn in Washita '92," *Proceedings of IGARSS '94, IEEE,* Pasadena, CA, August 8-12, 1994, Vol. III, pp. 1585-1587.

O'Neill, P. E., A.Y. Hsu, and J.C. Shi, "Soil Moisture Estimation Using Time-Series Radar Measurements of Bare and Vegetated Fields in Washita '92," *Proc. IGARSS '95, IEEE,* Florence, Italy, July 10-14, 1995, Vol. I, pp. 498-500.

O'Neill, P. E., J. J. Petrella, and A. Y. Hsu, "Comparison of Multifrequency Truck Radar and SIR-C Backscatter for Soil Moisture Estimation in Washita '94," *Proc. IGARSS '95, IEEE,* Florence, Italy, July 10-14, 1995, Vol. I, pp. 368-370.

O'Neill, P. and J. Petrella, "Comparison of Truck-mounted Radar Measurements with SIR-C Microwave Data for Soil Moisture Estimation," *NASA Research and Technology Report,* GSFC, 1994, pp. 124-126.

O'Neill, P., A. Hsu and T. Jackson, "Use of Active and Passive Microwave Measurements from Multiple Platforms for Soil Moisture Estimation," AGU Spring Meeting, Paper H32G-3, *EOS*, 76 (17), April 25, 1995 (Supplement), p. 5127.

Pauwels, V., et al., "A Combination of Remote Sensing and Hydrological Modeling to Estimate Soil Moisture at the Basin Scale," under review, 1995.

Shi, J., J. Wang, A. Hsu, P. O'Neill, and E. Engman, "Estimation of Soil Moisture and Surface Roughness Parameters Using L-Band SAR Measurements," *Proc. IGARSS '95, IEEE*, Florence, Italy, July 10-14, 1995, Vol. I, pp. 507-509.

Wang, J. R., P. E. O'Neill, E. T. Engman, R. Pardipuram, J. C. Shi, and A. Y. Hsu, "Estimating Surface Soil Moisture from SIR-C Measurements Over the Little Washita Watershed," Proc. IGARSS '95, IEEE, Florence, Italy, July 10-14, 1995, Vol. III, pp. 1982-1984.

Wood, E. F., V. Pauwels, T. Jackson, E. Engman, P. O'Neill and F. Schiebe, "Using SIR-C Shuttle Radar Laboratory (SRL) for Soil Moisture Remote Sensing in the Little Washita Catchment: Initial Results," AGU Spring Meeting, Paper H32G-4, *EOS*, 76 (17), April 25, 1995 (Supplement), p. S127.

Recent research results are also available on the Princeton SIR-C homepage:
(http://earth.princeton.edu).

Dr. Tom G. Farr
Mail Stop 300-233
JPL/Caltech
4800 Oak Grove Drive
Pasadena, CA 91109

Co-Investigators:

Oliver Chadwick	JPL/Caltech
Diane Evans	JPL/Caltech
Alan Gillespie	University of Washington
Gilles Peltzer	JPL/Caltech
Paul Tapponnier	University of Paris

Climate Change and Neotectonic History of Northwestern China

OBJECTIVES

To compare the types, rates, and magnitudes of surficial modification processes that have operated in NW China and the SW U.S.

To quantify and understand the basis of the remote sensing signatures of these processes to allow extrapolation from field sites to regional maps and to allow comparisons between widely separated arid regions.

To use the resulting chronologies to help define the temporal and spatial distribution of continental climate changes.

Determine the ages of movements on some of the active faults in NW China.

PROGRESS

Extensive SIR-C/X-SAR coverage was obtained with the two flights of SRL. Approximately 30 swaths were obtained that nearly mosaic to cover a large percentage of the region of northwestern Tibet, the Kun Lun Mountains, and southwestern Tarim Basin. This region contains many examples of landforms produced by past climate changes that have not been buried by the extensive loess deposits more common to the east. The region is also host to large faults, similar to California's San Andreas strike-slip fault and the blind thrust faults of Los Angeles Basin. From the NW China swaths, approximately 25 SIR-C and 40 X-SAR scenes have been processed, of which about 10 have been analyzed in depth for a just-completed field trip.

Other data sets have also been used in this investigation: Landsat MSS images provided synoptic coverage; SPOT images geocoded by Eric Fielding provided valuable high-resolution coverage of the main site; ERS-1 image coverage of the test sites has proved useful for regional coverage; both SIR-C and ERS-1 interferometric pairs were processed by Eric Fielding to produce DEMs of the main test site. The DEMs will be important for studies of the alluvial fans and their fault offsets and potentially lake shorelines.

An important step in the investigation was accomplished in August: A one-month field expedition. Participating were Farr, Evans, Chadwick, Peltzer, Doug Clark (a graduate student of Alan Gillespie's), and Rick Ryerson (specializing in cosmogenic dating techniques at Lawrence Livermore National Laboratories (LLNL). The Chinese fielded a team of five from the Institute for Remote Sensing Applications (IRSA), including Dr. Guo Huadong (the director) and four other scientists that were interested in paleoclimatology and neotectonics.

Objectives for the field work included: relative dating of fan surfaces, terraces, and moraines; collection of samples for soil descriptions, and for thermoluminescence, cosmogenic nuclide, and carbon dating; mapping and correlation of fan units, terraces, moraines, cirques; measurement of

fault offsets of fans, terraces, and moraines; collection of GCP for stereo SPOT and INSAR data reduction.

Four main sites were targeted: 1) Hotien Faults. Same area as visited by Farr, Evans, Peltzer, Avouac (Avouac and Peltzer, 1993). East of Hotien, between Lop and Qira. Interest was in normal faults and terraces. 2) Yecheng Folds. Along road between Hotien and Yecheng. Main interests were folds in gravel beds, road and stream cuts, and terraces. 3) Karakax Valley in Kun Lun Mountains. Main interests were in glacier moraines, alluvial fans on sides of valley, and terraces in larger side valleys. 4) Aksayqin Basin. Area around Aksayqin Hu and from Karakax Valley road to Lung Mu Co, and to Gozha Co, including up to the large ice cap north of Gozha Co. Main interests were alluvial fans on edges of basin, shorelines around lakes, volcanic deposits, and glaciers coming off the ice cap.

All four of the sites were visited, with most of the field time spent in the Karakax Valley. Sites one and two proved less amenable to remote sensing investigations because of the thickness of loess covering the surfaces. However, interesting observations relative to the folding and faulting of young gravels at the front of the Kun Lun were made, and samples were collected that may allow dating of the deformation. Activities in the Karakax Valley centered on mapping of moraines to constrain the glacial history and detailed mapping and sampling of several alluvial fans. Salt weathering is a much more important process in this area than was realized, however, sampling strategies to minimize its impact on the dating of the fans and moraines were devised in the field. The visit to the Aksayqin Basin, at over 5000 m, was in a reconnaissance mode, to gather information on the moraines and shorelines for potential future study. The glacial history appears to be consistent with that for the Karakax Valley. The shorelines were spectacular, and it is probable that with some good DEMs from SIR-C and ERS-1 a study of the lake history of the area would yield useful results. One of the Chinese scientists along on the trip may be interested in pursuing this topic.

Approximately 250 kg of samples were collected and shipped back to the U.S. for analysis of soil formation processes and for dating of the surfaces using thermoluminescence and the relatively new technique of cosmogenic nuclide measurement. The latter technique makes use of the fact that various isotopes (e.g., Be10, Al26, He3, Cl36) build up in the surface layers of rocks exposed to cosmic rays. The production rates for these nuclides are relatively well known, so the amount of a given nuclide can be used to calculate the duration of exposure. The technique has been used for several years, and has proved to be fairly reliable, if geologic conditions are adequately accounted for.

In addition to my main investigation, I have supported two Associate Investigators: Dr. Guo Huadong's investigation of the use of radar remote sensing at several test sites in China, and the archaeological investigations of China's Silk Road by How-Man Wong and Derrold Holcomb. My major activities with Dr. Guo have been to advise on coverage and parameter options for his sites. For the Silk Road investigations, I have helped plan coverage, ordered processed scenes, and analyzed the data.

SIGNIFICANT RESULTS

Using the remote sensing data, it was predicted that the processes acting in the Karakax Valley were different from those in the SW U.S. Specifically, it appeared that loess deposition was the dominant process, making the area more similar to central Nevada than to Death Valley. The field work just completed added to this interpretation, finding that salt weathering was also important, preventing the formation of thick coatings of desert varnish.

Another result of the field work will be at least three press releases: On the faulting and folding in the Tarim Basin, the glaciers of the Aksayqin Basin, and remote sensing of the oases along the Silk Road.

FUTURE PLANS

The major emphases for the next two years will be on 1) determination of remote sensing signatures of surfaces, 2) sample analyses for dating the surfaces, and 3) topographic analyses of faults and fans. Most of the radar data are already in hand; few additional SIR-C or X-SAR scenes will likely be requested. Additional images from other sensors are needed, however. Additional SPOT scenes are needed, for their high resolution, to help in mapping some of the landforms, and Landsat TM data are needed to add the multispectral, visible near-infrared channels which are sensitive to soil formation and desert varnish development. These additional data sets will allow mapping and correlation of fan units over the entire valley as well as better, more quantitative comparisons with the SW U.S.

Sample analyses will require significant funding over the next fiscal year. A cooperative arrangement has been reached between Alan Gillespie at the University of Washington (UW), Rick Ryerson at Lawrence Livermore National Laboratories (LLNL), and myself for sharing the costs of cosmogenic dating of the samples. If the dating works as we hope, significant progress will be made in understanding the glacial chronology and landscape evolution in this part of the world. This will feed into ongoing studies of lakes, glaciers, ice caps, rivers, and oases being pursued by a variety of researchers. Successful dating of these surfaces will prove a major breakthrough.

As with the remote sensing part of the investigations, topographic analyses require little additional data. The PI has an ongoing (unfunded) ERS-1/2 investigation which will provide any needed interferometric SAR data. One SIR-C interferometric swath over the area has already been processed, as has a single ERS-1 pair. These data will be used with models of alluvial fan formation to help constrain the uplift and offset histories of the fans in the Karakax Valley. This will also provide a way to compare quantitatively fans in NW China with the SW U.S.

Further in the future, two new areas of study may develop: Monitoring the evolution of oases, and Determination of paleolake shoreline elevations. Field observations indicate that the oases of the southern Taklamakan Desert enjoy a marginal existence. Extreme vigilance is necessary to protect the oases from erosion by desertification and moving dunes. The past history of the Silk Road is further proof that the area is susceptible to climatic shifts. Radar and other remote sensing techniques may be used to monitor the health of the oases and to search for changes in the land brought about by climate changes. This will be explored using historical remote sensing data sets. A graduate student at Caltech is currently interested in this project.

As discussed earlier, the new DEMs produced by interferometric SAR provide data that may be used to map accurately shoreline levels from past lakes in western Tibet. Accurate maps may be used to deduce climate changes through water-balance models, and to observe tectonic tilts, if present. Scientists at IRSA are interested in this project, which could be combined with results from recent French expeditions to the area.

Finally, as this project winds down, an effort will be made to archive all the remote sensing, field, and laboratory results onto one or more recordable CD-ROMs so that future researchers will be able to reconstruct these important data sets.

PUBLICATIONS

Farr, T. G., O. A. Chadwick, 1995, "Geomorphic processes and remote sensing signatures of alluvial fans in the Kun Lun Mountains, China," in preparation for the special *J. Geophys. Res.*, SIR-C/X-SAR issue.

Farr, T. G., 1995, Remote mapping of alluvial fan surfaces in western China, *Geol. Soc. Amer.*, Abs. with Program.

Farr, T. G., 1995, Mapping alluvial fan surfaces in western China with SIR-C/X-SAR, *Abs., Progress in Electromagnetic Research Symposium, Seattle.*

Fielding, E. J., C. L. Werner, T. G. Farr, G. F. Peltzer, 1995, High-resolution DEMs of the Altyn Tagh fault in the Kunlun of Tibet by interferometric processing of SIR-C and ERS-1 SAR, *Abs., Geol. Soc. Amer.,* New Orleans.

Logan, P., 1994, Synthetic aperture radar applied to China's ancient Silk Road, *Abs., UN/China/ESA Workshop on Microwave Remote Sensing Applications,* Beijing.

Farr, T. G., 1994, Use of radar and other remote sensing data for mapping alluvial fan surfaces in western China, *Geol. Soc. Amer., Abs.* with Program.

Avouac, J. P., G. Peltzer, 1993, Active tectonics in southern Xinjiang, China: Analysis of terrace riser and normal fault scarp degradation along the Hotan-Qira fault system, *J. Geophys. Res.*, v. 98, p. 21,773-21,807.

Holcomb, D. W., 1992, Shuttle Imaging Radar and archaeological survey in China's Taklamakan Desert, *J. Field Archaeology,* v. 19, p. 129-138.

Dr. Pierre Flament
Hawaii Institute of Geophysics
University of Hawaii at Manoa
1000 Pope Road
Honolulu, HI 96822

Co-Investigators:
Hans C. Graber Woods Hole Oceanog. Inst.
D. Halpern JPL/Caltech
B. Holt JPL/Caltech

Reconstruction of the Mesoscale Velocity Shear Seaward of Coastal Upwelling Regions from the Refraction of the Surface Wave Field

OBJECTIVES

The objective of this project is to study fronts that develop at the boundary between cold water recently upwelled to the surface through Ekman divergence, and warmer surrounding waters. This specific objective was suggested by studying the small scale structure of upwelling fronts (coastal, island, and equatorial) through shipboard surveys and infrared satellite images.

Constraints on the shuttle equator crossing imposed by other land sites precluded a coverage of the area targeted in the initial SIR-C proposal, the California Current. The site was then relocated to the Equatorial Pacific upwelling tongue, that can be satisfactorily imaged for a wide range of longitudes of the equator crossing.

Some limited data was nevertheless obtained over coastal upwelling off California in 1989, using the JPL AIRSAR in multifrequency mode, and over island upwelling off Hawaii in 1990, using the radar in along-track interferometric mode.

Aircraft Work

Coastal Upwelling

In summertime, the California Current is characterized by intense jets carrying cold water from near shore upwelling towards offshore; they appear as cold filaments in satellite infrared images of sea surface temperature. These jets are delimited by sharp thermal and velocity fronts, which are often convergent, and are subject to small-scale instabilities.

In previous shipboard surveys, clusters of surface drifters were deployed to measure the horizontal velocity gradient across these filaments. In the anticyclonic region, the flow was generally nondivergent with a shear of -0.3 f, but at the cyclonic front, the flow was discontinuous at the 1 km resolution of the clusters, with a shear larger than 4.5 f, associated with a cross-frontal surface convergence larger than 0.7 f, visible as a ~20 m-wide accumulation of debris of seaweed, and sometime variations of surface roughness.

A complete SAR survey of the filament rooted near Point Arena (northern California) was acquired on 8 September 1989, using infrared images from the NOAA satellites to guide the aircraft to features of interest. The radar was illuminating the ocean at C-, L- and P-bands, and was operated in polarimetric mode, including horizontal, vertical, and cross-polarization at each wavelength.

At all frequencies, the signatures of the thermal fronts appeared as bright delineations in the radar images, presumably made visible where waves were undergoing refraction by the current shear, resulting in increased amplitude. Several dark delineations, often parallel to the front, were also observed, possibly corresponding to internal waves radiating away from the front, made visible by biological films concentrated along convergence zones, thus reducing the amplitude of Bragg-scattering waves.

Island Upwelling

The Hawaiian Islands present obstacles to the northeasterly trade winds, creating calm regions in the lee. Sharp horizontal shear lines usually separate the 10-15 m/s trades from the calm regions. These shear lines extend several island radii downwind.

The variations of wind stress along the cyclonic shear line to the northwest of the Island of Hawaii, and the response of the ocean, were studied in August 1990 including along-track interferometry in the L-band. Concurrent data were obtained from a ship using a towed undulating CTD (SeaSoar), an acoustic Doppler current profiler and satellite-tracked drifting buoys, and from the NCAR Electra meteorological aircraft conducting boundary layer flights. Infrared images from the NOAA satellites, and 10-m resolution sun glint images from the SPOT satellite were also available.

Backscatter intensities in the L- and C-band were strongly modulated by the variations of surface wind stress, and showed that the cyclonic shear line was just a few tens-of-meters wide, much narrower than the ~2 km height of the planetary boundary layer. There was a strong gradient coinciding with the shear line in the along-track phase image, suggesting downwind surface flow in the trade wind regime, and a slight flow towards shore in the calm lee; however this phase variation did not correspond to detectable surface current variations in the acoustic Doppler current meter data. The correlation image showed high correlation in the lee, and much smaller correlation in the trade wind regime, where white capping was frequent.

Two effects of these wind stress variations on the upper ocean were observed during the ship survey. One-dimensionally, the mixed-layer depth was modulated by the wind stress: outside the calm region, a deep mixed layer was observed, whereas in the calm region, the mechanical energy provided by the wind was not sufficient to erode the 2-4 m warm buoyant layer resulting from solar heating. Intense diurnal warming was observed at the surface and a thermal front coincided with the shear line observed in the SAR images. Two-dimensionally, the curl of the wind stress along the cyclonic shear line induced upward Ekman pumping, spinning up a strong cyclonic eddy.

Shuttle Radar work

The surface front separating cold equatorial water from warmer tropical water at 2-7N in the Central Pacific was studied twice for one week in April and October 1994 between 115W and 155W by the shuttle synthetic aperture radar imaging in L-, C- and X-bands, with supporting NOAA satellites infrared images.

During the October flight (the peak of the equatorial upwelling season), zonal linear features of enhanced backscatter intensity were observed at all wavelengths, and corresponded closely to the thermal front seen in the infrared images. On some data takes, several linear features were found at different latitudes, suggesting that the front may not have been unique. The motion of the front estimated from successive daily images was consistent with the westward propagation found by previous studies. In contrast, no fronts were observed in the images taken during the April flight, which were dominated by the surface signature of rain cells.

The front was also visible as brightness changes in AVHRR images of the sun glint, and photographs of the glint taken from the Space Shuttle show the equatorial front as a quasi-linear feature, often darker than surrounding water.

These observations are consistent with *in situ* fR data collected during the Tropical Instability Wave Experiment in 1992 and 1995, which indicated that the temperature front was 1.2 deg C over 1 km or less, and was confined to the ~100-m-thick mixed layer. Fine-structure was observed,

suggesting northward subduction of cold, high salinity equatorial water, beneath warmer less saline ITCZ water. A 40 km drifter array deployed on the cold side of the front became aligned with the front in less than three days. The velocity averaged over five frontal crossings showed a 10 km-wide westward jet of 90 cm/s and a cross-frontal convergence of 15 cm/s, both confined above the thermocline.

During these cruises, white capping was frequently enhanced over a band ~100 m wide near the front, presumably due to surface wave refraction by the velocity gradient. Presumably, the linear features observed in the SAR images correspond to these bands of enhanced wave breaking.

PROGRESS

Preliminary results on both the AIRSAR and SIR-C/X-SAR work have been presented at IGARSS-95. Seminars have been given at NATO/SACLANT in June 1995, at DLR in July 1995, and at WHOI in February 1990.

We are now at the phase of completing the data requests:

- 95% of the 1989 AIRSAR data have been delivered
- 20% of the 1990 AIRSAR data have been delivered (this has been delayed by R. Carande's departure)
- approximately 75% of the X-SAR data and 45% of the SIR-C data have been received.

All ancillary in-situ data have been processed. AVHRR data for the Shuttle Radar missions will be processed during Fall 1995.

Final scientific analysis and preparation of publications will take place in 1996 - 1997. We anticipate four or five refereed publications to result from this work:

- "A Synthetic Aperture Radar survey of an upwelling filament," to be submitted to the *Journal of Geophysical Research* in Spring 1996 by Flament, Holt and Bernstein);

- "Along-track interferometric radar mapping of an Ekman divergence line," to be submitted to the *Journal of Geophysical Research* (pending delivery of the data by JPL) by Flament, Sawyer, and Carande.

- "SIR-C / X-SAR views the Equatorial Front," short report to be submitted to *Science*, by Flament, Runge, Sawyer and Holt in Winter 1996.

- "Synthetic Aperture Radar mapping of the Pacific subequatorial convergence," by Flament, Sawyer, Holt, to be submitted to *Journal of Geophysical Research* in Winter 1997.

- "Multifrequency SAR imaging of rain cells and associated surface processes in the Intertropical Convergence Zone," (tentative).

Dr. Anthony Freeman
Mail Stop 300-235
JPL/Caltech
4800 Oak Grove Drive
Pasadena, CA 91109

Co-Investigators:
K. Sarabandi U. of Michigan

Multifrequency, Multipolarization External Calibration of the SIR-C/X-SAR Radars

OBJECTIVES

Assess the accuracy at which the SIR-C/X-SAR standard data products can be calibrated through the use of ground calibrators to estimate the end-to-end system polarization calibration constants (or distortion parameters) and incorporate the constants into the data processing.

Study the cross-calibration between three multipolarization systems: SIR-C, the National Aeronautics and Space Administration/Jet Propulsion Laboratory (NASA/JPL) DC-8 SAR, and the University of Michigan ground-based polarimetric scatterometer.

Evaluate the calibration "stability" of SIR-C/X-SAR (measured by variations in the calibration constants) over the range swath width and over a specified distance in azimuth. Variations over a 12-hour period (between ascending and descending passes) will also be studied.

Develop a cost-effective calibration plan including development of inexpensive polarimetric active calibrators.

PROGRESS

JPL - during the two SIR-C missions, ground calibration equipment was deployed at the Death Valley supersite. Equipment included over 30 corner reflectors, six transponders and ground-based receivers. The transponders included two single antenna polarimetric active radar calibrator (SAPARC) devices developed by our co-investigator team at the U. of Michigan. The Principal Investigator's (PI's) team also participated in deployment of corner reflectors at the Manaus, Brazil supersite. In a collaborative effort with a team from the Institute of Navigation of the University of Stuttgart, high-precision transponders and ground receivers, similar to those at the DLR Oberpfaffenhofen test site, were deployed at the Chickasha, Oklahoma supersite. Corner reflectors and instructions/guidelines for their deployment were also distributed to PI's at several other supersites.

During the SIR-C missions, information on the location and configuration of the calibration devices deployed at participating supersites was relayed by PI's back to JPL. These data were used to 'manually' calibrate SIR-C data products during the actual missions. Calibrated SIR-C data were then passed on to the "real-time" science team, to be processed into geophysical products such as soil moisture, biomass and land cover maps.

Thus far, over 50 SIR-C scenes have been processed and analyzed which contain corner reflectors or other calibration devices, or which represent suitably uniform scenes to verify the SIR-C antenna patterns.

Working in collaboration with B. van den Broek of FEL-TNO of the Netherlands, an algorithm which fits a simple set of scattering models to SIR-C data has been applied to data from the Flevoland supersite and the Manaus supersite. The results of the model fit have been used as the

basis of an unsupervised classifier which divides SIR-C data up into several different land use categories.

The University of Michigan team were involved in a calibration campaign in the Raco Calibration Supersite. In each calibration campaign an array of point calibration targets including trihedral corner reflectors and polarimetric active radar calibrators (PARCs) were deployed. For this project two types of calibration targets for imaging radars were invented: (1) single antenna polarimetric active radar calibrator (SAPARC), and (2) self-illuminating optimum corner reflector. In addition to the deployment of point calibration targets, polarimetric backscatter measurements of distributed targets were collected using L-, C-, and X-band polarimetric, truck-mounted, scatterometer systems during the SIR-C flights. The scatterometers were calibrated against a precision metallic sphere and measured 100 independent spatial samples for characterizing the differential Mueller matrix of distributed targets to achieve the desired calibration accuracy. The measured Mueller matrices of the distributed targets are intended to be compared with those derived from SIR-C images. Two different calibration methods, one based on the application of point targets and the other based on the application of the distributed targets, are considered for calibration of the SIR-C data. So far, some encouraging preliminary results for two C-band images of the first mission have been obtained.

FUTURE PLANS

Summary and research plans for the next two years, including anticipated new data requests and new publications.

JPL - Radiometric calibration results and uncertainties for SIR-C data so far have been assessed from corner reflector signatures, which have inherent uncertainties of their own. We intend to revise our estimates of the SIR-C radiometric calibration performance by examining signatures of transponders and tropical rain forest areas, which should have smaller variations. The results will be published as a communication in a refereed journal.

A study has begun in collaboration with Dr. Francesco Holecz of the University of Zurich (currently seconded to JPL) to study the radiometric calibration errors in SIR-C data over areas with significant relief. The study involves registration of SIR-C data with a high-resolution DEM, correction for the 'true' incidence angle and elevation angle, and the comparison of fully corrected backscatter values with the original SIR-C data. It is also intended to study the radiometric errors caused by using a lower-resolution DEM to correct the data. The results of this aspect of the study will have implications for SRL-3 data, should that mission be manifested. The results of our collaboration with Dr. Holecz will be published in a refereed journal paper or papers.

In collaboration with Dr. van den Broek, we will continue to develop the model-fitting approach to understanding polarimetric SAR data from SIR-C and AIRSAR. We intend to pursue an avenue of adaptive model-fitting, in which for example, areas which are clearly dominated by surface scatter will be subjected to higher-order surface scatter models, areas which are clearly forested will be subjected to higher-order forest scatter models, and so on. This will probably involve a two-layer approach, in which the L- and C-band SIR-C data is used in an initial classification, followed by a higher-order model fit to give better estimates of surface properties. This will then be applied to SIR-C data from several different sites around the world. The result will be a generalized model-fit/simple classification software package and a refereed journal paper describing the approach, which should be applicable to any L- and C-band SIR-C data set.

The University of Michigan team will process the backscatter data collected with the truck-mounted scatterometer and compare with measurements extracted from calibrated SIR-C and X-SAR products. All the SIR-C and X-SAR data available over the Raco supersite will be orthorectified

using a modified version of a software package developed by Vexcel Corporation. This will make exact identification of the sites measured by the scatterometer much simpler, and lead to improved comparison data. The University of Michigan team will also study the effects of applying different calibration algorithms to the SIR-C data. The output of this analysis will be used to refine our estimates of calibration uncertainties in SIR-C/X-SAR data. The University of Michigan team will also construct and test a prototype of a "next-generation" corner reflector they have designed. The results of the University of Michigan team's investigations will be published as a series of refereed journal papers.

PUBLICATIONS

Freeman, A., Cruz, J., Alves, M., Chapman, B., S. Shaffer and Turner, E., SIR-C Data Quality and Calibration Results, *IEEE Trans. Geosci. Remote Sensing,* vol. 33, no. 4, July 1995.

Sarabandi, K., L. Pierce, M. C. Dobson, F. T. Ulaby, J. Stiles, T. C., Chiu, R. De Roo, R. Hartikka, A. Zambetti, and A. Freeman, Polarimetric calibration of SIR-C using point and distributed targets, *IEEE Trans. Geosci. Remote Sensing*, vol. 33, no. 4, July 1995.

Sarabandi, K., and T. C. Chiu, An optimum corner reflector for calibration of imaging radars, *IEEE Trans. Antennas Propagation,* submitted for publication (Feb. 1995).

Freeman, A. and Durden, S., Fitting simple scattering models to polarimetric SAR data, in preparation.

Freeman, A., Cruz, J., Chapman, B., Alves, M., Turner, E. and Shaffer, S., Calibration of SIR-C data products, *Proc. IGARSS '95*, Florence, Italy, pp. 1585-1587, July 1995.

Holecz, F., Freeman, A. and van Zyl, J. J., Topographic effects on the antenna gain pattern correction, *Proc. IGARSS '95*, Florence, Italy, pp. 587-589, July 1995.

Freeman, A. and van den Broek, B., Mapping vegetation types using SIR-C data, *Proc. IGARSS '95*, Florence, Italy, pp. 921-923, July 1995.

van den Broek, B., Davidson, M. and Freeman, A., Vegetation and soil characteristics in SIR-C data, *Proc. IGARSS '95*, Florence, Italy, pp. 1064-1066, July 1995.

Daida, J., Freeman, A. and Onstott, B., Evaluation of a hybrid symbiotic system on segmenting SAR imagery, *Proc. IGARSS '95*, Florence, Italy, pp. 1415-1417, July 1995.

Freeman, A., Cruz, J., Alves, M., Chapman, B., S. Shaffer and Turner, E., SIR-C Calibration Results, in *Proc. IGARSS '94,* Pasadena, California, August 1994.

Dr. Alan R. Gillespie
Dept. of Geological Sciences AJ20
University of Washington
Seattle, WA 98195

Co-Investigators:
John B. Adams — Univ. of Washington
Milton O. Smith — Univ. of Washington
Robin Weeks — Univ. of Washington

Alluvial Fan Evolution in the Western Great Basin

OBJECTIVES

Describe systematic morphologic changes with surface age in terms of multiparameter radar backscatter for dated chronosequences on alluvial fans at one or two sites in the Western Great Basin. Compare these changes to chemical weathering patterns observed for the same fans using visible/near-infrared (VNIR) and thermal infrared (TIR) images.

Construct a depositional and weathering history for the studied alluvial fans based on SAR, other images, and field investigations; use this to constrain paleoclimatic interpretations for the Great Basin. Use project as prototype for paleoclimate study of entire Great Basin or other geomorphic provinces, where multiparameter SAR data can be acquired regionally.

Test the application of spectral mixing analysis on multiparameter SAR images of alluvial fans in arid and semiarid regions. Define radar endmembers (from the spectral mixing analysis) physically, in terms of Bragg scattering, volume scattering, specular and corner reflectors, dielectric constant, etc. Develop and test mixing models for comparative analysis of images spanning multiple spectral regions.

PROGRESS

Summary of Activities Since February 1995

Organized field trip and field workshop in Death Valley, California. This was attended by members of various science teams.

Made combined measurements of roughness, close-up VNIR multispectral images, and field spectrometer data in Death Valley, designed to test joint SAR/VNIR analysis of roughness.

Fifty low altitude (1:1000 scale) aerial photographs obtained over alluvial fans in the Stovepipe Wells area of Death Valley.

Roughness estimates obtained at two spatial scales using stereo photography: The subcentimeter to meter scale, and the 10's cm to 10's meters scale. Available roughness spectra now span four orders of magnitude in length scale at ten sites in Death Valley.

Developed and installed software designed to simulate natural rough surfaces and to calculate the radar backscatter from them. The solutions use complete solutions of Maxwell's equations. This software complements our currently available radiosity models which calculate VNIR reflectance for the same rough surfaces, including the effects of multiple scattering interactions.

Collected samples from alluvial fan surfaces of various ages in Death Valley. In conjunction with LLNL we will be dating the ages of the surfaces.

Currently participating in field work in China with SIR-C PI Tom Farr, where similar sample collections for dating will be made.

Requested and obtained numerous SIR-C scenes over Death Valley, one over Owens Valley, two over the Amazon Basin, and one over Hawaii. Requested and obtained a number of AIRSAR images from Death Valley and Owens Valley.

Exchanged roughness/dielectric models, results, and information with Pascale Dubois at JPL, and J.C. Shi at UC Santa Barbara.

Presentation made at Spring AGU in Baltimore.

Negotiations with Bruce Jakosky on submission of three papers to SIR-C special of JGR planets, including visit of Bruce Jakosky to our laboratory.

Two manuscripts are in preparation for JGR Planets special issue. Deadline for submission, October 1995.

We will be presenting invited talks at the IEEE conference in Toulouse, France on "Retrieval of bio- and geophysical parameters from SAR data for land applications". We have also been invited to present a talk at the AIRSAR workshop at the University of New South Wales, Australia in November 1995.

Requested and obtained day/night flights of the C130 aircraft to collect TIMS, NS-001 data and color IR photography over Death Valley and Owens Valley.

We have made considerable progress towards our goal of using SAR images to recover roughness and moisture information for desert chronosequences. We have begun to understand what parameters of surface roughness description are important in controlling radar backscatter, and hence how we might expect to be able to invert SAR data for roughness information. Admittedly, some of our progress has consisted of discovering and documenting unanticipated, but inherent complexities. We have, however, shown that joint analysis of VNIR and SAR images is feasible and improves quantitative roughness recovery. We have explored the possibility of ground water correction using g-ray data and we have explored the use of apparent thermal inertia to correct desert scenes for dielectric changes other than those due to soil moisture. We have collected a large quantity of field data in Death Valley, Owens Valley, Hawaii, China and Australia for the purposes of documenting roughness, dielectric, spectral characteristics, and age of surfaces.

SIGNIFICANT RESULTS

Since February, we have advanced our efforts to evaluate the techniques of determination of surface roughness from SAR data and VNIR data. Our interest is in the joint use of data types as well as their separate use. In addition, within the last month, day/night pair TIMS data, as well as NS-001, have been taken over Death Valley and Owens Valley at our request (C130 flights). We will be examining the joint use of TIMS and SAR in determination of the ground dielectric constant by taking advantage of a physical relationship between thermal inertia and dielectric constant. The availability of these data mean that we will be able to bring three independent data types to bear on the problem of remote determination of roughness and dielectric constant. We are particularly interested in the use of FIR filters, a generalization of the linear mixing approach, for analysis of these combinations and types of data. Our field measurements (Figure 1) and the semi-empirical models of Dubois et al., and J. C. Shi, will be used to test our approach and we will also be evaluating the success of these models. In the Winter of 94/95 we commissioned low altitude stereo aerial photographs to be taken over Death Valley alluvial fans at a scale of 1:1000 (Figure 1).

We now have roughness results from these photographs which overlap in spatial scale with roughness determinations made on the ground using close-up stereo photography (Figure 2). Data delineating roughness on the alluvial fans, and covering four orders of magnitude of spatial scale, now exist for ten sites in the Stovepipe Wells area (Figures 1 & 2). These measurements are to be used in evaluating the success of inversions of SAR, VNIR and TIMS data for dielectric and roughness. Close-up stereo photographs have also been obtained at eight sites in the Owens Valley and twenty sites on the flanks of Kilauea Volcano on the Island of Hawaii. Roughness determinations will soon be available from these sites.

Collections of rock samples have been made for dating purposes at sites in Death Valley: - we propose to date the exposure of fan surfaces using cosmogenic Be10 techniques (Bierman et al., in press) and are doing this in conjunction with LLNL. The purpose of these measurements is to establish the connection between surface age and roughness on alluvial fans and thus to facilitate the use of SAR data to map relative age of alluvial fans on a regional scale. We are currently participating in field work in China with Tom Farr and will again be processing samples for the dating of fan surfaces in the Kunlun area for which SIR-C data has been obtained.

In order to provide a theoretical/modeling basis for the individual and joint use of different types of data we have started running backscatter simulations on our Dec alpha computers. Rough surfaces with the characteristics of field measured surfaces are simulated and the backscatter calculated using a complete solution of Maxwell's equations (Figure 3a). We now also have the ability to calculate the VNIR reflectance of these same surfaces using a radiosity model to take into account multiple scattering interactions (Figure 3b). The radiosity model is also used to simulate IR emission. We can thus examine the response of surfaces of varying roughness at VNIR, IR, and radar wavelengths, and under differing illumination and viewing geometry's. Our preliminary backscatter simulations have shown that the parameters of surface power spectrum (slope and offset) are inadequate and that the phase information contained in the Fourier Transform is perhaps more important (Figure 3a). This means that inversions of SAR data for slope and offset of surface power spectra are highly nonunique unless a third parameter, describing the degree of correlation of the phase of the surface, is introduced. This phase component really defines the shapes of elements of the surface (for example, the cobbles on alluvial fans in Death Valley) and these elements are the scattering elements of the surface. What might be required is that an initial assumption, based on field knowledge, defines the type of surface (shape/phase characteristic) after which a relation between slope and offset for that type of surface can be used.

FUTURE PLANS

We will be extending the efforts described above. This will involve further development of the integration and joint analysis of SAR, VNIR, and IR data to determine roughness parameters and dielectric constant. With regard to radar backscatter and surface roughness we will examine the response of radar to important aspects of real surfaces that have hither to been ignored. We will examine the ability to invert SAR data for these and other parameters. We will expand our simulation and modeling effort to include 2-D (surface) backscatter calculations to be made on a super computer in Hawaii. We will be working with SIR-C, AIRSAR, TIMS, NS-001, and Landsat TM data in various settings in Death Valley, Owens Valley, Hawaii, Australia and China. These regions will be used to test the applications we develop. We will determine age dates on many geologic surfaces of interest in Death Valley, Owens Valley, and China and hence better determine the relationship between age and backscatter in these regions. We anticipate a minimum of three publications and three abstracts per year for the next two years.

PUBLICATIONS

Since the February science team meeting we have presented a poster at the Spring AGU meeting in Baltimore. In addition, we have been invited to give presentations at the IEEE meeting in Toulouse (October) and the AIRSAR workshop in Sydney, Australia in November 1995. An additional, related abstract on roughness and VNIR reflectance will be given at the ERIM conference in Las Vegas in February.
We have been in close correspondence with Bruce Jakosky (editor of JGR Planets) on the organization and timetable for the SIR-C special issue in JGR Planets. Preliminary titles for submission to that special issue are:

(a) "Simulations of radar and VNIR scattering from rough surfaces: A basis for joint analysis".
(b) "The use of adaptive filters in the joint analysis of SAR and VNIR data for retrieval of geophysical parameters".

A later paper, to be submitted this year will be on the application of adaptive filters to roughness determinations on alluvial fans in the Western USA and China and the dating of chronosequences. This paper would be submitted to the proposed SIR-C special issue of Remote Sensing of the Environment.

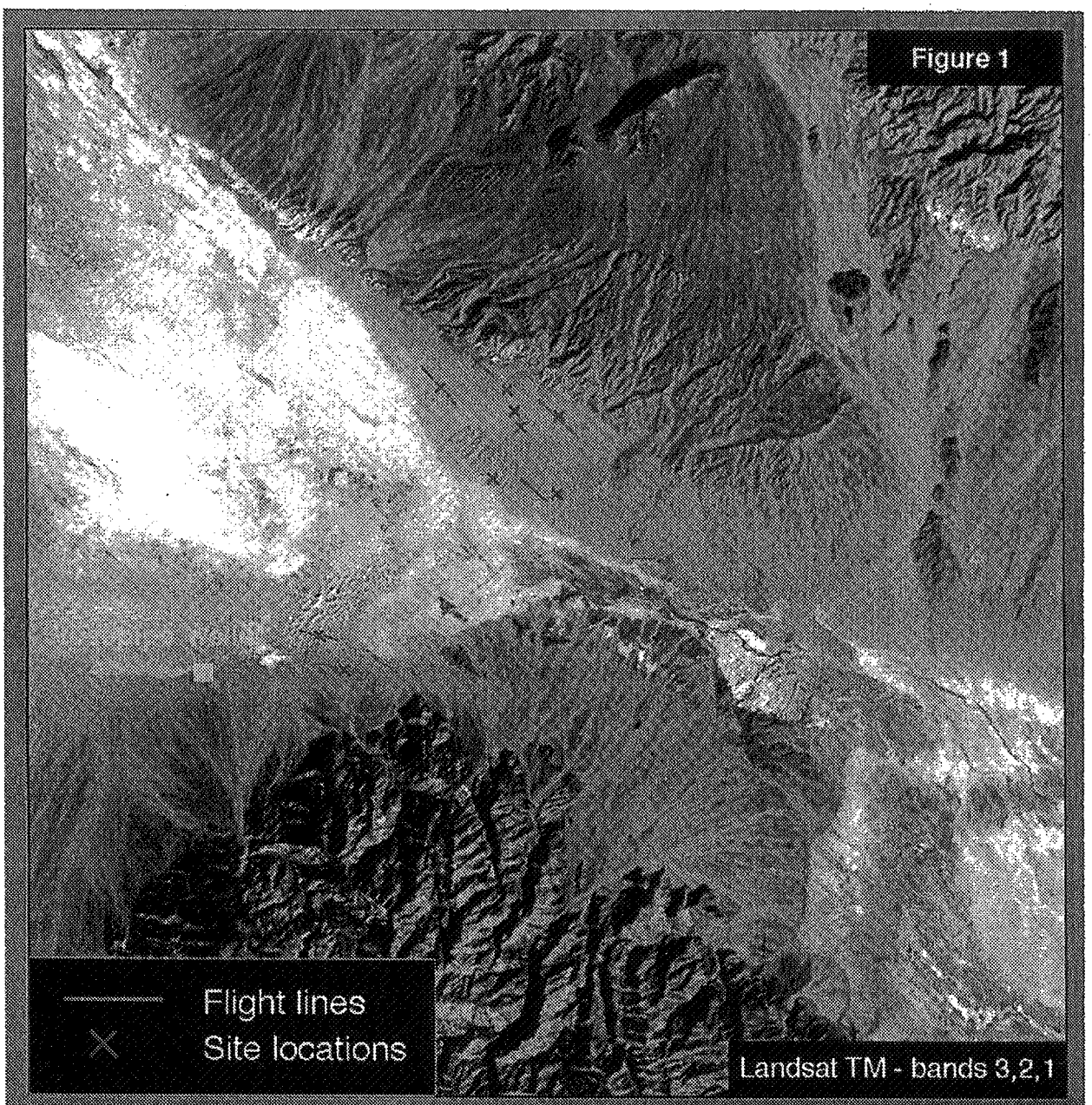

Site locations in the Stovepipe Wells area. Measurements at each site have included roughness measurements using close-up stereo photography, roughness measurements using a pin-profiler, low altitude (1000') stereo aerial photograghy for roughness, spectral measurements including variable filter CCD camera photography, and soil moisture samples. There are additional sites on Trail Canyon Fan to the south.

Figure 2

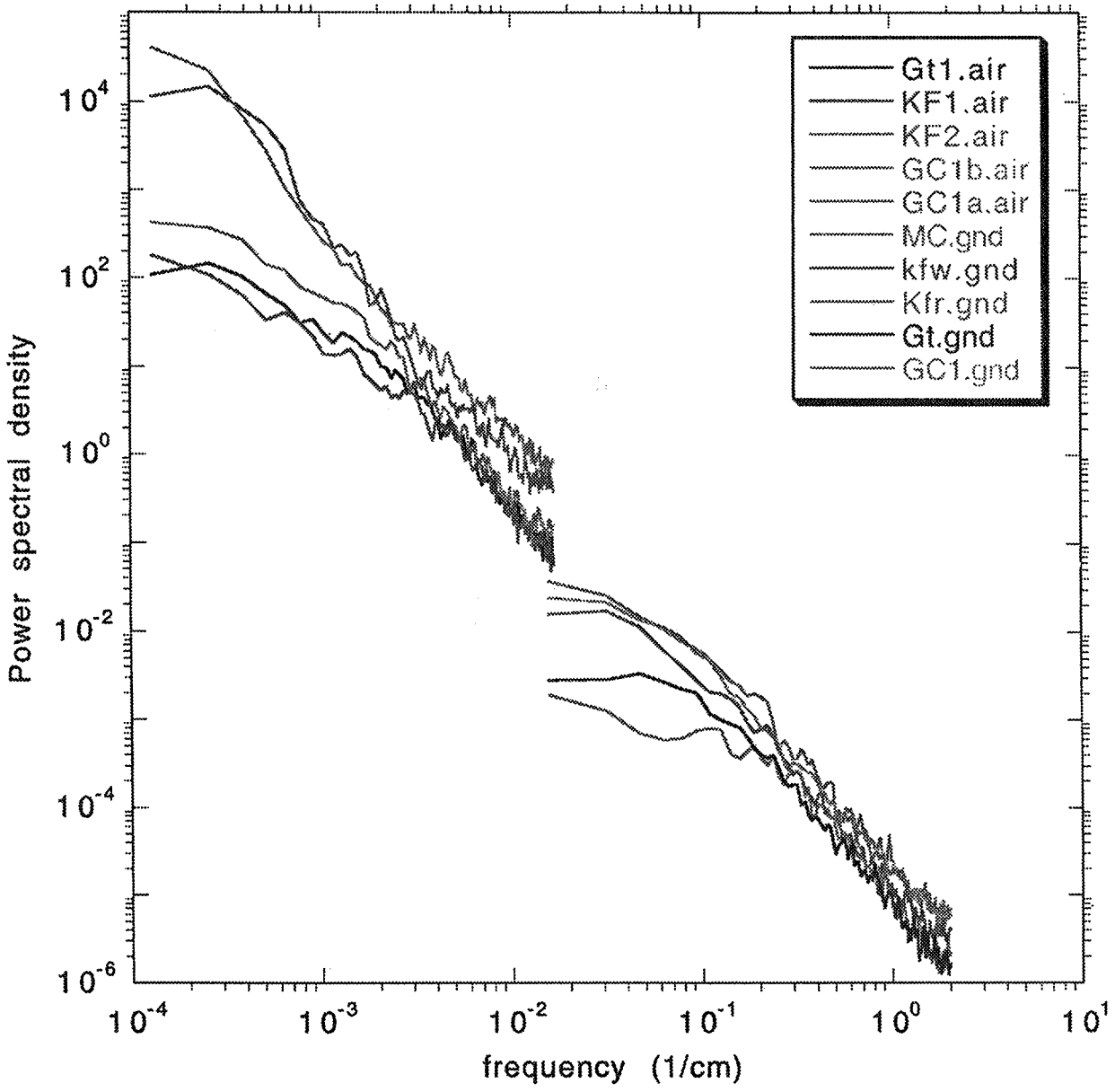

Power spectra of surface roughness in Death Valley. Spectra are taken from height profiles made from stereo photographs. Those spectra labelled '.air' are taken from aerial photographs while those labelled '.gnd' are taken from close-up ground photographs.

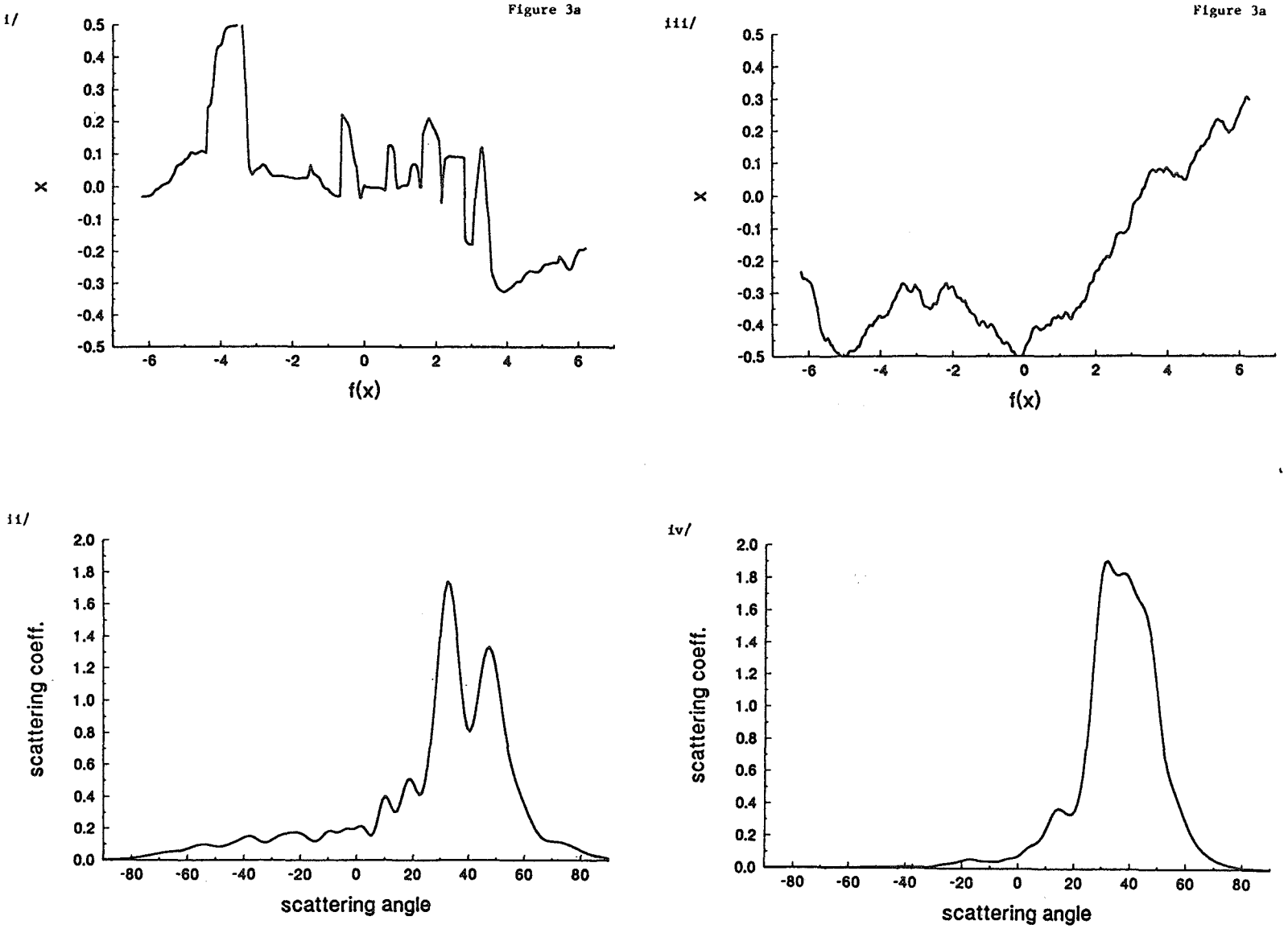

1D backscatter simulations showing the scattering coefficient with scattering angle for an angle of incidence of 40°. i/ Example of a real topographic profile taken from the Kit Fox fans in Death Valley. ii/ Backscatter calculated for the topographic data from the Kit Fox fans (24 profiles). iii/ Example of a profile simulated using the slope and offset of the power spectra obtained from i. iv/ Backscatter calculated for the simulated profiles. In the backscatter direction (-40°) results are very different.

Figure 3b

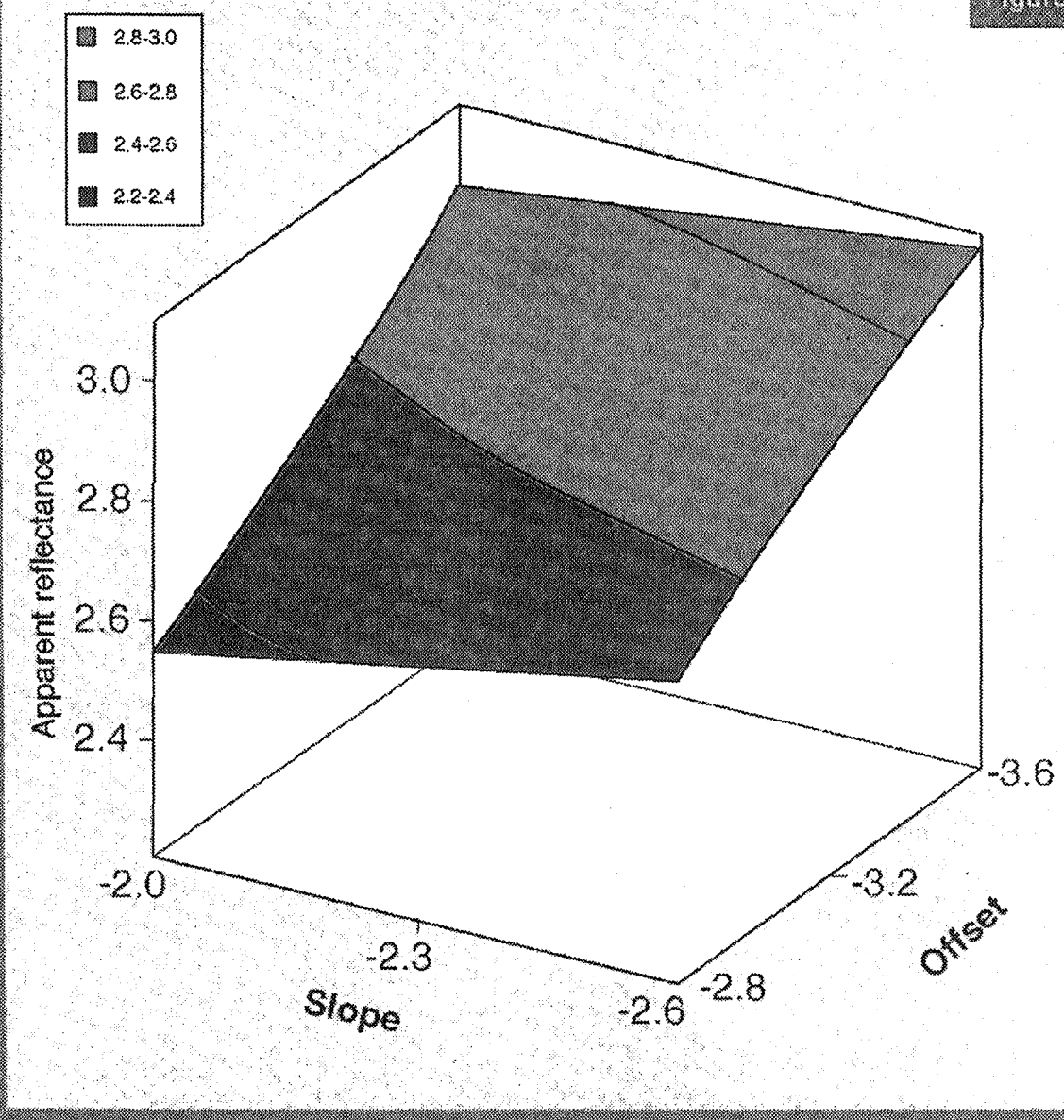

Variation of apparent VNIR reflectance with surface roughness. The x-y axes are slope and offset of the surface power spectrum respectively, and the z axis is in arbitrary units of reflectance. Contour lines are lines of equal reflectance and the color coding in units of reflectance.

Dr. R. M. Goldstein
Mail Stop 300-227
JPL/Caltech
4800 Oak Grove Drive
Pasadena, CA 91109

Co-Investigators:
A. K. Gabriel JPL/Caltech
Fuk K. Li JPL/Caltech
C. L. Werner JPL/Caltech
Howard A. Zebker JPL/Caltech

Differential Radar Interferometry

OBJECTIVES

Test differential radar interferometry as a new monitoring technique for remote sensing of a forest site, a farm site, and a desert site.

Generate topographic maps of test sites from radar data.

PROGRESS

Fort Irwin Site

We have acquired L- and C-band, single look, complex images of the Fort Irwin area on three successive days of the second SIR-C flight. The repeat-pass navigation was superb, resulting in interferometer baselines with perpendicular components of 66 m and 28 m.

The C-band interferogram enabled us to produce a digital elevation map accurate to better than 8 m rms when compared to a careful survey of the area. Most of this error was caused by turbulent mixing of water vapor in the atmosphere. The presence of the water vapor was revealed by small inconsistencies in the two interferograms, which were afforded by the three SIR-C passes.

The rms, one-way time delay of the atmospheric turbulence was found to be 0.24 cm. Identical results were found from the L-band data set.

A paper describing these results has been accepted for publication in *Geophysical Research Letters.*

Gulf Stream Site

The first and third leaf of the SIR-C C-band antenna were connected to separate receivers in a mode which enabled front-back interferometry. The shortness of the baseline (4 m) notwithstanding, interferograms of the gulf stream area were able to image the stream boundary directly. The boundary is seen as a change in the line-of-sight velocity.

Preliminary results of this effort were presented at the IGARSS '95 meeting. A journal article is in work.

Top of the Orbit Site

Good interferometer fringes have been obtained of the Meade Glacier, along the Canadian-Alaskan border. The fringes contain information on both the glacier motion and its topography. At this time we have been able to separate out the part due to motion and to quantify the line-of-sight component.

We are currently working on the motion-corrected topography.

FUTURE PLANS

We plan to develop our technique of glacier study using three-pass radar interferometry with the Meade Glacier observations and with other data sets along the SIR-C repeat tracks.

We plan to do the same with respect to atmospheric limitations to the accuracy of measuring small displacements and of measuring topography. The Fort Irwin data represent an extreme because of its desert environment. Other areas will give more representative observations, and, perhaps, stronger limitations.

We expect these plans to result in several more journal articles.

Dr. Ronald Greeley
Department of Geology
Arizona State University
Tempe, AZ 85287-1404

Co-Investigators:

Dan Blumberg	Arizona State University
A. Dobrovolskis	NASA Ames Research Center
James Iverson	Iowa State University
Nicholas Lancaster	Desert Research Center, NV
Bruce White	University of California, Davis
Keld Rasmussen	Aarhus University
Haim Tsoar	Ben Gurion University
Stephen Saunders	JPL/Caltech
Jakob van Zyl	JPL/Caltech
Stephen Wall	JPL/Caltech
Howard Zebker	JPL/Caltech

Development of a Technique to Relate Eolian Roughness to Radar Backscatter Using Multiparameter SIR-C Date

OBJECTIVES

To develop a technique to obtain values of aeolian roughness for geologic surfaces from values of surface roughness determined from calibrated L- and C-band, like- and cross-polarized, multiple incidence angle radar data from SIR-C.

To define the optimal combination of radar parameters from which aeolian roughness can be derived.

To gain an understanding of the physical processes behind the empirical relationship.

PROGRESS

Field work in preparation for SRL - two sites in Death Valley were instrumented with micrometeorology masts in preparation for the SRL missions. Field work was also conducted with JPL's calibration team to select appropriate sites for corner reflectors, transceivers, and receivers.

During the first SRL flight, field work was carried out in Death Valley combined with an education outreach program. High school students and teachers from two schools in Arizona assisted with the field work. The field work included measuring surface roughness by means of electronic distance meters, laser profilers, and a surface template.

As part of the second flight, field work was conducted at the Lunar dry lake site in Nye county, Nevada, August 18-20, 1994. A single micrometeorology mast was deployed and field observations conducted.

Following both flights, several impact crater sites modified by wind activity were identified in the survey data set. These include the three pretargeted sites: Zhamanshin (Kazakhstan), Roter Kamm (Namibia), and Wolf Creek (Australia).

Additional sites fortuitously imaged include: Oasis structure, Libya; BP structure, Libya; Auronga, Chad; Amguid, Algeria; Henbury and Spider structures in Australia.

A workshop was held at ASU in March 1995. The three-day workshop included investigators from Iowa State University, Univ. Calif./Davis, JPL, GSFC, Israel, Denmark, and Russia. The first day was dedicated to discussing progress on the analysis of the data covering the impact crater sites. The second day was dedicated to discussion on aeolian processes, and the third day was devoted to planning future work and publications.

FUTURE PLANS

a Extend testing of the correlation between aerodynamic roughness and radar backscatter to new areas including desert sites in the Middle East and vegetated sites in Denmark.

b. Continue experiments in wind tunnels on the role of roughness on the threshold wind speed and flux of particles.

c. Generate an aerodynamic roughness map from SRL data for a specific region and test the regional variation.

d. Explore applications of radar-derived aerodynamic roughness to GCMs and sensible heat flux.

e. Blumberg will be teaching a university class in Radar Remote Sensing at Ben Gurion University of the Negev, Israel. The class will be using SRL data.

Analysis of data

Our research involves photogeology and quantitative analysis of returned signals (backscatter cross sections). Hence, our analysis has included the generation of images in print form for several scenes in Death Valley, Denmark, Israel, and the impact craters named above. We have also conducted quantitative analysis on several of these scenes. This required writing software and modifying code provided by JPL. Future work will require further modification of the code to generate aerodynamic maps, RMS height and dielectric constant maps. Some of this is in progress and we are at the stage of debugging. In the future we will request more scenes of desert sites in the Middle East, Mojave, and Africa.

PUBLICATIONS

Blumberg, D. G. , J. F. McHone, R. Kuzmin, and R. Greeley, "Radar Imaging of Impact Craters by SIR-C/X-SAR," *Lunar and Planetary Science Conference*, XXVI, pp. 139-140.

Blumberg, D. G. and R. Greeley, 1993, "AIRSAR Views of Aeolian Terrain," *Summaries of the Fourth Annual JPL Airborne Geoscience Workshop,* pp. 9-12.

Blumberg, D. G. and R. Greeley, 1993, "Field Studies of Aerodynamic Roughness Length," *Journal of Arid Environments*, vol. 25, pp. 39-48.

Blumberg, D. G. and R. Greeley, 1994, "Spaceborne Radar Laboratory-1; Estimates of Aerodynamic Roughness," Geological Society of America, (in) *Remote Sensing: New Results from SIR-C/X-SAR: Geology from Spaceborne Radar*, Seattle, Washington, pp. A128.

Blumberg, D. G. and R. Greeley, 1995, *"New Observations of Bolivian Wind Streaks by JPL Airborne SAR; Preliminary Results,"* Summaries of the Fifth Anuual JPL Airborne Geoscience

Workshop, JPL Publication 95-1, vol. 3, pp. 1-4, Jet Propulsion Laboratory, Pasadena, CA. January 23-26, 1995.

Blumberg, D. G. and R. Greeley, 1995, "Study of Aeolian Processes from the Spaceborne Radar Laboratory," American Geophysical Union, Baltimore, (invited paper), *EOS*, vol. 76, 17, p. 196.

Blumberg, D. G. and R. Greeley, 1995, "Study of Potential Windblown Processes Using SIR-C/X-SAR: Preliminary Results," *IEEE PIERS 95 - Progress In Electromagnetics Research Symposium*, University of Washington, Seattle WA, (invited paper).

Blumberg, D. G., R. Greeley, N. Lancaster, C. Breed, G. Schaber, and J. McCauley, 1995, "Spaceborne Radar-Imaging of Dune Fields - New Results from the SIR-C/X-SAR Mission," *Association of American Geographers,* Chicago, IL, p. 26.

Greeley R. and D. G. Blumberg, "Preliminary Analysis of Shuttle Radar Laboratory (SRL-1) Data to study Aeolian Features and Processes," *IEEE Transactions on Geoscience and Remote Sensing,* in press.

Greeley, R. , D. G. Blumberg, J. F. McHone, R. Kuzmin, B. Ivanov, J. Garvin, R. Grieve, S. D. Wall, 1995, "SRL-1: Radar Scenes of Impact Craters," American Geophysical Union, Baltimore, *EOS,* Vol. 76, 17, p. 197.

McHone, J. F. , J. R. Underwood, Jr., D. G. Blumberg, R. Greeley, 1995, "Space Shuttle Radar Images of Terrestrial Impact Structures: SIR-C / X-SAR," *Meteoritics '95* (in press).

McHone, J. F., Blumberg, D. G., Greeley, R., Underwood, R., "Orbital Radar Images of Libyan Impact Structures," *Geological Society of America*, 1996 (in press).

Xu, P., D. G. Blumberg, and R. Greeley, 1995, *"Preliminary Study Of Kelso Dunes Using AVIRIS, TM, And AIRSAR,"* Summaries of the Fifth Anuual JPL Airborne Geoscience Workshop, JPL Publication 95-1, vol. 1, pp. 159-161.

Publications in preparation include three *Jour. Geophys. Res.* papers (an aeolian paper, an impact crater paper, and a planetary analog paper). Two papers will probably be submitted to the centennial meeting of the *Egyptian Geologic Survey.*

Prof. Guo Huadong
Institute of Remote Sensing
Applications (IRSA) Chinese
Academy of Sciences (CAS)
P.O.Box 9718
Beijing 100101
China

Co-Investigators:
Wang Chao, CAS-IRSA
Shao Yun, CAS-IRSA

Multi-Parameter SIR-C/X-SAR for Geoscience Study in China

OBJECTIVES

Establish the backscatter models for the typical targets at the land surface and study the penetration phenomena.

Develop the techniques for multi-frequency and multi-polarization SAR image processing and specific geoscience information extraction.

Study the geology and mineralization both in arid and subtropic regions, the archaeology and other geoscientific fields with the shuttle imaging radar.

Develop interferometric and polarimetric SAR data analysis methods and evaluate their roles in geoscience study.

PROGRESS

a. Airborne campaign and real-time observation during the SIR-C/X-SAR mission.

During the SRL-1 mission, the Chinese airborne SAR campaign was carried out simultaneously at the Beijing test site. The truck-based scatterometer measurement was performed on the various kinds of land types. Meanwhile, the soil moisture and crop phenologic parameters were observed. In the Inner Mongolia test site, 12 corner reflectors were deployed on the surface and in various depths of the sand sheets for penetration study.

b. Analysis of SIR-C/X-SAR data and ground-truth data

In the Inner Mongolia test site, the responses of the deployed corner reflectors were analyzed on the SIR-C/X-SAR images. The penetration depths through the sand sheet of multi-frequency radar signals were calculated and explained. At the Beijing test site, the truck-based scatterometer measurement was used for calibration of Chinese airborne CASSAR and SIR-C survey images over the Beijing site. The cross-calibration is going on. The relations between soil moisture, plant water content, and CASSAR images were analyzed. At the Zhaoqing site of south China, SIR-C data proved to be useful for geological exploration in subtropic areas with heavy vegetation cover. At the Shandong site of the east China, an impact crater was identified on the SIR-C/X-SAR images. At the Kunlun site of west China, a joint field investigation was carried out with JPL. Using the SIR-C data, nine summit craters and calderas with various shapes and types of lava flows have been detected in the northeast of Aksayqin Lake, west Kunlun. At the Yanchi site of north-central China, the first-step field

investigation for the Great Wall has been done based on the analysis for SIR-C data.

c. SIR-C Interferometry

SIR-C interferometry data over the Kunlun site were processed. After the resampling and registration, the fringe was produced. This technique will be used for the Karakax Fault study.

Dr. Bryan Isacks
Department of Geological Sciences
Snee Hall
Cornell University
Ithaca, NY 14853

Co-Investigator:
Arthur L. Bloom Cornell University

SIR-C/X-SAR Analysis of Topography and Climate in the Central Andes

OBJECTIVES

Understand large-scale interactions between tectonic and climate-controlled erosional processes that created the Andes.

Determine the modern and Pleistocene snow-line altitudes and gradients in a poorly known but critical latitude range of the central Andes, and interpret ice-age changes in atmospheric circulation.

PROGRESS

Since the launch of the April mission our project has focused primarily on the analysis of the enormous amount of new SIR-C/X-SAR data for the Patagonian Icefields. The North and South Patagonian Icefields represent 62% of the glacial area in the southern hemisphere outside of Antarctica, with the South Patagonian Icefield (SPI) ranking as the third largest ice mass on Earth after Antarctica and Greenland. Although little studied, these glaciers are some of the most dynamic in the world, with annual precipitation exceeding 7 m in the accumulation areas and ablation rates as high as 6 cm/day at sea level, allowing them to respond quickly to climatic variations. Monitoring the response of these glaciers is important for the study of the regional climate as well as the relationships between climate changes in the northern and southern hemispheres. The new radar data will have a major impact on the understanding of these important icefields and glaciers.

Radar interferometry analysis of the San Rafael glacier, one of the fastest moving glaciers in the world, has produced spectacular results revealing new information regarding its flow characteristics. The extremely fast velocities at the terminus are not characteristic throughout its length and slow down by an order of magnitude up glacier. Within the interior of the icefield the glacier acts as a well defined ice stream with slower moving ice on its flanks.

Analysis of the Patagonian SIR-C/X-SAR data has lead us to new discoveries regarding the spatial and temporal characterization of snow and ice conditions on the Patagonian Icefields, and has demonstrated the utility of combining multitemporal SAR with meteorological and hydrological data to detect the effects of synoptic weather systems and seasonal changes on snow and ice conditions.

The Patagonian results have spawned collaborations with the Chilean and Japanese glaciologists who have been responsible for much of the previous research on the icefields. We are planning to conduct a joint field trip with them to measure ice depth profiles and snow and ice conditions on the San Rafael glacier. The ice depth measurements will be made with an ice penetrating radar and are needed in order to use the ice velocity measurements to calculate ice flux and test models of glacier flow.

In April 1995 we received our first four TOPSAR scenes processed through the new AIRSAR integrated processor. These four scenes cover two glacier sites in the Cordillera Real, Bolivia and the Quelccaya Ice Cap, Peru. The focus of our recent research has been to assess the usefulness of this data for glaciological studies, especially as a high resolution data source for detection of glacier change. We are collaborating with researchers at the Unidad de Glaciology Recursos Hedricos de Electroperu to use TOPSAR data to update the glacial inventory of the Cordillera Blanca which was originally done using aerial photographs taken in the 1950s and 60s.

FUTURE PLANS

Spaceborne Imaging Radar (SIR-C/X-SAR) Glaciological Observations of the Patagonian Icefields

A mosaic of the North Patagonian Icefield and the northern half of the South Patagonian Icefield (SPI) is being constructed from the 14 SIR-C scenes acquired during SRL-1. Because of the persistent cloud cover this is the first complete mosaic of the icefields since a series of TM acquisitions in 1986. Terminus position changes of 15 glaciers are determined and the spatial distribution of these changes correlated with glacier characteristics including aspect, area, length, accumulation area/ablation area ratio, equilibrium line altitude (ELA) and gradient. Snowlines are mapped and compared to previous estimates of ELAs. Several ice divides on the SPI are defined for the first time. Other previously undetected glacial features include: buried crevasses, small icefalls, and ogives. The complete set of SRL-2 data provides a comprehensive view of seasonal change for the northern SPI.

Snow and Ice Conditions inferred from Scattering Mechanism Decomposition of SIR-C/X-SAR images of the Patagonian Icefields

The scattering mechanism decomposition technique of Cloude, modified for SIR-C data by van Zyl and Rignot, is used to interpret the snow and ice conditions of the Patagonian Icefields. Several large areas on the icefields are dominated by a double bounce scattering mechanism which has never been reported for a snow and ice target. We presently interpret this to be the result of subsurface refrozen ice on a 5 cm scale. Inverse backscatter modeling together with the limited published field data will be used to constrain the physical parameters of the snow and ice such as: grain size distribution, snow wetness, density, surface roughness and the orientation and structure of subsurface refrozen ice. We hope to further constrain the snow and ice parameters with our own measurements from snow pits on the Patagonian Icefields.

Ice Velocity and Surface Topographic Mapping of the Moreno Glacier area of the South Patagonian Icefield from Spaceborne SAR interferometry

Interferometric analysis similar to that done on the San Rafael Glacier will be applied to the fast-moving Moreno Glacier and several slower glaciers in the area. The glaciers in the southern portion of the SPI act as a coalescence of individual glaciers rather than outlet glaciers draining a common icefield as they do on the NPI, therefore, comparisons of the velocity and strain maps of this area with those of the San Rafael area will illustrate the differences in flow characteristics of these two glacial regimes.

Results from San Rafael Glacier Field Experiments

If we are successful in obtaining ice depth profiles and characterizing the snow and ice conditions on San Rafael Glacier during our planned trip to Chile then we will be in the position to provide important ground validation results for both the San Rafael interferometry results (Rignot, et al., 1995) and the Patagonian radar glacier zones (Forster and Isacks, 1995).

Mapping of Glacial Geomorphology in the Cordillera Real, Bolivia with SIR-C/X-SAR images

Various geomorphic features are easily identifiable on the SIR-C/X-SAR images that are not as evident on VNIR images. The extent of Pleistocene glaciation can be mapped from moraine positions prominently displayed on the SAR images because of the enhancement of subtle topography to the side-looking geometry. Rock glaciers, talus and bedrock outcrops can be distinguished through the variations in surface roughness.

A comparison of DEMs generated from SAR interferometry and stereo pairs in the Cordillera Real, Bolivia

We have a unique opportunity to compare DEMs generated from SIR-C and TOPSAR interferometry, SPOT stereo pairs, and from aerial photograph stereo pairs for an area with extreme relief for which we also have good ground control from 1:50,000 maps. This will serve as a test for the accuracy and coverage of a spaceborne interferometer in the presence of large topographic variations.

Himalayan Radar Glacier Zones observed with SIR-C/X-SAR

We will apply our interpretation of the Patagonian radar glacier zones to the SIR-C/X-SAR data acquired over the Himalayan Glaciers. The climatic setting in the Himalayans is dominated by monsoonal and winter precipitation as opposed to the year-round precipitation in Patagonia. We anticipate this to be reflected in the spatial and temporal distribution of the radar glacier zones. The seasonal changes induced by the 1994 monsoon season (mid-summer) should be recorded by the differences in the April and October radar glacier zones. Analysis of the radar zones will not be limited to relatively flat areas (as they were in Patagonia) because we can correct the SAR data for radiometric and geometric topographic influences with the high resolution DEM available at Cornell.

A multitemporal analysis of the Radar Glacier Zones in Patagonia and British Columbia with ERS-1 and SIR-C/X-SAR

Based on the Patagonian radar glacier zones defined from our SIR-C/X-SAR analysis we are observing those zones as shown by C-VV from a continuing series of ERS-1 and 2 SAR acquisitions of the Patagonian Icefields and British Columbia. These images are correlated with elevation of the snow and ice surfaces and with weather conditions to determine the dynamics of climate/glacier interactions over time scales of synoptic weather to seasonal change.

TOPSAR Data for Bolivia and Southern Peru

Our research has focused primarily on assessing the geometric accuracy of the data to determine if it can be used as part of a glaciological time series. Glacier boundaries are clearly discernible on the SAR imagery and can be easily mapped. Rectification of

TOPSAR data to other datasets is more problematic. The glacier recession that has occurred in the region over the past 30-40 years is measured in 10's of meters, so accurate coregistration is required. The small footprint of a TOPSAR scene has hindered coregistration simply because there is often a limited number of good ground control points that can be used to accurately define the transform. In an attempt to improve coregistration we have begun to focus on better visualization of the radar imagery. We have also recently begun to integrate TOPSAR digital elevation data with SAR imagery to create stereo radar imagery. This combination has resulted in dramatically improved visualization of radar data. It offers several advantages over even geocorrected data in mountainous regions. First and foremost it allows radar backscatter signatures to be seen in their true landscape position. This is crucial for proper interpretation of geomorphic features such as moraines or debris left by retreating glaciers as well as accurate mapping of the position of glacier termini. Secondly, it allows much better registration with other datasets as ground control points become much easier to identify. Lastly, It also allows radar imagery to be used by a much wider community. Nonradar scientists can find using SAR data, especially in mountainous regions, a frustrating task as layover and foreshortening render the landscape nearly unrecognizable. However, through the creation of stereopairs, radar data is presented in a form identical to widely used aerial photographs that researchers, even in underdeveloped countries, are familiar working with. We intend to use this technique with the DEM that will be created for the Cordillera, Real region using SLR-2 data as well.

Anticipated new data requests:
SIR-C/X-SAR
Patagonia sites (10)
Bolivia, Southern Peru and other South American sites (15)
Himalayan glaciers (10)

Integrated TOPSAR processing:
We require the entire coverage of the Peruvian Cordillera Blanca and the Bolivian Cordillera Real.

PUBLICATIONS

Forster, Richard R. and Bryan L. Isacks, Spaceborne Imaging Radar Reveals South Patagonian Icefield Responses to Seasonal and Synoptic Weather Changes, submitted to *JGR*, Planetary Science, 1 October 1995.

Rignot, E. J. M., R. R. Forster and B. L. Isacks, Interferometric radar observations of Glaciar San Rafael, Chile, *J. Glaciology*, (in press), 1996.

Rignot, E. J. M., R. R. Forster and B.L. Isacks, Mapping of glacial motion and surface topography of Hielo Patagonical Norte, Chile, using satellite SAR L-band interferometry data. *Annals of Glaciology*, vol. 213, 1996, (in press).

Presentations at Scientific Meetings

Forster, R. R., and B. L. Isacks, The Patagonian icefields revealed by space shuttle synthetic aperture radar (SIR-X/XSAR), *EOS*, Transactions, American Geophysical Union (Abstracts), v. 75 (44), p. 226, 1994.

Forster, R. R., B. L. Isacks, and A. G. Klein, Modern and LGM glaciation of the Bolivian and Patagonian Andes, *Geological Society of America annual meeting (Abstracts)*, v. 26 (7), p. 129, 1994.

Forster, R. R., B. L. Isacks, and A. G. Klein, Spaceborne Imaging Radar (SIR-C/X-SAR) Glaciological Observations of the Patagonian Icefields, submitted to *AGU* Fall 1995.

Dr. Arthur R. Jameson
Applied Research Corporation
8201 Corporate Drive, Suite 920
Landover, MD 20785

Dr. Fuk Li
Mailstop 300-227
JPL/Caltech
4800 Oak Grove Drive
Pasadena, CA 91109

The Joint Analyses of Single- and Dual-Frequency/Experimental Dual-Polarization SIR-C and X-SAR Measurements in Precipitation

OBJECTIVES

Determine the vertical and horizontal spatial distribution of hydrometeors in precipitating clouds.

Measure the spatial distribution of liquid water and ice in the clouds.

Measure and determine the limits of measurement of the polarization characteristics related to the shapes and orientations of hydrometeors in precipitating clouds.

PROGRESS

In spite of the severe constraint allowing only four nadir rolls during each mission, we were able to collect limited data on one occasion through a rainband of Typhoon Odille, on the first mission (Fig. 1), and much better data over tropical cyclone Seth, on two occasions during the second mission (Fig. 2). Although we apparently lost the best data take because of an error in the setting of radar parameters by the operations center, we did end up apparently with one good data take through intense convection and surrounding stratiform precipitation. This alone is a remarkable achievement with an estimated likelihood of success of less than 0.1% because of the spatial and temporal variability of the precipitation and limited (8) number of Shuttle nadir rolls during the two missions. We feel very lucky indeed and appreciate the hard work at the operations center to make sure we got these data takes.

While the focus of this research is on nadir data, other observations off-nadir through rain clouds were also collected. Several instances of these were processed first. While SAR side-looking images of rainstorms are interesting qualitatively, they are not very useful for quantitative studies because of the large vertical extent of the radar beam and because the geometry of the observations precludes unambiguous interpretation of the data. It is for these reasons that our primary concern here is with the nadir data. However, the request for these data from the second mission was at the bottom of the processing heap so that we are just now getting access to our SIR-C data and are still awaiting the X-SAR data. A preliminary inspection of the qualitative nature of the SIR-C data are, nevertheless, encouraging and warrant detailed quantitative analyses.

In particular these data include a transition from convective to stratiform precipitation clearly exhibiting a 'bright-band' associated with the melting layer (Fig. 2). The region of convection is well suited to a dual-frequency (C-band and X-band) analysis for the quantitative estimation of rainfall. The software for rainfall estimation is ready as demonstrated in Fig. 1.

Nevertheless, while waiting for access to the nadir data, we have made good use of the time by using ancillary data and performing theoretical studies of benefit to the upcoming analyses. In particular, an analysis of JPL/NASA ARMAR (Airborne Rain Mapping Radar) data collected at nadir shows that in heavier rain, the larger raindrops are oscillating leading to the generation of linear depolarization (LDR) (Jameson and Durden 1996). This not only has significant implications for ground-based polarization measurements of precipitation but could also prove to be a useful new method for detecting heavy rainfall from space. We will be looking for this signature in the upcoming analysis of the SIR-C data. Moreover, the ARMAR data clearly show enhanced LDR associated with the melting level. Knowing the altitude of this melting level is important in order to accurately retrieve rainfall measurements from space using either radar or radiometers or a combination of the two technologies. These two features are illustrated in Fig. 3.

Of much greater importance, perhaps, is a theoretical result having quite general applicability to many types of radar, scatterometer, radiometric, and other types of measurements. Since at nadir we use the SIR-C as a real aperture radar, we were interested in the smoothing effects of the beam as well as the signal statistics of a spaceborne radar passing through rapidly changing meteorological conditions. While investigating this situation, we (see Jameson and Kostinski 1996) found the general result for any instrument scanning through regions where the mean is changing while sampling, that the amplitudes, in general, are not Rayleigh distributed, as illustrated in Fig. 4.

Consequently, the distributions of the intensities are not, in general, negative exponential. This effect can lead to bias for some detectors (linear and logarithmic) and, more importantly, can significantly increase the uncertainty of the estimate of, say, the mean intensity at times and locations where conditions are changing rapidly. Moreover, it is shown that the beam filtering effect extends over twice the beam width (for one estimate per beam width) thus considerably broadening the storm boundaries and dimensions unless 'block' scanning is used. Fortunately, the SIR-C/X-SAR nadir data are optimum in the sense that these problems are minimized.

FUTURE PLANS

We anticipate accessing nadir data collected on data take 103 in mid-September and will then request multiple polarization and multiple frequency data through interesting segments. We should have these data within two months so that we can perform detailed quantitative analyses in November and December. The analysis software is ready (see Fig. 1) and simply requires getting the data. We hope to have a manuscript ready by the end of January 1996.

The first stage will be the processing and analysis of C-band data, especially looking for the melting layer and for enhanced LDR in heavier rain. The second stage will be combining the C-band and X-SAR data to deduce a profile of rain through deep convection. This will be a first, if successful, and should generate one to two publications. Finally, in the future, we would like to scan side-looking cloud images in order to look for unusual data for possible analysis. These will have to be primarily at small look angles in order to reduce the mixing of ground and rain signals. This may lead to additional publications, depending on what is uncovered.

PUBLICATIONS

Jameson, A. R. and A. B. Kostinski, 1995: "Non-Rayleigh signal statistics caused by changing conditions during sampling," *J. Appl. Meteor.*, submitted.

Jameson, A. R. and S. L. Durden, 1996: "A possible origin of linear depolarization observed at vertical incidence in rain," *J. Appl. Meteor.*, in press.

Haddad, Z. S., A. R. Jameson, E. Im, and S. L. Durden, 1995: "Improved correlated Z-R and k-R relations and the resulting ambiguities in the determination of the vertical distribution of rain from the radar backscatter and the integrated attenuation," *J. Appl. Meteor.*, in press.

Jameson, A. R., 1994: "The meteorological parameterization of specific attenuation in rain viewed at nadir," *J. Appl. Meteor.*, 1026-1033.

Jameson, A. R., 1994: "On the estimation of rainfall parameters using spaceborne and airborne nadir pointing radars," *J. Appl. Meteor.,* 33, 230-244.

Kostinski, A. B., J. M. Kwiatkowski, and A. R. Jameson,1993: "Spaceborne radar sensing of precipitation above an ocean surface: Polarization contrast study," *J. Atmos. and Oceanic Technol.*, 736-751.

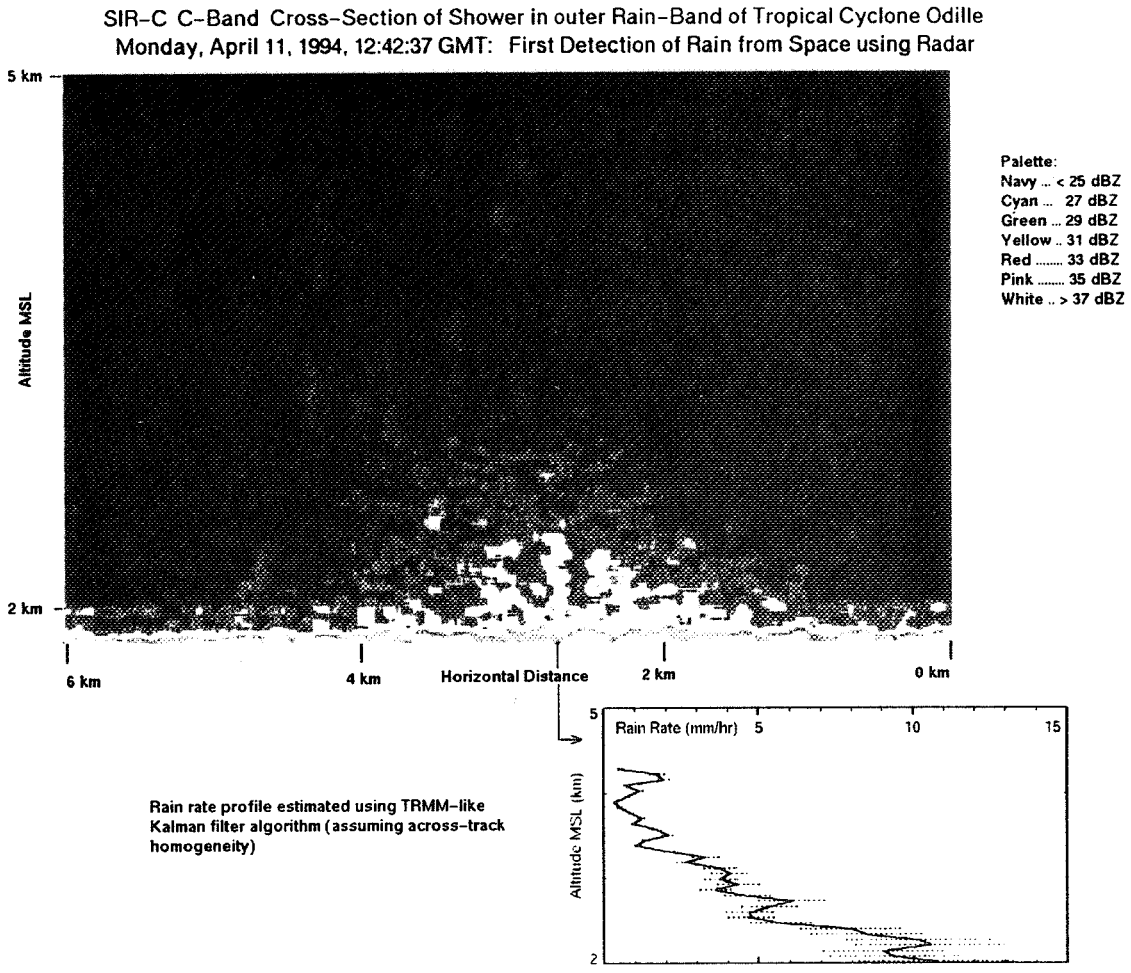

FIG.1: *Plot of the co-polarized radar reflectivity factor at C-band from part of a rainshaft associated with Tropical Cyclone Odille. A profile of rainfall rate as a function of altitude above the ocean surface (from Dr. Haddad) through the core of the rain is plotted as well.*

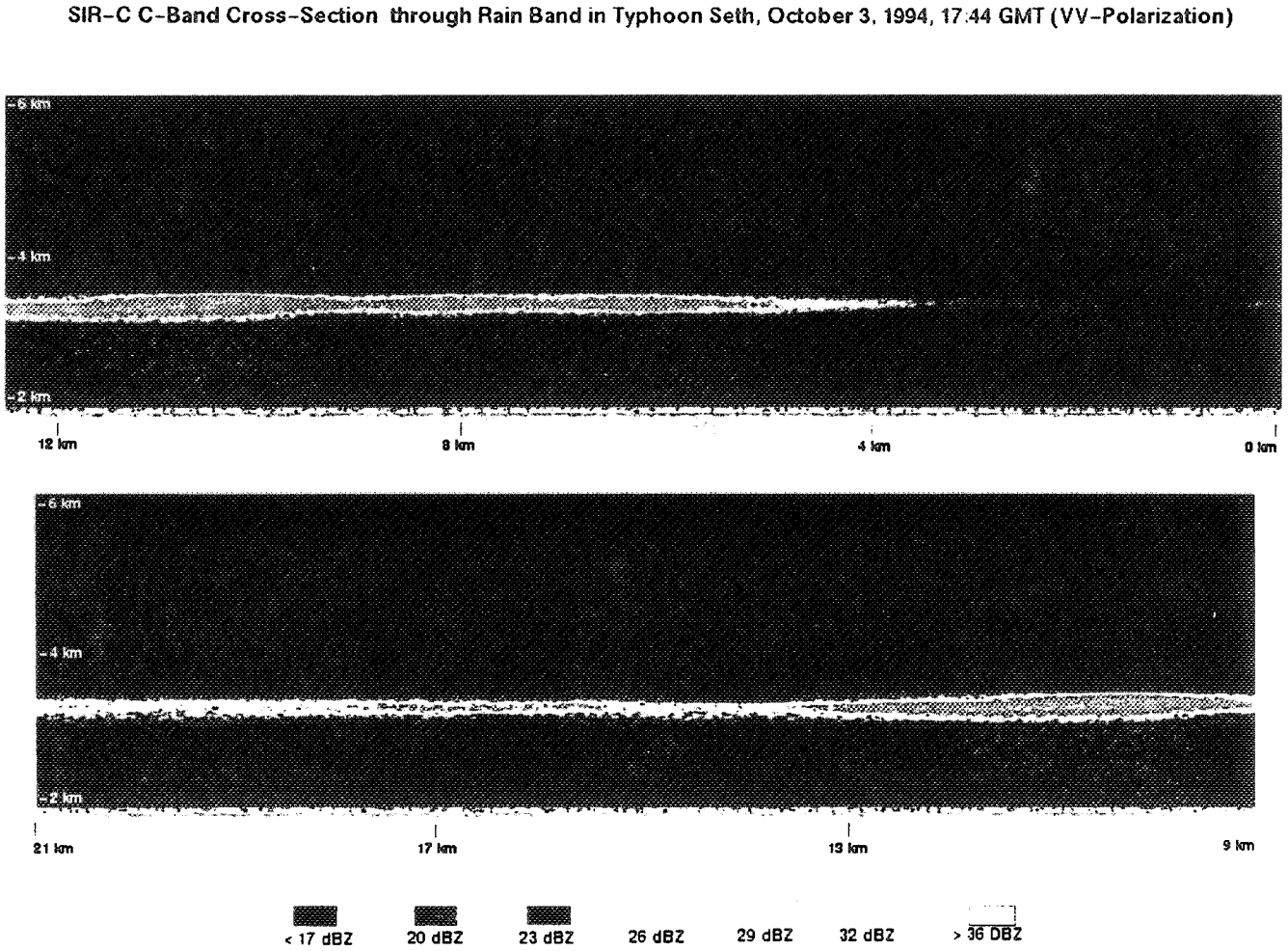

FIG.2: *Plot of the co-polarized radar reflectivity factor at C-band from a radar 'bright-band' arising from the melting of icy hydrometeors in a region of stratiform precipitation associated with Tropical Cyclone Seth. Note the rain falling beneath the bright-band at 13 and 6 km in the top panel and at 11 km in the lower panel.*

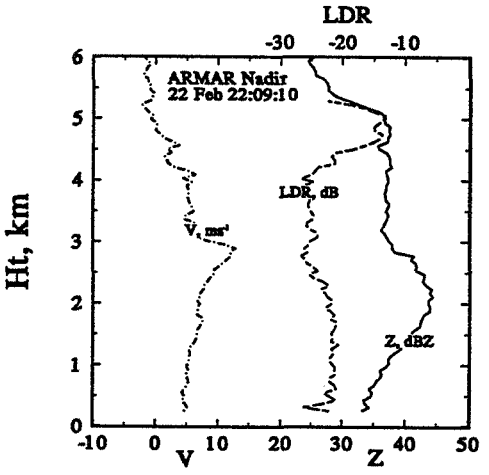

FIG 3: *An example of ARMAR data collected at nadir illustrating the linear depolarization ratio (LDR), the co-polar reflectivity factor (Z) as well as the mean Doppler velocity (V). The melting level is around 5 km above the ocean surface. (From Jameson and Durden 1996)*

Of much greater importance, perhaps, is a theoretical result having quite general applicability to many types of radar, scatterometer, radiometric and other types of measurements. Since at nadir we use the SIR-C as a real aperture radar, we were interested in the smoothing effects of the beam as well as the signal statistics of a spaceborne radar passing through rapidly changing meteorological conditions. While investigating this situation, we (see Jameson and Kostinski 1996) found the general result for any instrument scanning through regions where the mean is changing while sampling that the amplitudes,in general, are not Rayleigh distributed as illustrated in Fig.4.

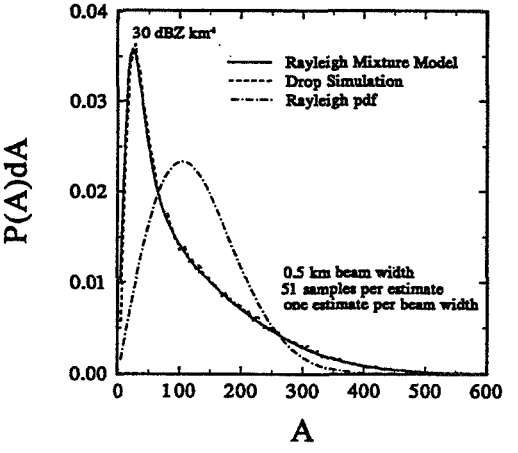

FIG.4: *The probability density functions (pdf) for the amplitudes of the estimate when the radar is at a typical rate of one estimate per beam width of distance covered while moving through a logarithmic linear radar reflectivity profile of 30 dBZ km^{-1}. Note the non-Rayleigh form of the pdf as well as the close agreement between theory (solid line) and results from the Monte Carlo drop simulation. (From Jameson and Kostinski 1995).*

Consequently, the distributions of the intensities are not, in general, negative exponential. This effect can lead to bias for some detectors (linear and logarithmic) and, more importantly, can significantly increase the uncertainty of the estimate of, say, the mean intensity at times and locations where conditions are changing rapidly. Moreover, it is shown that the beam filtering effect extends over twice the beam width (for one estimate per beamwidth) thus considerably broadening the storm boundaries and dimensions unless 'block' scanning is used. Fortunately, the SIR-C/X-SAR nadir data are optimum in the sense that these problems are minimized.

Dr. Eric S. Kasischke
Radar Science Laboratory
ERIM
P.O. Box 8618
Ann Arbor, MI 48107

Co-Investigator:
Norman Christensen Duke University

Estimation of Total Aboveground Biomass in Southern United States Old-Field Pine

OBJECTIVES

The overall goal of the NASA-sponsored research project is to develop methods to use spaceborne SAR imagery to monitor patterns of carbon storage in the pine forests found in the southeastern United States. This project is part of an overall program being carried out by scientists at ERIM and Duke to develop techniques to use satellite-based remote sensors to monitor carbon flux in this region. Towards this end, funding has also been secured from the Environmental Protection Agency to pursue research beyond the scope of the SIR-C project. Specifically, EPA funding is being used to obtain and analyze Landsat TM and MSS imagery over the test site to monitor changes in forest cover in this region from 1975 to present, to develop models describing patterns of below-ground carbon storage, and to develop an integrated approach using information derived from SIR-C and Landsat with ground-based models to study landscape scale patterns of carbon storage and flux.

Specific objectives of the overall program are to:

Develop optimum algorithms to estimate aboveground biomass/carbon in pine forests of the southeast U.S. using multichannel, spaceborne SAR data (NASA funded).

Develop models which link aboveground biomass/carbon with ground-layer carbon in pine forests in the southeast U.S. (EPA funded).

Based on (1) and (2) above, estimate patterns of carbon storage in the pine forests surrounding Durham, North Carolina at the times of the SIR-C overflights
(NASA funded).

Evaluate the utility of using SIR-C/X-SAR data to improve maps of forest cover in the study region (NASA funded).

Develop methods to monitor changes in forest cover from 1975 to 1994 in the study site using Landsat TM and MSS data (EPA funded).

Develop methods to combine the information derived from Landsat and SIR-C data to study patterns of carbon flux over the past 20 years (EPA/NASA funded).

PROGRESS

Prior to March of 1994, our activities focused on investigations of AIRSAR and ERS-1 SAR data to develop approaches in using radar imagery to monitor changes in biomass in southern U.S. pines. Towards this goal, a set of 80 test sites were established in the Duke Forest. These test sites were measured and techniques developed to estimate patterns of biomass present in these forests based on in situ measurements as well as allometric equations available in the literature. The utility of SAR data to monitor biomass patterns was clearly established during these initial

experiments. These data were also used in theoretical modeling studies to better understand the relationships between EM scattering and tree characteristics. This research resulted in eight published journal articles (see reference list).

The activities pursued during the past eighteen months were first focused on collection of ground-truth data sets to support the analysis of SIR-C/X-SAR data. These ground truth data included measurement of stand characteristics for 60 different pine stands, collection of soil moisture measurements during the SIR-C overflights in April and October of 1994, collection of local meteorologic conditions during the SIR-C overflights, and collection of canopy hemispherical photographs. The support of two SIR-C overflights within a seven-month period stretched the financial resources available at Duke University to the fullest, and required expending funds not received until November of 1994. Thus, we were not able to begin to fully reduce the ground data until the spring of 1995, when additional funding was received. In addition to supporting the experiments themselves, the PI for this experiment (E. Kasischke) also served as Co-Chairman of the Ecology Discipline Panel for the National Research Council's review of the utility of Spaceborne SAR for earth science applications. This activity required considerable efforts from the PI during the time period from November 1994 through February 1995, and severely strained the funding resources available for analysis of SIR-C data until a further funding increment was received in March of 1995.

Since March of 1995, we have begun to seriously analyze the SIR-C/X-SAR data sets. Our activities during this time period have focused on reducing the ground-truth data and on extracting signatures from the radar data sets. The data are currently being used in two separate analyses, each of which should result in a journal article. The first analyses is being conducted jointly with Frank Davis (UCSB) and Yong Wang (ECU). This is a modeling study on the sensitivity of radar backscatter to variations in surface moisture and changes in incidence angle. The second analyses is exploring the effects variations in imaging geometry and seasonal variations (e.g., leaf on versus leaf off, soil moisture) on the ability of SAR to estimate aboveground biomass. The approach being used is through a multistage approach, where canopy biomass is estimated from radar imagery, which in turn is used to estimate total stand. These journal articles are currently in preparation and should be submitted by the end of the year.

PLANNED ACTIVITIES - FY '96/'97

In addition to submitting the two journal articles mentioned above, during FY96/97 we plan the following activities (each of which will result in a separate journal article):

1. Analysis of Different Approaches to Estimation of Aboveground Biomass Using SIR-C/X-SAR Data

Several different methodologies have been proposed to estimate aboveground biomass in forests. In addition to the two-step approach developed by this program, Jon Ranson uses a polarization ratio to estimate biomass, while Craig Dobson uses a multiple-step approach where longer wavelength SAR data are used to estimate tree height and basal area and shorter wavelength data are used to estimate canopy biomass. Under this study, we will compare all three approaches to determine which approach is best suited for the forest conditions found in the southeast U.S.

2. Regional Estimates on Patterns of Carbon Storage in a Southeast U.S. Pine Forest Complex using Spaceborne SAR Data

This study will take the results from the algorithm from the previous analyses and use them to estimate patterns of biomass present in the pine forests in the Duke Forest Region. This analysis

will also utilize the below-ground carbon models developed by the EPA study to develop a total carbon budget for these forests.

3. Analysis of the Effects of Imaging and Scene Parameters for Detection of Floodingin a Bald Cypress Forest Wetland

Duke Forest contains a test stand of Bald Cypress which was continuously flooded during the SIR-C overflights. In the April flight, the leaves on the trees of this stand had just begun to flush, while during the October flight, the leaves were fully flushed. This study will focus on determining how well the different wavelength/polarizations of the SIR-C/X-SAR detected this flooded forest wetland as a function of incidence angle and leaf on/off conditions. The study will employ both empirical analyses as well as theoretical scattering models.

4. Mapping Forest Cover using Combined Landsat TM and SIR-C/X-SAR Data

This study will investigate whether imaging radar's unique capabilities in mapping forest structural characteristics can be used to improve maps of forest/land cover which are traditionally derived from MSS data.

5. Patterns of Carbon Storage and Flux in a Southern U.S. Forest from 1974 to 1994

This is the culmination of the overall program. This study will combine information (within a GIS context) derived from three separate sources (e.g., ground-based models, SIR-C/X-SAR, and Landsat) to look at how patterns of forest cover change have influenced carbon flux in the forests surrounding Durham, North Carolina.

PUBLICATIONS

Dobson, M. C., F. T., Ulaby, T. Le Toan, A. Beaudoin, E. S. Kasischke, and N. C. Christensen, Dependence of radar backscatter on conifer forest biomass, *IEEE Trans. Geosci. Remote Sens.*, 30, pp. 412-415, 1992.

Kasischke, E. S. and N. L. Christensen, Jr., Connecting forest ecosystem and microwave backscatter models, *Int. J. Remote Sens.*, 11, pp. 1277-1298, 1990.

Kasischke, E. S., L. L. Bourgeau-Chavez, N. L. Christensen, Jr., and E. Haney, Observations on the sensitivity of ERS-1 SAR image intensity to changes in aboveground biomass in young loblolly pine forests, *Intern. J. Remote Sens.*, 15, pp. 3-16, 1994.

Kasischke, E. S., Christensen, N. L., Jr., and E. Haney, Modeling of geometric properties of loblolly pine tree and stand characteristics for use in radar backscatter models, *IEEE Trans. Geosci. Remote Sensing*, 32, pp. 800-822, 1994.

Kasischke, E. S., Christensen, N. L., Jr., and L. L. Bourgeau-Chavez, Correlating radar backscatter with components of biomass in loblolly pine forests. *IEEE Trans. Geosci. Remote Sensing*, 33, 643-659, 1995.

Ustin, S. L., C. A. Wessman, B. Curtiss, E. Kasischke, J. Way, and V. Vanderbilt, Opportunities for Using the EOS Imaging Spectrometers and Synthetic Aperture Radar in Ecological Models, *Ecology*, 72, pp. 1934-1945, 1991.

Wang, Y., F. W. Davis, J. M. Melack, E.-S. Kasischke and N. L. Christensen, Jr., The Effects of Changes in Forest Biomass on Radar Backscatter from Tree Canopies, *Int. J. Remote Sens.*, 16, pp. 503-513, 1995.

Wang, Y., E. S. Kasischke, F. W. Davis, J. M. Melack, and N. L. Christensen, Jr., The Effects of Changes in Loblolly Pine Biomass and Soil Moisture Variations on ERS-1 SAR Backscatter - a Comparison of Observations with Theory, *Remote Sens. Env.*, 49, pp. 25-31, 1994.

Dr. Gordon Keyte
GEC-Marconi Research Centre
F/218/3388
Great Baddow
Space Division-Chelmsford
Avionics Laboratory-Essex CM2 8HN
England

Co-Investigators:
J.P. Matthews — Univ. of N. Wales
G.J. Wensink — Delft Hydraulics, NAL
R. Cordey — Marconi Research Centre

An Investigation of the Imaging of Ocean Waves and Oil Slicks with SIR-C and X-SAR

OBJECTIVES

To improve our understanding of ocean-wave imaging by synthetic-aperture radar (SAR).

To test the assumptions of backscattering theory with regard to short-wave properties.

To develop new techniques for retrieving ocean-wave spectra from multiparameter SAR.

PROGRESS

Multilook SIR-C/X-SAR data have been acquired for all the orbits coinciding with buoy measurements at the N. E. Atlantic site in the first mission (April 1994). There were no in-situ measurements during the second mission. The April 1994 experiment was successful, with many clear instances of the imaging of ocean swell waves at times of buoy measurements, and some clearly imaged artificial oil slicks. An initial analysis of the wave imaging has been made, and a more detailed study of the mean backscatter and backscatter statistics is currently in progress.

SIGNIFICANT RESULTS

An initial analysis was undertaken to assess the wavelengths and directions of the dominant swell waves imaged on two orbits. Good agreement was found with the simultaneous buoy data, although the SAR data showed a small but significant rotation of the position of the spectral peak with changing radar frequency. These results have been reported at IGARSS 95.

Further analysis has shown that the imaged wave modulations have a strong polarization dependence close to the range direction, but not in the azimuth direction. This agrees with the expected strong polarization dependence of the tilting imaging mechanism. Other initial results confirm the successful imaging of oleyl alcohol films deployed during this experiment.

However, the main thrust of our work has been the analysis of the mean backscatter and backscatter statistics. Empirical models of the mean backscatter have been tested. There is very good agreement, to 1 dB (standard deviation), with the ERS-1 C-band scatterometer model functions CMOD-3 and CMOD-4. Theoretical models show some systematic disagreements with radar frequency, pointing to a need to modify existing descriptions of short-wave spectra.

The single-look image statistics fit the K distribution, but all the multilook cases fit the lognormal distribution. Modelling of backscatter variances has been studied. It has been found that the observed variances can be explained in terms of the contribution from resolved ocean waves. We have applied wave-imaging theory to estimate this contribution from our buoy data. We find agreement with observations if the hydrodynamical modulation is increased above the level

predicted by the simple action-balance theory of Alpers & Hasselmann. This result agrees with tower-radar measurements.

FUTURE PLANS

New Data Requests

We now have all the multilook data-sets needed for comparison with our simultaneous wave-buoy measurements at the N. E. Atlantic site in the first mission (April 1994). We envisage a need for more single-look, complex scenes over this site, and the images and raw data from the SCANSAR passes over the N. Atlantic. We expect to define our requirements when our present program of work finishes in February 1996. We do not have any immediate plans to study data from the second mission (October 1994) as no in-situ measurements were made at our site.

Future Work

Our present work on the mean backscatter and backscatter statistics is scheduled to finish in February 1996. We are considering the possibility of follow-on work to examine alternative ways of combining the simultaneous SIR-C/X-SAR channels to reduce ocean-clutter false alarms in target detection. Analysis of the imaged oil slicks by DRA Winfrith is expected to commence in 1996.

PUBLICATIONS

The following paper was presented at IGARSS 95:

First results from the SIR-C/X-SAR experiment on ocean-wave imaging in the N. E. Atlantic, G. E. Keyte, R. A. Cordey, R. Larsen & J. T. Macklin, *Proc. IGARSS '95,* Firenze, Italy, 10 - 14 July 1995, pp 1320 - 1322.

The following internal report describing the conduct of the experiment has also been produced:

SIR-C Trials in N. E. Atlantic, R. Larsen & P. R. Dovey, GEC-Marconi Research Centre Report MTR 94/32A on DRA Contract RAE1B/89, August 1994.

New Publications

An outline abstract, SAR Backscatter Properties from the Sea Surface During the SIR-C/X-SAR Experiment in the N. E. Atlantic by N. R. Stapleton & J. T. Macklin, was sent by e-mail to Dr. Ben Holt (JPL). This is a contribution to a proposed special issue of the *Journal of Geophysical Research* on SIR-C/X-SAR oceans results. It is anticipated that a paper will be prepared for submission in early 1996.

An abstract, Radar Backscatter Statistics from the Sea Surface: Implications of SIR-C/X-SAR Observations for Maritime Surveillance by R. A. Cordey, N. R. Stapleton, J. T. Macklin, R. Ringrose, N. A. Robertson & G. E. Keyte, has been submitted to the NATO/AGARD Mission Systems Panel - 5th Symposium Space Systems as Contributors to the NATO Defence Mission. A paper will be prepared in early 1996.

Prof. Jin A. Kong
Department of Electrical Engineering
Massachusetts Institute of Technology
Cambridge, MA 02139

SIR-C Polarimetric Radar Image Simulation and Interpretation Based on Random Medium Model

OBJECTIVES

Demonstrate the applicability of the random medium model in simulating SIR-C imagery.

Analyze and interpret SIR-C imagery for remote sensing applications.

Investigation of seasonal variations and atmospheric effects.

PROGRESS

The work during this period has been focused on the use of spaceborne polarimetric radar measurements for monitoring, mapping, and retrieving the above ground vegetation biomass. Fully polarimetric radar data obtained from the SIR-C/X-SAR missions in April and October 1994 over the Landes Forest in Southwestern France have been analyzed in detail. The Landes forest is the largest plantation forest in France, and covers nearly one million hectares of flat topography. This forest is almost totally formed by maritime pine (pinus pinaster), and it has been managed in such a way that the forest is divided into various areas of large and statistically homogeneous tree stands of the same age. The acquired SIR-C data has been compared with the previous AIRSAR campaign (L- and C-band, fully polarimetric, 40-50 degree incidence angle), ERS-1 data (C-band, VV, 23 degree incidence angle), and JERS-1 data (L-band, HH, 35 degree incidence angle) to assure the consistency of measurement.

In the investigation of the application of SIR-C data to vegetated terrain classification and biomass inversion, the measured backscattering coefficients σ°_{hh}, σ°_{vv}, and σ°_{hv},), the derived complex correlation coefficient (ρ) of HH and VV polarizations as well as the ratio between cross- and co-polarization ratio ($\sigma^\circ_{hv} / \sigma^\circ$ vv) are fully utilized. A validated pine forest scattering model, which is based on the radiative transfer theory with the specific branching structure of pine tree taken into account, is used to interpret the SIR-C/X-SAR polarimetric backscattering measurements from the Landes forest. From the analysis of measured data and the theoretical simulation, the cross-polarization backscattering coefficients at L-band and the correlation between HH and VV backscattering returns at both L- and C-band are found to be most useful for the biomass retrieval. Bayesian classifications using data with known ground truth and with theoretical simulation are applied to classify the forest for biomass up to 50 tons per hectare with the available data at this time (26 degree incidence angle). With the use of pine forest scattering model, biomass inversion has been shown to be feasible over a wider biomass range (up to 100 tons per hectare) for angles of incidence around 45 degrees. In addition to the analysis of SIR-C/X-SAR data, we have refined our forest scattering model by taking into account the double scattering mechanism between trunk and branches which shows more effects on the cross-polarized backscattering return. We have also studied the collective scattering and absorption effects of clustered objects like the branches and leaves in a vegetation canopy. A new approach for studying the polarimetric response of various types of forest is also developed by using the L-systems technique to generate different kinds of plants.

In this work, we have collaborated closely with Dr. Le Toan's research group at the Center d'Etudes Spatiale De La Biosphere (CESBIO) of France. During the different flights of SIR-C/X-SAR over the test site, extensive ground truth data had been collected by Dr. Le Toan's team. These consist of an updated biomass map which provides the location and ages of more than 50 stands of maritime pines, as well as the statistical information about the densities and sizes of trees and branches. In addition, a clear-cut map is also available with some ground truth measurements including soil moisture and surface profiles. These valuable descriptions provide the key input parameters for our theoretical pine forest scattering model.

SIGNIFICANT RESULTS

The fully polarimetric backscattering measurements over the Landes forest from the first SIR-C flight was taken at a 26 degree incidence angle. In Figures 1 and 2, we compare the backscattering coefficients and the correlation coefficients between the SIR-C measured and model predicted data for both forest stands and clear-cuts at L- and C-band frequencies. The comparison between experiment and theory shows good agreement. The clear-cuts are areas where the biomass is lower than 5 tons/ha. For the area with bare soil surface, the magnitude of the correlation coefficient is close to 1 either at L- or C- band. When the area with forest stands is considered, the magnitude of rho drops to a value of 0.35 for older stands.

During the second SIR-C flight, measurements with different incident angles (18 and 51 degrees) were obtained. We then performed theoretical simulations to examine the scattering mechanisms involved in the angular variations with backscatter from forest. It is found that at a higher incident angle (51°), where the scattering from tree crown dominates for both L- and C-band, the cross-polarized return at L-band has larger dynamic range than lower incident angles. For small incident angles, the copolarized return from ground is more important for forest stands with low biomass. This suggests that the results may differ with surface conditions.

Classification and Biomass Estimation of the Landes Forest

With the ground truth from biomass map, the supervised classification of forest stands between 0 tons/ha and 50 tons/ha has been performed with a set of multi-look (5 x 5), fully polarimetric data at 26 degrees. The data are divided into 5 classes: from 0 to 7 tons/ha, from 8 to 20 tons/ha, from 21 to 33 tons/ha, from 34 to 50 tons/ha, and the one with more than 50 tons/ha. Using Bayes classification algorithm, an accuracy of 86% has been achieved. The accuracy of classification with backscattering coefficients only is 62%. Unsupervised classification of forest stands using theoretical models gives an accuracy of 70%. It is also found that for the classification of bare soil with forest areas, the ratio $\sigma^\circ_{hv}/\sigma^\circ_{vv}$ and the magnitude of ρ yield the best results. For both L and C-band frequencies, the forest can be classified with ratio higher than -11 dB or the magnitude of ρ lower than 0.85. As for the biomass retrieval, the magnitude of ρ gives the best performance.

Collective Scattering and Absorption Effects

For a locally clustered medium, the scatterers are clumped together like branches and leaves in a vegetation canopy. In such cases, the scatterers will scatter collectively. Collective scattering effects include correlated scattering, which takes into account the relative phase of scattered waves from the scatterers and their neighbors. The mutual coherent wave interactions between scatterers are also included. The locally clustering structure has important effects in determining the cluster's electromagnetic properties. We have shown that, in locally clustered media, the absorption of the cluster can be several times greater than the incoherent sum of the absorption of its components.

This suggests that in random media problems the effects of the clustered geometry on both scattering and absorption must be considered.

Theoretical Modeling of Forest Using L-Systems

The Monte Carlo approach has also been applied to study the scattering of electromagnetic waves by plants that are grown using the L-systems technique. The position, size, and orientation of every element in a generated tree can be obtained from the computer simulation. The scattering fields from all tree elements are added coherently to calculate the total scattering field. The results are further averaged over many tree realizations. Simulations of different types of trees show that the polarimetric backscattering behavior of forest is affected by the inner structure of plants.

FUTURE PLANS

The overall objective of this study is to investigate the application of spaceborne polarimetric data for classifying, mapping, and parameter retrieval of vegetated terrain using SIR-C/X-SAR polarimetric data. Based on our research goals, the planned investigations include:

Classification of Various Types of Forests

We will investigate the capabilities of radar data to achieve the classification of forests in a worldwide scale into major types according to the tree architectural forms. For each type of forest, the corresponding SIR-C/X-SAR images will be requested, and the backscattering coefficients will be evaluated. We will also investigate the relationships between polarimetric discriminations and tree structures and species. In addition to the Landes pine forest, the forest of eucalyptus in Congo, and the rain forest in Amazon will be studied. For different types of trees, the corresponding tree architecture model and the backscattering model will be set up with the use of L-systems technique.

Monitoring Rice Growth

In this study, the identification of rice fields at various growth stages, as well as the classification into different species will be investigated. At present, a theoretical scattering model for rice field at different growth stages has been developed at MIT, it will be applied to interpret the radar measurements. The test sites will be some rice fields at Indonesia and Japan. These sites have been the subject of remote sensing project using ERS-1 data to monitor rice growth. ERS-1 data will also provide us with samples of measurement at various rice growth stages for comparison.

Soil Moisture and Roughness Inversion

In order to assess the inversion of soil moisture from polarimetric data, a forward rough surface scattering model has been developed at MIT. This model is using the Monte Carlo approach which solves a 3-D random rough surface scattering problem numerically. A neural network is trained based on the direct scattering model and will be subsequently used to invert the SIR-C/X-SAR data. The selected sites with supporting ground truth are the Landes forest in France and Matera in Italy.

PUBLICATIONS

C. C. Hsu, J. A. Kong, T. Le Toan, S. Paloscia, and P. Pampaloni, "Microwave Emission and Backscattering from Crops," *Proc. PIERS '94 Symp.*, Noordwijk, Netherlands, July 1994.

F. Scire-Scappuzzo, C. C. Hsu, L. Wang, J. A. Kong, and T. Le Toan, "Biomass Inversion for Pine Forest using Polarimetric Backscattering Models," *Proc. PIERS '94 Symp.*, Noordwijk, Netherlands, July 1994.

L. Tsang, G. Zhang, K. H. Ding, C. Hsu, and J. A. Kong, "Microwave Scattering by Vegetation Based on Wave Approach," *Proc. PIERS '94 Symp.*, Noordwijk, Netherlands, July 1994.

L. Tsang, K. H. Ding, G. Zhang, C. Hsu, and J. A. Kong, "Backscattering Scattering Enhancement of Volume-Surface Interaction of a Layer of Scatterers Overlying a Homogeneous Dielectric Half Space," *AP Dig. Joint Symp.* IEEE-APS/URSI, Seattle, WA, June 1994, pp. 2338-3341.

L. Tsang, Z. Chen, K. H. Ding, C. Hsu, and G. Zhang, "Collective Scattering Effects in Vegetation Canopies at Microwave Frequencies Based on Monte-Carlo Simulations," *Proc. IGARRS '94 Symp.*, Pasadena, CA, August 1994, pp. 548-550.

C. C. Hsu, H. C. Han, R. T. Shin, J. A. Kong, A. Beaudoin and T. Le Toan, "Radiative Transfer Theory for Polarimetric Remote Sensing of Pine Forest at P-band," *Int. J. Remote Sensing*, Vol. 15, pp. 2943-2954, 1994.

A. Beaudoin, T. Le Toan, S. Gozc, E. Nezry, A. Lopes, E. Mougin, Hsu, C.C., H.C. Han, J.A. Kong, and R.T. Shin, "Retrieval of Forest Biomass from SAR Data," *Int. J. Remote Sensing*, Vol. 15, pp. 2777-2794, 1994.

W. C. Au, L. Tsang, and J. A. Kong, "Absorption Enhancement of Scattering of Electromagnetic Waves by Dielectric Cylinder Clusters," *Microwave Opt. Tech. Lett.*, Vol. 7, 454-457, 1994.

L. Tsang, J. A. Kong, Z. Chen, K. Pak and C. Hsu, "Theory of Microwave Scattering from Vegetation on the Collective Scattering Effects of Discrete Scatterers," *Proceedings of the ESA-NASA Workshop on Passive Microwave Remote Sensing of Land-Atmosphere Interaction,}* VSP Press, Netherlands, 1994.

J. C. Souyris, T. Le Toan, C. C. Hsu, and J.A. Kong, "Assessment of SIR-C/X-SAR Polarimetric Data for the Estimation of Forest Parameters," *Proc. Third International Workshop on Radar Polarimetry*, Nantes, France, March 1995, pp. 636-645.

L. Tsang, K. H. Ding, G. Zhang, C. C. Hsu, and J.A. Kong, "Backscattering Scattering Enhancement and Clustering Effects of Randomly Distributed Dielectric Cylinders Overlying a Dielectric Half Space Based on Monte-Carlo Simulations," *IEEE Trans. Antennas Propagat.*, Vol. AP-43, pp. 488-499, 1995.

J. C. Souyris, T. Le Toan, J. A. Kong, and C. C. Hsu, "Inversion of Landes Forest Biomass Using SIR-C/X-SAR Data: Experiment and Theory," *Proc. IGARRS '95 Symp.*, Firenze, Italy, July 1995, pp. 1201-1203.

Wang, L., K. H. Ding, C. C. Hsu, Y. E. Yang, and J. A. Kong, "Electromagnetic Scattering Model for Vegetation Based on L-Systems," *Proc. PIERS '95 Symp.*, Seattle, WA, July 1995, pp. 278.

Souyris, J. C., T. Le Toan, Y. Zhang, C. C. Hsu, and J. A. Kong, "Inversion of Biomass with Polarimetric Data from SIR-C/X-SAR," *Proc. PIERS '95 Symp.*, Seattle, WA, July 1995, pp. 902.

Hsu, C. C., J. A. Kong, J. C. Souyris and T. Le Toan, "Application of Radiative Transfer Modeling to the Polarimetric Backscattering of Forest," *Proc. PIERS '95 Symp.*, Seattle, WA, July 1995, pp. 903.

Hsu, C. C., L. Wang, J. A. Kong, J. C. Souyris and T. Le Toan, "Theoretical Modeling for Microwave Remote Sensing of Forest," accepted for the International Symposium on the Retrieval of Bio- and Geophysical Parameters from SAR Data for Land Applications,} Toulouse, France, October 1995.

Souyris, J. C., T. Le Toan, C. C. Hsu, and J. A. Kong, "Inversion of Landes Forest Biomass Using SIR-C/X-SAR Data: Experiment and Theory," accepted for the International Symposium on the Retrieval of Bio- and Geophysical Parameters from SAR Data for Land Applications, Toulouse, France, October 1995.

Le Toan, T., F. Ribbes, N. Floury, L. Wang, K. H. Ding, C. C. Hsu, and J. A. Kong, "On the Retrieval of Rice Crop Parameters from SAR Data," accepted for the International Symposium on the Retrieval of Bio- and Geophysical Parameters from SAR Data for Land Applications, Toulouse, France, October 1995.

Au, W. C., L. Tsang, R. T. Shin, and J. A. Kong, "Collective Scattering and Absorption Effects in Microwave Interaction with Vegetation Canopies," submitted to *Progress in Electromagnetics Research,* 1995.

Le Toan, T., J. C. Souyris, C. C. Hsu, and J. A. Kong, "Inversion of Landes Forest Biomass Using SIR-C/X-SAR Data: Experiment and Theory," to be submitted.

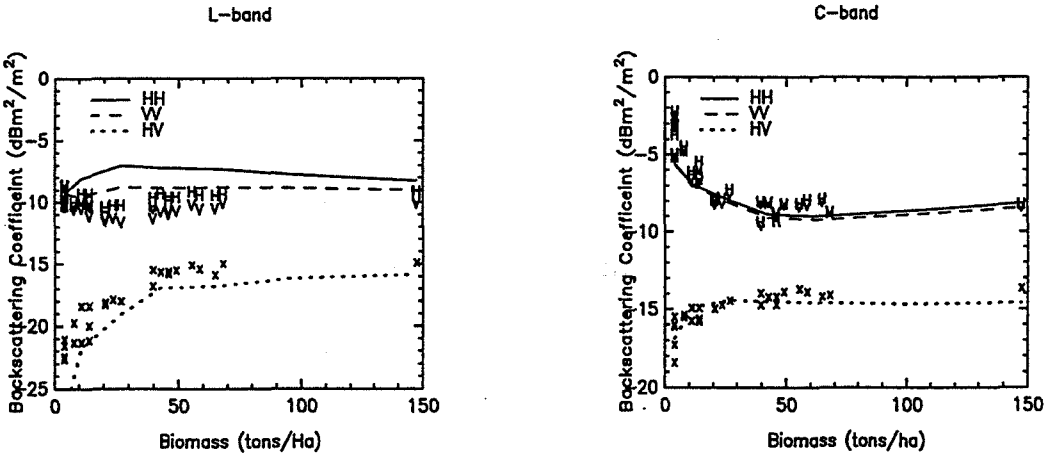

Figure 1: Comparison of measured and model backscattering coefficients at L-band and C-band.

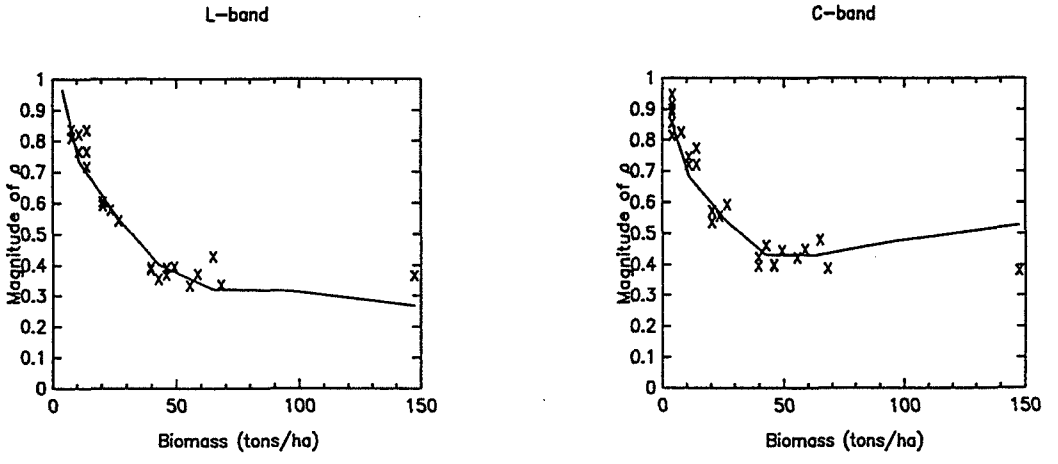

Figure 2: Comparison of measured and model correlation coefficient ρ at L-band and C-band.

Dr. Fred A. Kruse
Analytical Imaging and Geophysics LLC
4450 Arapahoe Ave, Suite 100
Boulder, CO 80303

Comparative Lithological Mapping using Multipolarization, Multifrequency Imaging Radar and Multispectral Optical Remote Sensing

OBJECTIVES

The objectives of this research have evolved over time based on experience with the data, definition of available SIR-C sites, and the availability of resources. The following summarizes the main objectives of the research.

To develop a better understanding of the current geomorphic expression of rock surfaces by determining the relationship between lithological variability, weathering, soil development, and vegetation distribution.

To use variation in radar backscatter as a function of wavelength and polarization to characterize the geometry, and indirectly the composition of rock units.

To compare radar characterization with visible/infrared characterization of surface materials.

To map the character and distribution of lithological variation with SIR-C/X-SAR by preparing detailed lithologic maps of selected sites.

PROGRESS

Until 31 March 1995, this research was supported with the University of Colorado. Effective 10 April 1995, this SIR-C research was transferred to Analytical Imaging and Geophysics LLC (AIG), Boulder, Colorado.

A Final Report was submitted on 31 March 1995. This report summarized significant results for research conducted at the University of Colorado. The research at CU concentrated on compiling and analyzing optical and SAR data sets, learning better how to use SAR data for geologic mapping, and establishing the framework for geologic analysis using SIR-C. This included much of the preparatory work for SIR-C, including acquiring NASA Airborne data and preparing multiple optical and SAR data sets for analysis and use with the SIR-C data. Data analyzed included Airborne Visible/Infrared Imaging Spectrometer (AVIRIS), Thermal Infrared Multispectral Scanner (TIMS), and JPL airborne SAR (AIRSAR). Small sample data sets for a site near the northern Grapevine Mountains, California/Nevada, were georeferenced and combined analysis was performed. The AVIRIS and TIMS data provided detailed lithologic information in the form of mineral maps and color composite images. The AIRSAR data were processed to color composite images and a small perturbation model was also used to extract surface roughness values from the data. Several sessions of field mapping and verification were conducted. Algorithms were developed that could be applied to the SIR-C data. Preliminary processing of SRL-1 data from the Death Valley Supersite included initial registration of X-SAR to the fully polarimetric SIR-C data, generation of gray scale and three frequency color composite images, and trial inversion of the SIR-C data to surface roughness. Two field checks of SIR-C processing results were conducted in January and March 1995. Significant results are summarized below.

-Research at AIG from 10 April 1995 to present has concentrated on utilizing the SIR-C and X-SAR data from SRL-1 and SRL-2 for geologic mapping. Six two-month research phases have been completed.

-Research during Phase I (10 April to 31 May 1995) of the AIG contract concentrated on analysis of SIR-C/X-SAR data for one area near Stovepipe Wells, California, the "Kit Fox Hills" area and two areas at the north end of Death Valley National Park. SIR-C and X-SAR data from SRL-1 DT 120.30 were processed to produce image-maps of these sites as the basis for detailed lithologic mapping and field investigations. Processing included extraction of compressed data products from 8 mm tapes, synthesis of individual frequency and polarization images for SIR-C data, interactive viewing and analysis of individual detected images and color composites, and generation of hard-copy images for visual analysis. SIR-C and X-SAR data were co-registered using ground control points (GCPs) and color composite images were made utilizing the three frequencies. JPL AIRSAR data were available for two of the above sites, the Kit Fox Hills area and one of the northern Death Valley National Park sites. Specific frequencies and polarizations were also synthesized for these data and visual comparisons made to the SRL-1 SIR-C/X-SAR data. Both LANDSAT Thematic Mapper (TM) and Thermal Infrared Multispectral Scanner (TIMS) data were available for the one northern Death Valley National Park site. These were co-registered to the SIR-C/X-SAR data and used for combined analysis. Limited field reconnaissance was conducted for all sites during April 1995 in conjunction with a JPL-sponsored coordination meeting with other SIR-C investigators conducting work at the Death Valley Supersite.

-Research during Phase II (1 June - 31 July 1995) of the AIG contract concentrated primarily on one area in Death Valley National Park. For Death Valley, SIR-C and X-SAR data from SRL-1 DT 120.30 were processed to produce image-maps of these sites as the basis for detailed lithologic mapping and field investigations. The key results are summarized in the significant results section below; additional results are described in a manuscript submitted to TGARS. Processing was a continuation of work conducted during Phase I and included synthesis of individual frequency and polarization images for SIR-C data, interactive viewing and analysis of individual detected images and color composites, and generation of hard-copy images for visual analysis. A small perturbation model was used to calculate the geophysical parameters "RMS surface roughness" and "Fractal Dimension." SIR-C and X-SAR data geometric corrections were refined using additional ground control points (GCPs). Images were coregistered with SPOT, TM, and TIMS and map located (geo-located). The combined data sets were used for integrated analysis.

Phase III (1 August - 30 September 1995) concentrated on one area in the Bighorn Basin, Wyoming. Data from SRL-1 DT 51.31 were processed and analyzed to produce image maps of portions of the Bighorn Basin near Greybull, Wyoming, as the basis for detailed lithologic mapping and field investigations. Processing and analysis included reading of SIR-C/X-SAR data from distribution tape, synthesis of individual frequency and polarization images for SIR-C data, interactive viewing and analysis of individual detected images and color composites, and generation of hard-copy images for visual analysis. The X-SAR data were registered to the SIR-C data using 20 manually-selected GCPs, Delaunay Triangulation warping, and nearest neighbor resampling. Both SIR-C and X-SAR data were further registered to LANDSAT TM images using 50 GCPs, Delaunay Triangulation, and nearest neighbor resampling. The images were used for digital analysis and manual interpretation followed by field reconnaissance during September 1995.

Phase IV (1 October - 30 November 1995) research concentrated on processing and analysis for a portion of the Death Valley SIR-C Supersite. Survey data from both the SRL-1 and SRL-2, CD-ROM sets were used to construct a mosaic covering the Death Valley Supersite. The purpose of this mosaic was to provide a regional overview of the site as an aid to structural interpretation, and to assist in selection, processing, and archiving of SIR-C/X-SAR data sets for precision processing. Two precision SIR-C/X-SAR data sets were also processed and analyzed to produce

image maps of portions of the Death Valley Supersite during the Phase IV effort. The effort using these products during this phase consisted of: selection of the data sets, reading of SIR-C/X-SAR data from distribution tapes, synthesis of individual frequency and polarization images for SIR-C data, interactive viewing and analysis of individual detected images and color composites, and generation of hard-copy images for visual analysis. Both sets of X-SAR data (SRL-1) and (SRL-2) were registered to the SIR-C data, and color-composite images were made for SRL-1 and SRL-2 data covering the same area. The objective of this work was to allow comparison of data from the two missions and assess the effect of specific radar acquisition parameters on the geologic information content of the imagery. Four AVIRIS scenes covering a subarea within the Death Valley Supersite were calibrated to reflectance using the ATREM atmospheric model during Phase IV. The data quality was assessed by interactive viewing, and preliminary analysis of individual scenes was started. Band 30 (0.66 mm) of all 4 scenes were map-referenced to allow future production of standard image maps from the data.

-Research conducted during Phase V was primarily a continuation of the Phase IV research and concentrated on processing and analysis of SIR-C data and AVIRIS data for portions of the Death Valley SIR-C Supersite. The Survey data mosaic constructed during Phase IV was printed at 1:250,000 scale and used to identify areas for further analysis. The precision SIR-C/X-SAR data sets processed during Phase IV were map-referenced during Phase V to produce high resolution image maps for comparison and combined processing with AVIRIS data. 1994 AVIRIS data processed during Phase IV were map-registered during Phase V and analysis products used to produce thematic image maps for comparison to SIR-C results. 1995 AVIRIS data for the northern Death Valley site were calibrated to reflectance using the ATREM atmospheric model, the data quality was assessed by interactive viewing, and mineral maps were made for sites previously analyzed using LANDSAT TM and SIR-C/X-SAR.

Phase VI research consisted of work at a variety of sites. Survey data from both the SRL-1 and SRL-2 CD-ROM sets were used to construct a mosaic covering the Bighorn Basin, Wyoming Site. The purpose of this mosaic was to provide a regional overview of the site as an aid to structural interpretation, and to assist in selection, processing, and archiving of SIR-C/X-SAR data sets for precision processing. SIR-C and X-SAR data were co-registered for a site in northern Sonora, Mexico, and multifrequency-multipolarization analysis was conducted. A digital elevation model derived by JPL from SIR-C data using interferometric methods was analyzed for a site at the southern end of Death Valley (the Owlshead Mtns.). The SIR-C DEM and SAR data were compared with standard USGS DEM products.

SIGNIFICANT RESULTS

Significant results of the research conducted under JPL Contract 958456 at the University of Colorado include:

Successful use of combined optical/SAR data to provide new insights for geologic mapping, particularly of alluvial materials. Mapping of selected locations within the Death Valley SIR-C Supersite.

Extraction of quantitative surface roughness using both AIRSAR and SIR-C to establish that under correct conditions (low topographic relief, composition and weathering characteristics closely linked, little surface moisture, and minimal vegetation cover), close associations do exist between lithology and fan roughness (e.g., hydrothermal alteration of granitic material produced smoother fan that fan derived from unaltered granite).

Demonstrated, that in most cases, however, fan morphology and lithology are more closely related to tectonics and fan age rather than directly to bedrock composition.

Training of graduate students in radar image processing at CSES and partial funding of one Ph. D. student for SIR-C studies in Sonora, Mexico.

Design, development, and delivery to JPL of the "Radar Analysis and Visualization Environment (RAVEN)" for analysis of polarimetric radar data. This software is now one of the standard software products released by JPL to the imaging radar community.

Partial support of a subcontract to VEXCEL corporation to develop model-based techniques and software for geometric registration and rectification of AIRSAR and SIR-C/X-SAR.

Hosted SIR-C PI Geoffrey Taylor from the University of New South Wales, Sydney, Australia, from July - November 1994, providing training and assistance for digital processing of AIRSAR and SIR-C data. Co-authored two papers based on cooperative research.

Significant results of research conducted under JPL Contract 960248 at Analytical Imaging and Geophysics LLC (AIG) include:

Processing and analysis of SIR-C/X-SAR data for several sites in Death Valley National Park, a regional study in the Bighorn Basin, Wyoming, and study of one site in Sonora, Mexico, indicate that the SIR-C data from both SRL-1 and SRL-2 are of high quality and useful for geologic mapping. Several test sites were analyzed in detail and field reconnaissance verifies image processing and analysis results.

Efforts towards SIR-C/X-SAR registration indicate that this is basically a non-issue other than the time and effort involved to perform the picking of ground control points. The two SAR datasets can be co-registered to acceptable error limits using standard image-to-image registration procedures available in many commercial remote sensing packages. Registration of images synthesized from the SIR-C MLC and the X-SAR MLD standard products is straightforward using ground control points. Registration of slant-range images synthesized from SIR-C SLC data is not as easy and errors are larger. It would be better if future multifrequency SAR missions would deliver inherently co-registered data sets to investigators.

Registration of optical data sets to the SIR-C data is more difficult than coregistration of SAR data, but still relatively easy. Standard image processing systems can be successfully used to perform the registrations. Because of the difference in the physics, however (active vs passive), and SAR artifacts such as layover and foreshortening and radar shadow, it is not possible to achieve the low RMS errors possible between SAR data sets. Registration for digital analysis requires significantly more ground control points to achieve the desired registration accuracy.

Standard image processing procedures available in many commercial remote sensing packages can be used effectively to extract useful geologic information from the SIR-C/X-SAR data. Simple color composites provided sufficient detail to make predictions that require only limited field verification. Some of the color distinctions required for interpretation are very subtle. Radar data simply do not make very colorful images for many geologic environments. This indicates that significant portions of the information are present in grayscale images of individual bands, which could just as well be used for the roughness interpretations.

Combined SAR/Optical data sets provide the best way to fully analyze the geology using remote sensing data sets. For alluvial fans in Death Valley, TM data are useful for providing a general overview of the geology. It does not adequately delineate the fans. TIMS data are particularly well suited to determining composition of the fans because of their ability to directly detect silica. In one case two areas were effectively separated corresponding to carbonates and silica. Fans in the

carbonate area, however, were not well separated using only the TIMS data. The SIR-C/X-SAR data were not able to separate the two compositions. They added significantly to the overall analysis, however, because they were able to discriminate the smooth fans with the same compositions (both quartzite and carbonate). The combination of these three data sets provides powerful tools for lithologic mapping. The results of this research show that the combination of optical remote sensing and radar data provides distinct advantages for geologic mapping, particularly of alluvial materials. Insights obtained during this research are being used to develop a model explaining the distribution of fans in the northern end of Death Valley and their relationships to bedrock lithology and tectonics.

Standard multispectral image processing procedures available in commercially available image processing systems were effective in extracting useful geologic information from combined SAR/Optical data sets. Simple color composites provided a wealth of detail for visual interpretation and mapping. Digital analysis and extraction of extended spectral signatures using "hyperspectral" analysis procedures were more effective in characterizing lithologic variability than the multispectral processing techniques. A procedure typically used for analysis of imaging spectrometer data consisting of a Maximum Noise Fraction (MNF) rotation and "Pixel Purity Index (PPI)" determination, followed by visualization using n-Dimensional scatterplots was effective in defining lithologic endmembers for subsequent classification and mapping. These results were also useful in assigning physical basis to colors presented on the color composites generated using multispectral methods.

In combination, these data sets provide complementary information that builds a picture of the geology; TIMS for rock forming minerals, TM and/or AVIRIS for weathering products and some rock forming minerals (carbonate), and SAR for surface morphology. The results of this research are summarized further in proceedings papers and peer-reviewed manuscripts listed below.

FUTURE PLANS (FY 1996)

In general, the focus during the remainder of FY '96 will be to use the SIR-C/X-SAR data from both SRL-1 and SRL-2 in combination with ancillary data sets to conduct geologic mapping at sites identified prior to the missions. The emphasis will be on producing refereed publications illustrating the research results. Specific milestones called for in the contract include the following:

Phase VII (1 April - 31 May 1996)
- Multifrequency/polarimetric analysis of Bighorn Basin, WY SIR-C/X-SAR data
- Comparison of ascending and descending track SIR-C data for Bighorn Basin
- Evaluation and processing of 1995 Bighorn Basin AVIRIS
- Submit bi-monthly report summarizing results to JPL

Phase VIII (1 June - 31 July 1996)
- Multifrequency/polarimetric analysis of Bighorn Basin, WY site (continued)
- Comparison of ascending and descending track SIR-C data for Bighorn Basin
- Integration of AVIRIS and SIR-C data for portions of Bighorn Basin site
- Preparation of draft manuscript summarizing selected SIR-C analysis results for submission to professional journal
- Submit bi-monthly report summarizing results to JPL

Phase IX (1 August - 30 September 1996)
- Co-registration of SIR-C/X-SAR for Palm Valley, Australia Site
- Map registration of TM data for Palm Valley
- Map registration of SIR-C/X-SAR data for Palm Valley
- Combined analysis of TM and SAR data for Palm Valley

- Submit bi-monthly report summarizing results to JPL

FY 1997 PLANS

The emphasis during FY '97 will be on regional mapping and refinement of regional tectonic and lithologic models. The following summarizes probable research directions.

- Map referencing and regional analysis using SIR-C/X-SAR data
- Combined analysis with LANDSAT TM and other available optical data
- Refinement of lithologic and tectonic models
- Final Field Checking and Verification
- Extension to other sites worldwide
- Refereed publications summarizing research results

PUBLICATIONS

Kruse, F. A., 1996, "Geologic mapping using combined LANDSAT TM, Thermal Infrared Multispectral Scanner (TIMS), and SIR-C/X-SAR data," *IEEE Transactions on Geoscience and Remote Sensing (TGARS)*, (in revision, 3/96).

Taylor, G. R., Mah, A. H., Kruse, F. A., Kierein-Young, K. S., Hewson, R. D., and Bennett, B. A., 1996, "Characterization of saline soils using polarimetric SAR data," *Remote Sensing of Environment*, (in press).

Taylor, G. R., Mah, A. H., Kruse, F. A., Kierein-Young, K. S., Hewson, R. D., and Bennett, B. A., 1996, "The extraction of soil dielectric properties from AIRSAR data," *International Journal of Remote Sensing*, (in press).

Kruse, F. A., Lefkoff, A. B., and Dietz, J. B., 1993, "Expert System-Based Mineral Mapping in northern Death Valley, California/Nevada using the Airborne Visible/Infrared Imaging Spectrometer (AVIRIS)," *Remote Sensing of Environment*, Special issue on AVIRIS, May-June 1993, v. 44, pp. 309 - 336.

Kruse, F. A., and Lefkoff, A. B., 1993, "Knowledge-based geologic mapping with imaging spectrometers," *Remote Sensing Reviews*, Special Issue on NASA Innovative Research Program (IRP) results, v. 8, pp. 3 - 28.

Ph. D. DISSERTATION

Kierein-Young, K. S., 1995, "Integration of quantitative geophysical information from optical and radar remotely sensed data to characterize mineralogy and morphology of surfaces," Unpublished Ph. D. Dissertation, University of Colorado, Boulder, p. 220.

PROCEEDINGS PAPERS

Kruse, F. A., 1996, "Geologic mapping using combined optical remote sensing and SIR-C/X-SAR data," in proceedings, 11th Thematic Conference, Applied Geologic Remote Sensing, 27 - 29 February, 1996, *Environmental Reserach Institute of Michigan (ERIM)*, Ann Arbor, MI, pp. II-142 - II-148.

Kruse, F. A., 1995, "Mapping spectral variability of geologic targets using Airborne Visible/Infrared Imaging Spectrometer (AVIRIS) data and a combined spectral feature/unmixing approach," in Proceedings, *AeroSense 95*, SPIE, 17-21 April 1995, Orlando, Florida, (in press).

Kruse, F. A., 1993, "Geologic mapping using integrated AIRSAR, AVIRIS, and TIMS data," in Summaries of the 4th JPL Airborne Geoscience Workshop, Washington, DC, JPL Publication 93-26, v. 3., pp. 29 - 32, Jet Propulsion Laboratory, Pasadena, CA.

Curlander, J., Leberl, F., and Kruse, F. A., 1992, "Geometric Ortho-Rectification and Generation of s-zero Image Products from Multiple Incidence Synthetic Aperture Radar Images," in Proceedings, *IGARSS '92*, 26-29 May, 1992, Houston, TX, IEEE Catalog Number 92CH3041-1, v. 1, pp. 111-113.

Kierein-Young, K. S., Kruse, F. A., and Lefkoff, A. B., 1992, "Quantitative analysis of surface characteristics and morphology in Death Valley, California using AIRSAR data," in Proceedings, *IGARSS '92*, 26-29 May, 1992, Houston, TX, IEEE Catalog Number 92CH3041-1, v. 1, pp. 392 - 394.

Kruse, F. A., 1992, "Geologic Remote Sensing - New Technology, New Information," in Proceedings, *IGARSS '92*, 26-29 May, 1992, Houston, TX, IEEE Catalog Number 92CH3041-1, v. 1, pp. 625 - 627.

Kierein-Young, K. S., and Kruse, F. A., 1992, "Extraction of Quantitative Surface Characteristics from AIRSAR Data for Death Valley, California," in Summaries of the *3rd Annual JPL Airborne Geoscience Workshop, AIRSAR Workshop*, JPL Publication 92-14, v. 3, pp. 46 - 48, Jet Propulsion Laboratory, Pasadena, CA.

Kierein-Young, K. S., Lefkoff, A. B., and Kruse, F. A., 1992, "Radar Analysis and Visualization Environment (RAVEN): Software for Polarimetric Radar Analysis," in Summaries of the *3rd Annual JPL Airborne Geoscience Workshop, AIRSAR Workshop*, JPL Publication 92-14, v. 3, pp. 78 - 80, Jet Propulsion Laboratory, Pasadena, CA.

Kruse, F. A., Dietz J. B., and Kierein-Young, K. S., 1991, (Extended Abst.), "Geologic Mapping in Death Valley, California/Nevada Using NASA/JPL Airborne Systems (AVIRIS, TIMS, and AIRSAR)," in Proceedings of the *3rd Airborne Synthetic Aperture Radar (AIRSAR) workshop,* 23 - 24 May 1991, JPL Publication 91-30, pp. 126-127, Jet Propulsion Laboratory, Pasadena, CA.

Kruse, F. A., and Dietz, J. B., 1991, "Integration of diverse remote sensing data sets for geologic mapping and resource exploration," *SPIE Symposium on Remote Sensing for Geology and Geophysics*, 1-5 April 1991, Orlando, Florida, v. 1492, pp. 326-337.

Kruse, F. A., and Dietz, J. B., 1991, "Integration of visible- through microwave-range multispectral image data sets for geologic mapping," in Proceedings of the Cinquiäme Colloque International, Mesures Physiques et Signatures En TÇlÇdÇtection, 14 - 18 January 1991, Courchevel, France, *European Space Agency*, esa SP-319, v. 2, pp. 481-486.

Kruse, F. A., and Dietz, J. B., 1991, "Integration of optical and microwave images for geologic mapping and resource exploration," in Proceedings, *International Symposium on Remote Sensing of Environment, Thematic Conference on Remote Sensing for Exploration Geology,* 8th, 29 April - 2 May 1991, Denver, Colorado, Environmental Research Institute of Michigan, Ann Arbor, pp. 535-548.

Kierein-Young, K. S., and Kruse, F. A., 1991, "Quantitative investigations of geologic surfaces utilizing Airborne Visible/Infrared Imaging Spectrometer (AVIRIS) and Polarimetric Radar (AIRSAR) data for Death Valley, California," in Proceedings, *International Symposium on Remote Sensing of Environment, Thematic Conference on Remote Sensing for Exploration Geology*, 8th, 29 April - 2 May 1991, Denver, Colorado, Environmental Research Institute of Michigan, Ann Arbor, pp. 495-506.

IN-HOUSE REPORTS

Kruse, F. A., 1995, Final Report - JPL Contract 958456, *Center for the Study of Earth from Space (CSES)*, University of Colorado, Boulder, p. 43.

Lefkoff, A. B., Kruse, F. A., and Kierein-Young, K. S., 1993, "Radar Analysis and Visualization Environment (RAVEN User's Guide, Version 1.0 (Prototype)," *Center for the Study of Earth from Space (CSES)*, p. 20.

TRADE JOURNALS

Kruse, F. A., 1992, T"he analysis of scientific data from NASA airborne systems," *Scientific Computing & Automation*, June 1992, Elsevier, pp. 15-22.

Dr. Thuy Le Toan
Centre d'Etudes-Spatiales
des Rayonnements
9 Av. Colonel-Roche, B.P. 4346
31029 Toulouse-CEDEX
France

Co-Investigators:
P. Hoogeboom Physics & Elect. Lab. TNO
A. Fiumara Telespazio

Relating Radar Backscatter Responses to Woody and Foliar Biomass of Pine Forests

OBJECTIVES

Demonstrate the use of spaceborne SAR images to detect forest parameters (biomass of different parts of the canopy).

Increase the understanding of the interaction between microwaves and vegetation canopies.

PROGRESS

Forest studies

The overall objective of forest studies developed in the frame of SIR-C/X-SAR data analysis has been to assess the capability of multi-incidence polarimetric data for the inversion of forest biomass, and for the monitoring of deforestation. SIR-C/X-SAR data acquired over Les Landes Forest test site in France have been compared with a theoretical modeling using a four layer radiative transfer model [Hsu et al. 1994].

The model has been subsequently used to determine the major contributions of the tree backscattering mechanisms, but also to define the optimal configurations (incidence, frequency, polarization) accordingly to the objectives (estimation of crown biomass, woody biomass, LAI,...).

Among the intensity information (i.e. backscattering coefficients σ° hh, σ° vv, σ° hv), L-band HV backscattering at 51 has been found to offer the highest sensitivity to biomass content on the range [0 tons/ha, 150 tons/ha].

Regarding the polarimetric information of the measurement, C-band degree of coherence between HH and VV signals at low incidence angle (26.4) provided the best results for forest/non forest segmentation. Based on the C-band coherence, the unsupervised extraction of regenerating forest has been achieved with an accuracy higher than 85%, while the discrimination between forest and nonforest areas has indicated an accuracy of 87%. Maps of coherence have been therefore derived, and compared with the corresponding color composite intensity images. Refined details of the area, as well as forest/nonforest segmentation have been shown to be emphasized on the coherence maps, showing complementarity between polarimetric and intensity information for forest segmentation and for forest parameters retrieval.

Retrieval of soil moisture from SIR-C/X-SAR data

The main objective of soil moisture studies based on SIR-C/X-SAR data analysis has been to investigate the effect of surface roughness and soil moisture on polarimetric SAR with the aim of

inverting SAR data either into roughness-states, or into soil moisture with a reduced effect of surface roughness.

For this, SIR-C/X-SAR data acquired during the first and second missions over bare fields located at the Landes (France) and Matera (Italy) test areas have been analyzed. In addition, the dependence of the copolarized correlation coefficient on the roughness state has been also addressed. In order to investigate the effect of polarization, the correlation coefficient has been derived for any pp-qq polarization states, where (p,q) is a basis of orthogonal polarizations. The results have indicated that the sensitivity of the correlation coefficient to the roughness state is enhanced at the circular polarization compared to the HH-VV polarization.

FUTURE PLANS

Forest

The technique developed over Les Landes test site for biomass inversion and deforestation studies will be assessed for other types of forest canopies. A study has been initiated over a tropical forest area in Brazil. The site of Sena Madureira, where extensive deforestation activities are in progress, will be of particular interest. The preliminary results show an obvious complement between intensity and coherence images, but require further ground truth informations to be fully understood. In addition, polarization synthesis techniques will be assessed for the improvement of biomass monitoring.

Soil moisture studies

The preliminary results have shown that the sensitivity of the correlation coefficient to the roughness state is enhanced when expressed in a circular polarization basis, compared to a linear basis. Polarization synthesis techniques are expected to be useful for filtering roughness effects in the backscattering from rough surfaces.

A topic for further studies will be to derive maps of soil roughness based on the degree of coherence expressed in a linear polarization's basis, and subsequently to assess the moisture inversion problem, provided that full polarimetric data are available.

In addition, within the frame of an IGPB project, SALT (Savanas in the Long Term) project, transitions between forest and desert in West Africa have been studied. These areas are expected to present similar moisture content from one year to the other, for a given period of the year. One particularity of these transition zones is the existence of inhomogeneous areas, composed of soils and scattered trees of very low density. These transition zones represent an opportunity to study radar responses of different transitional regions, from sub tropical forest to desert. SIR-C/X-SAR data requested will concern a Sahel transect. The research topics related to these subjects will deal will responses of different surface types (i.e. roughness mapping), as well as the modelling of mixed radar pixels.

Rice

A topic for future studies is the mapping of rice fields in different parts of the world, the classification of rice fields at various stages of growth.

In the past few years, investigations have been carried out using X-band airborne Synthetic Aperture Radar (SAR) in France [Le Toan et al., 1989]. The results showed an increase of the radar backscatter with days after transplantation until a plateau approximately at heading stage. This increase coincides with the increase of biomass and has been explained by the dominant vegetation-

water interaction scattering mechanism. Récent studies lead in Japan [Kurosu et al., 1995] and in Indonesia [Le Toan et al., 1995] confirmed this temporal behavior of the radar backscatter.

A theoretical model of scattering from rice plants at different growth stages [Le Toan et al., 1995] has been developed. The result shows that the specific structure of rice fields (vertical sticks distributed on a flooded surface) produces a backscattered response critically dependent of the polarization state. Hence, the use of SIR-C/X-SAR to identify rice fields appears promising.

The aim of the future study will be to study the polarimetric/multifrequency behavior of rice fields, in order to derive robust methods of rice monitoring.

The investigations will be performed on multitemporal and multipolarization X and C band SAR images over test sites where rice fields maps are available, including the following steps :

- the retrieval of radar backscatter values from SAR images,
- the analysis of the polarization and temporal responses of the vegetation cover to highlight the particular behavior of flooded rice fields and to determine the information carried by multipolarization,
- the interpretation of the observations of rice fields by simulation using a, theoretical model.

PUBLICATIONS

Souyris J. C., Le Toan T., Hsu C. C., Kong J. A., "Assessment of SIR-C/X-SAR polarimetric data for the estimation of forest parameters," *Conference proceedings Third international workshop on radar polarimetry*, pp. 636-645, Nantes (France), March 1995.

Souyris J. C., Le Toan T., Kong J. A., Hsu C. C., "Inversion of Landes Forest biomass using SIR-C/X-SAR data : experiment and theory," *Conference Proceedings IGARSS '95*, pp. 1201-1203, Firenze, Italy.

Wang L., Johnson J. T., Hsu C. C., Kong J. A., Souyris J. C., Le Toan T., "Application of neural networks to the inversion of geophysical parameters," *Conference proceedings PIERS '95*, University of Washington, Seattle, USA, p. 278, July 24-28, 1995.

Souyris J. C., Le Toan T., Zhang Y., Hsu C. C., Kong J. A., "Inversion of biomass with polarimetric data from SIR-C/X-SAR," *Conference Proceedings PIERS '95*, p. 902, University of Washington, Seattle, USA, July 24-28, 1995.

Hsu C. C., Kong J. A., Souyris J. C., Le Toan T., "Application of radiative transfer modeling to the polarimetric backscattering of forest," *Conference Proceedings PIERS '95*, p. 903, University of Washington, Seattle, USA, July 24-28, 1995.

Hsu C. C., L. Wang, J. A. Kong, Souyris J. C., T. Le Toan 2 Theoretical modeling for microwave remote sensing of forest, accepted to International Symposium 2 Retrieval of bio- and geophysical parameters from SAR data for land applications, Toulouse, France, October 10-13, 1995.

Souyris J. C., Le Toan T., Hsu C. C., Kong J. A., 2 Inversion of Landes Forest biomass using SIR-C/X-SAR data, accepted to International Symposium 2 Retrieval of bio- and geophysical parameters from SAR data for land applications, Toulouse, France, October 10-13, 1995.

Mattia F., T. Le Toan, J. C. Souyris, De Carolis, G., G. Pasquariello, F. Posa, P. Smacchia, N. Floury, 2 Soil moisture estimation from multipolarization and multifrequency SAR data, *Proceedings IEEE Workshop Retrieval of bio- and geophysical parameters from SAR data for land applications*, Toulouse, 10-13 October 1995.

New publications scheduled

Le Toan T., Souyris J.-C., Hsu C. C., Kong J. A., "Inversion of Landes Forest biomass using SIR-C/X-SAR data : Experiment and Theory." In preparation. To be submitted to IEEE/TGRS, or IJRS.

Souyris J. C., T. Le Toan, N. Floury, C. C. Hsu, J. A. Kong, 2 Use of polarization synthesis for deforestation studies based on SIR-C/X-SAR data analysis accepted to *IGARSS '96*, Lincoln, Nebraska.

Le Toan T., J. C. Souyris, C. C. Hsu, L. Wang, J. A. Kong, 2 Microwave remote sensing of natural targets: theory and experiment, accepted to Agard Symposium on 2 remote sensing, a valuable source of information, Toulouse, France, 22-25 April 1996.

Le Toan T., Ribbes F., Floury N., Wang L., Kong J. A., Kurosu T. and Fujita M., 1996. Rice crop monitoring using ERS-1 data: experiment and modelling , Submitted to IEEE Transactions on Geoscience and Remote sensing.

References

Hsu, C. C., H. C. Han, R. T. Shin, J. A. Kong, A. Beaudoin and T. Le Toan, "Radiative transfer theory for polarimetric remote sensing of pine forest," *International Journal of Remote Sensing*, Vol. 15, no. 14, pp. 2943-2954, September 1994.

Kurosu T., Fujita M. et Chiba K., 1995. Monitoring of rice crop growth from space with ERS-1 C-band SAR. Submitted to *IEEE. Trans. on Geoscience and Remote Sensing.*

Le Toan T., Laur H., Mougin E., Lopes A., 1989. Multitemporal and dual- polarization observations of agricultural vegetation covers by X-band SAR images. *IEEE Transactions on Geoscience and Remote Sensing*, vol. GE-27, N6, Nov. 1989, pp. 709-717.

Le Toan T., Ribbes F., Floury N., Wang L., Kong J. A., Kurosu T. and Fujita M., 1996. Rice crop monitoring using ERS-1 data: experiment and modelling, Submitted to *IEEE Transactions on Geoscience and Remote sensing.*

John McCauley
Northwestern Arizona University
USGS Emeritus
189 Wilson Canyon Road
Sedona, AZ 86336

Co-Investigators:

Gerald Schaber	Northwestern Arizona University & USGS Emeritus
Carol Breed	NAU & USGS Emeritus
Bahay Issawi	Egypt
Hugues Faure	France
André Simonin	France
Joachim Pachur	Germany
Stefan Kroepelin	Germany

Paleodrainages of the Sahara, SIR-C

OBJECTIVES

Use SIR-C/X-SAR data in a synoptic mode with other remotely sensed data, field, and cartographic data to map relic Cenozoic drainage systems across the Sahara from the Red Sea Hills, Egypt, to the Chad Basin and Atlantic Ocean.

Demonstrate applicability of SIR data, used with Landsat, SPOT and high-altitude photographic data, as a new, cost-effective remote geophysical tool for exploration geology.

Produce a major report on the distribution of paleodrainages in the Sahara, their relations to the basic tectonic elements of North Africa (basins and swells), and their economic potential.

PROGRESS

CDs containing relevant Sahara "Data Takes" have now been received (two key CDs arrived as recently as mid-September '95). Most CDs containing survey data in areas of interest have been distributed to our Co-I's. A list of some 50 scenes we have selected for special processing has been submitted to JPL, primarily for sites in eastern Libya, northern Sudan, and the Sinai Peninsula, where several promising examples of sand-buried paleodrainage patterns are revealed by the L-band radar. We estimate that our total request for special processing will be about 250 scenes, when all of the inputs are received from our foreign Co-I's.

We have completed preliminary review of all the Saharan swaths received by the Paleodrainage Team (to Sept. '95). This was done on the PI's Pentium computer system which allowed the production of enhanced and scaled survey images at the 1:500,000-scale, which were then registered to 1:500,000-scale Tactical Plot charts of North Africa, provided to us by the U.S. Army Topographic Engineering Center, Ft. Belvoir, VA. These charts show all of the visible (surface) drainage systems located by conventional mapping system. By comparing them with the SIR-C radar images, because of the ability of SIR-C to image into the shallow subsurface in sand covered areas, we are able to delineate previously unrecognized watercourses. Our ultimate objective is to produce a map at the largest practical scale (1:2,000,000?) showing the newly found drainages against a background of those already mapped. This map is expected to have broad practical applications for water resources, mineral exploration, and land use in several parts of North Africa. This effort will also make use of the astronaut photography and ERS-1 data. Extensive collaboration has taken place over the past eighteen months with our foreign Co-I's and Collaborators, both by fax, e-mail, and in person before, during and after the Uberlingen meeting.

(1) Data analysis plans and long range plans were discussed and an invitation was extended to our group to participate in field work in the Sahara with the newly funded German desert team under the direction of Dr. Stefan Kroepelin, University of Cologne, Germany. New vehicles, equipment, base camp buildings, etc. are currently being assembled as part of this new project, entitled "Environmental and Cultural Change in Arid Africa." We intend to follow up on this opportunity at the earliest possible time (probably Oct./Nov. '96).

(2) Also in Germany, Dr. Joachim Pachur, Free University of Berlin has agreed to take the lead in investigating the SIR-C coverage of the Wadi Kufra area in southeast Libya. We reported preliminary work on this river system at the Spring AGU Meeting in Baltimore. A graduate student of Prof. Pachur (Mr. Frank Rottinger, who attended the Uberlingen Meeting) who will do his Ph.D. on newly defined paleoriver systems in the southern Sahara will be coming to our facility in Flagstaff this fall to begin work with SIR-C data. Both German groups have access to Libya whereas we do not and are happy to defer to them.

(3) Data analysis planning with the French group at the University of Marseilles also took place after the Uberlingen meeting and we had preliminary discussions about their possible return to northeastern Chad for various Quaternary studies and visits to key paleodrainage localities that are also presently out of reach of U.S. investigators for political reasons.

(4) Bahay Issawi, former Director of the Egyptian Geological Survey, spent nine days at the Sedona office of the P.I. and also visited the USGS offices in Flagstaff. This time was spent relating the SIR-C data to regional geology of Egypt and preparing the first draft of the paper submitted to the IEEE Special Issue and demonstrating various data analysis techniques for use in Egypt. Meetings were also held in Flagstaff with a representative of the Saudi Arabian SIR-C Paleodrainage Experiment. Plans for a special session on imaging radar results in Egypt were first formulated. During the time period we also spent much time revising the requirements for our experiment in order to obtain the best mission plan for possible Sahara coverage consistent with the needs of other experiments for SRL-2. The overall plan was presented to all interested geology investigators at the June 19, '94 Team Meeting at JPL.

(5) Carol Breed and the P.I. attended the SRL-2 launch (at our own expense) where we had the opportunity to discuss the merits of SIR with Dr. John Hansen, Director of Research at the Topographic Engineering Center, U.S. Army Corps of Engineers, Ft. Belvoir, VA. This led to further discussions, cartographic support, and a minor amount of funding for a demonstration project by Carol Breed for the purpose of finding desert water resources. We also helped to prepare after the mission several PIO captions (particularly SafSaf, Egypt) for JPL.

(6) Briefed the SRL-2 Astronaut Crew (May 4-5) at our facility in Flagstaff on the objectives of the Paleodrainage experiment and desert landforms in general. This was followed by an overnight field trip to the Painted Desert east of Flagstaff where they gained visual experience with sand-filled river channels, wind erosion features, sand sheets and sand dunes. Later in the year (Sept. 23), we met with SRL-1 astronaut Linda Godwin in Flagstaff to discuss preliminary results of the first flight and to attend her lecture at Northern Arizona University where our SIR work was amply referenced.

FUTURE PLANS

As explained above, we anticipate needing an additional 150 to 200 specially processed segments of SIR-C data, in order to do justice to the data and to take advantage of the field expertise of our foreign Co-I's and Collaborators. This requirement stems from the areal scope of the Saharan Paleodrainage Investigation, which covers an area roughly equivalent to that of the USA.

Prepare a synoptic map (as described above) of the newly defined SIR-C paleodrainages of North Africa.

Participate in the special conference on North African radar applications as part of the EGSMA Centennial, and submit paper.

Participate in a field campaign with the newly-formed German desert group (with direction of S. Kroepelin). Emphasis will be on radar response studies at Safsaf (in cooperation with P.I. G.G. Schaber) and the applications of SIR-C data to hydrological and archaeological prospecting. One of the key German radar experts has stated, during training sessions for desert researchers, that the paleodrainage results were the most significant of the entire mission. We expect numerous publications to come from this work, both in European and U.S. journals.

We also anticipate close cooperation and multiple publications with our numerous French colleagues. These will not necessarily be limited to paleodrainage features, but will also include studies of duricrusts (calcrete, gypcrete, ferricrete), and landscape evolution as a function of the interplay between running water and wind driven by climate change in the Sahara.

PUBLICATIONS

Schaber, G.G., McCauley, J.F., and Breed, C.S., 1994, New radar images of Safsaf Oasis and vicinity, southern Egypt, *Geological Society of America Abstracts with Programs*, v. 26, no. 7, p. 127. 1994 Annual Meetings, Seattle, WA.

McCauley, J.F., Breed, C.S., and Schaber, G.G., 1995, SIR-C definition of the Serir-Kufra River system in SE Libya: Poster no. P51A-4, AGU Spring Symposium, *EOS Supplement*, p. 5194.

McCauley, J.F., Breed, C.S., and Schaber, G.G., 1995, Mapping the Wadi Kufra paleodrainage system in eastern Libya using spaceborne imaging radar, Poster presentation at Symposium on Retrieval of bio and geophysical parameters for SAR data for land applications, Toulouse, France (October 1995), in press.

Schaber, G.G., McCauley, J.F., Breed, C.S., and Issawi, Bahay, 1995, The roles of wavelength and polarization in geologic studies at Bir Safsaf (Egypt) using SIR-C/C/XSAR data, 1995, Abstracts and Programs, *Geol. Soc. of America,* Annual Meetings (New Orleans, LA, November 6-9, 1995), in press.

Dr. John N. Melack
Department of Biological Sciences
University of California
Santa Barbara, CA 93106

Co-Investigators:
Laura Hess Univ. of Calif., Santa Barbara
Yong Wang
Solange Filoso
Dalton Valeriano
Leal Mertes

Determining The Extent Of Inundation On Tropical And Subtropical Floodplains Beneath Vegetation Of Varying Types And Densities

OBJECTIVES

Develop a procedure for recovering the presence, absence, and patchy presence of water and its spatial distribution beneath different floodplain plant communities of varying crown closures, densities, stand geometries, and canopy states for sites in Georgia. Test the applicability of the procedure to the Amazon and Alligator river floodplains in Brazil and Australia.

Modify, extend, and verify the Santa Barbara radar model for different floodplain vegetation types and densities.

Test both discrimination procedures and model predictions for leaf-on/leaf-off and water-on/water-off states against SIR-C/X-SAR and aircraft radar images.

Couple the above modeling and discrimination procedures for floodwater detection and delineation for input to conceptual flood stage/flood area hydrologic models.

PROGRESS

During Space Radar Laboratory (SRL) mission 1 (April 1994), and SRL mission 2 (October 1994), field teams were deployed to the Manaus Supersite in Brazil, the Pantanal Backup site in Brazil and a secondary site near Darwin, Australia. Classified images of the central Amazon within the Manaus supersite were produced within two days of image acquisition during SRL 1 and 2. These images were used widely by TV and newspaper coverage of the missions. In December 1994, a manuscript derived from these images and associated field measurements was submitted to the IEEE Transactions on Geoscience and Remote Sensing; it appeared in the July 1995 issue. Subsequently, analysis has continued on other SIR-C scenes from the central Amazon, Pantanal and northern Australia. A summary of scenes processed, publications, presentations and planned publications is shown in Table 1.

SIGNIFICANT RESULTS

Our research has focused on developing techniques for using synthetic aperture radar (SAR) data to decipher hydrologic and vegetative conditions on floodplains. Knowledge of the seasonal dynamics of inundation and vegetation is the basis for understanding biogeochemical processes such as methane generation and for managing resources such as fisheries and other wildlife. Such information is lacking for most floodplains, particularly in the tropics.

In order to realize the potential for SAR to delineate floodplain inundation and vegetation, robust classification methods are needed which do not require repeated optimization by scene or date. We have therefore employed a rules-based approach, using a decision-tree model to construct

classification rules. Decision tree classifiers are hierarchical multistage classifiers that can use different predictor variables at different stages of the decision process. The decision-tree classification approach was developed and tested using JPL AIRSAR data obtained for the Altamaha River, Georgia. A scene including floodplain and upland was classified using the full set of AIRSAR variables (HH, VV, HV backscattering coefficient and HH/VV phase difference for C-, L- and P-bands) and using subsets of these variables to simulate SIR-C, ERS-1, JERS-1, and Radarsat datasets. Using the full AIRSAR and SIR-C inputs, error rates (percent of training pixels misclassified) were less than 5%. In both cases, the decision tree model selected both long and short wavelengths (C and P or C and L) and both HH and HV polarizations. Error rates were higher using the JERS input (L-HH only); the overall error rate was 11%. Classifications using either ERS-1 (C-VV) or Radarsat (C-HH) configurations had error rates over 35%. High accuracies could be achieved by combining single-wavelength sensors; the overall error rate with a C-HH plus L-HH combination was only 5%.

The SIR-C/X-SAR missions offered the opportunity to test the ability of multi-frequency SAR to accurately delineate tropical floodplain inundation and vegetation from space. Because SIR-C data for our main study area were downlinked and processed during the missions, we were able to test whether such analyses could be completed very rapidly, as would be required for applications such as disaster assessment. We also tested whether decision rules based on a combined (two-date) training set would be significantly less accurate than rules tailored to the individual dates.

During Space Radar Laboratory (SRL) mission 1 (April 1994) and SRL mission 2 (October 1994), field teams were deployed to the Manaus Supersite in Brazil, the Pantanal Backup site in Brazil and a secondary site near Darwin Australia. A field team was also in Brazil during August 1994 in anticipation of the aborted launch of SRL 2. Field measurements in Brazil included ground and boat surveys and over-flights in light aircraft. Ground measurements of vegetation and hydrology included estimates of stem density, plant height above the water, phenology, dielectric constants, canopy closure and water depth. Corner reflectors were deployed to aid calibration of the SAR data. Helicopter over-flights were conducted during the missions in Australia. In late March 1995, Melack revisited the study area and made ground observations and additional over-flights. During AIRSAR transects over our Altamaha site in Georgia, USA, flown in October 1994, boat and aerial surveys were done. SIR-C data were acquired during both Space Radar Lab flights, and "realtime" data were received at ICESS during the missions for the Barroso study area, spanning the floodplains of the Negro and Solimoes (Amazon) rivers about 50 km west of their confluence near the city of Manaus, Brazil. Classified images were produced and tested within two days of SIR-C data acquisition. In December 1994 , a manuscript derived from these images and associated field measurements was submitted to the IEEE Transactions on Geoscience and Remote Sensing; it appeared in the July 1995 issue (Hess et al. 1995, see Table 1). Both C-band and L-band were necessary to distinguish the landcover types. HH polarization was most useful for distinguishing flooded from non-flooded vegetation (C-HH for macrophyte vs. pasture, and L-HH for flooded vs. non-flooded forest), and cross-polarized L-band data provided the best separation between woody and non-woody vegetation. Between the April and October missions, the Amazon River level fell about 3.6 m and the portion of the study area covered by flooded forest decreased from 23% to 12%. Using decision rules derived from the individual scenes, misclassification rates of test pixels were 3% for April and 4% for October. Using rules based on the combined April and October datasets, the misclassification rate for the combined test pixels was 5%. This is a positive indication that it will be feasible to build multidate knowledge on which to base decision rules.

During SRL 1 and 2 we were engaged in public relations activities. Our classified images of the Amazon floodplain were featured repeatedly by CNN News. Melack gave interviews televised on Santa Barbara's TV station KEYT, and our research was reported in a full page article in Santa Barbara's News Press. UCSB highlighted our SIR-C research in its alumni magazine, Coastlines, and its newspaper to faculty and staff, 93106. Some analysis has been conducted for two other wetland SIR-C sites: the Pantanal (Mato Grosso do Sul, Brazil), and the Alligator River (Northern

Territories, Australia) (Hess and Melack-1995). Both sites offer conditions not found in the Amazon or Altamaha sites. The Pantanal landscape is dominated by grasses rather than trees. Some of the aquatic macrophyte communities found at the Alligator River site are quite different structurally from those at the Brazilian or Altamaha sites. For both the Pantanal and Alligator River, we will integrate X-SAR and SIR-C data, which should improve discrimination of macrophyte communities.

In order to better understand the scattering mechanisms operating in flooded and nonflooded forests, and to predict the effect of changes in forest structure variables on backscattering at different wavelengths and polarizations, we simulated C-, L-, and P-band backscatter from a tropical flooded forest using the Santa Barbara microwave canopy backscatter model (Wang et al. 1995). Extensive forest stand data collected at the Anavilhanas flooded forest, a large fluvial archipelago in the lower Negro River near Manaus, were supplemented with published values for similar forest types. Given the same wavelength or incidence angle, the ratio of backscatter from the flooded forest to that from the nonflooded forest was higher at HH polarization than at VV polarization. Given the same wavelength or polarization, the ratio was larger at small incidence angles than at large incidence angles. Given the same polarization or incidence angle, the ratio was larger at a long wavelength than at a short wavelength. As the surface soil moisture underneath the nonflooded forest increased from 10 to 50% of volumetric moisture, the flooded/nonflooded backscatter ratio decreased; the decreases were small at C- and L-band but large at P-band. When the leaf size was comparable to or larger than the wavelength of C-band, the leaf area index (LAI) had a large effect on the simulated C-band (not L-band or P-band) backscatter from the flooded and nonflooded forests.

The Anavilhanas forest is taller and about as dense as other Amazonian closed-canopy varzea forests and igapo forests on clay soils; it is significantly taller and denser than most igapo forests on sandy soils or open-canopy varzea stands. Compared to published values for cypress-tupelo and bottomland hardwood stands of the southeastern U.S., and to seasonally flooded Melaleuca woodlands of Australia, the Anavilhanas forest is denser and has higher LAI and branch biomass. The results from the Anavilhanas modeling thus roughly bound the high end (i.e. maximum canopy attenuation) of the spectrum of several major subtropical and tropical floodplain forest structures. We therefore expect a flooded/nonflooded ratio of at least 2 to 3 dB at small incidence angles for the majority of floodplain forests (which would have lower canopy attenuation than the Anavilhanas stand), at CHH, LHH and PHH. At CVV, we would expect much less contrast between flooded and nonflooded unless the canopy was rather open.

Melack played a key role in preparing for the review of NASA's SAR program by the National Academy of Science's Committee on Earth Sciences. He chaired and hosted the SAR Ecology workshop, co-edited the Ecology chapter in the report to the NAS (Kasischke and Melack 1995) and co-presented the perspectives of the ecological community to the NAS committee.

The research activities at UCSB have a major educational component. The primary team is composed of three graduate students (L. Hess, S. Filoso and D. Valeriano) and one post-doctoral researcher (Y. Wang), who is now an Assistant Professor. Weekly meetings concerned with SAR science and applications also have included other students and faculty, and an increasing number of visitors from abroad or the USA.

FUTURE PLANS

Our research on inundation and ecology of floodplains during the next two years will include (1) further analysis of SIR-C/X-SAR scenes and (2) synergistic use of multisensor data. We estimate that these activities will require about 40 additional SIR-C/X-SAR scenes.

Further analysis of SIR-C/X-SAR and related data: During the next six months we will focus our analyses on two datasets: SIR-C/X-SAR April and October scenes of the Cabaliana reach of the Amazon floodplain and neighboring upland scenes, and 1990, 1991, and 1994 AIRSAR datasets for the Altamaha River. We have conducted extensive field documentation in both areas.

Results from the Cabaliana analysis will be used to refine and extend our classification of aquatic vegetation and will be combined with our Landsat and passive microwave work (see below) to improve regional estimates of methane emission. Our examination of upland forests will evaluate the possibility of retrieving information about tropical forest strucure from SIR-C data. Our measurements of upland forest structure include stem density, basal area, stand height and canopy closure as measured by hemispherical images taken with videography. The study areas have large tracts of primary forest and stands of secondary forest at different stages of regeneration. Several band-polarization combinations will be analyzed for development of algorithms to acquire information on stand structure from SAR data. Similar analysis has been completed using C band data collected during the SAREX mission for a study site near the Tucurui dam in the eastern Amazon.

The Altamaha site has an unusually large range of floodplain forest stand densities, and multiple AIRSAR swaths were obtained over a wide range of incidence angles. These data are therefore being used to document how incidence angle effects on backscattering vary with forest stand type. These results will help in determining guidelines on appropriate incidence angle ranges to use at given wavelength/polarization combinations for wetlands monitoring.

The next step in our SIR-C/X-SAR analysis will be to use the Amazon, Pantanal, Alligator River, and Altamaha datasets to determine the degree to which our classification algorithms are applicable to widely varying types of wetlands, as a step towards a global wetlands mapping strategy. The decision-tree model we are using is well suited to this problem because it is easily updated and can include categorical data such as date, soil or general wetland type. Analysis of the multisite, multidate SIR-C/X-SAR and AIRSAR dataset will allow us to estimate realistically the accuracy achievable and recommend appropriate strategies for wetlands mapping initiatives. For example, Melack is chairing an IGBP workshop designed to develop a strategy for producing a global inventory of inundation and wetland vegetation to be used in conjunction with hydrological, ecological and biogeochemical projects within IGBP and MTPE.

Synergistic use of multisensor data: Inundation of a floodplain is the product of the hydrology of different water types that enter the floodplain. The spatial and temporal patterns are in turn influenced by the topography, soils and vegetation of the floodplain. As a result of such complexity, ecological consequences of inundation and hazards associated with floods vary from river to river and season to season. Our strategy for investigating the processes influencing water, sediment, and nutrient transport to and from floodplains is to insure, through a combination of field, numerical simulation, and remote sensing techniques, that we have hydrologic, geomorphic and vegetation data at sufficient temporal and spatial resolutions to determine the significant processes influencing the pattern of flooding. From a remote sensing perspective, we can determine the following critical elements: (1) the relationship between inundation and water stage for predictive models, (2) the general pattern of vegetative cover, (3) the degree of incursion of different water types, and (4) the seasonal boundaries of inundation. The first element requires fine temporal resolution, as provided by passive microwave sensors. The second and third elements require optical (visible and infrared) and active microwave data at sufficiently fine spatial resolution that flood characteristics can be described as the pattern changes. The boundary of inundation or saturation (element 4) can be mapped using multiband SAR data.

To accomplish these ambitious objectives we have initiated several activities: We have successfully proposed to become ERS-SAR and Radarsat investigators; hence, we will receive ample C-band data for our study sites in Georgia and Brazil, albeit without funding for data analysis. We are

participating in a collaboration with JPL, the Japanese space agency (NASDA), the Brazilian space agency (INPE) and the Brazilian Institute for Amazonian Research (INPA) to acquire and interpret JERS-SAR (L-band) data for the Amazon. Furthermore, deployment of corner reflectors and collection of secondary forest biometric measurements and canopy closure videography were conducted near Manaus in September 1994 for the acquisition of calibrated JERS-1 data under an agreement between NASDA, INPE and the Brazilian State Oil Company (Petrobras). Calibrated data for this overpass as well as for an overpass at about the same time as the April SIR-C mission have been provided by NASDA and data analysis is in progress. With on-going support from NASA, we are continuing our application of passive microwave data (SMMR and SSMI) to determine seasonal inundation in the major floodplains of South America. In association with an EOS IDS investigation (Soares of INPE and Dunne of UCSB and Univ. of Washington), we are using Landsat imagery, in part derived from the Humid Tropics Pathfinder, to classify vegetation along the Amazon floodplain.

Our synergistic use of multisensor data is benefitting from the active participation of Dr. Leal Mertes, Dept. of Geography and ICESS. She has applied spectral mixture analysis of Landsat data to detection of sediment distributions and floodplain habitats and has developed numerical simulation models of flooding. As her interests in SAR have increased, she has joined J. Melack as a Co-I on our ERS and Radarsat projects. Furthermore, Mertes and Melack have a proposal pending with Hydrological Processes at NSF to fund additional examination of SAR data and to combine those results with on-going hydrological, geomorphological, ecological and biogeochemical studies. Additional collaboration is beginning with Dr. Geoff Henebry (Univ. of Kansas) in the analysis of texture in SIR-C/X-SAR and Radarsat scenes from the Pantanal, and with Dr. Max Finlayson (ERISS, Australia) in interpretation and application of SAR imagery in northern Australia.

TABLE 1: **SUMMARY OF ACTIVITIES: JAN '94 - SEP '95**

SIR-C DATA ANALYSIS
Scenes
Processed

	SRL1	**SRL2**
Manaus Anavilhanas	4	3
Manaus Cabaliana	5	5
Manaus Barroso	1	1
Pantanal	2	1

PUBLICATIONS

Hess, L. L., and J. M. Melack. 1994. Mapping wetland hydrology and vegetation with synthetic aperture radar. *Int. J. Ecol. Environ. Sci.* (special issue-Recent Studies on Ecology and Management of Wetlands) 20: 197-205.

Hess, L. L., J. M. Melack, S. Filoso, and Y. Wang. 1995. Delineation of inundated area and vegetation along the Amazon floodplain with the SIR-C synthetic aperture radar. *IEEE Trans. Geosci. Rem. Sens.* 33: 896-904.

Kasischke, E., and J. M. Melack. 1995. Ecology. Pages 2-1 to 2-31. *In Spaceborne synthetic aperture radar: current status and future directions.* Report to Committee on Earth Sciences, Space Science Board, National Academy of Sciences. NASA Tech. Memorandum 4679.

Melack, J. M., L. L. Hess, and S. Sippel. 1994. Remote sensing of lakes and floodplains in the Amazon Basin. *Rem. Sens. Reviews* 10: 127-142.

Mertes, L. A .K., D. L. Daniel, J. M. Melack, B. Nelson, L. A. Martinelli and B. R. Forsberg. Spatial patterns of hydology, geomorphology and vegetation on the floodplain of the Amazon River in Brazil. *J. Geomorphology* (in press).

Sellers, P. J., B. W. Meeson, F. G. Hall, G. Asrar, R. E. Murphy, R. A. Schiffer, F. P. Bretherton, R. E. Dickenson, R. G. Ellingson, C. B. Field, K. F. Huemmrich, C. O. Justice, J. M. Melack. N. T. Roulet, D. S. Schimel and P. D. Try. 1995. Remote sensing of the land surface for studies of global change: models-algorithms-experiments. *Rem. Sens. Environ.* 51:3-26.

Wang, Y, L. L. Hess, S. Filoso, and J. M. Melack. 1995. Understanding the radar backscattering from flooded and nonflooded Amazonian forests: results from canopy backscatter modeling. *Rem. Sens. Environ.* 53: (in press).

Proceedings

Filoso, S., J. M. Melack, and M. Williams. Spatial and temporal variation among lakes of the Anavilhanas Archipelago (Negro River, Brazil). *Proc. Internat. Assoc. appl. theor. Limnol.* (in press).

Hess, L. L., and J. M. Melack. 1995. Delineation of inundated area and vegetation in wetlands with synthetic aperture radar. *Proceedings, Wet-Dry Tropics Management Workshop.* Office of the Supervising Scientist, Australia (in press).

Hess, L. L., J. M. Melack, and F. Davis. 1994. Mapping floodplain inundation with multifrequency polarimetric SAR: use of tree-based model. *Proc. Int. Geocsci. Remote Sens. Sympos.* vol. II, pages 1072-1073.

Melack, J. M. and Y. Wang. Delineation of flooded area and flooded vegetation in Balbina Reservoir (Amazonas, Brazil) with synthetic aperture radar. *Proc. Internat. Assoc. appl. theor. Limnol.* (in press).

Wang, Y., L. L. Hess, S. Filoso, and J. M. Melack. 1994. Canopy penetration studies: modeled radar backscatter from Amazon floodplain forests at C-, L-, and P-band. *Proc. Int. Geosci. Remote Sens. Sympos.* vol. II, pages 1060-1062.

Abstracts

Hess, L. L., J. M. Melack, S. Filoso, and Y. Wang. 1995. Delineation of inundated area and vegetation along the Amazon floodplain with the SIR-C synthetic aperture radar. Poster presentation, Ecological Society of America Annual Meeting, July 1995, Snowbird, Utah.

Melack, J. M. 1994. Synergistic use of multisensor data for wetland studies. 30th COSPAR Scientific Assembly. Invited talk-Symposium A3.1 Calibration and applications of satellite sensors for environmental monitoring. Hamburg, Germany.

Planned Publications

Filoso et al. Forest structure and seasonal inundation in the Anavilhanas archipelago, Negro River, Brazil. Vegetation.

Hess et al. Microwave backscattering response of wetland communities of a southeastern U.S. floodplain as a function of frequency, polarization, and incidence angle. IEEE Trans. *Geoscience Rem. Sens.*

Hess et al. Characterizing seasonal changes in vegetation and hydrology on the Amazon floodplain with the SIR-C SAR. *Rem. Sens. Environ.*

Hess et al. SAR mapping of wetlands: integrating multiple SIR-C dates and sites.

Ecological Applications

Melack et al. Active and passive remote sensing of inundation on the Amazon floodplain and regional estimates of methane emission. Global Biogeochemical Cycles or Nature.

Melack et al. A remote sensing-based strategy for a global analysis of wetlands. IGBP workshop report and an article for *EOS.*

Valeriano et al. Evidence for detectability of tropical forest canopy closure with C band SAR data: analysis of SAREX data at the Tucurui dam study site. *Int. J. Rem. Sens.*

Valariano et al. Detection of forest parameters and canopy closure in central Amazonia using SIR-C multipolarized data. *Rem. Sens. Environ.*

Valeriano et al. Analysis of multi-angle, multi-polarization AIRSAR data for detection of forest structural parameters in a flooded forest in southeastern Georgia. *Int. J. Rem. Sens.*

Wang et al. Applying decomposition theory to SIR-C wetland sites. *Rem. Sens. Environ.*

Planned Conference Presentations

Hess et al. SAR mapping of wetlands: integrating multiple SIR-C dates and sites. IGARSS 96.

Melack, J. M., L. L. Hess, and S. J. Sippel. Delineation of flooding by large South American rivers with active and passive microwave remote sensing. *AGU 1995 Fall Meeting*, Union Session on Monitoring of Floods and Droughts with Remote Sensing.

Mertes, L. A. K., D. L. Daniel, and L. L. Hess. Patterns of flooding derived from Optical and Microwave Remote Sensing Data. Invited paper. *AGU 1995 Fall Meeting*, Union Session on Monitoring of Floods and Droughts with Remote Sensing.

Dr. Frank M. Monaldo
Johns Hopkins University
Applied Physics Laboratory
Johns Hopkins Road
Laurel, MD 20707-6099

Co-Investigator:
R. Beal Applied Physics Laboratory

Optimization of SAR Parameters for Wave Spectra

OBJECTIVES

Maximize the amount of ocean wave information extracted from SAR imagery.

Determine those SAR parameters --- look angle, frequency, polarization, etc. --- which produce highest fidelity ocean wave spectra.

This project can be considered joint and involves collaboration from the Southern Ocean experiment (PI: R. Beal, CI: F. Monaldo, T. Gerling), with largely overlapping tasks and common goals, that is, the application of spaceborne SAR to operational ocean wave monitoring and forecasting.

PROGRESS

With both the SRL-1 and SRL-2 missions, we have acquired a SAR wave imaging and comparison data set more than two orders of magnitude greater than in any previous U.S. SAR mission. The SRL data set is all the more unique and valuable to us, since it was acquired at both a low altitude and low off-nadir angle. These are both necessary conditions for any future free flyer dedicated to global ocean wave monitoring. The data set for our SRL investigation consists of:

Over 100,000 SAR Image Spectra over the Southern Ocean from the real-time APL SAR Processor: 45,000 from April, and 55,000 from October.

Eighteen precision, high resolution SAR imagery data-takes correlated by NASA/JPL, both over the Southern Ocean and over the North Atlantic.

Numerical wave model (WAM) nowcasts for the periods covering both April and October missions, from both the US Navy Fleet Numerical and Meteorological Center (Monterey) and the European Centre for Medium Range Forecasting (ECMWF)(Reading).

ERS-1 SAR derived wave spectra from the Max Planck Institute covering the entire globe for the time intervals of both the April and October missions.

APL Processor SAR Data

Aboard the Endeavour, an APL-built processor correlated SAR imagery from the SIR-C C-band HH-polarization signal and produced image spectra which were transmitted to the ground in real time. More than 100,000 image spectra from the APL-processor were stored from 120 data takes in SRL-1 and 126 data takes in SRL-2. The wave spectra cover most of the Southern Ocean from 45S to 60S. The data set includes measurements where the ocean significant wave height varied from near zero to over 12 m, spanning nearly the full range of naturally occurring sea states.

NASA Precision, High-Resolution Data

SAR signal outside the southern oceans was acquired in the Northeast Atlantic supersite. During SRL-1 and SRL-2, 20 and 18 data takes were acquired from the Northeast Atlantic, respectively. We now have, in house from SRL-1, precision-processed multilook data from the following data takes: 19.20, 31.30, 35.30, 35.3, 47.10, 51.6, 63.10, 79.00, 83.40, 95.3.,110.0, 127.10, 131.5, 143.10.

We plan to request a similar data set from SRL-2. Unlike the first data set, we plan to order single-look complex data to allow for the application of more advanced speckle noise elimination strategies.

WAM Nowcasts

During SRL-1 and SRL-2, the Navy's Fleet Numerical Oceanography and Meteorology Center (FNMOC) retained the nowcast spectra made from their version of the operational WAM forecast model. An analogous comparison model data set is also available from ECMWF through collaborators at the Max Planck Institute (Hamburg).

ERS-1 SAR Imagery

Given the broad geographical coverage of data from the APL processor, there are at least 30 times in each mission when ERS-1 wave spectra and APL-processor image spectra were located less than 50 km apart and acquired within one hour of one another. Loosening the colocation criteria only slightly will produce more than 100 such comparisons sets.

SIGNIFICANT RESULTS

Using real-time APL-processor data received at Johnson Space Center, we merged SAR wave vector estimates over the Southern Ocean with wave vector forecasts from FNMOC and daily placed the combined products on a World Wide Web site. During the mission, the site was visited more than 150 times by investigators from as far away as South Africa and Australia. This effort demonstrated the potential of providing wave information from spaceborne SAR quickly enough to be usefully assimilated into wave forecast models. The site

ftp://fermi.jhuapl.edu/sirc/sirc.html

currently shows recent data and analyses from the SRL missions. In the past year, we have processed image spectra with only a simple SAR modulation transfer function. Even these results show quality retrievals of wave direction and wavelength. In the future, we will employ more sophisticated retrieval schemes that may permit the accurate measurement of ocean SWH as well.

FUTURE PLANS

Given the totality of the SIR-C image spectra, ERS-1 SAR spectra and WAM model estimates, we intend to 1) make a definitive determination of what ocean wave parameters can be extracted from spaceborne SARs and with what accuracy, 2) specify the SAR satellite configuration which optimizes this retrieval, and 3) to demonstrate with a statistically significant data set the value of SAR for improved global wave forecasting.

We are currently collaborating with William Plant, who while a visiting scientist at the Max Planck Institute this last year, applied nonlinear retrieval algorithms to estimate wave spectra from

coincident SIR-C and ERS-1 data. We expect to submit a joint paper in the upcoming year, documenting the comparison of ERS-1 and SIR-C derived image spectra.

We intend to extend our analysis to the North Atlantic, multipolarization and multifrequency data set using the precision-processed SAR data to confirm the relative contributions of the various wave imaging mechanisms. In addition, we will use the data to test more sophisticated schemes to alleviate the effects of speckle noise in the SAR image.

We intend to make a systematic comparison, wave system by wave system, to ascertain systematic differences between WAM model wave estimates and SIR-C measurements for the entire Southern Ocean data set. We will then determine whether these differences are due to input wind field errors, model problems and/or SAR wave imaging limitations.

PUBLICATIONS

Monaldo, F. M. and R. C. Beal, Real-Time Observations of Southern Ocean Waves Fields from the Shuttle Imaging Radar, *IEEE Transactions on Geoscience and Remote Sensing*, vol. 33, No. 4, pp. 942-949, 1995.

Beal, R. C., S. F. Oden, J. L. MacArthur, and F. M. Monaldo, Real Time Ocean Wave Monitoring from Space: A Thirty Year Quest Achieved, *Johns Hopkins APL Technical Digest,* vol. 15, No. 3, pp. 237-241.

Monaldo, F. M. and R. C. Beal, SRL Real Time Wave Forecasting in the Southern Ocean, *Proc. 1995 International Geoscience and Remote Sensing Symposium,* Florence, Italy, July, 1995.

Plant, W., S. Hasselmann, C. Bruning, R. Beal, and F. Monaldo, Comparison of Ocean Wave Spectra from a Non-linear SAR Inversion Scheme using ERS-1 and SIR-C Data Sets, *Proc. 1995 International Geoscience and Remote Sensing Symposium*, Florence, Italy, July, 1995.

Gerling, T. G and P. A. Wittmann, Comparison of SAR-estimated Wave Spectra with WAM Model Estimates During the SRL Southern Ocean Experiment, *Proc. 1995 International Geoscience and Remote Sensing Symposium*, Florence, Italy, July, 1995.

Wittmann, P. A., R. M. Clancy, and R. C. Beal, FNMOC Supports Wave Modeling Around the World and into Space, *Naval Meteorology and Oceanography News*, July 1995.

Beal, R. C., The SRL Real Time Wave Forecasting Experiment and its Implications for a Future Satellite Design, invited seminar to NOAA/NESDIS, 15 December 1994.

Beal, R. C., The SIR-C Real-Time Southern Ocean Experiment, invited seminar to the Max Planck Institute for Meteorology, 6 July 1995.

Beal, R. C., Ocean Applications of Spaceborne SAR, invited presentation at the US-ROC Oceanic Microwave Remote Sensing Workshop, U. Delaware, 16 August 1995.

Dr. Richard K. Moore
University of Kansas
Center for Research, Inc.
2291 Irving Hill Drive-Campus West
Lawrence KS 66045-2969

Co-Investigators:
Julian C. Holtzman Univ. of Kansas

Inflight Antenna Pattern Measurement for SIR-C

OBJECTIVES

Obtain the vertical antenna patterns of the SIR-C radars to allow improved radiometric calibration of data for other investigators.

To determine how much the vertical antenna pattern changes after launch to aid in designing future space radars and to determine if such measurements are needed on all future space radars.

PROGRESS

The University of Kansas Radar Systems and Remote Sensing Laboratory is studying the elevation pattern of the SIR-C and X-SAR antennas using backscatter from homogeneous targets. Specific passes were requested and obtained over the Amazon rain forest, the world's largest homogenous flat forest area. In addition, passes over the Amazon area requested by other investigators are useful for this purpose.

We now have patterns for both SIR-C and X-SAR antennas from some of the SRL-1 passes, but not all. The patterns obtained are for a limited set of conditions because the antenna has many modes (VV, HH, HV, VH at each frequency of SIR-C, with 10 beam-spoiling modes). Too few passes are available to test the various beam-spoiling modes. For X-SAR, which has only one mode, we have a complete pattern and published the results {Fang and Moore, 1995}.

The X-SAR pattern obtained is close to that used in correcting the data. For some SIR-C modes the pattern is close, but not as close as the X-SAR in most cases. For the one beam-spoiled mode we have studied, there is a major inconsistency between

* beamwidth in tape header,
* beamwidth from radiometric correction table,
* beamwidth from our calculations.

For no beam spoiling, we find differences between our measured one-way pattern and the radiometric table up to about 1 dB at the edges of the swath.

SIGNIFICANT RESULTS

The use of radar returns from large homogeneous areas requires selection of areas that are flat and, at least in the average, uniform in content. They should be flat so that slope effects on radar backscatter do not distort the data. The Amazon rain forest is the largest flat, homogeneous area in the world, so it was selected as the primary area for pattern determination. However, images of the rain forest show that low hills occur in some places, and in this case, we exclude the hilly areas from processing.

Areas that are largely homogeneous frequently contain regions with signals greatly different from the average; examples are water bodies and cities. We remove the effect of these by preparing a histogram of the signals. If the histogram is multimodal, with a low mode for water, a large central region, and possibly a high mode for cities, the points in the upper and lower modes are excluded from the analysis. Some images show rivers that are at essentially constant range; these cannot be used because the river return at a given range would leave to few forest returns to get a valid point at that range.

We then average the remaining data in long strips; each strip is 100-1000 m wide and as long as the useful part of the image (typically tens of km). Each strip corresponds to a particular angle off the beam center. The average power in the strips is then plotted vs. beam angle. At this point we fit the data with an appropriate function. Although we have used quadratic and quartic polynomial fits, the best fit comes from a form

$$G(f) = d \cos^b [c(f-a)].$$

The best-fit function is then used to determine the beamwidth, This can be compared with the beamwidth given in the tape header. Moreover, we can plot the pattern using this beamwidth and the theoretical shape to find how the measured pattern deviates from that reported in the header.

A third pattern source is available; the radiometric correction table used in processing the data. This is also provided on the tapes. We also plot and measure a beamwidth for this information. By plotting all four curves (measured, fit to measured, header-stated, and radiometric correction), we can compare results at each angle in the beam to see how large errors might be using one of the curves based on preflight measurements and calculations.

Table 1 summarizes the results for SIR-C for SRL-1. The beamwidths are reasonably close, but never identical for LVV and LHH with no beam spoiling. They are not quite as close for C-band. Note that our beamwidths are smaller than the header beamwidth for L-band, but larger for C-band. The only beam-spoiled pass we had available was 78.60. The differences between the three beamwidths are quite large for this case. It appears that the header value may have been taken from a beam-spoil-zero mode table, whereas both measured and radiometric correction beamwidths are more than twice as large as that reported on the header. Note also that the differences between measured and radiometric correction beamwidths are rather large in this case, suggesting that the correction was inadequate at the edges of the beam.

Fig. 1 shows one of the better cases, where the three fits are not far apart. Even here the difference between our measured pattern and the radiometric correction is about 0.6 dB at the edge of the beam (2-way difference would be 1.2 dB).

Fig. 2 shows the bad beam-spoiled case. The difference between our pattern and the radiometric correction is not too bad, but the pattern based on the header is not even close. Unfortunately, this only beam-spoiled case was for a rather narrow swath (in terms of percent of the beam width), so the fits over the entire beam are not as reliable as they would be if the data covered a wider part of the beam.

We requested SRL-2 tapes, but have not received any to date.

The same method was used to determine the X-SAR pattern. The results were very close to the predicted pattern, as shown in our paper (Fang and Moore, 1995). X-SAR images were obtained for all passes for which SIR-C images were requested. However, some of them were not usable.

The SIR-C patterns we obtained for SRL-1 are moderately close to those from the beamwidths in the tape headers and the radiometric correction tables when there is no beam spoiling. For the one beam-spoiled tape available, the beamwidth in the header is obviously very wrong, and the radiometric correction differs quite a bit from our measured pattern. Based on this limited information, we would warn users that beam-spoiled data may have poor radiometric quality. A report has been prepared that gives the details of these results and comparisons.

The measured X-SAR patterns for SRL-1 agree well with the values used in data processing. As with SIR-C, we have no data tapes processed. Some tapes arrived just as this report was being written.

FUTURE PLANS

We plan to obtain as complete a set of patterns as possible for the SRL-2 mission. We also plan to revisit SRL-1 to determine if suitable non-Amazon targets will let us get patterns for different beam-spoiling modes. This may be difficult, as most of the supersites fail either the homogeneity test or the flatness test, or both.

A main purpose of this effort is to improve the radiometric data for other users. We hope that our first report will allow some modification to the patterns used for no beam spoiling. We have insufficient data to help much for passes where beam spoiling was used, but at least we can provide information that serves as a warning to users of such data. We intend to publish a short paper on the preliminary results after JPL personnel have had a chance to review the report.

We plan to process all of the SRL-2 data, when they become available, as we did the SRL-1 data. We will then prepare reports and papers presenting the results.

Because of the paucity of C-band data and data with beam spoiling, we will devote special effort to identifying passes at C-band with various polarizations from other possible useful targets. We will also try to find passes with beam spoiling in
areas that may allow pattern determination.

PUBLICATIONS

Fang, Y., and R. K. Moore (1995), "Inflight Vertical antenna Patterns for X-SAR from Amazon Rain-Forest Observations," *IEEE Trans. GRS*, vol. 33, pp. 1083-1085.

Table 1. Summary of Results

Prod. ID	Data Take ID	Beam Spoil. Mode	Beam Steer. Angle	Inc.[1] Angle	Freq. Pol.	Cosine Fitting [2]		Our 6-dB BeamWidth	JPL 6-dB [3] Beamwidth (Rad. Corr.)	JPL 6-dB BeamWidth (Header)
						b	c			
11389	39.60	0	2.2°	44.0°	LVV	4165	0.312	9.45°	9.99°	9.57°
					LHH	1.722	14.46	9.37°	9.95°	9.57°
11390	39.60	0	2.1°	44.0°	LVV	6209	0.259	9.33°	10.15°	9.57°
					LHH	2.524	12.21	8.95°	9.83°	9.57°
11342	55.62	0	14.7°	26.3°	CVV	20237	0.121	11.01°	9.65°	8.47°
					CHH	61140	0.237	10.25°	9.33°	8.47°
12347	78.60	6	11.3°	29.8°	LVV	592680	0.009	26.26°	30.92°	10.71°
					LHH	753	0.273	25.14°	31.36°	10.71°
12348	78.60	6	11.3°	29.8°	LVV	235	0.514	24.22°	30.92°	10.69°
					LHH	219480	0.017	23.96°	32.36°	10.69°
12092	103.60	0	6.4°	48.7°	LHH	3833	0.435	7.05°	N/A	6.40°
12093	103.60	0	6.4°	48.7°	CHH	1975	0.623	6.87°	N/A	6.40°

1. Incident angle are defined at the center of the image.
2. Cosine function used to fit the data is $d\cos^{b}[c(x-a)]$, x is in degree.
3. The data in the radiometric correction table was extended by using cosine fit.

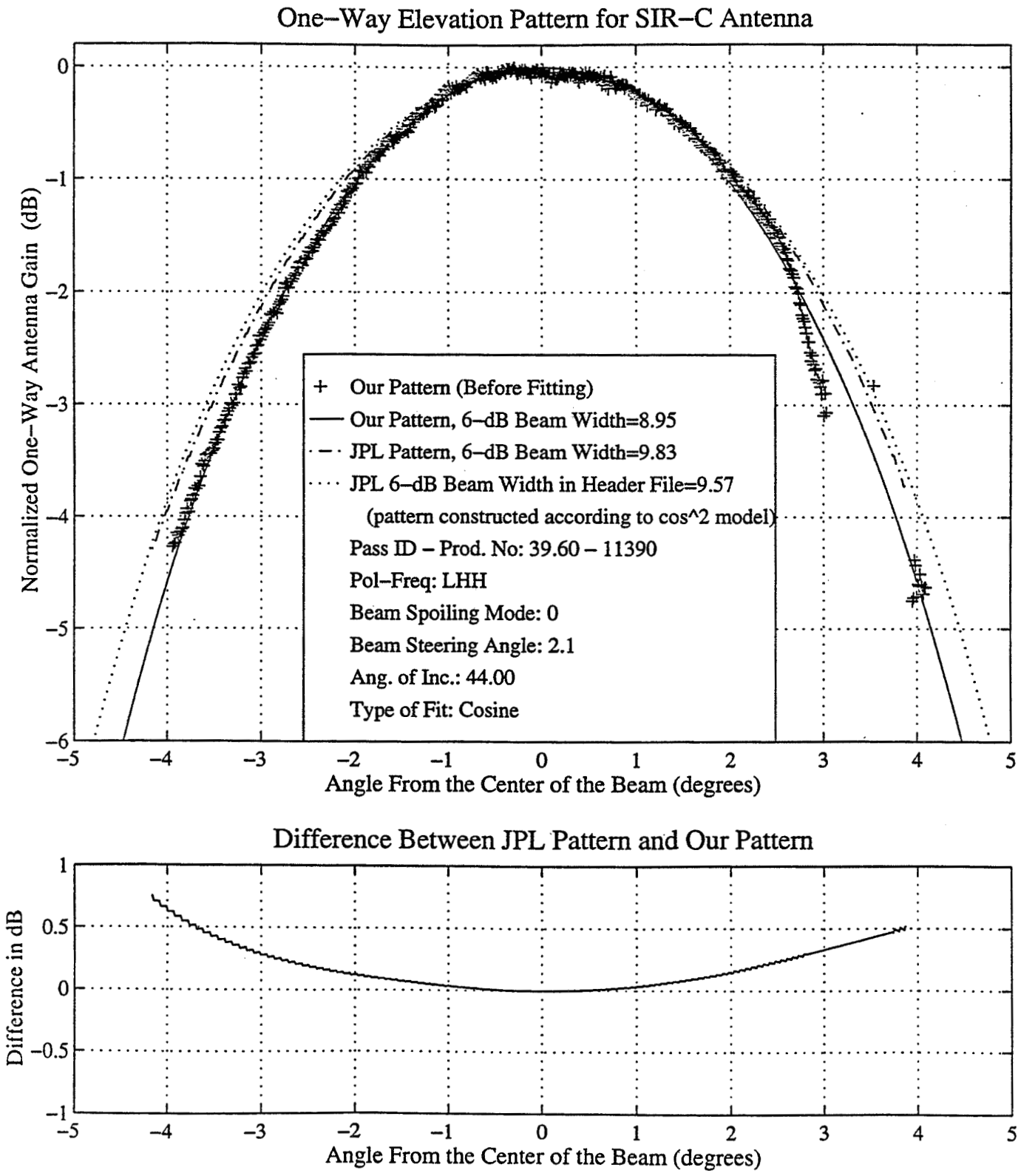

Fig. 1. A case where fits are not far apart.

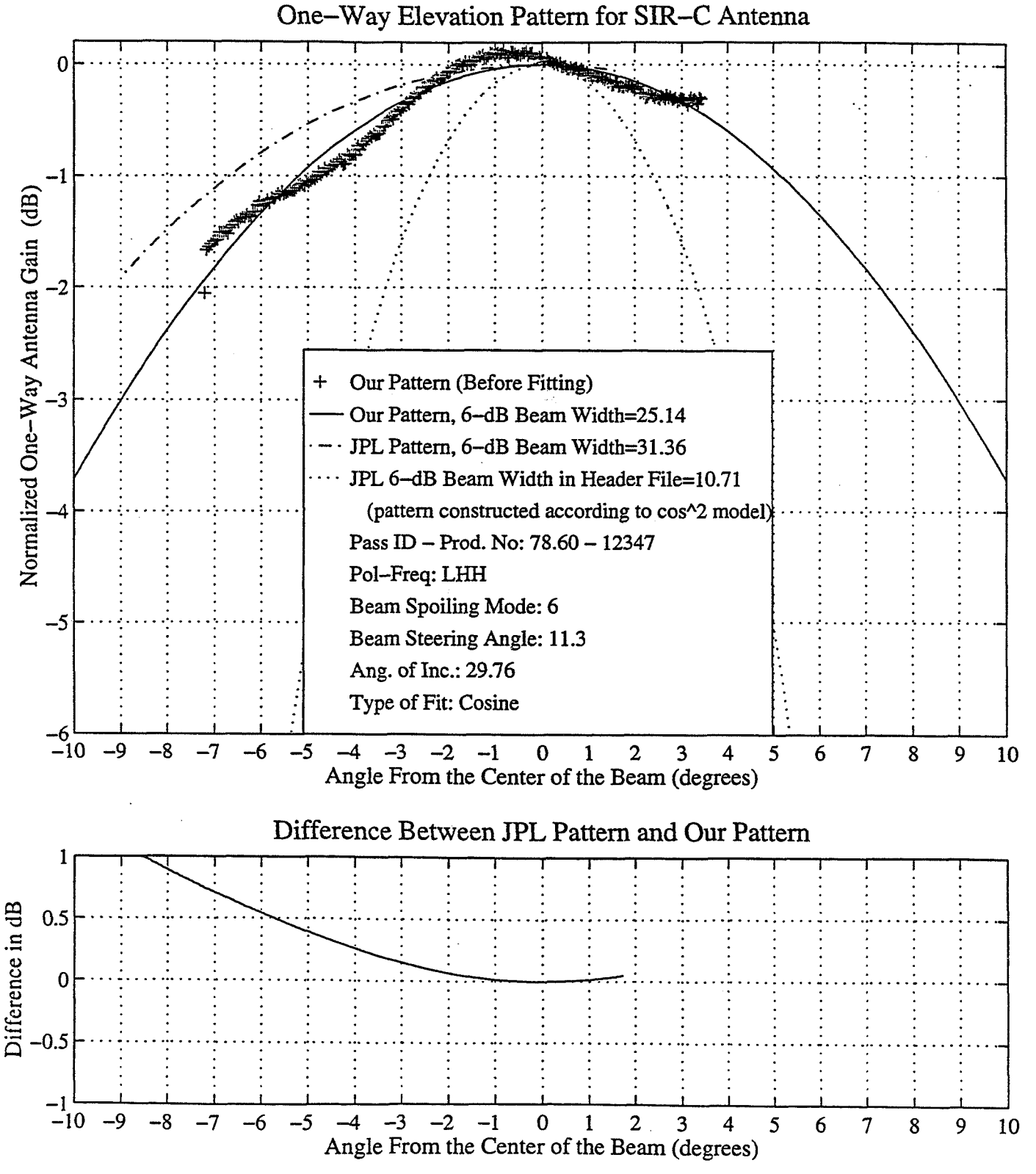

Fig. 2. The bad beam-spoiled case.

Table 2. Data Used from SRL-1 and Ordered for SRL-2

Frequency	Beam Spoil Mode	Polarization		
		VV	HH	Cross
SRL-1 DATA				
L	0	2	3	
	6	2	2	
C		1	2	
X		3		
SRL-2 DATA				
L	0	3	5	
	3		1	
	4		3	
C	0		2	
X		9		

Dr. Peter J. Mouginis-Mark
Planetary Geosciences Division
University of Hawaii
2525 Correa Road
Honolulu, HI 96822

Co-Investigators:
V.H. Kaupp University of Arkansas
H.C. MacDonald University of Arkansas
W.P. Waite University of Arkansas

Eruptive Styles Of Basaltic Shield Volcanoes From Shuttle Imaging Radar-C (SIR-C) and X-SAR Data

OBJECTIVES

To provide a comprehensive understanding of the distribution of volcanic materials on classic examples of balsaltic shield volcanoes in Hawaii, Reunion Island (Indian Ocean) and Galapagos (Eastern Pacific).

Interpret the preserved eruptive history of each volcano, draw contrasts between each test site in terms of the role of the tectonic setting on basaltic volcanism, and make inferences about the internal structure of the volcano and its magma chamber.

PROGRESS

Since the SRL-2 mission (October 1994), we have recognized the importance of the repeat-orbit phase of the mission for conducting new volcanological research with interferometric radar data. Over the last eight months we have therefore undertaken a vigorous program to develop our own interferometric SAR processing scheme at the University of Hawaii through a close collaboration with Howard Zebker and Paul Rosen at JPL. The processing scheme that we have developed is based on a program in use at JPL, and on the mathematics outlined by Curlander (1991). From raw SIR-C data we can now construct images, co-register repeat-pass images, produce interferograms between images, unwrap interferogram phase, and minimize baseline uncertainties. We have performed the mapping from interferometric phase to topography, and calibrated the topography to produce digital elevation models. Our ultimate processing goal, which we expect to reach by the end of 1995, is to use repeat-pass interferometry to produce quantitative phase correlation maps in order to describe surface change on volcanoes such as Kliuchevskoi (Kamchatka). Our interferometry work in Hawaii mirrors studies conducted at JPL, and we have collaborated on one of their papers (Zebker et al., submitted to Science) on the surface changes due to the emplacement of new lava flows at Kilauea volcano during SRL-2 (see Fig. 1).

For test data we have worked with SIR-C data for our "Super Site" on Isabela Island (Galapagos). Figs. 2 and 3 demonstrate our current capabilities to perform this interferometry work, which allows us to go from the raw data to a DEM. This DEM is being used to study the relationship between lava flow widths and slopes (a good indicator of changing lava flow rheology) as well as test our phase unwrapping algorithms for SIR-C via a comparison with the TOPSAR DEM that was obtained as part of the 1993 South America deployment of the NASA DC-8 aircraft. As our SIR-C investigations advance from algorithm development to scientific application, we shall concentrate on creating images and DEMs for Kliuchevskoi, Taal (Philippines), the Virunga Chain (Zaire), and Piton dela Fournaise (Reunion Island), and on deformation mapping of Kilauea and Kliuchevskoi. For the Galapagos, by comparing DEMs from SIR-C data with pre- and post-eruption SPOT images (together with TOPSAR results), we will investigate topographic control of lava flows.

As a parallel activity, we expect to be able to demonstrate within a few months a fully-functional SAR processing scheme together with full satellite downlink capabilities (using our own X-band ground station). With the capability to process SIR-C data, and with the ability also to downlink ERS and JERS data, we will be in a good position to support any future NASA radar missions, including any SRL-3 or TOPSAT mission. This university-based capability should be particularly useful as NASA attempts to find low-cost methods for radar data reception and processing in order to fly these future missions.

We have obtained 11 data takes over Hawaii (including Mauna Loa, Kilauea and Haleakala -- all places where we have on-going research), and 31 data takes over other volcanoes. As part of this investigation, a total of 27 interferometric data sets have also been obtained or are requested, making 69 data requests in all. Currently, we have research underway using SIR-C data to investigate the relationship between extensional tectonism and volcanism at Erta Ale (Ethiopia), the structure of Taal caldera and the regional distribution of volcanic land forms in the Virunga volcanic chain. The Virunga chain includes Nyamuragira and Nyiragongo volcanoes, and gives us the opportunity to study the radar scattering properties, the noise floor of the radar data, and the radar system calibration in an area where the distribution of flow types and vegetation is poorly known, thereby building on our experience with SIR-C data at Kilauea. We have SIR-C data for the Virunga Chain that were obtained at three different pulse bandwidths and two look-directions, and have on order a SPOT multispectral image for the same area. In addition to describing the volcanology of this area, we will also study the effects of different pulse bandwidths for mapping the numerous cinder cones and lava flows in this rarely studied area.

SIGNIFICANT RESULTS

As we work through the radar interferometry data sets, we are starting to see some fascinating new things. Our paper (Zebker et al., submitted to *Science*) shows for the first time how an orbital radar can be used to measure the daily change in area of new lava flows on Kilauea volcano, Hawaii. Such data provide new insights into the eruption characteristics of the volcano, and the growth of lava flow fields. By approximating the average thickness of the flow to 50 cm, we have estimated an average effusion rate of ~2 cubic meters per second over the four-day observation period. Furthermore, the derivation of the phase correlation maps (needed to detect new lava flow surfaces) also revealed some unexpected phenomena that we believe are due to atmospheric moisture. This was totally unexpected, and we plan to process additional interferometry pairs as fast as we can in order to search similar phenomena in different climatic settings.

As a part of our efforts to educate the volcanology community on the value of orbital radars, and SIR-C in particular, we have published a general review (in *Earth Observation Quarterly*) of radar interferometry in volcanology, and have a review article in press in *IEEE Trans. Geosci. Rem. Sen.* The P.I. has also served on the NASA NRC Review Panel (John McElroy, Chair) advocating a new NASA interferometric radar mission. Invited papers on the SIR-C results have been given at the 1994 GSA meeting (Seattle) and the 1995 IUGG General Assembly (Boulder, CO). Another review will be given at the All-Union special session on "Radar Interferometry" at the Fall 1995 AGU meeting in San Francisco.

Surface change at Kliuchevskoi volcano, Kamchatka, during the October 1994 eruption. As luck would have it, there was a major explosive eruption of Kliuchevskoi volcano five hours after the launch of SRL-2. While most of the explosive activity took place during the early parts of the mission, pyroclastic flows and mudflows were reported during the repeat-orbit phase of the mission between October 7th - 10th. We are currently processing these interferometric data to search for surface change. If we find any, we will place these results into the general context of the eruption with the aid of reports made by other volcanologists on the ground and images taken by the SRL-2 crew during the mission. This work is in an early phase, but will be submitted to

Bulletin Volcanology either as a complete study, or as a component of a paper on the use of radar-derived digital elevation models and surface change detection.

For our Galapagos Super Site, we have used the SIR-C data to help with the mapping of Fernandina volcano, particularly in determining flow types. The goal of this project is to determine the long-term magma production rates and eruption patterns of the volcano. This is being done by mapping the distribution of flows of various relative ages, mapping the distribution of eruptive vents, and by calculating the volumes of the flows of these various ages. Calculating the volumes requires knowledge of the flow thicknesses, and this is where we are using TOPSAR data. So far only the volumes of the youngest flows have been determined, and they total 25.5 cubic kilometers. They have been preferentially erupted from the upper and lower SE and NW flanks. One result of having the good topography is that it has highlighted the fact that there are essentially no eruptive vents on the steeper slopes, which no doubt reflects some aspect of the stress field within the volcanic edifice. This work is being prepared for publication in the special SIR-C issue of *J. Geophysical Research.*

FUTURE PLANS

Our plans for the next two years are heavily focused on the analysis of the interferometry data, both for the detection of surface change and atmospheric effects (i.e., analysis of the phase correlation data) and on the derivation and analysis of the digital elevation models that we will produce. We have a specific set of priorities and collaborations planned for these studies and intend that each of these investigations will result in a manuscript being submitted for publication:

Kliuchevksoi volcano, Kamchatka (SRL-2 data takes 121.10, 137.10, 153.10 and 169.20, all of which are in-hand). We wish to study the later parts of the eruption, searching for evidence of moving pyroclastic flows, mudflows, and the waning phases of the eruption plume. Quantitative decorrelation maps will be produced from the SRL-2 data collected on October 7th, 8th, 9th and 10th, 1994 to show how the flows may have moved on a daily basis. Through this study we hope to learn more about the emplacement of these flows -- we expect to see changes not only at the leading edge but also in the up-slope parts of the flow if the flow is a mudflow that remained fluid during to the release of melt water from the snow-capped peak of the volcano, as suggested from our inspection of the accompanying hand-held photography obtained by the crew of STS-68.

Morphology and structure of the Virunga volcanic chain, Africa (SRL-2 data takes 154.90 and 170.90). These data encompass virtually the entire Virunga volcanic field, including the recently active Nyiragongo volcano of Zaire. Parts of Nyamuragira volcano lie within the interferometry pair, and all parts of the volcano were imaged as part of the multilook data (SRL-1 DT 58.60, 171.10, SRL-258.61 and 154.90). We plan to produce a DEM for the eastern area of the Virunga volcanic field, which includes the Karisoke Research Center -- home of the endangered mountain gorillas -- and to use this DEM to study the distribution of the maar volcanoes in this area as a function of elevation. Here we wish to use the elevation data to help us remotely discriminate between cinder cones ("dry" eruptions at relatively high elevations) and maar cones ("wet" eruptions at lower elevations) close to nearby Lake Kivu; there are many dozens of cones surrounding the main volcanoes and we hope to deduce some structural aspects of this mono-genetic volcanic field through a study of cone volume and size of the summit craters. In addition, there are some unusually thick lava flows on some of the volcanoes that can be seen in the multilook data; we want to measure their slopes on the DEM to help with rheological studies of flows. Nyiragongo and Nyamuragira are characterized by extremely fluid lava flows that can travel long distances very quickly, posing an extreme hazard for nearby populated areas, such as Goma (and the surrounding Rwandan refugee camps). Also, the formation of Lake Kivu has heightened the risk of explosive activity due to magma/groundwater interactions. Although volcanic hazards mitigation is largely beyond the scope of this study, SIR-C data can provide the

basis for geologic maps of the region, particularly in otherwise accessible areas. This study will provide a regional context for field observations that can be used by other investigators to further understand the past behavior and future risks in this area.

Structure of Taal volcano (SRL-2 data takes 126.30, 142.30, and 158.30 all of which have already been requested). In collaboration with Dr. Stephen Self (Univ. Hawaii) and Dr. R. Punongbayan (Philippine Volcano Observatory), we plan to create a digital elevation model of Taal volcano in order to investigate the structure of southwestern Luzon island, Philippines. Detailed knowledge of the topography will greatly aid our analysis of the erosional characteristics of the ignimbrite sheets that dominate the area surrounding Taal caldera. Some areas of deeply eroded (steep slopes?) and other areas of relatively shallow valleys (lower slopes?) can be identified in individual SIR-C images. Our main study area is the Taal ignimbrite sheet north of the caldera, which is extremely difficult to map on the ground due to dense vegetation and the lack of roads.

Piton de la Fournaise, Reunion Island was our third original SIR-C/X-SAR target. During the last 3 months, we have been discussing with Jean-Francois Lenat (Center for Volcanology Research, Clermont Ferrand, France) the possibility of detecting changes in the large-scale morphology of the volcano between 1990 (when he produced a DEM of the volcano using SPOT stereo data) and 1994 (the SRL-2 interferometry pair from Data Takes 146.60 and 162.60, both already requested). Because this volcano erupts almost every year, there is a good possibility that we will be able to detect differences in the volume of the summit crater and/or flank flows. This will also be a valuable test for comparing DEMs produced from photogrammetric data with DEMs derived via interferometry methods.

We have had several requests for producing digital elevation models of other volcanoes, partly in support of our EOS interdisciplinary investigation, and partly to assist our colleagues in the international volcanology community. Mt. Etna (SRL-2 data takes 141.10 and 157.10 both requested) is a key area of interest for Dave Pieri and Vince Realmuto (both at JPL) and Dave Rothery, John Murray and Bill McGuire (all in England). Detailed knowledge of the topography of Etna is required for rheological studies of the numerous lava flows on the flanks, as well as for sulfur dioxide retrievals using TIMS data. Ray Punongbayan is very interested in the production of a DEM of Pinatubo (SRL-2 data takes 126.30, 142.30, and 158.30) because of the continuing hazards due to lahars on this volcano. Vesuvius (DT 130.40, 146.40, and 162.40 all requested) is a high priority for Italian and German members of the X-SAR Team, since they wish us to produce a DEM using our code that can then be compared to their result. In addition, we already have a TOPSAR DEM for Vesuvius, and will take this opportunity to compare our SRL-2 topographic map with these aircraft measurements.

PUBLICATIONS

Evans, D. L., J. Apel, R. Arvidson, R. Binschadler, F. Carsey, J. Dozier, K. Jezek, E. Kasischke, F. Li, J. Melack, B. Minster, P. Mouginis-Mark, and J. van Zyl. Spaceborne synthetic aperture radar: Current status and future directions. NASA Tech. Mem. 4679, 1995.

Mouginis-Mark, P.J. Analysis of volcanic hazards using radar interferometry. *Earth Observation Quarterly*, No. 47, p. 6 - 10, 1995.

Mouginis-Mark, P.J. Preliminary observations of volcanoes with the SIR-C radar. *IEEE Trans. Geosci. Rem. Sen.*, in press, April 1995.

Zebker, H. A., P. Rosen, S. Hensley, and P. J. Mouginis-Mark. Analysis of active lava flows on Kilauea volcano, Hawaii, using SIR-C radar correlation measurements. Submitted to *Science*, August 1995.

Students Supported:
Ph.D. dissertation completed:

"Frequency Analysis of SAR: Optimization for Imaging Unvegetated Lava Surfaces" C. M. Ting, Ph. D. Dissertation, University of Arkansas, May 1995.

M.S.E.E. thesis completed:

"Multi-resolution Decomposition of Radar Images Using Wavelet Transforms" S. Ramamurthi, M.S.E.E. Thesis, University of Arkansas, December 1994.

Ph.D. dissertation in progress:

Title: TBD. J. F. Hug, University of Arkansas, September 1996 (projected).

MSc dissertation in progress:

Title: TBD. S. Siddiqui, University of Hawaii, December 1996 (projected).

Figure Captions

Figure 1: Radar detection of surface change at Kilauea volcano, Hawaii, during the repeat-orbit phase of the mission. Top left: panel shows the lava flow field down slope of Pu'u O'o volcano on October 9, 1994. Arrows connect parts of the flow field to the same areas on the radar phase diagram. Top right: Details of active flow; arrow connects this flow to the same area seen in the radar phase image. Flow thickness is about 50 cm. Bottom three panels show radar phase correlation maps for period October 7-10 for the three 24-hour periods indicated. Zero phase correlation corresponds to the three active flow fields (Flow regions 1, 2, and 3). Other areas that are decorrelated are the vegetated slopes of the volcano.

Figure 2: Examples of the radar processing capabilities that have been developed at the University of Hawaii. Input data are the raw reformatted signal data provided by JPL. We can process these data to produce the SAR backscatter image (top left), create a raw radar interferogram (top right), display these two data sets together (bottom left) and generate a digital elevation model via our own phase unwrapping algorithm (bottom right). The test data that we display here are for part of Alcedo volcano, which is a part of our SIR-C supersite in the Galapagos Islands.

Figure 3: Oblique perspective view of Alcedo volcano, Galapagos Islands, generated by combining our in-house produced DEM and the radar backscatter image. View is from the northeast.

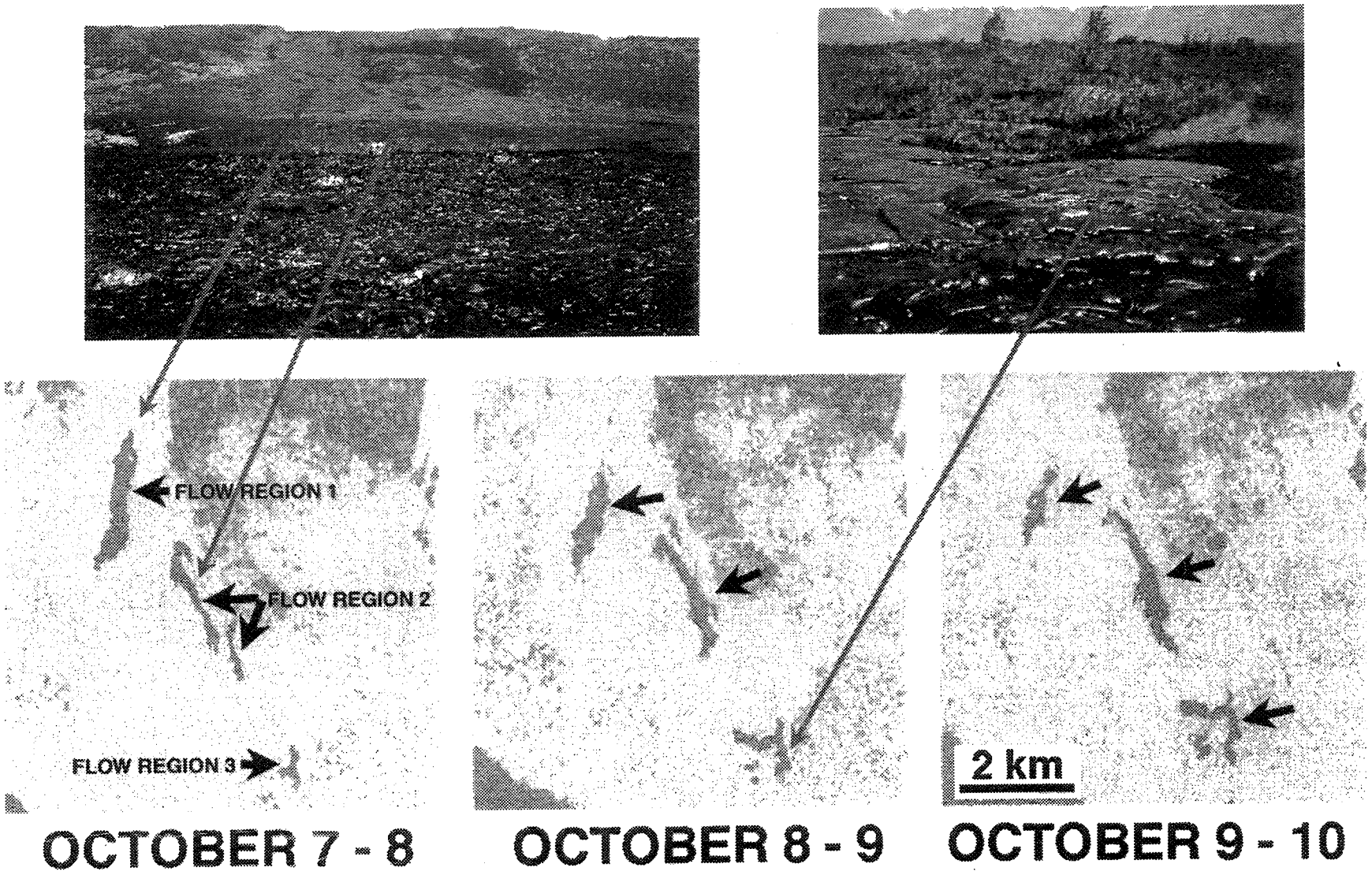
SHUTTLE RADAR INTERFEROMETRY:
GROWTH OF HAWAIIAN LAVA FLOW
FLOW REGION 1
FLOW REGION 2
FLOW REGION 3
2 km
OCTOBER 7 - 8
OCTOBER 8 - 9
OCTOBER 9 - 10

Figure 1

SRL-2 INTERFEROMETRY
ALCEDO VOLCANO, GALAPAGOS

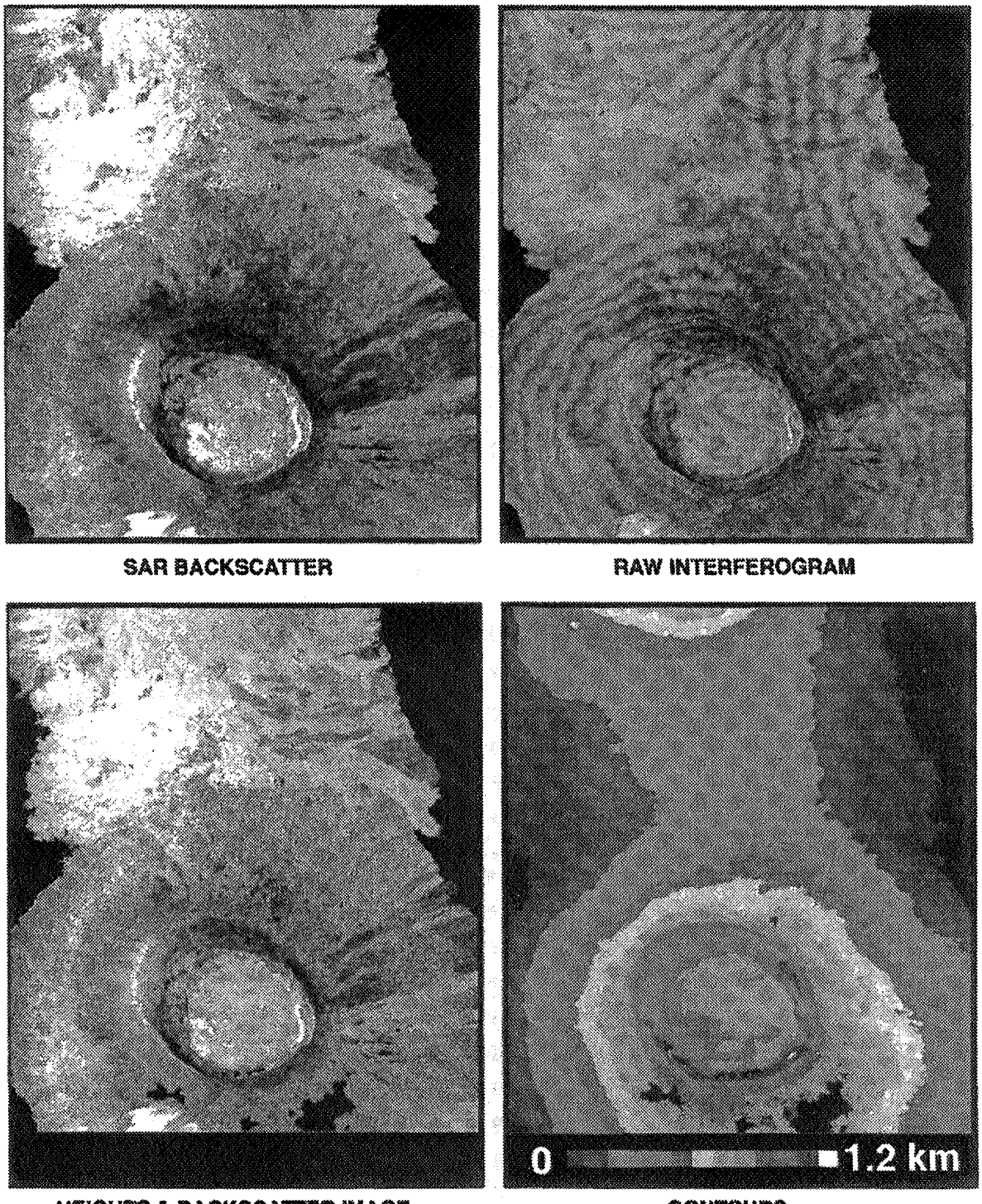

Figure 2

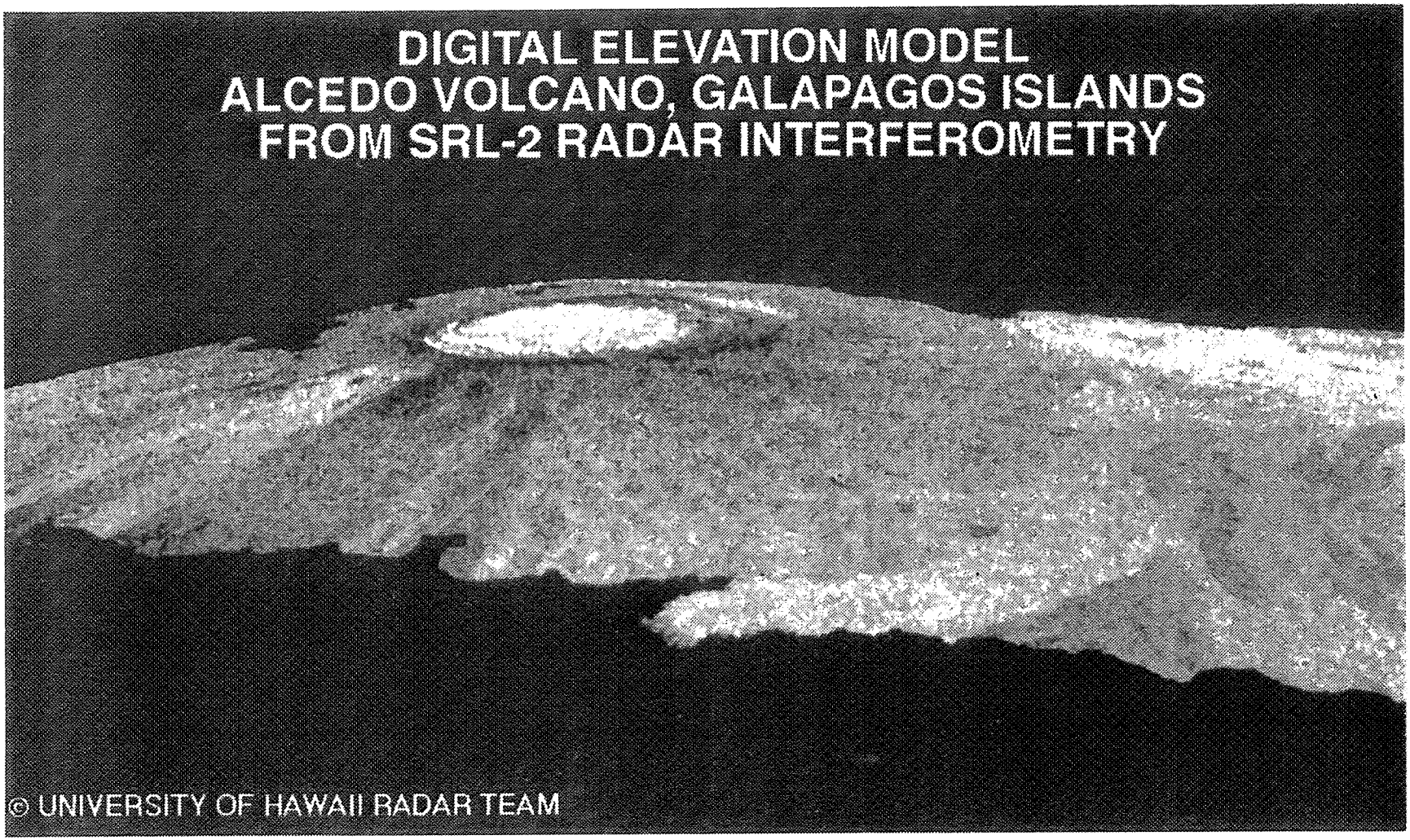
DIGITAL ELEVATION MODEL
ALCEDO VOLCANO, GALAPAGOS ISLANDS
FROM SRL-2 RADAR INTERFEROMETRY
© UNIVERSITY OF HAWAII RADAR TEAM

Figure 3

Prof. Pasquale Murino
Instituto U. Nobile
Piazzale V. Tecchio, 80
80125 Napoli, Italy

Co-Investigators:
Lucio Castellano
Luciano Russo
Mario Ferri

SIR-C/X-SAR data analyses in Campania Test Site

OBJECTIVES

The overall objective of this investigation is the evaluation of SIR-C/X-SAR data collected over the Campania test site in geological analyses.

Specific objectives include the following:

To determine effective procedures to process SAR data to extract information useful in geological analyses, in particular lithology mapping;
To evaluate the relative utility of multifrequency quad-pol SAR data in morpho-structural analyses.

In particular a processing algorithm based on a covariance matrix approach, which permits us to take advantage of the polarization agility of dual-channel multifrequency SAR, has been developed. Unfortunately only one quad-pol single-look image was available so a great amount of work was carried out on dual-pol data which do not allow a complete electromagnetic characterization of targets.

PROGRESS

The Picentini Mountains

The Picentini mountains have been selected because of their very articulated morphology and structure. The area is characterized by many geological formations and structural typologies (faults, overthrusts, klippens, and tectonic windows). The geological analysis of SAR images has been carried out locally (the selected area does not exceed 400 km^2) so, for example, structural trends have not been considered. The study has been focused on both geological details (e.g., the analysis of the limit between limestone and dolomite of the Stella mountain) and structural lineament identification.

The Phlegrean Fields

The Phlaegrean Fields area offers the opportunity to study a morphology characterized by several crateric rims having different ages and histories. For this area SIR-C/X-SAR data have been integrated by ERS-1 and JERS-1 data imagery (lower incidence angles and different looking directions).

The Somma-Vesuvius complex

Vesuvius a very interesting test site, which was observed during a number of spaceborne and airborne remote sensing missions. For that reason we are able to compare the results obtained using SIR-C/X-SAR data with those obtained using other SAR imagery acquired by ERS-1, JERS-1, and AIRSAR missions.

Available SIR-C/X-SAR data

The following data takes have been used:

- SRL-1/DT 114.31 (L-, C-band, mode 11X, incidence angle 52.6°, 4 looks, pixel spacing rng 12.5m / az 12.5m);
- SRL-1/DT 146.30 (L-, C-band, mode 11X, incidence angle 47.8°, 4 looks pixel spacing rng 12.5m / az 12.5m)
- SRL-1/DT 098.20 (L-, C-band, mode 16X, incidence angle 48.5°, 1 look, pixel spacing rng).
- SRL-2/DT 130.40 (X-band, incidence angle 55.4°, SSC and MGD, pixel spacing rng 6.66 / az 5.23)
- SRL-2/DT 146.40 (X-band, incidence angle 55.3°, SSC, pixel spacing rng 6.66 / az 5.23)
- SRL-2/DT 162.40 (X-band, incidence angle 55.4°, SSC, pixel spacing rng 6.66 / az 5.23)

Methodology

Color and B/W images have been generated from both dual-pol (11x) and quad-pol (16x) L- and C-band data takes and from fixed polarization X-band acquisitions respectively.

Dual-pol data color images have been obtained by combining the HH, HV and SPAN information on three (Red, Green and Blue) 8-bit color planes. That combination is especially helpful in the L-band where the cross-polarized return is mainly contributed by the high depolarization effect of dense vegetation. In such a way the green appearance of HV return facilitates the geologist to detect some variations in the lithology.

A more sophisticated processing has been developed and applied to quad-pol data takes. First and second order statistics of co-polarized and cross-polarized measurements can be easily extracted from scattering matrix or Stokes scattering operator and used to build a covariance matrix. If single-look data are available these statistics can be computed assuming both a temporal average of values (single look) or assuming a spatial average of values (multi look), the latter being less noisy. If HV=VH, the covariance matrix (now 3x3) can be decomposed, according to Cloude, Van Zyl, and Castellano, in the sum of three scattering mechanisms (the product of each eigenvector for its transpose with opposite phase) weighted by the respective eigenvalues. Even though the basis of such a decomposition is rotating in the target space for different targets (when the eigenvalues change the eigenvectors rotate in a plane), it can be shown that, if at a first approximation we assume a fixed basis of the decomposition, the eigenvalues will differentiate among targets with a different scattering behavior. In addition three eigenvalues (normalized or not) can be represented on three color planes for visual photo-interpretation.

Geology

The SIR-C/X-SAR images, generated as above mentioned, have been analyzed by using photo-interpretation techniques and integrated with images of comparable spatial resolution acquired by other sensors (ERS-1 ascending, descending and roll-tilt mode, JERS-1, AIRSAR). The results have been compared and/or integrated with geological sheets and when possible with aerial photos, geological sheets and field checks.

Brightness, color, texture, shading and pattern information is used for discriminating among geological features and lithologies. Foreshortening/layover effects, in the case of the Picentini mounts and of the Phlaegrean Fields, have been verified by comparing SAR images and geological cartographic profiles.

SIGNIFICANT RESULTS

Data Processing

Tables 1 (L-band) and 2 (C-band) show some experimental results obtained by decomposing the normalized covariance matrices computed over 9 sample windows (11x11 pixels). Each target (Vesuvius cone, 1944 lava flow, pine forest and sea) has been selected at most twice in order to check about the effects of slight different looking directions and/or incidence angles. Sea samples have been extracted from AIRSAR images since on these data the incidence angle ranges from 23° to about 58°.

For each sample have been computed the ratio HH/VV (second column), the ratio VV/HH (third column), the third eigenvalue (fourth column), the module (fifth column) and phase (sixth column) of correlation coefficient between co-polarized channels, the first (seventh column) and second (eighth column) normalized eigenvalues. The target "entropy", here defined as the sum of the normalized eigenvalues, is reported in the last column.

As can be noted, if the target is constituted by sand/ash as in the case of the Vesuvius cone, the first eigenvalue represents more than the 70% and 80% of target entropy for L-band and C-band respectively. These values suggest that, also for L-band scattering, the surface effect dominates the volumetric effect. A comparison made with P-band AIRSAR data shows a probably more consistent volumetric scattering at these frequencies (a value of 60% is typical on the Vesuvius cone). The analysis of λ_3 (η in the Tables) confirms these remarks; the L-band (5-6 %) and C-band (12-13%) values show clearly, for the latter, a higher depolarization effect suggesting that the pyroclastic products of the Vesuvius cone are rougher at a centimeter scale than at a decimeter scale.

For concerns of the 1944 lava flows, the depolarization effect increases sensibly with respect to the cone in the L-band as well as the C-band. The first eigenvalue is now only 50-55% of target entropy while the second and third eigenvalues reach about the 20-25%. It may be concluded that the roughness at a centimeter scale is comparable to the roughness at a decimeter scale.

Pine Forest data confirm that trend since the entropy increases and λ_1 is still decreasing (40-45% in L-band and 45-50% in C-band).

This decomposition of covariance matrix can be used also in the analysis of sea scattering. Some investigations which have been carried out show that at low incidence angles (23°)

the specular reflections largely dominate and target entropy is very low especially for L-band where the sea acts like a deterministic target and λ_1 constitutes about the 98% of total entropy. As the incidence angle increases the entropy increases as well and the VV return becomes also up to three times the HH return (L-band at 58°).

Geology

SIR-C/X-SAR images, because of the high incidence angle (about 50°) clearly show the differences between the western side of the Picentini mounts and the Avella mountains. The first ones are characterized by a complex overlapping of structures while the second ones are simply crossed by a normal fault.

The following classes have been easily discriminated:

1) Alluvium, pyroclastic products (ignimbrite campana), colluvium, flisch, and "melange" of the sicilide unity;

2) Carbonatic-dolomitic rocks of the "Campano-Lucana" platform;

3) Bedded sands and conglomerate of the Altavilla unit.

At low incidence angles (i.e., about 20-25°) discrimination between conglomerates and sands of the Altavilla unit, and the carbonatic formations is not possible. On the investigated area, the differences between calcareous-dolomitic and alluvium/flisch terrains are simply detected while the discrimination between flisch and alluvium is a difficult task. On the Mai mountains (a part of Picentini mountains), some Trias-Giura limits seems to be actually tectonic and not stratigraphic as pointed out in the literature.

In X-SAR imagery, the morphology of the Mounts Lattari stands out clearly as well as the boundaries among carbonatic rocks, colluvium and alluvial fan and tuff or eruptive volcanic products less or more pedogenized. The alluvial fan presents a very thin texture while the Vesuvius 1944 lava flows are less evident.

In the Somma-Vesuvius area, the limit between the products of pre-Mount Somma and the undiversified pyroclastic products has been recognized by using differences of intensity, color and texture which are due to changes of morphology, vegetation cover and drainage pattern. Good discrimination is achieved among the characteristics of the recent lavas, principal quarries, Mount Somma caldera rim, the drainage pattern and the pyroclastic products of the Vesuvius cone.

A detailed analysis of the Phlegrean Fields area requires the integration of data acquired with different incidence angles and from different looking directions in order to achieve a good detection of the crateric morphology and, in some cases, for the detection of zones affected by volcano-tectonic collapses. This is the case of Mount Gauro which is characterized by eastern and western crateric slopes slightly concave toward the exterior, with the sides higher than the center. The east and west slopes of the Gauro are related, according to some authors, to volcano-tectonic collapses following explosive events that occurred about 5000 years ago. SIR-C/X-SAR images show a more realistic morphology and the shadow distribution allows a good identification of the heights of this crateric edge.

HH polarization allows a good characterization, in terms of tone and texture typologies, of terrains and anthropic constructions while in the HV images, the texture is more homogeneous.

FUTURE PLANS

Research activities are still in progress. New sub-areas included in the Campania test-site will be considered, especially for what concerns INSAR and DINSAR data processing. For example, 16 corner reflectors have been already installed in the area of Sannio-Matese and new installations are planned in the next months.

Polarimetry

Further investigations both theoretical and experimental will be carried out on quad-pol data.

In particular the following items are under study:

- significance of eigenvector rotation and its potential for supervised/unsupervised target identification and characterization;
- simulation of covariance matrices of some targets. Currently a model "cloud of cylinders" with different distributions has been tested.

Interferometry

Since interferometric SLC L-band and C-band data were not yet available for Vesuvius or Etna, the work has been conducted on X-SAR SSC products which include the Vesuvius and a part of Matese area. Differential INSAR processing is under progress and the results will be compared with those extracted from ERS-1 SLC data.

PUBLICATIONS

[1] Castellano, L., A. Siciliano, and P. Murino, "Characterization of Natural Targets in Volcanic Areas Using SAR Polarimetric Covariance Matrix," *45th Congress of the International Astronautical Federation*, Jerusalem, Israel, 9/14 October 1994.

[2] Murino, P., M. Ferri, L. Castellano, L. Russo, and A. Siciliano, "Using SIR-C/X-SAR Data in the Analysis of Volcanic Areas. The Campania test site (Southern Italy)," *IGARSS '95*, Firenze, Italy.

[3] Castellano, L., "Nuovi Metodi di Analisi di Dati SAR Polarimetrici Ripresi da Piattaforme Aerospaziali," Ph.D. Dissertation, National Libraries of Rome and Florence (Italy), 1994.

[4] Castellano, L., P. Murino, and A. Siciliano, "Characterization of Natural Targets Using Multiparametric Spaceborne-SAR imagery," To be presented at *AGARD/NATO Meeting on Remote Sensing: A Valuable Source of Information*, Toulouse, France, 22-25 April 1996.

[5] Castellano, L., and P. Murino, "On the Usefulness of Interferometric SIR-C/X-SAR Data for Geological Investigations in Campania Test Site," To be presented *at 47th Congress of the International Astronautical Federation*, Beijing, China, October 7-11, 1996.

L-band	1/ζ	ζ	η	|ρ|	(deg)			
Cone 1	1.0003	0.9997	0.1210	0.8654	-2.5208	1.8655	0.1345	2.1210
Cone 2	1.0405	0.9611	0.1764	0.8119	-4.8326	1.8136	0.1879	2.1780
44' Lava 1	0.9608	1.0408	0.5562	0.3886	-7.2830	1.3914	0.6102	2.5578
44' Lava 2	0.9775	1.0230	0.5736	0.4111	-7.4226	1.4120	0.5885	2.5741
Forest 1	1.0956	0.9127	0.7312	0.2185	3.6549	1.2410	0.7673	2.7395
Forest 2	1.1336	0.8821	0.6097	0.2737	-1. 3037	1.3092	0.7066	2.6254
Sea (23∞)	0.9580	1.0439	0.0195	0.9613	-0.8334	1.9632	0.0386	2.0214
Sea (45∞)	0.4371	2.2879	0.0746	0.8739	0.8260	2.6363	0.0897	2.7996
Sea (58∞)	0.3176	3.1483	0.1835	0.7040	7.0143	3.3137	0.1522	3.6494

Tab. 1 - Decomposition of the covariance matrix (9 sample windows 11x11 pixels), L-band results.

C-Band	1/ζ	ζ	η		(deg)			
Cone 1	1.1558	0.8652	0.2873	0.6742	3.0451	1.7001	0.3208	2.3083
Cone 2	1.1588	0.8630	0.3033	0.6022	3.9899	1.6310	0.3908	2.3251
44' Lava 1	1.0277	0.9731	0.4983	0.4785	-5.0762	1.4796	0.5211	2.4991
44' Lava 2	0.9644	1.0369	0.4388	0.5211	-7.7925	1.5231	0.4782	2.4401
Forest 1	1.1808	0.8469	0.6669	0.2561	7.0226	1.3195	0.7081	2.6946
Forest 2	1.1566	0.8646	0.7099	0.2500	-8.8327	1.3001	0.7211	2.6002
Sea (23∞)	0.9222	1.0843	0.0070	0.8966	-13.3407	1.9035	0.1030	2.0135
Sea (45∞)	0.4770	2.0996	0.2048	0.7164	2.1040	2.3695	0.4141	2.7814
Sea (58∞)	0.5555	1.8003	0.5000	0.2681	0.7945	1.8556	0.5002	2.8558

Tab. 2 - Decomposition of the covariance matrix (9 sample windows 11x11 pixels), C-band results.

Dr. Jack F. Paris
Department of Biology
California State University
Fresno, CA 93740-0079

Co-Investigator:
Elizabeth Taylor Northern Arizona University

OBJECTIVES

Study the impact of tropical forest fragmentation on local populations of endangered and threatened species of certain mammals, butterflies, birds and plants. Vegetation information from SIR-C/X-SAR data over three tropical-forest intensive-study sites will aid an independent, broader study of forest fragmentation and its effects on biodiversity.

Add the unique, detailed information on forest fragmentation from spacecraft-based SAR to the broader study begun ins 1988.

Use imaging data from the Landsat Multispectral Scanner (MSS) and the National Oceanographic and Atmospheric Agency (NOAA) Advanced Very-High Resolution Radiometer (AVHRR) to assess on a biome scale, but with less spatial resolution than that of the SIR-C/X-SAR data.

Evaluate the use of the unique information about forest distributions and stand conditions expected from multiparameter synthetic aperture radar (SAR) relative to that from the MSS and AVHRR.

PROGRESS

Most of the effort has focused on preprocessing issues. CSUF staff developed and used an adapted version of the CEOS reader software package to enable the translation of original 6-10 byte SIR-C data or the 4 byte X-SAR data to raster formats compatible with off-the-shelf image processing software packages like the Map and Image Processing System (called TNTmips) from MicroImages, Inc. TNTmips is used by CSUF and by GeoEcoArc (Dr. K. Pope). TNTmips is also at UC Davis. The basic departure in our approach to SIR-C/X-SAR data preprocessing is to produce 16-bit integer rasters (rather than 8-bit integer) rasters from the compressed data produced by JPL or DLR. In addition, CSUF-derived indices (combinations of SIR-C data) are produced such as the Volume Scattering Index (VSI), the Canopy Structure Index (CSI), and the Interaction Type Index (ITI) (see Pope et al., 1994).

Another area of great attention during the last year has been the processing of ground truth data for the Manaus site. These consist of video tapes by Dr. Taylor, her sketch maps, her notes, and scans of maps for the region (1:50,000 scale and 1:250,000 scale). Relatively large-scale maps for the Manaus study site are rare.

Yet another processing issue of interest to CSUF is the question of the generation of textural information (by aggregate spatial analysis algorithms) from single-look complex (SIR-C SLC or X-SAR SSC) data. Dr. R. Smith has been exploring this issue in depth. Our focus is on ways and means for the aggregation of complex scattering data (one look) to multiple looks with attention to the correct handling of magnitude and phase data.

Begun many years ago, CSUF staff continue to work on the analyses of AIRSAR data taken over the UC Davis Winters site. Basically, the AIRSAR analysis is complete. We are waiting for an analysis of optical image data (Landsat TM and AVIRIS) by the UC Davis group. An extensive draft has been in existence for some time for a published paper on this effort.

SIGNIFICANT RESULTS

Preliminary results, from a general inspection of both the SIR-C and X-SAR data for common sites support the following significant results.

Proportion-based indices (PIs), in comparison with single-parameters, serve well to isolate certain biophysical properties of terrestrial landscapes with radar data. The set of PIs introduced by Pope et al. (1994) work well in hilly landscapes. In such landscapes, the effects of slope and aspect variations on a given solitary radar magnitude are severe and detract from their usefulness for estimation of biophysical conditions on the landscape. A PI is based on a ratio-like formulation, B*255/(B + A); thus, with both Raster A and Raster B being affected in the same way by slope and aspect, these effects divide out in the PI, and the PI indicates biophysical conditions on different slopes. With the availability of both C- and L-band radar parameters, a PI involving cross polarization parameters at the two different wavelengths is a good indicator of woody biomass. These results, first explored by Pope et al. (1994) in a Belizian test site and later explored by CSUF staff in the Winters test site, are holding true in the Manaus test site. The Winters results are significant in that they indicate that the landscape characterizations needed for turbulent land-air exchange modeling (Landscapes project, UC Davis, Dr. K.T. Paw U) can be obtained in part from multiparameter radar (like that of AIRSAR and SIR-C). Other parameters needed in the exchange model are likely to be obtained from optical multispectral data (work in progress at UC Davis).

FUTURE PLANS

With all of the requested SIR-C/X-SAR data in hand now (since August, 1995), we are moving ahead with the analysis phases of our investigation. We expect, with the cooperation of our many colleagues at other institutions, to reach many conclusions with regard to the SIR-C/X-SAR project by the end of FY96. In fact, we anticipate having several papers submitted by the time of the SIR-C/X-SAR meeting at UCSB in February 1996.

PUBLICATIONS

Pope, K. O., J. M. Rey-Benayas, and J. F. Paris, 1994: Radar remote sensing of forest and wetland ecosystems in the Central American tropics. *Remote Sensing of Environment,* 48:205-219.

Ustin, S. L., J. F. Paris, A. Palaceos, K. T. Paw U, 1995: Modeling turbulent exchange with remotely-sensed landscape parameters. Draft written and being reviewed by authors for submission to *Remote Sensing of Environment.*

Paris, J. F., 1995: Interaction Type Index (ITI): Physical basis and applications. In preparation for submission to an *IEEE* journal.

Smith, R., J. F. Paris, 1995: Aggregation techniques for single-look, multiparameter radar data. In preparation for submission to an image processing journal.

Dr. Kyaw Tha Paw U
Department of Land, Air &
Water Resources
University of California, Davis
Davis, CA 95616

Co-Investigators:
Roger Shaw Univ. of California, Davis
Susan Ustin Univ. of California, Davis
Jack Paris California State Univ., Fresno

Turbulent Exchange at Vegetated Surfaces and Evaluation of Estimates of Canopy Structure Using SIR-C Data; Ecology Science Team

OBJECTIVES

To characterize the turbulent exchanges of momentum, heat and gases from plant surfaces.

To evaluate the effects of foliage density, structure and height on the exchanges.

To evaluate the use of SIR-C/X-SAR remotely sensed data for estimating information regarding the type, structure, and status of vegetation needed for estimating the exchanges of momentum, heat and gases.

PROGRESS

We have made moderate progress in obtaining data needed for the analysis of the feasibility of using SRL data in addition to other remotely sensed data to assess biometeorological-surface exchange processes. We have carried out several experiments, and developed several analytical techniques following and surpassing our objectives on the biometeorological aspects of our projects. We have used optical data in several areas and are in the process of analyzing SRL data on the radar aspects of our project.

During the past 1.5 years, we have developed a new wavelet-like technique to analyze turbulent data, especially in identifying the large 'coherent structures' which are responsible for the majority of the exchange processes (such as for trace gases and momentum). This methodology has yielded results that imply plant height is a very important scaling factor, along with mean wind speed. We have also found in related research that true orthonormal wavelets are not suitable for many types of turbulence research, including some types that have been published (possibly by people jumping on a trendy bandwagon). Therefore the method we have developed appears to be a good alternative.

We have developed a plant-atmosphere biometeorology model which includes a higher-order closure description of turbulence. This model now includes current physiological process models in addition to its sophisticated turbulence description. A preprint is listed below, which describes the significant differences (implying errors) between simpler Si-B like models and higher-order closure models, for predicting global change responses of canopies. The higher-order closure model has given insights into the type of data and the accuracy of data needed by SRL and optical platforms (see below for a further description).

Important inputs include canopy height, Leaf Area Index (LAI), and a general idea of the plant type (for inclusion of appropriate plant physiological response parameterization).

In our field experiments, we have begun analysis of the biometeorological data obtained during the SRL-1 and SRL-2 overflights for the Howland, Maine site and Davis site. One preprint describes progress in assessing water vapor and carbon dioxide exchange at the Davis site associated with an

SRL-2 overflight intensive field campaign period. In this and a related preprint we have established that the surface-renewal method, which depends on knowledge of the canopy height, works reasonably well.

The processing of the AVIRIS optical data for the Davis-Winters site has taken place and preliminary results include assessment of vegetation type, and therefore an indirect estimation of canopy height, LAI, and gap fraction. We are also investigating the measurement of these canopy properties and fraction woodiness, woody biomass, and water content using radar and optical datasets. We have evaluated multivariate spectral mapping of soil types and found we were able to separate very similar soils having different organic content and texture, properties related to the water holding capacity differences. Another aspect of our investigations is to use SRL and optical data to detect quantify surface heterogeneity at different spatial scales. Current biometeorological models assume homogeneity in the spatial domain and the sharp discontinuities in flux processes and surface roughness actually found between agricultural fields violate these simple assumptions. The turbulence model we are developing should provide better energy balance estimates using this information on landscape structure.

We have pioneered a new approach to spectral analysis using finite impulse response filters (FIR) and Gabor transforms (a form of wavelet analysis; we note in passing that wavelet analysis was originally developed for image processing although it has been used, sometimes inappropriately, in many other fields). This method allows us to separate small spectral signals such as differences in some biochemical properties of the plant canopy. It has considerable promise for time-series analyses of landscape change. We have also explored the potential for radiative transfer modeling to estimate canopy biochemicals. We have revised the PROSPECT model to include estimates of pigments, carbon, nitrogen, and water contents for leaves. This model has been incorporated into a canopy model, the IAPI model for predicting canopy reflectance and from satellite sensors. The biochemical functions from PROSPECT have been incorporated into a new ray-tracing model of the leaf that explicitly considers leaf cellular structure. These new approaches appear promising to provide detailed information on the functional status of canopies for the biometeorological model.

Radar data processing has been delayed greatly by the lack of time by one of the co-PI's on the project, Jack Paris. Originally, all radar data were to be processed by him, but there have been delays. Currently, another co-PI, Susan Ustin, is beginning to analyze the radar data instead, in addition to her general analysis of the optical data. Despite these difficulties, we have already written a second draft of a paper describing research in modeling the sensitivity of exchange estimates to remotely-sensed vegetation parameters. The higher-order turbulence and biometeorology model is being used, along with data inputs representing errors in the estimated plant parameters, obtained from SRL and optical sensors. This is listed below under the "in preparation" manuscripts.

PUBLICATIONS

Refereed Journals

Paw U, K. T., Qiu, J. , Su, H. B., Watanabe, T., and Brunet, Y., 1995. Surface renewal analysis: a new method to obtain scalar fluxes without velocity data. *Agric. For. Meteorol.* 74:119-137.[1]

Qiu, J., Paw U, K. T. and Shaw, R. H., 1995. Pseudo-wavelet analysis of turbulence patterns in three vegetation layers. *Boundary-layer Meteorol.* 72:177-204.[2]

Paw U, K. T., Y. Brunet, S. Collineau, R. H. Shaw, T. Maitani, J. Qiu and L. Hipps, 1992. On coherent structures in turbulence within and above agricultural plant canopies. *Agric. For. Meteorol.* 61:55-68.[1]

Paw U, K. T., 1992. Development of models for thermal infrared radiation above and within plant canopies. *J. Photogrammetry Remote Sens.* 47:189-203.[3]

Zhang, Changan, R. H. Shaw and K. T. Paw U, 1992. Spatial characteristics of turbulent coherent structures within and above an orchard canopy. In Precipitation Scavenging and Atmosphere-Surface Exchange, Vol. 2, coordinators Schwartz, S. E. and Slinn, W. G. N., Hemisphere Publishing Co., Washington. pp. 741-751.[1]

Paw U, K. T., 1992. A discussion of the Penman form equations and comparisons of some equations to estimate latent energy flux density. *Agric. For. Meteorol.* 57:297-304.[3]

In Press:

DeFries, R., C. Field, I. Fung, C. Justice, J. Townshend, S. Los, P. Sellers, C. J. Tucker, P. Matson, E. Matthews, K. Prentice, H. Mooney, P. Vitousek, C. Potter, and S. Ustin, 1995. An approach to characterize the land surface with continuous fields for global atmosphere-biosphere models. *J. Geophys. Research* (in press).[4]

Submitted:

Su, H.-B., Paw U, K. T., and Shaw, R.H., Development of a coupled leaf and canopy model for the simulation of plant-atmosphere interaction. Submitted to *J. Appl. Meteorol.* [3]

Orueta Palaceos, A., and S. L. Ustin, Multivariate statistical classification of soil spectra. Submitted to *Remote Sensing of Environment* (in review).[4]

Jacquemoud, S., S. L. Ustin, J. Verdebout, G. Schmuck, G. Andreoli, and B. Hosgood. Prospect Redux. Submitted to *Remote Sensing of Environment* (in review).[4]

Grossman, Y. L., S. L. Ustin, E. Sanderson, S. Jacquemoud, G. Schmuck and J. Verdebout, Examination of regression and correlation approaches for extraction of leaf biochemistry information from leaf reflectance data. Submitted to *Remote Sensing of Environment* (in revision).[4]

Govaerts, Y. M., S. Jacquemoud, M. M. Verstraete, and S. L. Ustin., 1995. Modeling plant leaf bidirectional reflectance and transmittance with a 3-d ray tracing approach. Submitted to *Applied Optics.*[4]

Xiao, Q. -F., S. L. Ustin, and W.W. Wallender, A spatial and continuous surface-subsurface hydrologic model. Submitted to *J. Geophys. Research* (in revision).[4]

Ustin, S. L. , Q. J. Hart L. Duan and G. Scheer, Vegetation mapping on hardwood rangelands in California, Submitted to *I.J. Remote Sensing* (in review, submitted 5/95).[4]

In Preparation:

Ustin, S. L., Paris, J. F., Palacios, A., and Paw U, K. T. Modeling Turbulent Exchange with Remotely-Sensed Landscape Parameters.[4]

Paw U, K. T. and H. -B. Su. Structure function analysis of sensible heat flux density and coherent structure characteristics.[2]

Pinzon, J. E., S. L. Ustin, M. Castenada, S. Jacquemoud, and M. O. Smith. Investigation of leaf biochemistry by foreground and background analysis.[4]

Preprints, Proceedings and Abstracts:

Paw U, K. T. and Su, H. -B., 1994. The usage of structure functions in studying turbulent coherent structures and estimating sensible heat flux. pp. 98-99. In preprints, *21st Conference on Agricultural and Forest Meteorology*, March 7-11, 1994, San Diego, California. American Meteorological Society, Boston, MA.[2]

Qiu, J., Paw U, K.T. and Shaw, R.H., 1994. Pseudo-wavelet analysis of turbulence patterns in three vegetation layers. pp. 106-109. In preprints, *21st Conference on Agricultural and Forest Meteorology*, March 7-11, 1994, San Diego, California. American Meteorological Society, Boston, MA. 2.

Paw U, K.T., 1994. Development of a higher order closure turbulence model for simulating particulate, pollen and spore transport within plant canopies. pp. 401-402. In preprints, *11th Conference on Biometeorology and Aerobiology,* March 7-11, 1994, San Diego, California. American Meteorological Society, Boston, MA.[3]

Pereira, A. R., and Paw U, K. T. 1994. A surface renewal description of the exchange of scalars between full canopies and the atmosphere. pp. 104-105. In preprints, *21st Conference on Agricultural and Forest Meteorology,* March 7-11, 1994, San Diego, California. American Meteorological Society, Boston, MA.[2]

Qiu, J., R. H. Shaw and K. T. Paw U, 1991. Comparison of turbulence statistics and structures at four vegetation canopies. pp. 66-67. In preprints, *20th Conference on Agricultural and Forest Meteorology,* September 10-13, 1991, Salt Lake City, Utah. American Meteorological Society, Boston, MA.[2]

Zhang, Changan, R. H. Shaw and K. T. Paw U, 1991. Translation velocity of turbulent coherent structures within and above an orchard canopy. pp. 193-194. In preprints, *20th Conference on Agricultural and Forest Meteorology*, September 10-13, 1991, Salt Lake City, Utah. American Meteorological Society, Boston, MA.[1]

Paw U, K. T., 1991. Anisotropy of thermal infrared radiation above and within plant canopies. pp. 199-200. In preprints, *20th Conference on Agricultural and Forest Meteorology,* September 10-13, 1991, Salt Lake City, Utah. American Meteorological Society, Boston, MA.[3]

Govaerts, Y. M., S. Jacquemoud, M. M. Verstraete, and S. L. Ustin., 1995. Modeling plant leaf bidirectional reflectance and transmittance with a 3-d ray tracing approach. *IGARSS-95.*[4]

Jacquemoud, S., S. L. Ustin, J. Verdebout, G. Schmuck, G. Andreoli, and B. Hosgood, 1995. Prospect Redux. In *Summaries of the Fifth Annual JPL Airborne Earth Science Workshop,* JPL Publication 95-1, pp. 99-104 Jet Propulsion Laboratory, Pasadena, CA. January 23-26, 1995.[4]

Pinzon, J. E., S. L. Ustin, Q. J. Hart, S. Jacquemoud, and M. O. Smith, 1995. Using Foreground/Background Analysis to Determine Leaf and Canopy Chemistry. In *Summaries of the Fifth Annual JPL Airborne Earth Science Workshop*, JPL Publication 95-1, pp.129-132, Jet Propulsion Laboratory, Pasadena, CA. January 23-26, 1995. [4]

Hart, Q. J., S. L. Ustin, G. Scheer, and L. Duan, 1994. Estimating dry grass biomass residues using AVIRIS image analysis. In *Int. Geosci. and Remote Sens. Symp. IGARSS '94.* August, 1994 California Institute of Technology.[4]

Ustin, S. L., L. Duan, Q. J. Hart, 1994. Seasonal changes observed in AVIRIS images of Jasper Ridge, California. In *Int. Geosci. and Remote Sens. Symp. IGARSS '94.* August, 1994 California Institute of Technology.[4]

Grossman, Y. L., E. Sanderson, and S. L. Ustin, 1994. Relationships between canopy chemistry and reflectance for plant species from Jasper Ridge, California, in *Int. Geosci. and Remote Sens. Symp. IGARSS '94.* August, 1994 California Institute of Technology.[4]

In Press:

Paw U, K.T., Su, H-B., Charlevoix, D., and Hsiao, T.C., Testing of an advanced plant physiology model linked with a plant-atmosphere higher order closure turbulence model for response to elevated CO2 concentrations. In Press, preprints, *22nd Conference on Agricultural and Forest Meteorology,* Atlanta, Georgia. American Meteorological Society, Boston, MA.[3]

Paw U, K. T., Su, H-B., and Braaten, D. A.. The usage of structure functions in estimating water vapor and carbon dioxide exchange between plant canopies and the atmosphere. in Press, preprints, *22nd Conference on Agricultural and Forest Meteorology,* Atlanta, Georgia. American Meteorological Society, Boston, MA.[2]

Paw U, K. T., Biermann, H. and Johnson, R., A comparison of FTIR and UVGA eddy covariance and surface renewal estimates of water vapor and carbon dioxide fluxes. In Press, preprints, *22nd Conference on Agricultural and Forest Meteorology,* Atlanta, Georgia. American Meteorological Society, Boston, MA.[4]

Su, H. -B., Shaw, R. H., Paw U, K. T., Moeng, C-H., and Sullivan, P.P. Modeling forest-atmosphere interaction by coupling a large-eddy simulation with a leaf and canopy model. In Press, preprints, *22nd Conference on Agricultural and Forest Meteorology,* Atlanta, Georgia. American Meteorological Society, Boston, MA.[3]

Su, H. -B., Paw U, K. T., and Shaw, R. H. Development of a coupled leaf and canopy model for the simulation of plant-atmosphere interactions. In Press, preprints, *22nd Conference on Agricultural and Forest Meteorology,* Atlanta, Georgia. American Meteorological Society, Boston, MA.[3]

Explanation of superscripts:

1 Uses data gathered at sites covered by SRL actual and proposed datatakes.

2 Development of analysis technique to assist in data processing, and to further the field of biometeorology.

3 Model development to be used in the assessment of sensitivity of exchange processes to SRL and optically derived plant variables.

4 Uses data and models to accomplish preliminary estimates of sensitivity of exchange processes to SRL and optically derived plant variables, or optical and/or SRL data to estimate variables related to estimating the sensitivity.

Kevin O. Pope
Geo Eco Arc Research
2222 Foothill Blvd. Suite E-272
La Canada, CA 91011

Co-Investigators:
Jack F. Paris Cal State University, Fresno
Eliska Rejmankova U. of California, Davis

SIR-C/X-SAR Investigations of Wetland Hydrology in the Seasonal Tropics

OBJECTIVES

Demonstrate the capabilities of spaceborne multifrequency polarimetric SAR imagery for monitoring seasonal flooding in tropical and subtropical regions.

Use the SIR-C/X-SAR imagery to map spatial patterns of wetland communities and determine spatial and temporal patterns of inundation in conjunction with a variety of ecological and geological studies. These studies include monitoring of breeding sites of the malaria transmitting mosquito, studies of wetland biogeochemical gradients, and studies of groundwater discharge systems and their relationship to the buried Chicxulub impact crater.

PROGRESS

Polarimetric L- and C-band and XVV radar imagery were acquired for dry (April) and wet (October) seasons for wetland sites in Chiapas and the Yucatan Peninsula. Field campaigns were conducted in both seasons in Chiapas and the Yucatan to record the biophysical character of the wetlands and to record seasonal changes in flooding. Analyses of field data from marshes in the Yucatan have been completed, while analyses of data from Chiapas and from forested wetlands and mangroves in the Yucatan are still underway.

Marshes in Yucatan are dominated by three species of emergent macrophyte: *Cladium jamaicense* (sawgrass), *Typha domingensis* (cattail), and *Eleocharis cellulosa* (rush). Communities of these three species occur as monospecific stands, mixtures of monospecific clumps, and mixtures with a single dominant species. Eleven marsh sites were studied in detail encompassing a wide variety height, density, and species composition. The only significant seasonal change observed in the marshes was in flooding. Changes from dry to continuously flooded, dry to partially flooded, partially flooded to continuously flooded, and changes in the depth of continuous flooding were observed in the 11 marsh sites. All field observations were located with a hand-held GPS receiver.

Wet and dry season SIR-C polarimetric L- and C-band imagery from data take 81.0 have been georeferenced and coregistered. Backscatter amplitude (HH, VV, CS= average of HV+VH) and phase (|H-V phase difference|=PD) statistics were extracted from the seasonal images for polygons corresponding to the survey areas of the 11 marsh sites and from a stable calibration site of closed canopy evergreen forest. Significant seasonal changes in amplitude and phase above the calibration limit were then determined for the marshes. A similar analysis is currently being conducted for the mangrove and swamp forest communities within the same coregisterd images and preliminary results have been obtained.

SIGNIFICANT RESULTS

Increased flooding in marshes can be detected by SIR-C by: 1) an increase in backscatter magnitude in marshes with tall, dense cover; 2) a decrease in backscatter amplitude in marshes with short, sparse cover; and 3) an increase in PD in all types of marshes. Magnitude increases result

from an increase in double bounce interactions between the emergent vegetation and water surface, while decreases result from an increase in forward scattering off the open water. Average PD values increase due to an absolute or relative increase in double compared to single bounce interactions. Changes from dry or partially flooded to completely flooded and increases in water depth could be detected by most of the polarimetric parameters, but changes from dry to partially flooded could not. CPD changed significantly for all 11 marshes studies, followed by LPD and LVV (9 marshes) and LHH, LCS, and CVV (7 marshes). CHH detected significant changes in five marshes, but produced near significant changes (±1.8-1.9 dB) in four others.

FUTURE PLANS

An analysis similar to the marsh study summarized above is near completion for mangroves and swamp forest in the Yucatan test site. A similar analysis is also planned for wetlands in the Pacific coastal plain of Chiapas. The Chiapas sites add an additional suite of wetlands including different marsh species and extensive tall mangroves.

The marsh monitoring capabilities developed in this study are being refined for application in a Radarsat ADRO project employing Radarsat, ERS-1, 2, and JERS-1 imagery of Belize to monitor malaria transmitting mosquito breeding sites in a program of malaria control.

The flood detection capabilities developed in this study are being applied to an analysis of groundwater discharge systems in the Yucatan and their relationship with the buried Chicxulub impact crater.

PUBLICATIONS

Pope, K. O., Rey-Benayas, J. M., and Paris, J. F. (1994). Radar remote sensing of forest and wetland ecosystems in the Central American Tropics, *Rem Sens. Environ.* 48:205-219.

Rejmankova, E., Pope, K. O., Post, R., and Maltby, E. (in press). Herbaceous wetlands of the Yucatan Peninsula: Communities at extreme ends of environmental gradients, *Int. Rev. Ges. Hydrobiol.*

Pope, K. O., Ocampo, A. C., Kinsland, G. L., and Smith, R., (in review). Surface expression of the Chicxulub crater, *Geology.*

Pope, K. O., Rejmankova, E., Paris, J. F., and Woodruff, R. (in review). Monitoring seasonal flooding cycles in marshes of the Yucatan Peninsula with SIR-C polarimetric radar imagery, *Rem. Sens. Environ.*

Dr. K. Jon Ranson
Biospheric Sciences Branch
Code 923
Goddard Space Flight Center
Greenbelt, MD 20771
e-mail: jon@taiga.gsfc.nasa.gov

Co-Investigators:
Herman Shugart University of Virginia
James A. Smith Goddard Space Flight Center
Guoqing Sun Science Systems Applic., Inc.

Collaborators:
Roger Lang George Washington Univ.
Narinder Chauhan
Ozlem Kilic
Randal Cacciola

John Weishampel Univ. of Central Florida
Eric Nielson University of Virginia
Lance Lockart University of Kansas
Bob Knox GSFC/Code 923
Sasan Saatchi JPL
Slava Kharuk Sukachev Forest Institute, Siberia, Russia

SIR-C/X-SAR - Imaging Radar Analyses For Forest Ecosystem Modeling

OBJECTIVES

Ecosystem characterization using SIR-C/X-SAR and AirSAR data.

Improving radar backscatter models for forest canopies.

Using SAR measurements and models with forest ecosystem models to improve inferences of ecosystem attributes and processes.

PROGRESS

To date we have analyzed multiple SIR-C/X-SAR data sets for Prince Albert, Canada; Howland, Maine; and Western Sayani, Siberia. In addition, we have requested and received data for Nelson, House, Manitoba; Wallops Island, Virginia and Voyageurs National Park, Minnesota. A brief summary of results follows.

Ecosystem characterization using SAR

Procedures and results of using SIR-C/X-SAR data to map forest cover type and above ground forest biomass were developed and applied to SIR-C X-SAR data of the Canadian boreal forest (i.e., Prince Albert , BOREAS study area). Forest cover type classification accuracies on the order of 80% were achieved with standard supervised classification techniques and the multiple frequency and multipolarization radar data. The results also show that maps of estimated biomass can be produced that match observed patterns and preliminary ground data. The sensitivity to boreal forest biomass in our study area was between 15 and 20 kg/m^2. Better sensitivity over the range of biomass in our study was attained using a ratio of L-band HV to C-band HV backscatter. We also found that using the backscatter ratio appeared to reduce the difference in backscatter due to different species or mixtures. This will be examined further as additional quantitative data become available.

A comparison of the April and October data sets was also conducted to understand the effects of seasons on the analysis. Frozen trees and wetter background contributed to increased backscattering observed in the April data. SIR-C/X-SAR data acquired during the growing season would be useful to determine the effects of deciduous leaves on biomass estimation. Results of mapping forest cover and biomass in our study area using SIR-C/X-SAR data are encouraging and should be useful for the study of above ground carbon in boreal ecosystems. Sensitivity to biomass was sufficient to map most of the types of stands in our area, but we need to examine additional ground measurements to verify this. We continue to expand the ground truth data base and test these results in a more rigorous fashion.

An evaluation of the SIR-C/X-SAR results with respect to AIRSAR in terms of different wavelengths (i.e. X-band and P-band) and resolution (28 m vs. 12 m) was performed for the Howland, Maine Backup Supersite and GSFC Forest Ecosystem Dyhamics study area. SIR-C/X-SAR data was analyzed to classify forest types, estimate above ground biomass and characterize forest spatial patterns for Howland, Maine. SIR-C/X-SAR performed well as compared with AIRSAR data, but was not able to discriminate forest types adequately. Continued work will focus on improving classification procedures and developing other techniques for spatial pattern analysis.

Improving radar backscatter models

In retrieval of forest parameters from radar images, one of the major concerns is the uncertainty or error induced by the variation of tree size and position. A new 3-D radar backscatter model was developed and tested which takes into account spatially distributed gaps and clustering of trees. This spatially explicit, 3-D model was used to simulate AIRSAR signatures from a test site in Howland, Maine. The results showed that the model worked well for our predominately coniferous forest test site by giving good prediction of total backscattering averaged over the site. Significant spatial correlations between AIRSAR and simulated images were also produced for all frequencies (P, L and C-band) and polarization combinations (HH, VV, HV).

Forest stands with different spatial patterns (random and clumped) were simulated. Results indicated that the total backscattering is higher for stands with randomly positioned trees than for a clumped stand. The textures of the simulated images were different because of the different tree position patterns. Lacunarity analysis was performed on the total HH backscattering images to reveal this difference.

SAR images of forests with hidden objects i.e., 2.43 m corner reflectors and metal cylinders (radius of 0.5 m and height 1 meter) were simulated for C, L and P bands. High-resolution (1-meter pixel) and low-resolution (12 meters of AIRSAR) images were simulated. The hidden objects were easily visible at L and P bands, but not at C bands. At C band, because of high attenuation, the hidden targets can only be seen through forest gaps. The hidden objects were not very distinct in low-resolution images even though speckles don't exist in these simulated images.

Using SAR with forest ecosystem models

Development of algorithms for using SAR data to infer biomass by using a forest succession model to simulate forest canopy parameters to run a radar backscatter model. A gap-type forest succession model was parameterized to simulate growth and development of a northern hardwood-boreal transitional forest typical of central Maine, USA. Forest model results of species, bole diameter, stem and crown heights of individual trees in a stand, plus density of trees were used to run a discontinuous canopy backscatter model to determine radar backscatter coefficients for the simulated forest stands. Using the model results, relationships of backscatter to forest biomass were developed and applied to an AirSAR image over a forested area in Maine. Using only

modeled results the derived relationship was found to underestimate biomass. Calibrating the model results with limited measurements improved the algorithm significantly.

Applying the calibrated model derived algorithm to SAR imagery produced reasonable results when mapped biomass was limited to 15 kg/m2 or less. These results can be improved as the forest and backscatter models are improved. For example a single species forest growth function was used in the model. Parameterizing the growth function for the species common to the study area would improve the forest composition and stand structure results.

FUTURE PLANS

Since our SIR-C/X-SAR project is closely allied with forest ecosystem dynamics research at GSFC we will continue analyze data over coincident study areas such as Howland, Maine; Prince Albert, Saskatchewan; Nelson House, Manitoba, Wallops Island, VA, Voyageurs and Itasca Parks in Minnesota and the Western Sayani Mountains, Siberia. Many of these data sets have been ordered and received. The JPL Radar Data Center is to be commended for the prompt attention given to our data requests.

We plan to use SIR-C/X-SAR data to examine the stratification of forest areas based on general surface cover prior to biomass mapping, the sensitivity of the biomass mapping to seasonal change of moisture and temperature conditions, the effects of radar illumination angle, and the combination of microwave and optical remote sensing data in forest classification and biomass mapping. Several publications are anticipated in the near future covering the various topics listed above.

Currently, radar models do not simulate cross polarized backscatter very well because of the lack of treatment of multiple scattering. This in an obvious area of future work. Our radar backscatter models will be further improved by incorporating higher-order scatterers. Radar backscatter modeling will be used to investigate the radar responses to successional forest structures by using the simulated forests from forest growth models as inputs. These modeling results will aid in improvement of forest parameter retrieval algorithms.

Given the emphasis of topography for SRL-3 we plan to explore the use of interferometric SAR for our forest ecosystem research. The Western Sayani Mountains test area we are working on with Dr. Slava Kharuk of the Sukachev Forestry Institute in Siberia poses topographic challenges to our ecosystem analyses. Fortunately, repeat pass SRL-2 data was obtained and are being ordered. The topographic information interferometrically derived from these data as well as DTM data (if available) will be used to improve and extend our current biomass mapping methods to mountainous areas through data correction for local incidence angle, layover and shadows.

Another extremely interesting possibility is the use of interferometry to estimate forest stand height. It may be difficult to retrieve actual heights from interferometry data because of the uncertainty in the position of scatter centers. Even this course level of information is useful for the ecosystem models and will aid in development of algorithms for forest attributes. We will also explore the possibility of detecting forest gaps and edges by retrieving heights of scattering centers.

The SIR-C/X-SAR missions are demonstrating the unique capabilities of multiple frequency and multipolarization SAR data for studies of the Earth. Similar measurements over a significant portion of the Earth's biomes will produce a unique and valuable source of data for terrestrial ecologists and climatologists. Global maps of important terrestrial vegetation parameters derived from these data sets can be used directly by scientists to gain further understanding of the current "state of the Earth" and develop insight into the global consequences of climate change. Thus we look forward to a third SIR-C mission that would map significant areas of the worlds forests with L-band co- and cross polarized channels in addition to the topographic data.

PUBLICATIONS (1994-1995)

Refereed Journal Articles

Lang, R.H., N.S. Chauhan and K.J. Ranson, (1994). Modeling of P Band SAR returns from a red pine stand. *Remote Sens. Environ.* 47(2):132-141.

Ranson, K. J., G. Sun , J.F. Weishampel , and R.G. Knox (1995) Forest biomass from combined ecosystem and radar backscatter modeling.

Ranson, K. J., Saatchi, S. and G. Sun. (1995), Boreal forest ecosystem characterization with SIR-C/XSAR. *IEEE Trans. Geosci. Remote Sens.* 33:867-876.

Ranson, K.J. and G. Sun, "Mapping biomass for a northern forest using multifrequency SAR data," *IEEE Transactions on Geoscience Remote Sensing*, 32(3):388-396, (1994).

Ranson, K.J. and G. Sun, (1994), "Northern forest classification using temporal multifrequency and multipolarimetric SAR images," *Remote Sensing of Environment*, 47(2):142-153.

Salas, W.A., K.J. Ranson, B.N. Rock and K.T. Smith. (1994). Temporal and spatial variations in dielectric constant and water status of dominant conifer species from New England, *Remote Sensing Environ.* 47(2):109-119.

Sun, G. and K. J. Ranson. (1995), A three-dimensional radar backscatter model of forest canopies, *IEEE Trans. Geosci. Remote Sens.* 33:372-382.

Waring, R., J. Way, R. Hunt, L. Morrisey, K.J. Ranson, J. Weishampel and R. Oren, (1995) Imaging radar for ecosystem studies, *BioScience*, 45(10) 715-723.

Weishampel, J.F., G. Sun, K.J. Ranson, H.H. Shugart and K.D. Lejeune. (1994). Inference of spatial resolution on forest texture derived from simulated SAR images. *Remote Sensing Environ.* 47(2):120-131.

Weishampel,J.F., K.J. Ranson and D. Harding. (1995). Remote sensing of forest canopies. Selbyana. (in press).

Book Chapters

Leckie, D, (1995), Manual of Remote Sensing: Radar Volume, Forestry Applications Chapter (J. Ranson contributing author) In preparation.

Moughin, E., K.J. Ranson and J.A. Smith eds., (1995). SPIE Conf. Multispectral and microwave sensing of forestry, hydrology, and natural resources, Rome, Italy, Sept 26-30, 1994. Vol. 2314, 630 pp.

Weishampel,J.F., R.G.Knox, K.J. Ranson, D.L. Williams and J.A. Smith, (1995). Integrating remotely sensed spatial heterogeneity with a 3-D forest succession model, in Gholz, H.L., Nakane, K. and Shimoda, H. (eds), The use of remote sensing in the modeling of forest productivity at scales from the stand to the globe. Kluwer Acad. Publishers, Dordrecht (in press).

Published Proceedings

Chauhan, N. S., R. Lang, J,. Ranson and O. Kilic, (1994), Multistand radar modeling from a boreal forest: Results from the BOREAS Intensive Field Campaign- 1993. *Proc. IGARSS '94,* Pasadena, CA, August 8-12.

Knox, R. G., K. J. Ranson, J. F. Weishampel and L. Prihodko, (1995), A vegetation context for scaling results within the BOREAS Southern Study Area. ESA Meeting, Snow Bird Utah.

Lang, R. H., K. J. Ranson, N. S. Chauhan and O. Kilic, (1994), Radar analysis and modeling of forest stands for biomass estimation, Progress in Electromagnetic Radiation Symposium, The Netherlands, July.

Lee, J. S., D. L. Schuler, R. H. Lang and K. J. Ranson, (1994), K-distribution for multilook processed polarimetric SAR imagery, *Proc. IGARSS '94*, Pasadena, CA, August 8-12.

Ranson, K. J. , J. A. Smith, G. Sun, J. F. Weishampel and R.G. Knox, (1995), Forest structure from combined optical and microwave modeling and measurements, by submitted to Combined Optical-Microwave Earth and Atmosphere Sensing (CO-Meas'95), Atlanta, GA April 1995.

Ranson, K. J., Guoqing Sun, John F. Weishampel and Robert G. Knox, (1995), Interfacing forest succession and remote sensing models for forest ecosystem studies, SPIE Conf. Multispectral and microwave sensing of forestry, hydrology, and natural resources, Rome, Italy, Sept 26-30, 1994. Vol. 2314, pp. 526-537.

Ranson, K. J., R. H. Lang, G. Sun N. S. Chauhan and R.J. Cacciola, (1995), Mapping of boreal forest biomass using synthetic aperture radar measurements and modeling, Retrieval of Bio- and Geophysical Parameters from SAR for Land Applications, Toulouse France, 10-13 October.

Ranson, K. J. and G. Sun, (1995), Dependence of radar backscattering on northern forest structure observed from AirSAR and SIR-C/XSAR. *IGARSS '95.*

Ranson, K. J., G. Sun , J. F. Weishampel and R. G. Knox, (1995), An evaluation of SIR-C/XSAR images for northern forest ecological studies in Maine, USA. *IGARSS '95*, Florence, Italy.

Saatchi, S., K. J. Ranson, G. Sun, (1995), Boreal Forest Characterization with SIR-C/X-SAR. Progress in Electromagnetic Research Symposium-95, Seattle, WA.

Sun, G. and K. J. Ranson, (1994), Forest ecological studies and radar backscatter modeling, UN/CHINA/ESA Workshop on Microwave Remote Sensing Applications, Beijing, China, Sept. 14-18, 1994.

Sun, G. and K. J. Ranson, (1994), Spatially explicit modeling of radar backscatter from forest canopies, Proceedings of EUROPTO, Vol. 2314, pp. 559-570. The European Symposium on Satellite Remote Sensing, 26-30 September, NRC of Italy Headquarters, Rome, Italy.

Poster Presentations

Sun, G. and K. J. Ranson, (1995), Three dimensional radar backscatter model for forest canopies, Remote Sensing Science Workshop, NASA/GSFC, Feb. 27-March 1.

Ranson, K. J., Lang, R. H., Sun, G. Chauhan, N. S. and R. Cacciola (1995), Mapping of boreal forest biomass using synthetic aperture radar measurements and modeling. BOREAS Workshop, October 10-13, 1995, Laurel, MD.

Dr. Helmut Rott
Institute for Meteorology and Geophysics
University of Innsbruck
Inrain 52
A-6020 Innsbruck, Austria

Co-Investigators:
D.-M Floricioiu Univ. of Innsbruck
T. Nagler
A. Siegel
C. Mätzler Univ. of Bern, Switzerland

High Alpine SAR Experiment

OBJECTIVES

The High Alpine SAR Experiment is aimed at the development of methods and the demonstration of applications of multifrequency polarimetric SAR for investigations of high alpine environment with emphasis on snow and glacier applications. The main activities, including extensive field campaigns and data analysis, were related to the test site Ötztal in the Central Alps of Austria which had been selected as SIR-C/X-SAR supersite for snow hydrology and glaciology. Complementary investigations on snow applications were carried out in the region near Innsbruck, where different snow types than at the high alpine site Ötztal were observed during SRL-1 in April 1994. Valuable glaciological information was derived from SIR-C/X-SAR data also for Viedma Glacier and Moreno Glacier of the Southern Patagonian Icefield. On Moreno Glacier the PI is leading a glaciological research project involving field measurements and satellite data analysis.

PROGRESS

During the two SIR-C/X-SAR missions SRL-1 (9 to 20 April 1994) and SRL-2 (30 September to 10 October 1994) extensive field measurements were carried out on glaciers and on ice-free parts of the test site. The measurements included:

During both SRL-1 and SRL-2:
- deployment and geodetic measurement of corner reflectors (1.25 to 1.8 m leg length) on glaciers,
- measurement of snow depth, density, grain size, dielectric constant, stratification, temperature in snow pits,
- surface roughness profiles of snow and ice,
- meteorological measurements,
- mapping of snow extent,

Additional measurements during SRL-1:
- backscattering of snow at 5 GHz and 35 GHz HH, VV, HV, VH,
- emission of snow at 21 and 35 GHz, H and V,

Additional measurements during SRL-2:
- backscattering of bare soil and alpine grassland at 5.3 GHz and 10.3 GHz HH, VV, HV, VH,
- measurements of soil humidity and surface roughness.

Measurements throughout the year:
- hourly mean runoff of two basins in the central part of the test site,
- ice ablation and accumulation for determination of glacier mass balance,
- meteorological stations.

During SRL-1 the glaciers were covered by dry winter snow, the air temperature at 3000 m was below -10°C, and snowfall was observed during several days. At lower elevations the

snow-structure was more complex, and the snowpack was partly humid. During SRL-2 the meteorological conditions changed drastically; the mean daily air temperature dropped by 12°C during the campaign, resulting in significant changes of snow properties and backscattering signatures on the glaciers.

All data, which had been acquired over the test site, were processed and delivered. We obtained the following scenes:

SRL-1, SIR-C (SLC): DT 14.2 (10-04-94), DT 46.1 (12-04-94), DT 78.0 (14-04-94),
SRL-1, X-SAR (SSC, MGD, GTC): DT 14.2 (10-04-94), DT 18.21 (10-04-94), DT 34.31 (11-04-94), DT 46.1 (12-04-94), DT 78.0 (14-04-94),
SRL-2, SIR-C (SLC), X-SAR (SSC, MGD, GTC): DT 14.2 (1-10-94), DT 18.21 (1-10-94), DT 34.31 (2-10-94), DT 46.1 (3-10-94), DT 78.1 (5-10-94).

Polarimetric signatures and frequency dependence of backscattering of snow cover, glaciers, and ice-free areas, including vegetated and un-vegetated terrain, were investigated and related to field data of target properties. The analysis included investigations of angular behavior of backscattering properties and studies of temporal changes. Significant short-term changes were observed over snow and ice during SRL-2 at X- and C-band, whereas the seasonal changes in snow and ice properties resulted in pronounced backscattering differences between SRL-1 and SRL-2 at all 3 frequencies. Supervised and unsupervised methods were applied for classification, based on various combinations of backscattering parameters.

SIGNIFICANT RESULTS

- During both SRL-1 and SRL-2 a near real time analysis was carried out over glaciers to determine the accumulation and ablation areas and estimate glacier mass balance.

- The signature analysis clearly demonstrates the importance of multifrequency and polarimetric data for separating different snow and ice regimes on glaciers and for mapping accumulation and ablation areas. L- or C-band co- and cross-polarized channels in combination with X-band were found to be of main importance for this application.

- The maps of accumulation and ablation areas, derived from SIR-C/X-SAR data of SRL-2, show low ratios of accumulation to ablation areas, and consequently significant loss of mass during summer 1994 for all glaciers of the Ötztaler Alpen. Good agreement was found for the mass balance estimated from the SRL-2 data in comparison with field measurements, carried out on two glaciers in the test site for the period 1 October 1993 to 30 September 1994.

Snow Studies in the Innsbruck Region

The region surrounding Innsbruck was covered by the same swathes of the ascending orbits as the test site Ötztal. During SRL-1 the mountain slopes above Innsbruck were covered by humid snow, an intense snowfall event was observed between DT 46.1 and DT 78.0. This enables studies of different snow conditions than at the high alpine site. Snow properties and soil humidity were measured in the field.

For the Innsbruck region so far the following X-SAR data (*MGD*) were obtained:
SRL-1: DT 78.0 (14-04-94),
SRL-2: DT 78.1 (05-10-94).

Wet snow cover can be very well identified in the X-SAR images due to low backscattering coefficients. Change detection techniques, based on the X-SAR images from SRL-1 and SRL-2, provide an excellent capability for mapping melting snow areas.

Glacier Studies on the Southern Patagonian Icefield

Glaciological and geodetic measurements have been made on two of the main glaciers, Viedma Glacier and Moreno Glacier, of the Southern Patagonian Icefield which were imaged by SIR-C/X-SAR. Because emphasis of field activities during SRL-1 and SRL-2 was on the test site Ötztal, the campaigns in Patagonia could not be carried out during the shuttle flights. Nevertheless, the information obtained in the field during the campaigns listed below, is of great importance for the analysis of the SIR-C/X-SAR data.

Measurements on Viedma Glacier (22 to 27 Feb. 1994):
- GPS measurements of ground control points along the glacier boundary,
- documentation of surface roughness in the ablation area, including the volcanic ash bands,
- collecting of ash samples and pumice stones from the ash bands on the glacier.

Measurements on Moreno Glacier (1 to 6 March 1994):
- measurement of ice motion and ablation at 4 stakes which had been drilled in Nov. 1993.

Measurements on Moreno Glacier (14 to 30 November 1995):
- drilling of 19 stakes (10 m to 12 m deep) at various locations on the glacier, including a transverse profile (11 stakes) situated 10 km above the glacier terminus,
- measurement of the geodetic position of the stakes by means of differential GPS,
- GPS measurements of ground control points along the glacier boundary,
- installation of an automatic meteorological station at the glacier terminus.

Further field campaigns are planned on Moreno Glacier in March 1996 and November 1996. The planned activities include re-measurement of stakes to determine ice motion and ablation, GPS measurements of glacier boundaries, ice thickness measurements along the transverse profile, echo-sounding of the lake depth in front of the glacier.

Analysis of SIR-C/X-SAR Data:

Emphasis of the analysis so far was on X-SAR data, received in early 1995. In November 1995 we obtained the first SIR-C data (interferometric) of Patagonia. The following data were received:

X-SAR (MGD), Viedma Glacier:
SRL-1: DT 13.06 (10-04-94), DT 25.03 (10-04-94), DT 41.05 (11-04-94), DT 57.05 (12-04-94), DT 73.03 (13-04-94),
SRL-2: DT 09.4 (01-10-94), DT 13.6 (01-10-94), DT 25.3 (01-10-94), DT 45.7 (03-10-94), DT 57.5 (03-10-94), DT 73.3 (04-10-94).

X-SAR (SSC), Moreno Glacier:
SRL-2: DT 121.3 (7-10-94), DT 153.3 (9-10-94), DT 169.3 (10-10-94).

SIR-C (ISLC L-band), Moreno Glacier:
SRL-2: DT 121.3 (7-10-94), DT 153.3 (9-10-94), DT 169.3 (10-10-94).

The boundaries of Viedma Glacier and of the glacier dammed lake *Laguna Viedma* were mapped from the X-SAR data. Extent and melting conditions of snow and ice areas on the glacier were investigated. Interferometric analysis was carried out for the region of Moreno Glacier, for X-SAR and L-band SIR-C data.

- A major change of the glacier dammed lake *Laguna Viedma* was found by comparing the X-SAR images from SRL-1 and SRL-2. The lake area decreased from 5.5 km^2 in April 1994 to 1.5 km^2 in October 1995 and the water level lowered considerably. This outbreak of the lake, after a long period of comparatively stable glacier position, may indicate changing climatic conditions and the start of a major glacier retreat.

- Good interferograms were obtained on Moreno Glacier from the SIR-C L-band data although the glacier surface was melting. No coherency was obtained over the glacier in the X-SAR data, because backscattering at the shorter wavelengths is more affected by melting. Ice velocities from the L-band interferogram show good agreement with the velocities measured in the field. From the interferogram a map of ice motion can be generated over the whole glacier terminus, most parts of which are inaccessible due to crevasses. Interesting features of the ice motion, including a secondary maximum of velocity just above the calving front, have been identified which had not been known so far.

FUTURE PLANS

- Improvements of target classification and characterization in high Alpine regions, including glaciers and ice-free areas.
- Test of feasibility and accuracy of inversion procedures for snow wetness and for dry snow using the Ötztal data set. The inversion procedures, which have been developed for the SIR-C data of Mammoth by J.C. Shi, will be applied.
- Studies of ice dynamic of Moreno Glacier, based on SIR-C interferometry and on field data. In addition to the campaign in Nov. 1995, the field activities planned for 1996 (ice thickness, motion, glacier boundaries) are of great significance for this task.
- Studies of morphologic characteristics and flow features of Viedma Glacier based on SIR-C and X-SAR data in combination with ERS-1 and ERS-2 SAR data.
- Development of methods for surface shape reconstruction and improvements of digital elevation models, using SIR-C/X-SAR data acquired over the test site Ötztal under various incidence angles and from two look directions (in cooperation with F. Leberl, TU Graz).

Further Data Needs

Innsbruck Region:
SRL-1, SIR-C (MGD): DT 14.2 (10-04-94), DT 46.1 (12-04-94), DT 78.0 (14-04-94),
SRL-2, SIR-C (MGD): DT 14.2 (01-10-94), DT 46.1 (03-10-94), DT 78.1 (05-10-94),
SRL-1, X-SAR (MGD): DT 14.2 (10-04-94), DT 46.1 (12-04-94), (ordered Dec. 28,1995),
SRL-2, X-SAR (MGD): DT 14.2 (01-10-94), DT 46.1 (03-10-94), (ordered Dec. 28,1995).

Moreno Glacier, Patagonia:
SIR-C (C-band ISLC, interferometric), Moreno Glacier:
SRL-2: DT 121.3 (7-10-94), DT 153.3 (9-10-94), DT 169.3 (10-10-94).

Viedma Glacier; Patagonia:
SIR-C (MGD) from SRL-1 and SRL-2, as available.

PUBLICATIONS

Skvarca P., H. Rott and M. Stuefer, 1995: Synergy of ERS-1 SAR, X-SAR, Landsat TM imagery and aerial photography for glaciological studies of Viedma Glacier, southern Patagonia. *Proceedings, VII Simposio Latinoamericano de Percepciòn Remota, SELPER,* Puerto Vallarta, México, Nov. 1995: 674-682.

Rott H., T. Nagler and D.-M. Floricioiu: Snow and glacier parameters derived from single channel and multi-parameter SAR. *Proc. of Int. Symp. on Retrieval of Bio- and Geophysical Parameters from SAR Data for Land Applications*, Toulouse, Oct. 1995.

Rott H.: Glacier studies by means of SIR-C/X-SAR. In: *The X-SAR Book*, W. Noack (Editor).

C. Mätzler, T. Weise, T. Strozzi, D.-M. Floricioiu, H. Rott: Microwave snowpack studies in the Austrian Alps during the SIR-C/X-SAR experiment in April 1994, in preparation.

Rott H., and D.-M. Floricioiu: Analysis of glacier properties with SIR-C/X-SAR. Contribution to the special SIR-C/X-SAR issue of Remote Sensing of Environment, in preparation.

Dr. Gerald G. Schaber
US Geological Survey
2255 N. Gemini Drive
Flagstaff, AZ 86001

Co-Investigators:

John F. McCauley	USGS-Emeritus, Sedona AZ
Carol S. Breed	USGS-Emeritus, Sedona AZ
Andre Simonin	CNRS-IMAGEO, Paris
Philip Rebillard	MATRA CAP SYSTEMES, Velizy Villacoublay, FRANCE
Nicholas Lancaster	Desert Research Institute Reno NV
James Teller	Manitoba, Quebec

SIR-C surface and subsurface responses from documented test localities in the Sahara, Namib, and Kalahari Deserts, Africa and the Jornada del Muerto, New Mexico

OBJECTIVES

To determine the optimum SIR sensor configuration for detection of desert duricrust and to use this understanding to reconstruct the paleoclimatic history of two large desert regions in Africa.

To determine the ability of SIR-C/X-SAR (alone and synergistically with other remotely sensed data) to delineate and map near-surface, regional caliche deposits and other "fossil" duricrusts formed during a series of less arid intervals in Africa, but now obscured by aeolian sand.

To test various sensor parameter configurations of SIR-C/X-SAR for discriminating among surface and near-surface stratigraphic units in well documented sites from the SIR-A and SIR-B experiments. The results will be used to calibrate the penetration and backscattering capabilities of the SIR-C/X-SAR.

PROGRESS

SRL-1 and SRL-2 Crew Training in Desert Geologic Processes

In May of 1993 and May of 1994 Gerald Schaber, John F. McCauley and Carol Breed planned and led two-day field trips into Northern Arizona and the Territory of the Navajo Nation for the purpose of briefing and instructing the astronaut crews of SRL-1 and SRL-2 in desert geologic processes and the scientific basis of the collaborative SIR-C/X-SAR Investigations of Schaber and McCauley. These field trips, initiated at the request of and coordinated through Dr. Tom Jones (Astronaut Office, JSC), were considered by the crew members participating to be extremely helpful and instructive. The first field trip in May 1993 was so successful that Dr. Jones requested a repeat for the crew of the second SRL mission.

Mission Planning, Targeting Activities

Between February 1994 and October, 1994 (SRL-2 mission) Carol Breed, Gerald Schaber and J. McCauley were quite active in helping JPL SIR-C Project personnel develop complex mission targeting scenarios, especially for the numerous study sites of interest in the Sahara, Namib, and Kalahari Deserts in Africa. During this same time period, this same team was also asked by the PI of the Saudi Arabia Investigation (Dr. A. Dabbagh) to act as his representative with JPL personnel in data-take planning and targeting for the Kingdom of Saudi Arabia.

Data Acquired

Numerous SIR-C/X-SAR data takes were successfully acquired for the PI over selected sites in the Sahara, Namib and Kalahari Deserts of Africa during both SRL-1 (April, 1994) and SRL-2 (October, 1994). Some of the Sahara data takes were acquired for joint use between this investigation and the Paleodrainage Investigation of PI F. McCauley. Overall, these data are of outstanding quality. External ground based and/or airborne radar interference patterns (especially at L-band, HH and HV) are visible to various degrees on some of the images acquired over the northeastern Sahara (e.g., Egypt). Because of the multiple passes required for the Death Valley Supersite, and other mission planning and operations constraints, no SRL data could be acquired of the Investigator's prime domestic test site at Jornada del Muerto NM. However, useful SRL data were acquired of the PI's domestic sand penetration study site located near Yuma, Arizona. A total of 22 standard processed SIR-C and X-SAR scenes have been specifically requested to date by the PI for research by the PI and his Co-I's and Collaborators: eleven of Bir Safsaf and vicinity (Egypt); eight of Algeria/Tunisia sites; and one each of sites in the Namib Desert (SW Africa), Yuma (AZ) and Death Valley (CA). An updated listing of all Co-Investigators and Collaborators actively analyzing SIR-C/X-SAR data in collaboration with G. Schaber is given above.

Since the first SRL mission (April 1994) the Principal Investigator (G. Schaber) has focused almost exclusively on qualitative and quantitative analyses of fully processed SRL-1 SAR scenes of Bir Safsaf and vicinity (Egypt)--the prime radar penetration and EM theory Supersite for both SRL-1 and SRL-2. A total of 10 SIR-C/X-SAR data takes (data takes) were acquired of the Bir Safsaf study site during SRL missions 1 and 2 (April and October, 1994) (three in quadpol mode 16, three in mode 11X, one in mode 8X, and three in interferometric mode 20X). These data have been calibrated for radar backscattering coefficients (Sigma 0) to 2.3 dB. Several of the Bir Safsaf data takes covered nearly identical image footprints for various reasons. Image data acquired on data takes 12.1 and 82.41 during SRL-2 were purposely targeted slightly away from the Bir itself in order to fill gaps in the data from SRL-1 and to acquire additional coverage. An additional three SRL-2 data takes that included Bir Safsaf were acquired in the "interferometric mode" at the same incidence angle (47.7) for the purpose of obtaining topographic information. The SIR-C image of Bir Safsaf with the widest swath width (48 km) was acquired during SRL-1 data take 130.4. This data take 130.4 was acquired in mode 11X, i.e., XVV, CHH, CHV, LHH, and LHV only. Fully processed X-SAR and SIR-C data requested for this site include 100-km long scenes from SRL-1 data takes 2.1, 82.41, 98.3, 114.4 and 130.4. No SRL-2 image scenes or interferometric data from the Bir Safsaf Supersite have yet been requested for standard processing.

SIGNIFICANT RESULTS

Progress on Studies of The Bir Safsaf (Egypt) Supersite

The most complete and most significant research results to date for this investigation center around the PI's analysis of data takes acquired over the Bir Safsaf Supersite in southern Egypt. Schaber et al. (1996) describe and illustrate how the X-, C-, and L- band SAR data each contribute unique types of significant paleoclimatic and geologic information that is virtually obscured on conventional Landsat TM-type sensors by the thin but pervasive cover of blow sand. For example, the outstanding portrayals of: (1) a NS-trending wind erosion pattern in the bedrock on only the X-band SAR images, (2) previously poorly mapped granitoid stocks and complexly fractured granitic gneisses and migmatites using C-cross polarization and L-band images, and (3) aggraded and blow-sand mantled, defunct, stream channels using all three SAR frequencies, document to a degree heretofore unprecedented the considerable benefits of using multi-frequency and polarimetric SAR imagery in geologic mapping and paleoclimatic studies of desert regions.

Based on detailed field documentation carried out by the PI and his colleagues (John McCauley, Carol Breed) at Bir Safsaf following the SIR-A and SIR-B missions (Schaber et al., 1986), the observed differences in backscatter response are interpreted to result primarily from: (1) increased "radar imaging depth" with increasing SAR wavelength (i.e., decreasing frequency), (2) the sensitivities of SAR signals of different wavelengths and transmit/receive polarizations to different scales of micro-roughness both on the surface and within the shallow subsurface, (3) the existence on the surface and in the shallow subsurface of iron oxides and other secondary deposits (e.g., calcite, gypsum, halite, etc.) with high dielectric permittivity, and (4) a combination of these and other affects. In simplest terms, the differences in geologic information portrayed on SIR-C/X-SAR images from the same data take are a direct result of the specific SAR frequency and polarization mode used. The effect of incidence angle on discrimination of geologic features on SIR-C/X-SAR images of the Bir Safsaf site was investigated first by simple visual comparison of images from SRL-1 data takes 82.41 (22.5 incidence angle), 114.4 (46.2), and 130.4 (47.9); and subsequently by quantitative analysis of the mean and standard deviation of backscatter values for selected geologic units. The smaller incidence angle (or steeper antenna depression angle) resulted in better overall image quality (in all polarization modes) for geologic analysis than the images acquired at a larger incidence angle (or shallower depression angles).

Progress on Central North Africa Studies

All relevant SIR-C and X-SAR CD-ROMs from missions 1 and 2 containing data takes primarily in Algeria and Tunisia, have been provided to Andre Simonin (CNRS-IMAGEO, Paris) (the PI's CO- I/Coordinator for the Northern Sahara). Specially requested, fully processed scenes thus far provided by the PI (through JPL) to Simonin include: Monastir, Tunisia (2 tapes), Chott Gharsa, Tunisia, El Borma, Tunisia, Chott Djerid/DJ Asker, Tunisia, Merkherrhane, Algeria (two tapes), and Tanezrouft, Algeria. Scenes processed independently by the G-PAF but copies provided to Dr. Simonin include: Side El Hani, Tunisia (two tapes); Mokine, Tunisia (two tapes); Nefta, Tunisia; Sahara/Algeria; Quargla, Algeria, Touggourt, Algeria; and El Oued, Algeria. While awaiting the receipt of the high resolution data, our Co-Is and Collaborators in Europe and North Africa have been active in the field evaluating the SRL-1 SAR Survey images. For example, in April, 1995, J.L. Ballais (U. Aix-Marseilles) completed a ground truth survey over the entire study site at Chott Gharsa, Tunisia - an area in which he has over 20 years of experience in geologic mapping. Ballais collected (with GPS location control) samples, surface properties, topography, vegetation cover, etc. His preliminary correlation of the SIR-C survey data with ground truth at Chott Gharsa resulted in very high expectations when comparing (in the near future) the fully processed SAR images with regard to geomorphology and geology in southern Tunisia--especially in synergy with Landsat and SPOT data.

At the Merkerrhane site in Algeria, Y. Callot (Univ. Tours) is presently conducting a visual evaluation of a print of an X-SAR, fully processed scene of the Sebkras Merkerrhane area. J. Chorowicz and C. Chalah (LGST Lab. Univ. P & M. Curie, Paris) are pursuing the processing and interpretation of an ERS-1 image over the Tanezrouft site (Algeria) that they intend to compare with SIR-C and X-SAR fully processed data. They report that, compared to Landsat and SPOT images, the ERS-1 images reveal some penetration of the sand sheets, allowing the interpretation of slightly buried structures.

Mauritanian Sites

Fully processed data will be provided by JPL on a Mauritanian site to Dr. J. P. Deroin (BRGM-Orleans) from data take 132.30 (Western Africa). Evaluation of an ERS-1 scene and field survey have been conducted over this area in 1995 (Deroin and Simonin), and will be presented at the Toulouse meeting in October 1995.

Progress on Namib Desert Studies (SW Africa)

Co-Investigator Nick Lancaster (Desert Research Institute-Reno NV) reports the SRL SAR images of the northern part of the Namib sand sea in southwest Africa provide an enhanced view of Quaternary fluvial deposits in the region. Previous studies (e.g., Lancaster, 1984; Ward, 1987) used aerial photographs to map several generations of Pleistocene fluvial deposits. The extent of these deposits to the west was not fully defined because they were covered by a thin aeolian sand cover. SRL images show clearly the extent of calcrete-cemented fluvial gravels in the area west and south of the Kuiseb River. These gravels extend much farther west than mapped by Ward (1987). C- and L-band HH polarized data provide the best images of these deposits, which have a bright radar signature as a result of their rough surfaces.

In the lower Tsondab River valley (also know as the Tsonab Flats) SRL images enable identification of fluvial gravels between 5- to 10-m-high linear and crescentic dunes. In many areas, the former meandering river channels can be accurately mapped, something that Lancaster (1984) was unable to achieve using aerial photographs. In the area south of the Kuiseb River, SRL images show that a dendritic drainage network is developed on older calcrete-cemented gravels. This drainage network is directed from east to west and has never previously been identified as such. They were suggested to be some form of patterned ground by Besier (1980) and Watson (1980). Ward (1987), however, suggested that these features were macro-scale fractures developed during diagenesis of the underlying Tertiary-age Tsondab Sandstone Formation. The channels are imaged as dark tones, suggesting that they are filled by thin aeolian or fluvial sands. The amount of the network discernible on the SAR images changes with radar wavelength. The best resolution of the channels and most complete network are obtained with X-band data, followed by C-, and then L-band. This suggests that there is penetration of the sands by longer wavelengths and gives a general impression of the depth of sand cover in the channels, which increases with stream order. Further studies are planned to explore the full potential of the SRL data, now that full- resolution images are available. These studies will include comparison between radar and Landsat TM data and estimates of the depth of radar penetration using information from past field studies by Lancaster. We plan to prepare at least one manuscript for submittal in early 1996. Some of the results of this study will be presented at the IGCP 349 meeting "Desert margins"... to be held in the United Arab Emirates in December, 1995.

FUTURE PLANS

Plans are currently under way to attend the Centennial Meeting of the Geological Survey of Egypt in Cairo and to present a paper on the role of wavelength and polarization in geologic studies of Bir Safsaf (Egypt) using SIR-C/X-SAR data. Additional field work at Bir Safsaf is being investigated as part of the Cairo meeting in order to field check the SIR-C/X-SAR data. There will be a possible group field trip for selected attendees of Cairo meeting.

The first oral presentation (by N. Lancaster and G. Schaber) on the SIR-C/X-SAR Namib results will be presented at the IGCP 349 meeting to be held in the United Arab Emirites in December, 1995 (See 2.2 above).

The February 1996 SIR-C/X-SAR Team meetings will be held at the U. of California, Santa Barbara; an oral progress report will be presented on the Namib and Algeria/Tunisia SIR-C results.

An "Estimate" of Additional Data Requests (SIR-C and X-SAR) (1996):

(1) 5-10 scenes from the Namib Desert (SW Africa).

(2) 10-15 scenes from the Central-Northern Sahara (Algeria, Tunisia, Morocco, Niger, Mali).
(3) 5-10 scenes from Egypt-Sudan.
(4) 2-3 scenes from Death Valley, CA and Yuma, AZ.

PUBLICATIONS

October, 1995 - Oral and Poster presentations (accepted) at the Symposium "Retrieval of bio- and geophysical parameters from SAR data for land applications"- Toulouse, France, Oct. 17-20, 1995.

November, 1996 - Presentations in scientific session S-08 "Shuttle Studies" at the Geological Survey of Egypt's Centennial Symposium, Cairo, Egypt, Nov. 11-14, 1996.

Abstracts

Schaber, G. G., McCauley, J. F., and Breed, C. S., 1994, New radar images of Safsaf Oasis and vicinity, southern Egypt, Geological Society of America Abstracts with Programs, v. 26, no. 7, p. 127, 1994 Annual Meetings, Seattle, WA.

McCauley, J. F., Breed, C. S., and Schaber, G.G., 1995, SIR-C definition of the Serir-Kufra River system in SE Libya: EOS Supplement April 25, 1995, p. S196 (AGU Spring Meeting, poster #P51A-4).

McCauley, J. F., Breed, C. S., and Schaber, G. G., 1995, Mapping the Wadi Kufra paleodrainage system in eastern Libya using spaceborne imaging radar, poster presentation at Symposium on "Retrieval of bio and geophysical parameters from SAR data for land applications, Toulouse, France (October 1995), in press.

Schaber, G. G., McCauley, J. F., Breed, C. S., and Issawi, Bahay, 1995, The roles of wavelength and polarization in geologic studies at Bir Safsaf (Egypt) using SIR-C/XSAR data, 1995.

Abstracts and Programs, Geol. Soc. of America, Annual Meetings (New Orleans LA-November 6-9, 1995), in press.

Musick, Brad, Schaber, G. G., and Breed, C. S., 1995, Use of AIRSAR to identify woody shrub invasion and other indicators of desertification in the Jornada (NM) LTER, in abstracts of the Ecology Society of America (ESA) Annual Meeting (Summer, 1994), *Bull. of the Ecology Society of America*, v. 75, no. 2, (supplement), p. 163.

Musick, Brad, Schaber, G. G., and Breed, C. S., 1995, Use of AIRSAR to identify woody shrub invasion and other indicators of desertification in the Jornada (NM) LTER, Summaries of the Fifth Annual JPL Airborne Earth Science Workshop (January 23-25, 1995), Publication 95-1, vol. 3, Jet Propulsion Laboratory, Pasadena, CA, pp. 31-34.

Open Literature

Schaber, G. G., McCauley, J. F., Breed, C. S., and Issawi, Bahay, The role of wavelength and polarization in geologic studies of Bir Safsaf (Egypt) using SIR-C/XSAR data, J. Geophy. Res.-Planets or Remote Sensing of Environment; 50+ pages, being submitted in October (1995).

Dr. Robert J. Stern
Center for Lithospheric Studies
University of Texas at Dallas
Box 688
Richardson, TX 75083

Co-Investigators:
Timothy H. Dixon — JPL/Caltech
Kent C. Nielson — Univ. of Texas at Dallas
Mohammed Sultan — Washington Univ., St. Louis

SIR-C Studies of the Precambrian Hamisana and Nakasib Structures, NE Sudan, in Arid Regions of Low Relief and in the Subsurface

OBJECTIVES

a) Develop techniques for optimizing structural analysis of basement trends in arid regions with extremely subdued topography and/or thin aeolian cover.

b) Apply results of (a) to map the southern extension of the Hamisana Shear Zone and the western extension of Nakasib Suture.

c) Apply results of (b) to constrain the roles of terrane accretion and strike-slip re-organization for late Precambrian crustal evolution in NE Africa.

PROGRESS

Our proposal called for evaluating the suitability of SIR-C/X-SAR imagery for resolving basement structures in hyperarid regions where visible and near-infrared imagery revealed only sand covering. Specifically, we proposed using the radar data to define the southern extension of the Hamisana Shear Zone in NE Sudan. This Precambrian basement structure lies in the Sahara Desert, earth's most hyperarid environment. We had previously exhausted efforts to use conventional imagery to resolve the structure. The study area that we originally proposed is shown as 'Original Proposed Study Area' in Fig. 1. In preparing for the SIR-C/X-SAR experiments, field studies led us to recognize that a parallel but more westerly structure was also important. This is the poorly exposed and consequently very poorly known Keraf Shear Zone. Following preliminary field studies which indicated that the Hamisana may terminate just south of its present outcrop limit, and that the Keraf Shear Zone may be more important than previously thought, we redirected our efforts towards studying the Keraf. This is a slight change in direction that has been justified by subsequent discoveries resulting from our interpretation of the SIR-C/X-SAR imagery.

Prior to receiving the SIR-C/X-SAR data, we carried out a field program based on structural interpretation of SIR-A data over the northern part of the Keraf Shear Zone. This was done in order to better prepare us to interpret the SIR-C/X-SAR images and to define the fundamental structural characteristics of the Keraf that were likely to be so identified. The location of this 'SIR-A pilot study' is shown in Fig. 1, and the results of this investigation have been published (Schandelmeier et al., 1994; Stern et al., 1993) or are now in press (Abdelsalam et al., in press). We also took advantage of the preparation phase to prepare an overview summarizing the sequence of events and global significance of the tectonic evolution of the Arabian-Nubian Shield (Stern 1994).

Progress in the Past 1.5 years

Our experiment continues to focus on using the multi-parameter characteristics of the SIR-C/X-SAR imagery to find, define, and interpret geologic features in hyperarid regions, and to understand the extent to which the radar is resolving structure by penetration through sand or back-

scattering from subtle topographic expressions of structure. Once the SIR-C/X-SAR data were acquired, we compiled SRL-1 and -2 survey data over all of NE Sudan. This involved obtaining reconnaissance L-band data takes (Alden prints) and compiling these with reference to known geologic structures. This comprehensive data set was then studied to identify where further processing efforts and field studies (ground-truth efforts) should be concentrated. This work was completed at the end of Spring 1995, and because the quality of the L-band Alden prints is very similar to that of SIR-A, we were well prepared to interpret these images on the basis of our pilot study in the northern Keraf Zone. This phase of our study indicated that the original focus - tracing the southern continuation of the Hamisana Shear Zone - was not likely to be fruitful, and we switched our primary focus to the heretofore unknown southern part of the Keraf Shear Zone, where we are confident that our original objectives can be attained. This area is labeled 'New Area of Primary Concentration' in Fig. 1. The first and most exciting result to date was our discovery on the radar imagery and subsequent ground verification of two previously unrecognized shear zones (which we have named 'Abu Hamed Shear Zone' and 'Abu Dis Shear Zone'; Fig. 2) along the Nile north of Atbara. This is the southern part of the Keraf zone, and while its existence has been long suspected to lie in this region on the basis of isotopic considerations, it was not until we examined the SIR-C/X-SAR imagery that the location, trend, and even the existence of this important lithospheric structure in this region was demonstrated.

This discovery was the result of the SIR-C/X-SAR imaging capabilities, and we are now concentrating on understanding and exploiting this result. We are convinced that this discovery dramatically demonstrates the importance of radar to geological studies in hyperarid, poorly known regions, among which the Sahara Desert is the type example. After careful study, we conclude that almost none of the structures visible on the radar images (Fig. 3) can be seen on images produced from a wide range of visible and near infrared sensors. We have studied Landsat TM images, Shuttle hand-held photography (acquired during the April 1994 flight), and 1:80,000 air photos in efforts to discern structures that are vividly revealed in the radar images. We conclude that there is no way that the visible and near-infrared images could have been processed or interpreted that could have resolved these structures.

It is presently unclear how much of the radar's sensitivity to structure is the result of penetration of sand drapes and how much is due to subtle variations in topography and low, nearly-hidden outcrops. Answering this question is an important part of the work that remains to be done in the next two years.

Just how spectacular the SIR-C images of the area are is shown in Fig. 3, a very small part of the region shown in Fig. 2. This scene was processed at UTD. The radar images show remarkable detail over the shear zone, revealing a complex, intensely folded region to the east of the Abu Dis shear zone and a less intensely deformed region to the west of the shear zone. We carried out three weeks of field studies in the region last April. This concentrated on refining our structural interpretations of selected portions of the region shown in Fig. 3, and on understanding how much of the structure is buried beneath dry, wind-blown sand (and how thick is this cover). Our preliminary estimate is that a variable thickness of sand covers a basement peneplain. Our preliminary estimate is that about 10-20% of the desert surface is low basement outcrop and the other 80-90% is 2-200 cm of windblown sand. The situation in the field is shown in Fig. 4, as is how the region appears with visible and near-infrared imagery.

SIGNIFICANT RESULTS

Our work is continuing, but we have prepared two abstracts on our results (Abdelsalam et al., submitted; Stern et al., submitted) that will be presented at the 1995 national meeting of the Geological Society of America meeting in November. We are also preparing a manuscript (Stern et al., in prep.) that will be submitted to the special volume of JGR-Green on geologic results from

SRL-1 and 2. Another manuscript nearing completion reports the results of our structural studies of southern Keraf Shear Zone, based on interpretation of the SIR-C/X-SAR data and field investigations (Abdelsalam et al., in prep.). Several other publications are planned following completion of our studies.

FUTURE PLANS

Our top priority is completing the analysis of data sets that cover the 'New Area of Primary Concentration' outlined in Fig. 2, and publication of these results. We have all of the radar data sets that we need, and we are proceeding with the following work plan: 1) Assembly of L-band total power image (black and white) over the entire area outlined in Fig. 2.; 2) Generation of individual false-color L-, C-, and L/C images for subscenes covering all of Fig. 2; 3) Coregistration of L-, C-, and X-band data sets for selected parts of the region outlined in Fig. 2; and 4) Field checking of results following final image processing. Items 1 and 2 are well in hand, and these tasks should be completed sometime in the next 2 months. We place a very high value on item 3. One of the few disappointments of the SIR-C/X-SAR experiment has been the scarcity of images that use all three wavelengths. This is unfortunate for two reasons. First, the international nature of the experiment means that a very real part of the collaboration is reflected by the products that use both data sets, and the relative lack of these products can all too easily be interpreted as indicating a lack of true co-operation. Second, the SIR-C/X-SAR platform is unique in acquiring simultaneous multi-wavelength data, and this aspect should be considered for future orbital radar platforms. Coregistration of all three wavelengths is a very high priority, and this task is being carried out with S. Okonek and other scientists at JPL. An important part of this effort will be comparing images produced from the three-wavelength coregistered data with images produced using only L-, C-, and L/C.

Finally, we require another 2- to 3-week field expedition to Sudan. This is needed in order to carry out GPS-controlled field checks of our structural interpretations, collect a few samples for radiometric age determinations needed to constrain the age of deformation, and to quantify the depth of sand cover and percentage of basement exposure. This work will be the focus of our efforts during most of FY 96.

In late FY 96 and early FY 97, following completion of the primary tasks outlined above, we will turn our attention to application of SIR-C/X-SAR data to another poorly exposed region along the Nile in Sudan, shown as 'New Area of Secondary Concentration' in Fig. 2. The work plan for this area will be similar to that outlined above or the Keraf area: 1) Assembly of L-band total power image; 2) Generation of detailed false-color images, either coregistered X-, C-, and L-band data, or L-, C-, and L/C, depending on the results of our study outlined above; and 3) Field work to verify and modify interpretations and provide data regarding amounts and depths of sedimentary cover. The data sets that we need to conduct this phase of the work are about half complete, and we expect to submit requests for another 10-15 precision products to both JPL and DLR.

Finally, in late FY 97, we hope to apply our refined techniques to a study of the Allaqi-Heiani suture. This fundamental lithosphere structure in SE Egypt is poorly known, but appears to be deflected by the northern extension of the Keraf Zone. If time and funds allow, we would like to carry out the sorts of investigations outlined above to studying this structure. If this work moves forward, we expect to require another 20 precision products from both JPL and DLR.

PUBLICATIONS

Abdelsalam, M.G., Stern, R.J., Daniels, A.T., Elfaki, E.M., Elhur, B., and Ibrahim, F., in press. Tectonic evolution of the Neoproterozoic Keraf Zone, Sudan. Geol. Soc. America, Ann. meeting (abs.).

Abdelsalam, M.G., Stern, R.J., Schandelemeier, H., and Sultan, M., in press. Deformational history of the Neoproterozoic Keraf Zone, NE Sudan revealed by Shuttle Imaging Radar. *Journal of Geology.*

Schandelmeier, H., Wipfler, E., Kuster, D., Sultan, M., Becker, R., Stern, R.J., and Abdelsalam, M.G., 1994. Atmur-Delgo suture: A Neoproterozoic oceanic basin extending into the interior of NE Africa. *Geology* v.22, p. 563-566.

Stern, R.J. 1994. Arc Assembly and Continental Collision in the Neoproterozoic East African Orogen: Implications for the Consolidation of Gondwanaland. *Annual Reviews of Earth and Planetary Sciences* v.22, p. 319-351.

Stern, R.J., Abdelsalam, M.G., and Daniels, A.T., in press. Shuttle Imaging Radar reveals a major deformation belt in the Sahara Desert of Sudan. Geol. Soc. America, Ann. meeting (abs.).

Abdelsalam, M.G., and Stern, R.J., submitted. Shuttle Imaging Radar imaging of buried and poorly exposed basement structures in hyper-arid terrains. *J. Geophys. Res.* - Planetology.

Stern, R.J., Abdelsalam, M.G., Schandelmeier, H., and Sultan, M., 1993. Carbonates of the Bailateb Group, NE Sudan: a Neoproterozoic (ca. 750 Ma) passive margin on the eastern flank of Gondwanaland, Geol. Soc. America, abs. with progr. v.27, p. 49.

Figure Captions

Figure 1: Locality map of Precambrian basement outcrops in NE Sudan and the locations of various study areas proposed in the text. Note that the area labeled "New Area of Primary Concentration" also shows the location of Figure 2.

Figure 2: Geologic sketch map of the southern Keraf Zone. The geology from west of the Nile is generally well-exposed and is taken from various published reports and our own field investigations. The geology east of the Nile is not exposed and represents our interpretation of SIR-C L-band survey images supplemented by field checking. Notice that the geology of this part of the Keraf Zone is complex, with ultramafic rocks defining the folded surface of the suture between the pre-1.0 Ga crust of the East Saharan Craton and the 0.85 - 0.65 Ga juvenile crust of the Arabian-Nubian Shield, and younger left-lateral strike-slip faults (Abu Hamed shear zone and Abu Dis shear zone) disrupting the older suture. The area of detailed work to date is shown in the rectangle labeled 'Figure 3.'

Figure 3: Area of detailed work on the Abu Hamed and Abu Dis shear zones. 'A' shows a SIR-C image (SRL-1, Data take 82.42) processed (HH polarization, red = L-band power, green= C-band power, blue = L/C). This image reveals a variety of previously unknown structures, interpreted in 'B.' Our field work in April 1995 concentrated on understanding the geometry of these structures. The location of the detailed image shown in Figure 4 is outlined by rectangle in 'A.'

Figure 4: Comparison of images of the study area. 'A' shows terrain along the Abu Dis shear zone, looking SSW from arrow 'a' in 4. The <1m high ridge is made up of mylonitized granite emplaced in the shear zone during deformation. 'B' shows terrane looking east from arrow 'b' in 4. Notice the low hills in the distance; these can be recognized as two NE-SW elongated ridges

about 6 km to the east. Notice very subdued outcrop in foreground. 'C' shows the SIR-C scene itself, processed as described for figure 3. This scene is about 20 km wide. 'D' shows the region in 4 outlined by a rectangle as photographed during SRL-1 (photo STS059-L19-OCF). Notice the absence of any structural features. All visible and infrared images are similarly featureless.

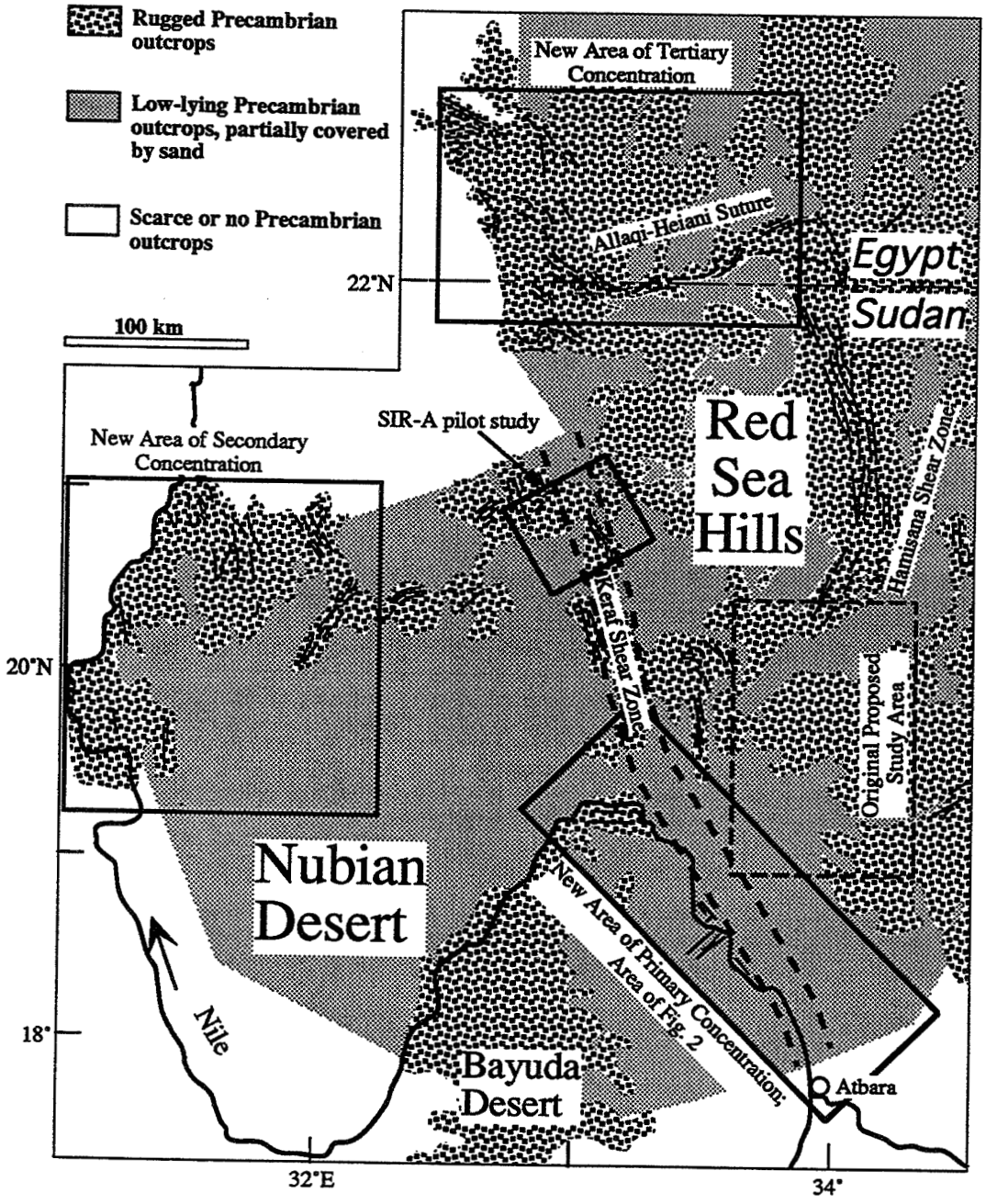
Rugged Precambrian outcrops
Low-lying Precambrian outcrops, partially covered by sand
Scarce or no Precambrian outcrops
100 km
New Area of Tertiary Concentration
Allaqi-Heiani Suture
Egypt
Sudan
22°N
SIR-A pilot study
New Area of Secondary Concentration
Red Sea Hills
Hamisana Shear Zone
Kerai Shear Zone
20°N
Original Proposed Study Area
Nubian Desert
New Area of Primary Concentration; Area of Fig. 2
Nile
18°
Bayuda Desert
Atbara
32°E
34°

Figure 1

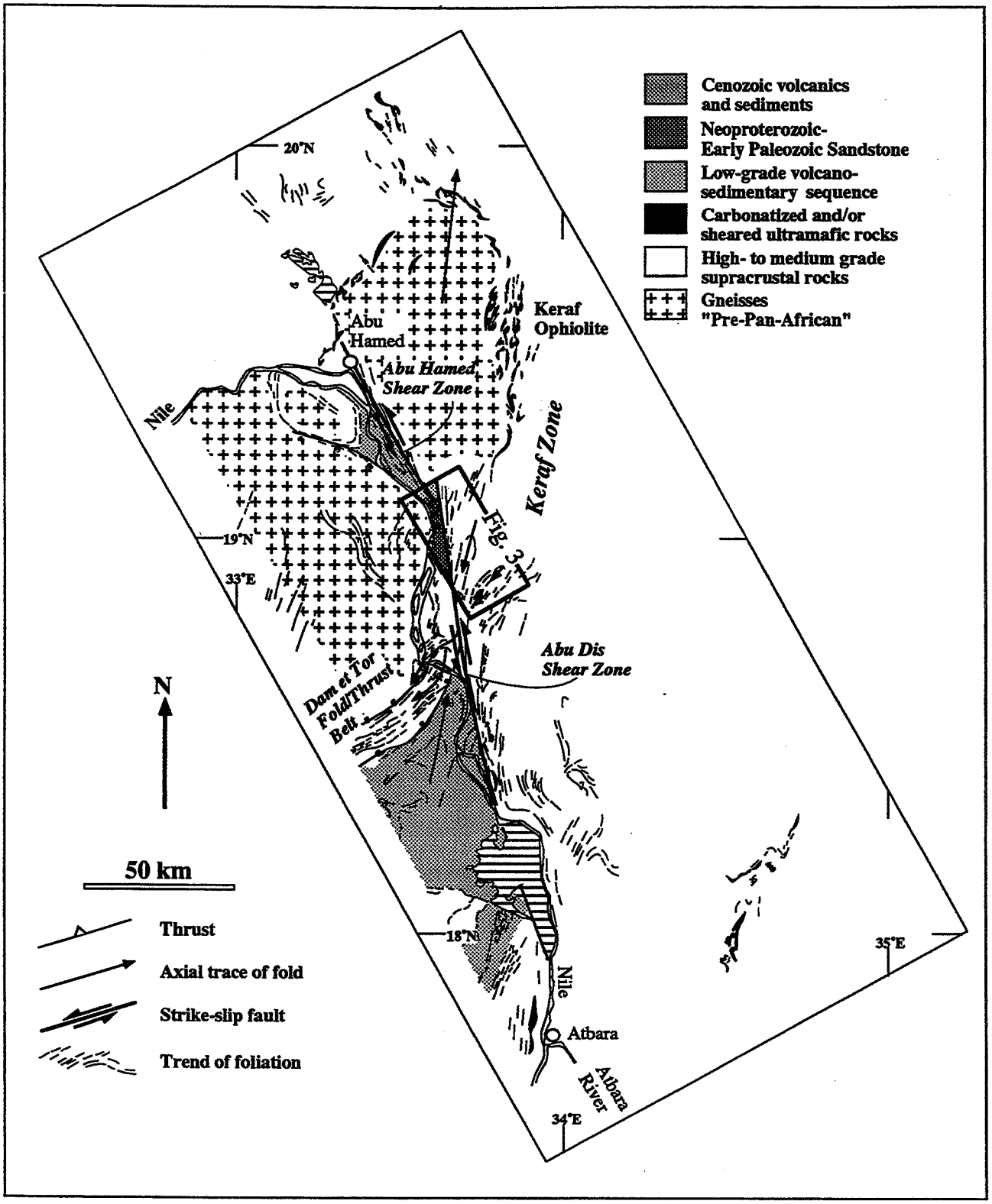
Cenozoic volcanics and sediments
Neoproterozoic-Early Paleozoic Sandstone
Low-grade volcano-sedimentary sequence
Carbonatized and/or sheared ultramafic rocks
High- to medium grade supracrustal rocks
Gneisses "Pre-Pan-African"
20°N
19°N
18°N
33°E
34°E
35°E
Abu Hamed
Keraf Ophiolite
Abu Hamed Shear Zone
Keraf Zone
Nile
Fig. 3
Abu Dis Shear Zone
Dam et Tor Fold/Thrust Belt
N
50 km
Thrust
Axial trace of fold
Strike-slip fault
Trend of foliation
Atbara
Atbara River

Figure 2

Fig. 3

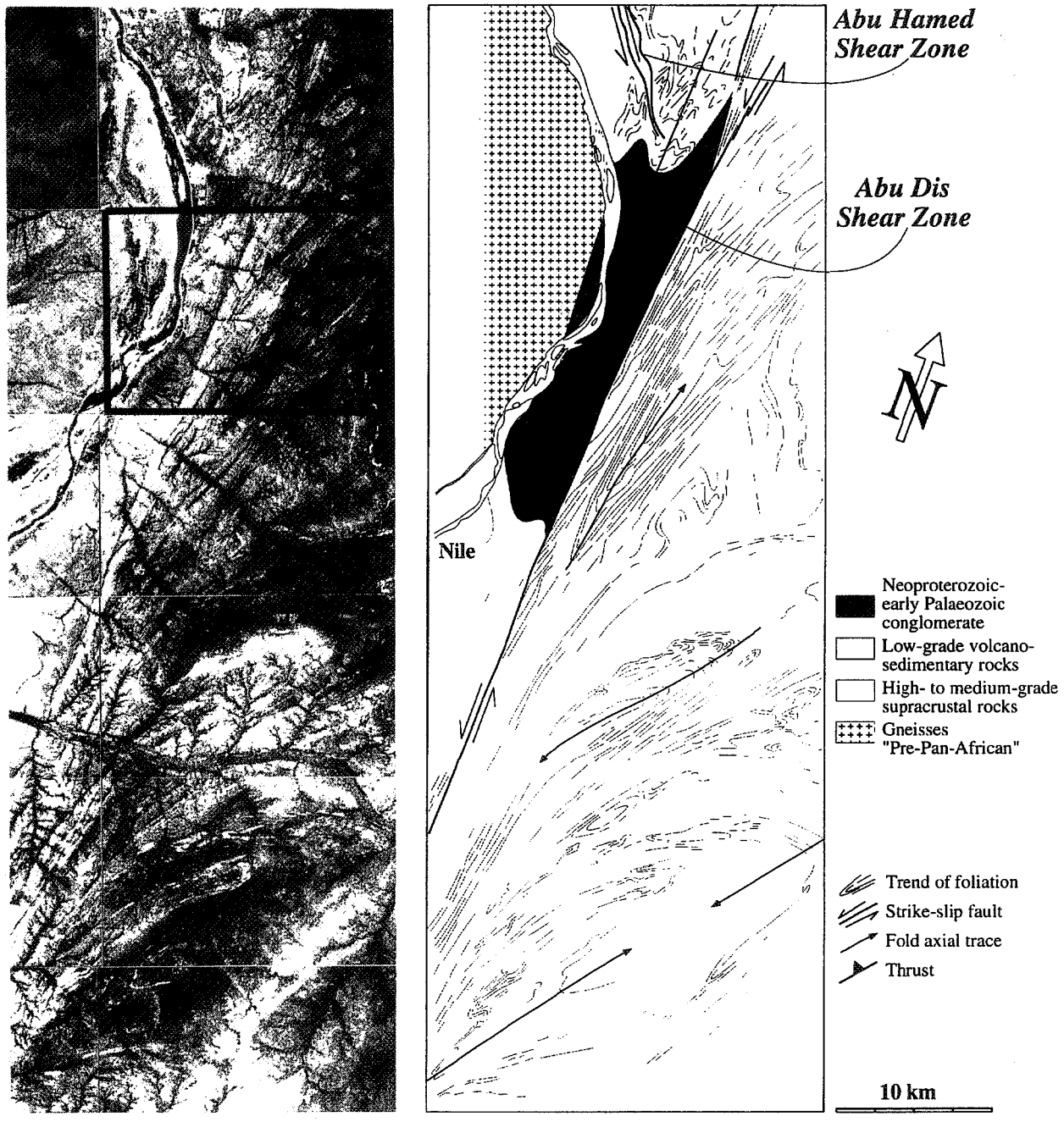
Abu Hamed
Shear Zone
Abu Dis
Shear Zone
N
Nile
Neoproterozoic-
early Palaeozoic
conglomerate
Low-grade volcano-
sedimentary rocks
High- to medium-grade
supracrustal rocks
Gneisses
"Pre-Pan-African"
Trend of foliation
Strike-slip fault
Fold axial trace
Thrust
10 km
A
B

Fig. 4

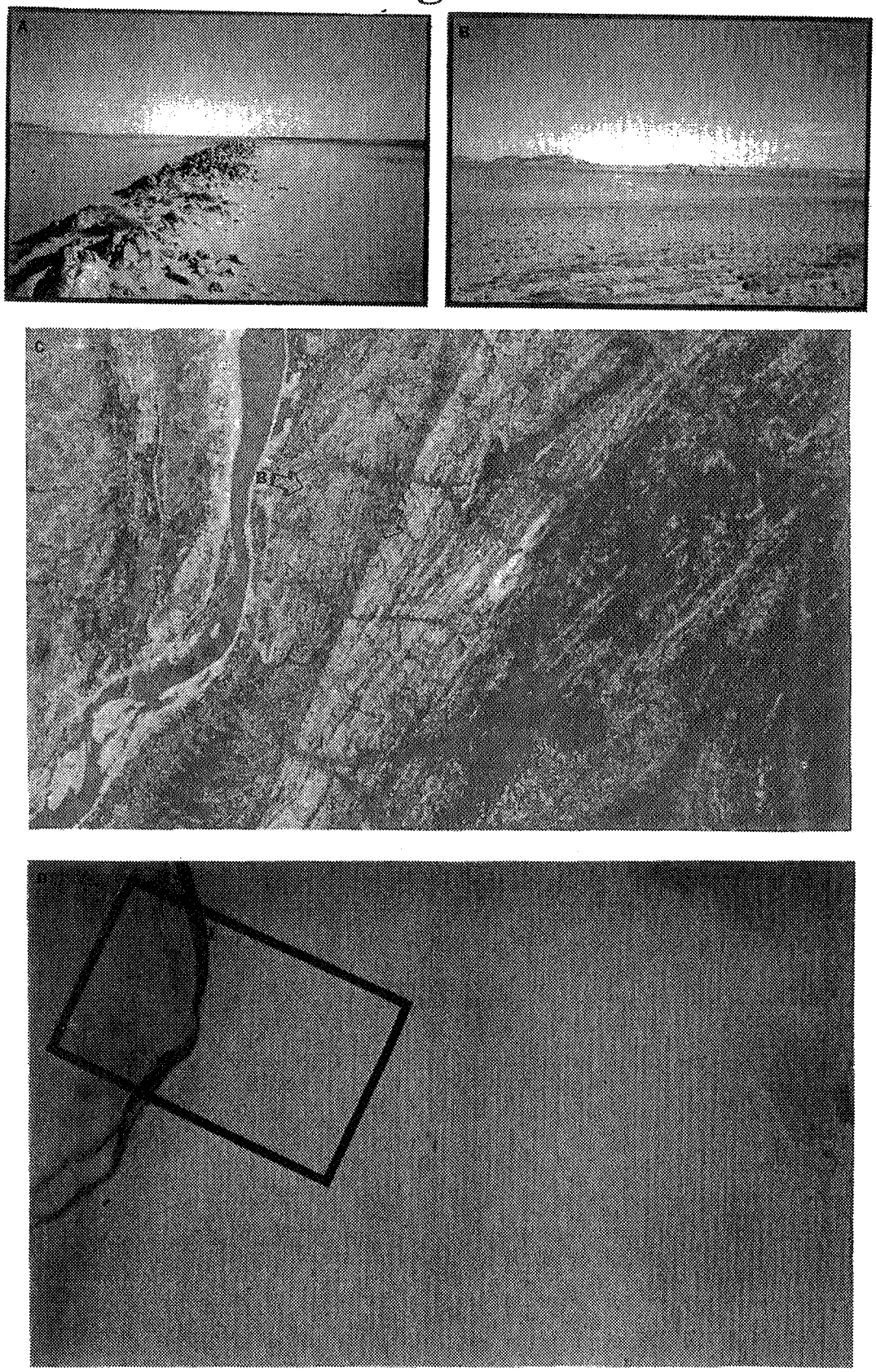

Dr. Geoffrey R. Taylor
Department of Applied Geology
Univ. of New South Wales
P.O. Box 1
Kensington NSW 2033
Australia

Geology and hydrology projects - Australia

OBJECTIVES

To assess the utility of multipolarization multifrequency spaceborne radar for surficial sediment mapping (lithology, rock weathering, and geochronology,) and groundwater management (arid regimes) in a variety of Australian environments.

To establish the utility of the SIR-C imagery for recognizing basement structures (tectonics and geologic boundaries) by mapping drape-related fractures in overlying surficial sediments.

PROGRESS

Data acquired

The Australian group was able to acquire data over several of its test sites during the AIRSAR campaign of September 1993 and the two SIR-C/X-SAR missions. The principal purpose of each site was as follows:

AIRSAR

Pyramid Hill (Kerang) - Soil salinity mapping with dielectric constant measurements
Palm Valley - 3-Dimensional geological structural analysis of the Palm Valley Gas Field
Fowlers Gap - Studies of the regolith and geological mapping
Yass - Dryland salinity mapping in an area of moderate relief

SIR-C/X-SAR

Pyramid Hill (Kerang) - Soil salinity mapping through dielectric constant measurements
Palm Valley - 3-Dimensional geological structural analysis of the Palm Valley Gas Field
plus
Northern Luzon, Philippines - geological, structural, and environmental mapping

SIGNIFICANT RESULTS

Pyramid Hill (Kerang) - Inversion of the AIRSAR data has allowed for the mapping of the Complex Dielectric Constants over the study region. Atypical wet soil conditions at the time of acquisition meant that variations in the dielectric constant were due mainly to the imaginary part of the complex constant, and hence due to salinity. The dielectric constant maps provide the best available maps of soil salinity for the region. The L-band-derived image provides the best indication of surface salinity (Figure 1). The dielectric maps

derived from C-, L- and P-band give indications of the extent of salinity at depth (Figure 2) and can be combined to give a color composite that clearly indicates the severity of salinity (Figure 3).

Comparison of the various available inversion techniques shows that in this region of low relief, the small perturbation model discriminates saline areas well but underestimates the magnitude of the dielectric constant. The semi-empirical method developed at JPL provides the best results. These may be compared qualitatively as follows:

Model	Mean	SD	Max	Variation/ incidence	dynamic range/discrim.
SPM UNSW	4.72	11.97	100	moderate	excellent
SPM Colorado	5.28	11.86	100	excessive	fair
JPL	10.12	10.05	88	slight	excellent
Empire	6.48	9.7	687	none	very poor

Other processing carried out on Pyramid Hill AIRSAR data:

Decompositions by MAPVEG
Surface roughness mapping with RAVEN
Polarization signatures with ENVI

These different processing strategies have been used to create three useful map products that show surface roughness, surface scattering mechanisms, and the multifrequency derived dielectric maps (Figure 4).

Both the UNSW small perturbation inversion and the semi-empirical JPL inversion have been applied to several of the available SIR-C scenes. Problems with modifying code to take appropriate account of incidence angle have delayed the work. To date we have found that the dielectric maps give a good indication of the local soil moisture content (Figure 5a). This in turn is related to the recent irrigation history. Only on one data take (SRL-2, 84.8), which was acquired after light rain, is there any indication of the soil salinity that was so visible on the AIRSAR images (Figure 5b). Inversions of the small incidence angle images appear to give much noisier maps of the dielectric constant than do the large incidence angle images. The RMS images produced by the JPL inversion are an accurate reflection of surface roughness.

3 -Dimensional geological structural analysis of the Palm Valley Gas Field

We have developed software, VECTOR3D, using the Interactive Data Language (IDL), that allows the elevation of any point along the trace of a geological feature visible in the remotely sensed image to be derived from the integrated digital terrain data. Several different methods are provided for the estimation of the dip and strike of the inferred geological structure and for testing the reliability of the determination. Additional tools are provided for annotation of interpreted features, modeling of geological structures, and the estimation of the depth to particular modeled structures.

We are currently undertaking an analysis of the 3-D orientation of all structures visible on the AIRSAR imagery of Palm Valley. This work has important petroleum exploration implications.

Fowlers Gap, western NSW

AIRSAR and TOPSAR imagery from Fowlers Gap has been thoroughly evaluated. The surface roughness aspects of the AIRSAR data form a useful ancillary data set to combine with other forms of remotely sensed data. The TOPSAR data have been used to create topographic surfaces upon which TIMMS imagery has been draped. This provides a very powerful image from which surficial geology can be mapped.

Yass, central NSW

The Yass AIRSAR imagery has been inverted, using a simple small perturbation model, to map soil dielectric constants. The results were disappointingly noisy, mostly due to the moderate topography and high levels of vegetation cover. We hope to develop an inversion algorithm which takes into account the topography, calculates local incidence angle for each pixel, and hence might give more reliable estimates of the surface dielectrics.

Northern Luzon, Philippines - Several SIR-C/X-SAR scenes have been received for the Zambales ophiolite belt which lies immediately to the north of Mount Pinatubo. Studies to date have utilized topography and image texture to map geology and structure. It is hoped that an interferometric DTM can be obtained that will allow the study to expand into an analysis of the role of topography in facilitating mapping of geology and landscape evolution. Local Philippine students under the supervision of UNSW academics are keen to use the DTMs for characterizing lahar deposits around Mount Pinatubo.

FUTURE PLANS

In order of priority, our outstanding objectives are:

*1. To produce a regional map of the soil salinity of the Tragowel Plains region around Pyramid Hill, Victoria. Requires JPL to process further AIRSAR imagery as requested in December 1995.

2. To fully evaluate the response to soil moisture and salinity shown in the SIR-C/X-SAR images on a temporal and incidence angle basis.

3. To fully evaluate the power of Cloude-type decompositions for mapping surface scattering components in both AIRSAR and SIR-C/X-SAR imagery.

*4. To develop inversion routines that will properly take account of local incidence angle variations in areas of moderate relief (Yass).

*5. To complete an evaluation of SIR-C/X-SAR and the derived DTMs for mapping geology, structure, and environmental features in tropical areas, using the data from northern Luzon.

* indicates objectives requiring further processed data

PUBLICATIONS

* Indicates papers describing AIRSAR or SIR-C/X-SAR results

Mah, A. H., G. R. Taylor, I. Acworth, B. A. Bennett, T. Calvert and R. D. Hewson, 1993 Dielectric properties of salinised soils and their implications for the possible use of radar to map and monitor such soils. Proc. Coming of age, 21 years after Landsat, Advanced Remote Sensing Conference. University of New South Wales, Kensington. pp. 17.

Bennet, B. A., G. R. Taylor, R. D. Hewson, and A. H. Mah, 1993, Spectral characteristics in the 1.3 to 2.5 micron range of saline areas and their implications for monitoring techniques. Proc. Coming of age, 21 years after Landsat, Advanced Remote Sensing Conference. University of New South Wales, Kensington. p. 7.

Vinayan, P. K., G. R. Taylor, L. Balia and P. G. Lennox, 1993, The integration of vector and raster-based remotely sensed data for geological exploration. Proc. Coming of age, 21 years after Landsat, Advanced Remote Sensing Conference. University of New South Wales, Kensington.

Mah, H., G. R. Taylor, P. Lennox, and L. Balia, 1995 Lineament analysis of Palm Valley Thematic Mapper images, Northern Territory, Australia. Photogrammetric Engineering and Remote sensing, 61, 761-773.

Taylor, G. R., B. A. Bennett, A. H. Mah,and R. D. Hewson, 1994, Spectral properties of salinised land and implications for interpretation of 24 channel imaging spectrometry. Proceedings of the First International Remote Sensing Conference and Exhibition, Strasbourg, France, Vol. 3, 504-513.

Taylor G. R., A. H. Mah, F. A. Kruse, K. S. Kierein-Young, R. D. Hewson, and B. A. Bennett, 1995, The extraction of soil dielectric properties from AIRSAR data. *International Journal of Remote Sensing*, in press.

*Taylor, G. R., A. H. Mah, F. A. Kruse, K. S. Kierein-Young, R. D. Hewson, and B. A. Bennett, 1995, Characterization of saline soils using airborne radar imagery. *Remote Sensing of Environment*, In Press.

Taylor, G. R., L. Balia, and JUSMADY, Integrated remotely sensed imagery and computer-based lineament analysis as an aid to tectonic analysis of an area adjacent to the Philippine Fault. Submitted to Tectonophysics, in review.

*Taylor, G. R., A. H. Mah, F. A. Kruse, K. S. Kierein-Young, R. D. Hewson, and B. A. Bennett, 1995, The extraction of soil dielectric properties from AIRSAR and SIR-C imagery. European Symposium on Satellite Remote Sensing II, Paris, 25-28 September 1995.

*Taylor, G. R., A. H. Mah, F. A. Kruse, K. S. Kierein-Young, R. D. Hewson, and B. A. Bennett, 1995, The extraction of soil dielectric properties from AIRSAR and SIR-C imagery. Significant Results of the AIRSAR Australia 1993 Mission. International Workshop on Radar Image Processing and Applications, University of New South Wales, 6-8 November 1995.

*Hewson, R. D. and G. R. Taylor, 1995. AIRSAR imagery as an ancillary data set for geological mapping at Fowlers Gap, Western New South Wales. Significant Results of the

AIRSAR Australia 1993 Mission. International Workshop on Radar Image Processing and Applications, University of New South Wales, 6-8 November 1995.

*Mah, A. H. and G. R. Taylor, 1995. The extraction of 3-dimensional structures from integrated DTM and remotely sensed data. Significant Results of the AIRSAR Australia 1993 Mission. International Workshop on Radar Image Processing and Applications, University of New South Wales, 6-8 November 1995.

*Taylor G R, A. Mah and Taylor M., 1996. The determination of the orientation in three dimensions of geological structures from remotely sensed radar and digital terrain data. Proc. 8th. Australian Remote Sensing Conference, Canberra, March 1996. In Press.

*Zaratan M L and Taylor G R, 1996. Analysis of multifrequency, multipolarization SIR-C/X-SAR data for Geologic Studies, in the Mount Pinatubo area, Philippines. Proc. 8th. Australian Remote Sensing Conference, Canberra, March 1996. In Press.

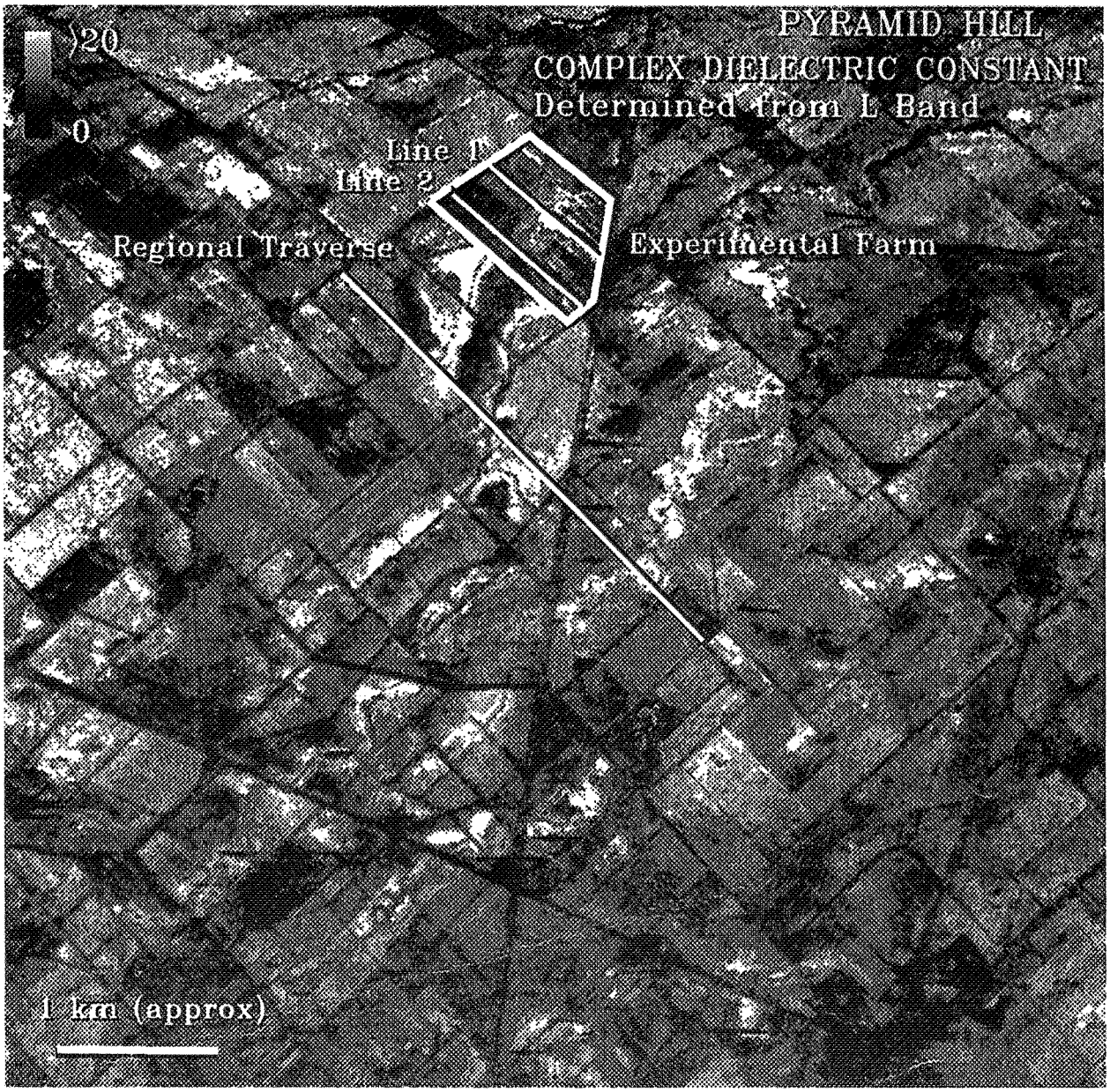
PYRAMID HILL
COMPLEX DIELECTRIC CONSTANT
Determined from L Band
>20
0
Line 1
Line 2
Regional Traverse
Experimental Farm
1 km (approx)

Figure 1

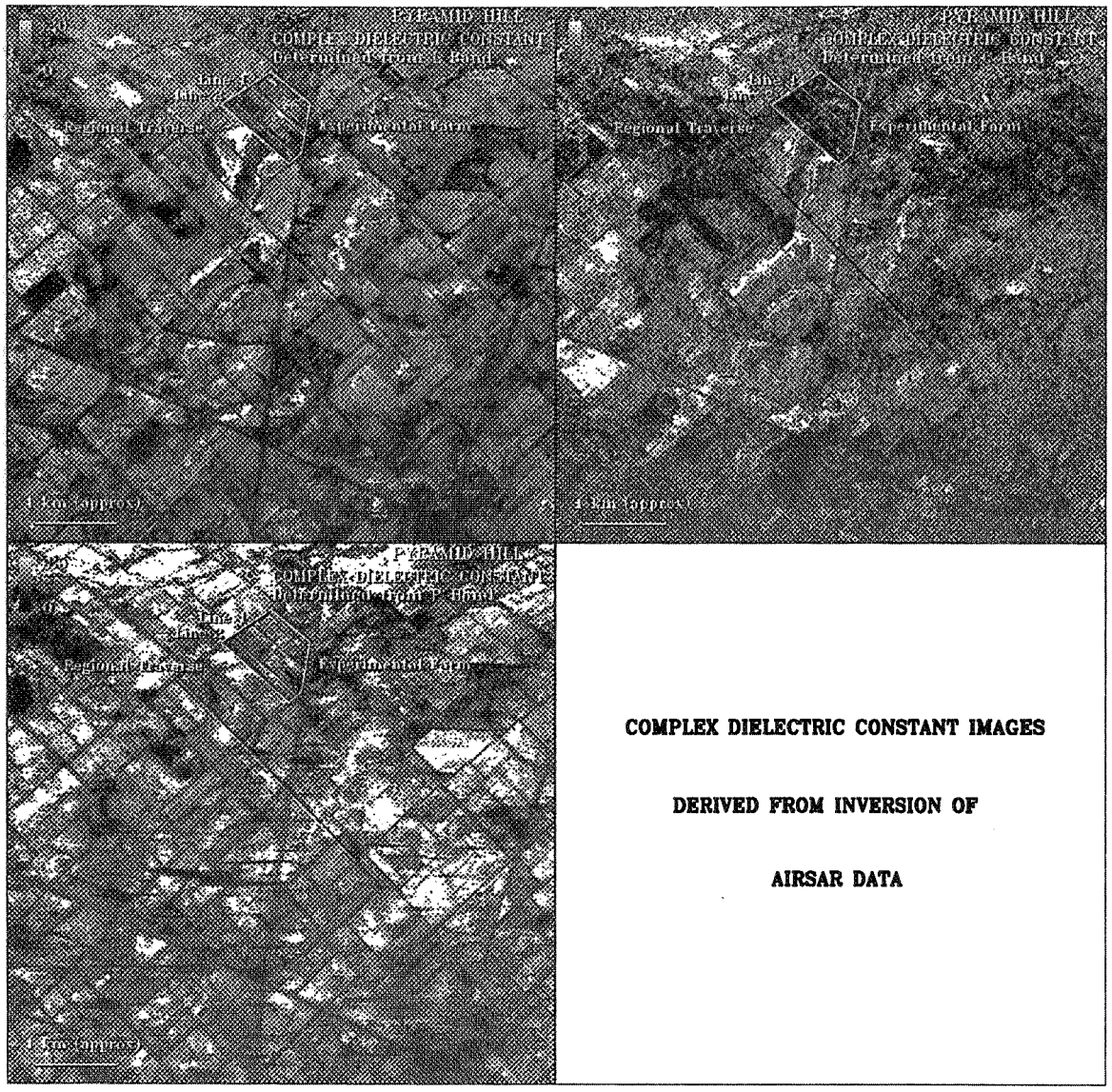
PYRAMID HILL
COMPLEX DIELECTRIC CONSTANT
Determined from L Band
Line 3
Line 2
Regional Traverse
Experimental Farm
4 km (approx)
COMPLEX DIELECTRIC CONSTANT IMAGES
DERIVED FROM INVERSION OF
AIRSAR DATA

Figure 2

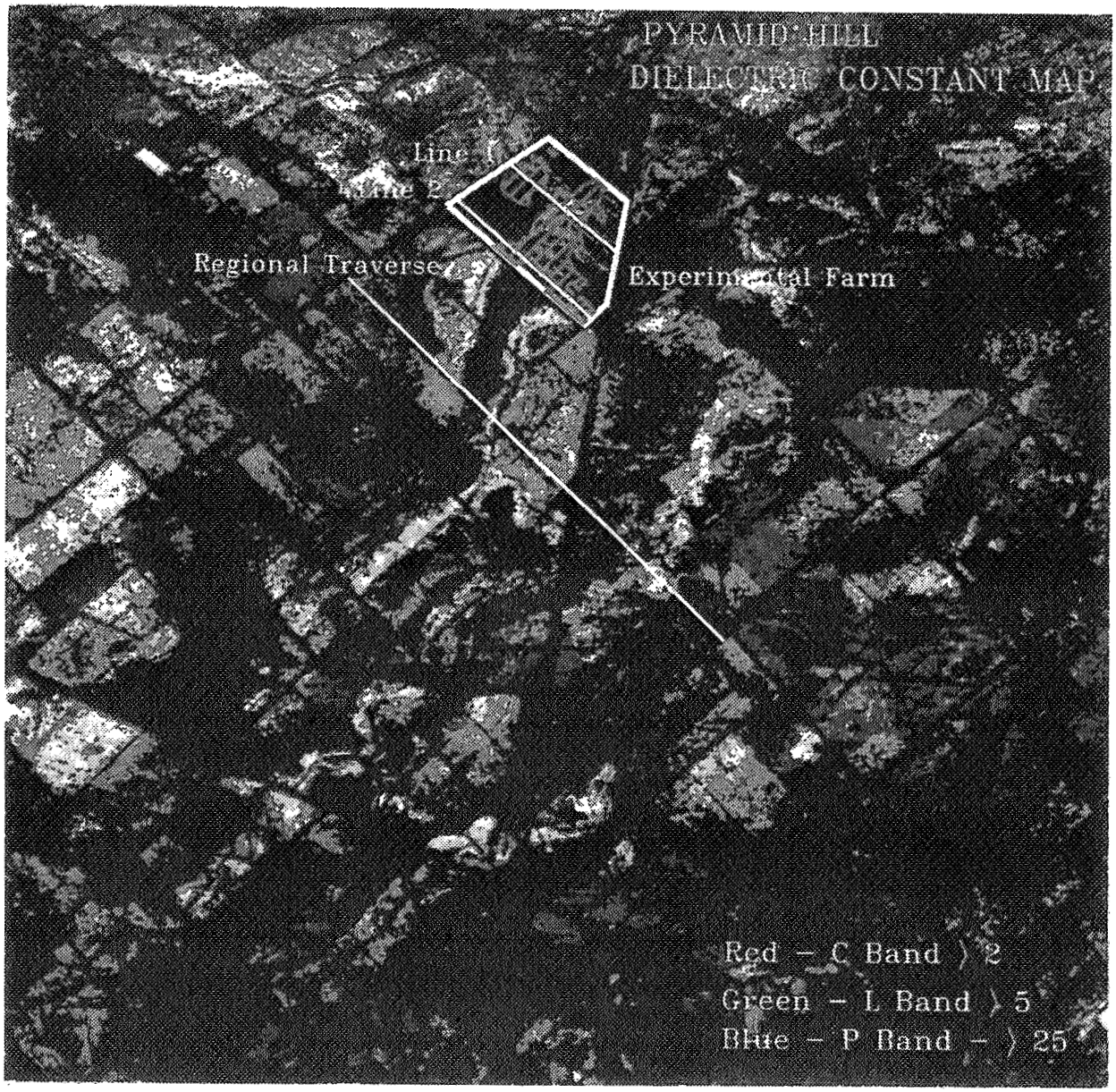
PYRAMID HILL
DIELECTRIC CONSTANT MAP
Line 1
Line 2
Regional Traverse
Experimental Farm
Red - C Band) 2
Green - L Band) 5
Blue - P Band -) 25

Figure 3

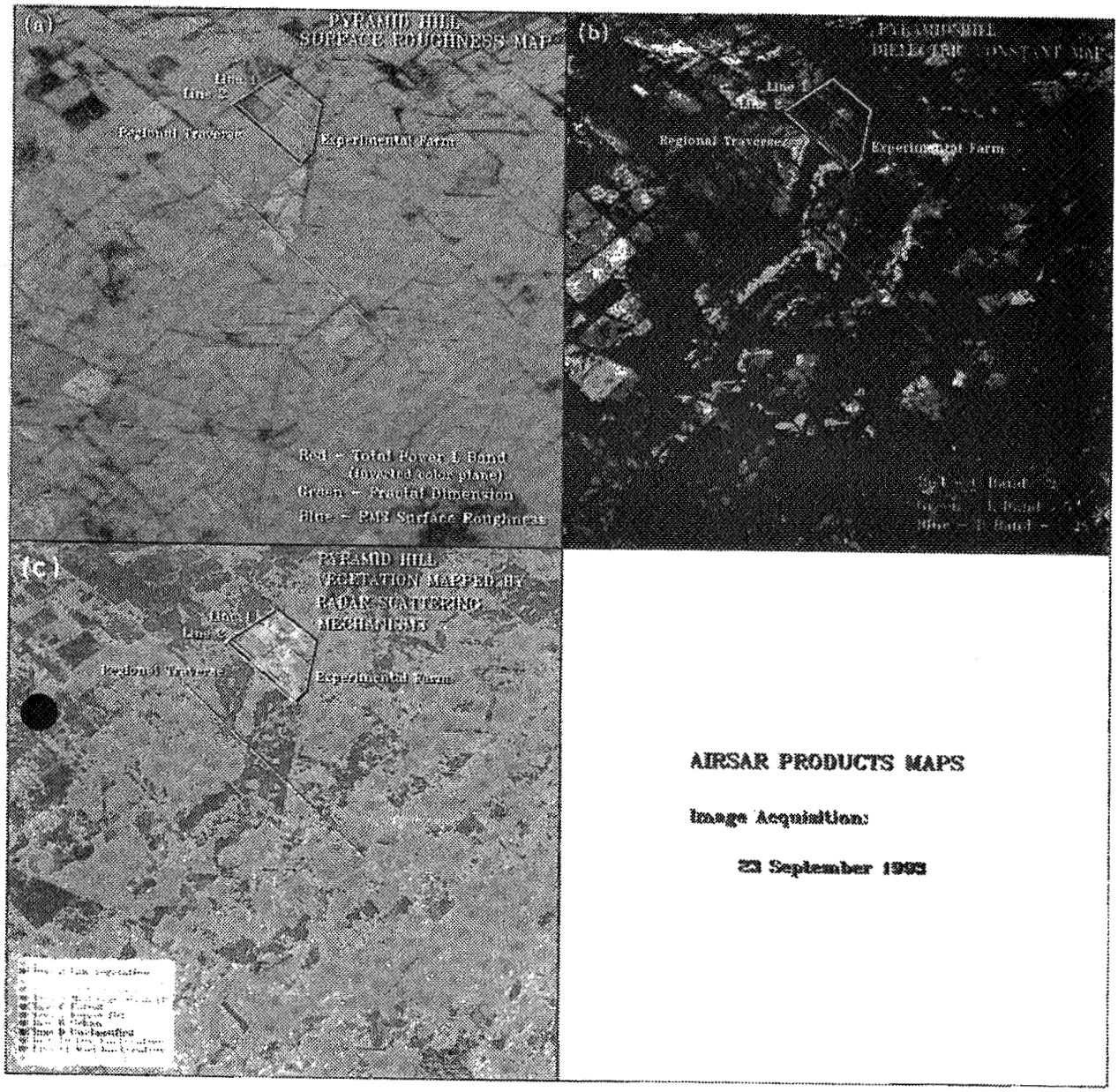
(a)
PAPANUI HILL
SURFACE ROUGHNESS MAP
Line 1
Line 2
Regional Traverse
Experimental Farm
Red = Total Power L Band
(Horizontal polarization)
Green = Fractal Dimension
Blue = RMS Surface Roughness
(b)
Line 1
Line 2
Regional Traverse
Experimental Farm
(c)
PAPANUI HILL
VEGETATION MAPPED BY
RADAR SCATTERING
MECHANISMS
Line 1
Line 2
Regional Traverse
Experimental Farm
AIRSAR PRODUCTS MAPS
Image Acquisition:
23 September 1993

Figure 4

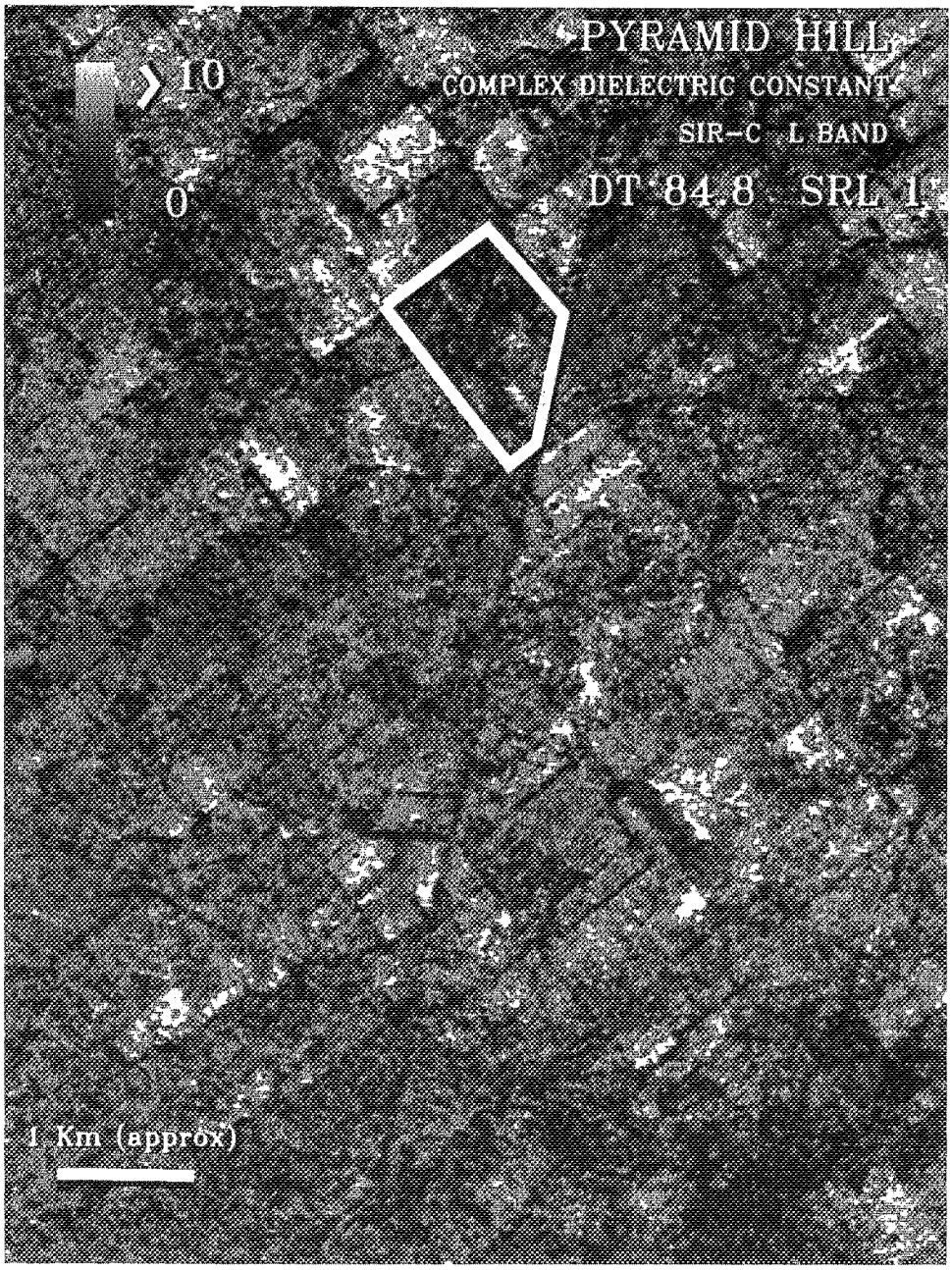
PYRAMID HILL
COMPLEX DIELECTRIC CONSTANT
SIR-C L BAND
DT 84.8 SRL 1
> 10
0
1 Km (approx)

Figure 5a

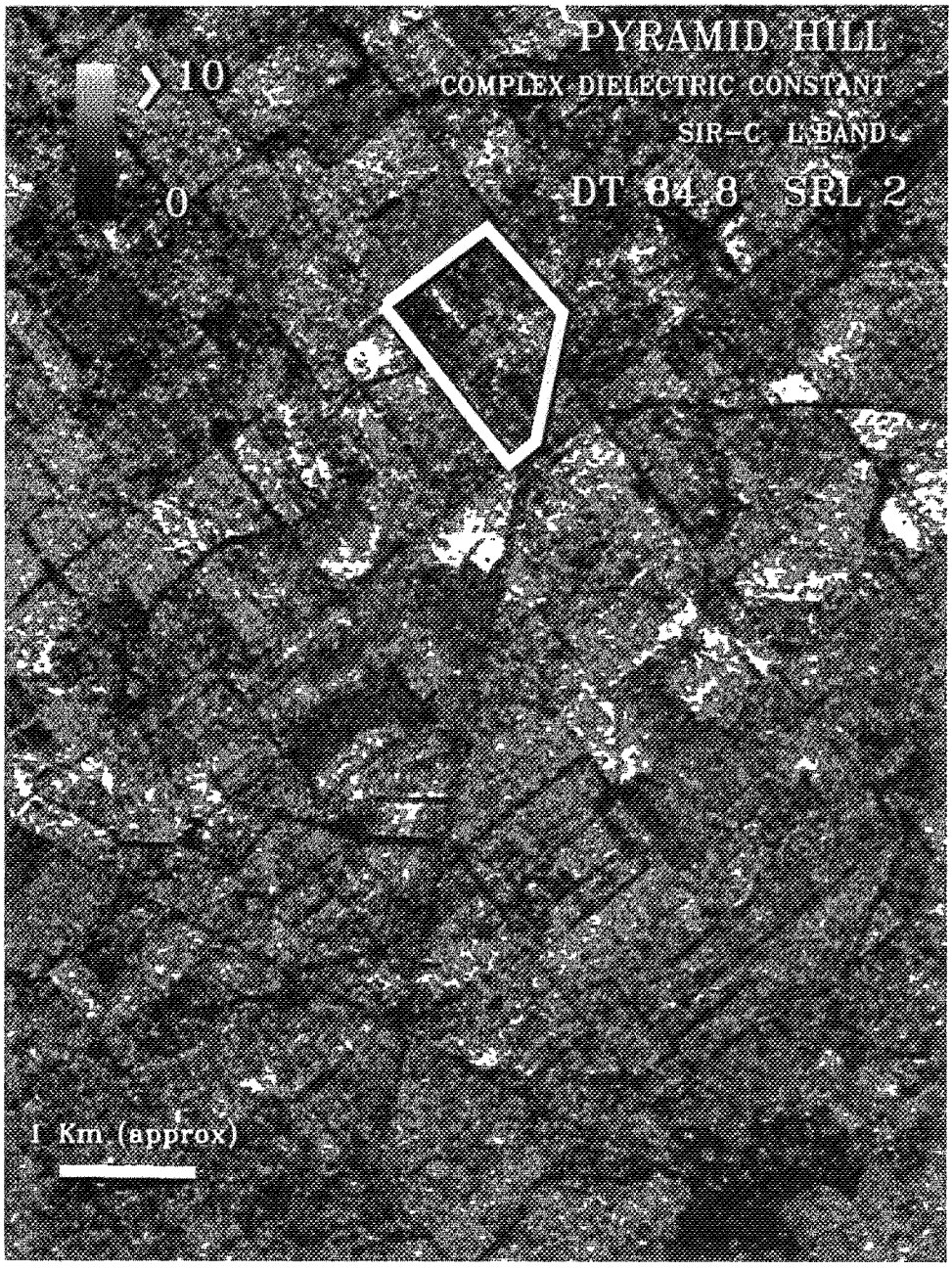
PYRAMID HILL
COMPLEX DIELECTRIC CONSTANT
SIR-C L-BAND
DT 84.8 SRL 2
> 10
0
1 Km (approx)

Figure 5b

Dr. Fawwaz T. Ulaby
University of Michigan
Radiation Laboratory
Department of EECS
1301 Beal
Ann Arbor, MI 48109-2122

Co-Investigators:
M. Craig Dobson Univ. of Michigan
T. Sharik Univ. of Utah

Polarimetric Radar Observations of Forest State for Determination of Ecosystem Process

OBJECTIVES

The objectives of this research are to test the hypotheses that ecologically significant forest state parameters may be estimated from SAR data. These include estimation of above ground biomass, plant water status, and near surface soil moisture under certain forest conditions.

Test hypotheses in the northern hardwoods forest community, refine them if necessary, and establish techniques for retrieving this information from orbital SARs such as SIR-C/X-SAR.

This report summarizes (1) recent progress, (2) significant results and (3) research plans concerning SIR-C/X-SAR research conducted under JPL Contract No. 951869. Significant progress has been made with regards to data acquisition, data analysis and dissemination of results during the 18-month period from March 1994 to August 1995. The data have been fully documented and the substantive findings have been thoroughly reported via technical reports, symposia and journals subject to peer review. The research plan for the next two years has two phases: (1) complete the analyses of the Raco Supersite data and (2) extrapolate significant results and methodologies to other SIR-C/X-SAR test sites.

PROGRESS

During the past 18 months, research efforts have concentrated on (1) acquisition of data before, between and during the two SRL missions, (2) reduction, documentation and distribution of the data, (3) analyses of the SAR and ancillary data concerning land-cover classification and retrieval of forest biophysical properties, (4) syntheses of research results and (5) dissemination of SIR-C activities and data to the general public. Progress in each of these areas is briefly reviewed. The amount of processed SIR-C data for the Raco Supersite was somewhat limited until just recently. Only 50% of the acquired data takes had been processed and delivered as calibrated SLC products prior to 8/15/95. However, we have received the remaining 50% of the data within the past two weeks. All X-SAR data were processed and delivered by May 1995. Data acquisition activities completed over the past 18 months include: (1) SAR calibration support, (2) extensive inventories of land-cover information, (3) updating biometric surveys of approximately 60 forest stands and (4) in situ observations of moisture, dielectric, precipitation and temperature conditions during the SRL missions. Over 35 persons have been involved in these efforts.

Calibration

The calibration activities consisted of deploying arrays of passive and active point targets of known radar cross-section as well as the measurement of distributed targets using a truck-mounted polarimetric scatterometer. In support of both SIR-C/X-SAR and associated under flights by the JPL AIRSAR, these targets were repositioned, as needed, to optimize performance for each overpass. The 3-D differentially processed GPS coordinates were obtained for each target and

forwarded to JPL during each mission, along with the expected RCS of each target, for use in the initial calibration of the SIR-C data. The distributed target measurements are being used under separate contract to improve estimates of the SIR-C distortion matrices. Accurate calibration of both amplitude and phase are essential for application of robust quantitative algorithms.

Land-Cover Classification

Much effort has been put into activities supporting land-cover classification using SIR-C/X-SAR. Classification is an essential precursor to accurate retrievals of geophysical properties (i.e., soil moisture) and biophysical properties (i.e., biomass). Small aircraft were chartered in April and October 1994 to acquire both video and still photography during each of the SRL missions. A 30-km x 50-km region surrounding the Raco Supersite was imaged. This imagery augments ground-level surveys and photography to document land-cover and land-use conditions over both the forested portion of the supersite and an adjacent agricultural area. These qualitative data are used in conjunction with more detailed quantitative information obtained for approximately 60 forest stands and 30 non-forested areas to provide independent training and testing populations used in development and evaluation of a land-cover classification.

To date, we have tested both simple hierarchical knowledge-based approaches to classification and also optimized Baysian classifiers (as well as hybrid techniques). For purposes of technique development and extension of prior results based upon JPL AIRSAR data, our efforts have concentrated thus far on a small number of data sets, SRL-1 data take 6.1 (at 31° incidence angle) and data take 22.2 (at 21° incidence angle) for both SRL-1 and -2. Our approach has been to (1) define and optimize a classification technique, (2) evaluate the role of azimuth angle and temporal effects (day-to-day variation in scene dielectric properties and seasonal phenologic changes) on classifier stability, (3) evaluate effects of angle of incidence on classification and (4) investigate the improvement in classification afforded by either multitemporal or multiangle classification techniques. Classifications developed using AIRSAR data have been successfully extended to SIR-C/X-SAR data and confirm expectations. Greater than 90% classification accuracy is generally achieved when land-cover classes are defined on the basis of structural attributes. Multitemporal classifications show some improvement over single-date classifications due primarily to phenologic changes in the crown layer. The SAR-based classifications provide structural information not possible using optical techniques.

Biomass Retrieval

Biometric surveys were conducted of approximately 60 forest stands within the Raco Supersite during the four-year period from 1990 to 1993. During a two-week period in July 1994, a team of 16 persons, including a group of high school students selected by the Johns Hopkins Center for Talented Youth, reinventoried 22 of the youngest stands for which annual growth leads to a significant percent change in total biomass. Approximately 20,000 stems were measured during this period. In addition, new allometric equations were generated on the basis of our data to estimate tree height from diameter and then applied to the full sample population of over 70,000 tree stems to provide an updated data base of forest biomass concurrent with the SIR-C/X-SAR data. This data base represents an investment of over 12,000 hours of effort. During the SIR-C/X-SAR missions in April, August and October, on site teams of about 15 persons collected daily measurements of moisture, density, temperature and dielectric properties of soil, snow and vegetation for a representative subsample of the 60 forest stands within the Raco Supersite. Surface roughness was also characterized at two scales for a subset of the forest stands using surveying equipment over 50-m transects and photographs of 2-m roughness panels to record micro relief. In addition, leaf area index was measured for all forest stands during August and September using a techniques based on the optical transmittance of the canopy. These data have been processed, edited and published in two technical reports.

The biomass data have been merged with the SIR-C/X-SAR data and completely analyzed for two data takes (SRL-1: 6.2 and 102.41); another pair of data takes are partially analyzed (data take 22.2 on SRL-1 and -2). A semi-empirical technique has been developed and tested that uses a three-step approach to yield final estimates of crown, trunk and total above-ground standing biomass. The approach utilizes the SAR-based land-cover classification, then estimates average tree height and basal area which in turn are used to estimate trunk-layer biomass. These estimates have been found to be highly accurate, and are generally within 10% of the allometrically-determined values (which themselves have associated uncertainties on the order of 15%). Hence, the SAR-based results are comparable to or better than those from detailed ground-based surveys costing on the order of $1,000/ha. These initial results have generated a high level of excitement within the ecological and forestry communities.

Soil Moisture

The descending passes of SIR-C/X-SAR acquired data over an agricultural region immediately to the southeast of the Raco Supersite. During SRL-2, detailed observations were made of vegetation cover (i.e., type, height, biomass, moisture, leaf area index), surface roughness and soil properties (moisture, density and dielectric constant). The soil data were collected on a daily basis during the last half of SRL-2 (repeat orbit phase). These data have been edited, compiled and published in a technical report. The purpose of these data is to test and validate improved algorithms to estimate near-surface soil moisture beneath short vegetation covers. The data are not yet analyzed for this purpose.

In addition to the conduct of experimental activities and analyses of the data, our team has contributed to a number of other associated activities. One or two team members have attended all SIR-C Team and Working Group meetings. We contributed heavily to the NRC review. A significant additional effort was put into (1) providing "real-time" analyses of land-cover classification and biomass retrieval during both SRL-1 and -2, (2) provision of both studio interviews and on site video of experimental activities for the JPL Public Information Office, (3) approximately 20 interviews with radio, television and print journalists, (4) classroom instruction and teacher assistance at the high school level as part of the SIR-C Public Education Initiative and (5) seminars and workshops to disseminate SIR-C results to working ecologists and foresters at the Hiawatha National Forest.

FUTURE PLANS

During the next two years, further analyses of SIR-C/X-SAR data will be conducted in two phases: (1) complete analyses of the Raco Supersite data and (2) extend the methodology and algorithms to other SIR-C sites. During the first phase, land-cover classification and biomass retrieval methodologies and algorithms will be completely evaluated using the full set of SRL-1 and -2 SAR data. For both activities, temporal variations in scene dielectric properties and phenologic conditions will be evaluated using same angle pairs of data takes both within a mission (day-to-day variation) and between SRL-1 and -2 (seasonal variation). The effects of angle of incidence will be evaluated using SIR-C/X-SAR data that range from 20° to 44° for a common azimuth view angle. The effects of azimuth viewing angle will be evaluated using data from three viewing directions but with two sets of common incidence angles (approximately 20° and 30°). This work is being done as part of a Ph.D. thesis. The added benefits of multitemporal or multiangle classification will also be evaluated. The semi-empirical technique for retrieval of biomass requires certain ancillary data for each forest structural type, a more theoretical approach that does not require this information will be tested with a subset of the SIR-C/X-SAR data. Finally, analyses will be conducted for purposes of soil moisture retrieval using the data acquired during SRL-2; the algorithms to be used are being developed under separate contract. All of the SIR-C/X-SAR data for the Raco Supersite have been processed and delivered for the SLC "calibrated" product. The only additional

processing that we need is for geo-coded products. We have found that our efforts have been considerably slowed by the absence of such a product and foresee great difficulty in extension of the Raco Supersite results to other regions of even modest relief until such a product is developed and distributed.

During the second phase, those techniques and algorithms found to be useful at the Raco Supersite will be tested at other SIR-C/X-SAR sites. This will allow us to test for robustness and take advantage of the ancillary data acquired at other US and foreign supersites. The ecology supersites will be used for this purpose. First, we will test the algorithms in biomes similar to the region of development (i.e., at Howland and Duke Forest), then the techniques will be assessed at other sites primarily those in Europe. Some of the processed SIR-C data have already been made available to us for this purpose. We do not expect to be requesting additional SIR-C/X-SAR processing beyond what is requested by site PIs for this purpose.

PUBLICATIONS

Pierce, L. E., F. T. Ulaby, K. Sarabandi, and M. C. Dobson,"Knowledge-Based Classification of Polarimetric SAR Images," *IEEE Transactions Geoscience and Remote Sensing*, Vol. 32, No. 5, pp. 1081-1086, Sept. 1994.

Dobson, M. C., F. T. Ulaby, and L. E. Pierce, "Land-Cover Classification and Estimation of Terrain Attributes Using Synthetic Aperture Radar," *Remote Sensing of Environment,* Vol. 51, No. 1, pp. 199-214, 1995.

Sarabandi, K., L. E. Pierce, M. C. Dobson, F. T. Ulaby, J. M. Stiles, T. C. Chiu, R. De Roo, R. Hartikka, A. Zambetti and A. Freeman, "Polarimetric Calibration of SIR-C Using Point and Distributed Targets," *IEEE Trans. Geoscience and Remote Sensing*, Vol. 33, No. 4, pp. 858-866, July 1995.

Dobson, M. C., F. T. Ulaby, L. E. Pierce, T. L. Sharik, K. M. Bergen, J. Kellndorfer, J. R. Kendra, E. Li, Y. C. Lin, A. Nashashibi, K. Sarabandi and P. Siqueira, "Estimation of Forest Biophysical Characteristics in Northern Michigan with SIR-C/X-SAR," *IEEE Trans. Geoscience and Remote Sensing*, Vol. 33, No. 4, pp. 877-895, July 1995.

Symposia, Workshops and Conferences

Dobson, M. C., L. E. Pierce, and F. T. Ulaby, "Semi-empirical Method for Estimation of Forest Biophysical Properties from Multifrequency Polarimetric SAR," 1994 International Geoscience and Remote Sensing Symp. (IGARSS '94), August 8 - 12, 1994, California Institute of Technology, Pasadena, CA.

Ulaby, F. T., L. E. Pierce, M. C. Dobson, S. Chacon, and K. Sarabandi, "Land Cover Classification by SAR," 1994 International Geoscience and Remote Sensing Symposium (IGARSS '94), August 8 - 12, 1994, California Institute of Technology, Pasadena, CA.

Sarabandi, K., L. E. Pierce, J. M. Stiles, M. C. Dobson, T. C. Chiu, and F. T. Ulaby, "Polarimetric Calibration of SIR-C Using Point and Distributed Targets," Proc. SAR Calibration Workshop, pp. 18, CEOS Calibration/Validation Working Group: SAR Calibration Workshop, Sept. 28-30, 1994, The University of Michigan, Ann Arbor, MI.

Dobson, M. C., "Retrieval of Forest Biomass Using SAR", Ecology Panel Workshop for the Committee on Earth Sciences, Space Studies Board, National Research Council, Univ. of CA at Santa Barbara, Nov. 14-17, 1994.

Dobson, M. C. and F. T. Ulaby, "Preliminary Results from SIR-C/X-SAR at the Raco Supersite," SIR-C/X-SAR Team Meeting, Uberlingen, Germany, Feb. 6-8, 1995.

Dobson, M. C., F. T. Ulaby, L. E. Pierce, and K. Sarabandi, "Land-Cover Classification and Estimation of Forest Biophysical Properties Using SIR-C/X-SAR," NASA Remote Sensing Science Workshop, NASA Goddard Space Flight Center, Feb. 27 - March 1, 1995.

Dobson, M. C., "Terrain Classification and Estimation of Forest Biophysical Properties Using SIR-C/X-SAR," Proc. CoHEMIS Workshop on Remote Sensing and Environmental Monitoring for the Sustainable Development of the Americas, San Juan, Puerto Rico, March 21-22, 1995.

Sarabandi, K., L. Pierce, J. Stiles, M. Dobson, T. Chiu and F. Ulaby, "Polarimetric Calibration of SIR-C Using Point and Distributed Targets," Int. Geoscience and Remote Sensing Symposium (IGARSS '95), *IGARSS '95 Digest,* Vol. 1, pp. 593, July 10-14, 1995, Florence, Italy.

Pierce, L., K. Bergen, C. Dobson, and F. Ulaby, "Land-Cover Classification with SIR-C/X-SAR Data," 1995 Int. Geoscience and Remote Sensing Symposium (IGARSS '95), *IGARSS '95 Digest*, Vol. 2, pp. 918-920, July 10-14, 1995, Florence, Italy.

Dobson, M., L. Pierce, K. Bergen, J. Kellndorfer, and F. Ulaby, "Retrieval of Above-Ground Biomass and Detection of Forest Disturbance Using SIR-C/X-SAR," 1995 Int. Geoscience and Remote Sensing Symposium (IGARSS'95), IGARSS'95 Digest, Vol. 2, pp. 987-989, July 10-14, 1995, Florence, Italy.

Kasischke, E., J. Melack, J. B. Way, and M. Dobson, "Ecological Applications of Imaging Radar," 1995 Int. Geoscience and Remote Sensing Symposium (IGARSS'95), IGARSS'95 Digest, Vol. 1, pp. 593, July 10-14, 1995, Florence, Italy.

Technical Reports

Bergen, K. M., M. C. Dobson, L. E. Pierce, J. R. Kendra, J. Kellndorfer, P. Siqueira, K. Sarabandi and F. T. Ulaby, "April 1994 SIR-C/X-SAR Mission: Ancillary Data Report Raco, Michigan Site," Radiation Lab Tech. Report. 026511-5-T, December 1994.

Dobson, M. C., K. Bergen, L. E. Pierce, J. Kellndorfer, K. Sarabandi and F. T. Ulaby, "October 1994 SIR-C/X-SAR Mission: Ancillary Data Report Raco, Michigan Site," Radiation Lab Tech. Report. 026511-6-T, August 1995.

Papers Submitted

Bergen, K. M., M. C. Dobson and L. E. Pierce, "Radar Aboard Space Shuttle Endeavor Images the Hiawatha for Purposes of Land-Cover Classification, Biomass Estimation and Detection of Forest Disturbance," Conference on Adding a Multiscale and Ecological Perspective to Wildlife and Vegetation Management in the Upper Peninsula of Michigan, Clear Lake, Hiawatha National Forest, Sept. 19 - 21, 1995.

van Zyl, J., C. Dobson, J. Dozier, P. DuBois, D. Evans, J. A. Kong, T. LeToan, J. Melack, E. Rignot, S. Saatchi, J. C. Shi, and F. T. Ulaby, "Preliminary Science Results from the SIR-C/X-SAR Mission," Int. Symp. on Retrieval of Bio- and Geophysical Parameters from SAR Data for Land Applications, Toulouse, France, Oct. 10-13, 1995.

Ulaby, F. T., M. C. Dobson, L. Pierce and K. Sarabandi, "Scene Classification and Biomass Estimation Using SIR-C/X-SAR Data," Int. Symp. on Retrieval of Bio- and Geophysical Parameters from SAR Data for Land Applications, Toulouse, France, Oct. 10-13, 1995.

Dr. Paris W. Vachon
Canada Centre for Remote Sensing
588 Booth Street, Ottawa,
Ont. K1A 0Y7
Canada

Co-Investigators:

Fred W. Dobson	Bedford Inst. of Oceanography
Roop Lalbeharry	Atmospheric Environ. Service
Harald Johnsen	NORUT

SIR-C/X-SAR Wind and Wave Observations In The Gulf of St. Lawrence

OBJECTIVES

Quantify the frequency/polarization dependence of the real aperture radar (RAR) modulation transfer function (MTF).

Extend wind retrieval models such as CMOD4 (valid for C-band VV polarization) to other frequencies/polarizations.

Test the ability of the SIR-C/X-SAR to detect wave patterns, including the effects of refraction and diffraction, in shallow areas near islands.

Data Set:

SRL-2 (October 1994)

Meteorological buoy and a directional wave buoy deployed in the Gulf of St. Lawrence, south of Iles de la Madeleine.

Six SIR-C/X-SAR passes obtained (three over the site, three nearby).

Canadian Spectral Ocean Wave model (CSOWM, third generation).

Status:

All six SIR-C/X-SAR images have been received in MLD and SLC format.

Image cross spectra have been calculated for all passes (28 cross spectra are available).

From the meteorological buoy, calibrated time series of wind velocity, sea level pressure, and air and sea temperature have been produced.

From the wave buoy, calibrated directional spectra of the wave fields at each of the six pass times have been derived (mean energy, direction, and spreading at a set of 13 wave frequencies).

CSOWM has been run in hindcast mode.

The small incidence angles, and corresponding poor calibration, will prevent further evaluation of wind retrieval models.

FUTURE PLANS

Further SIR-C/X-SAR data requests are not anticipated.

The wind/wave frequency/polarization dependence of the RAR MTF will be studied using empirical methods.

All cross spectra will be inverted to heave spectra using the wave model spectra as a starting point.

The cross spectrum methodology will be evaluated using the buoy spectra.

These analysis results will be published in the special issue on SIR-C/X-SAR oceans results (JGR?) to be organized by B. Holt.

PUBLICATIONS

Vachon, P. W., F. W. Dobson, and R. Lalbeharry, "SIR-C/X-SAR wind and wave observations in the Gulf of St. Lawrence," *Proc. IGARSS '95*, 10-14 July, Firenze, Italy, IEEE 95CH35770, pp. 1314-1316.

Dr. Sergio Vetrella
Cattedra di Ingegneria dei
Sistemi Aerospaziali
Facolta di Ingegneria
Piazzale Tecchio, 80
80125 Napoli, Italy

Co-Investigators:
Antonio Moccia — DISIS, Univ. of Naples
Salvatore Ponte — Second Univ. of Naples, Italy
Francesco Posa — Polytechnic of Bari, Italy
Vincenzo Schena — CO.RIS.T.A., Napoli, Italy
Giacomo De Carolis — CGS-ASI, Matera, Italy

Passive and Active Calibrators for Multifrequency and Multiangle X-SAR/SIR-C Image Radiometric and Geometric Corrections

OBJECTIVES

Prove that despite the considerable number of variables contributing to SIR-C/X-SAR image formation, the data can reveal system descriptors by studying the system response to "known targets" (either point-like or extended) within the scene.

PROGRESS

The analysis of SIR-C/X-SAR data started from our previous work and airborne SAR campaigns in preparation for the April and October 1994 spaceborne missions. Our attention was focused on the data sets gathered during several passages over the Calibration Backup supersite CB1 (Matera, Southern Italy). The main purpose of the experiment is to prove that, despite the considerable number of variables contributing to SIR-C/X-SAR image formation, the data can reveal system descriptors by studying the system response to "known targets" (either point-like or extended) within the scene. To this end, the authors have been designing and developing passive and active L-, C- and X-band calibrators, which were used to instrument approximately 10 square kilometers of the Matera test site, and were accurately located with respect to the geodetic network. This instrumentation was accurately calibrated by using anechoic chamber measurements, and successively tested and validated by means of airborne SAR campaigns (AIRSAR, MAC Europe 1991, TOPSAR).

The step-by-step research program planned and developed in the past allowed us to test and operate a set of ad-hoc multifrequency instrumentation for SAR calibration and data validation, as well as to implement effective radiometric calibration procedures. The insight gained into SAR processing and calibration techniques is being validated by analyzing SIR-C/X-SAR data. In particular, we have available at our Department the SLC (Single-Look Complex), MLD (Multi-Look Detected) and RSD (Reformatted Signal Data) products for all the April 1994 passages of the sensor over the CB1 test site. SIR-C data were acquired during the first half of 1995 from the SIR-C Radar Data Center, whereas the I-PAF provided us with the X-SAR raw (RAW), single-look (SSC) and multilook (MSD) images. Analogous data requests for the October 1994 mission (SRL-2) are going to be fulfilled by SIR-C RDC and the D-PAF.

As it will be explained in the following sections, we performed our analysis mainly on SLC and RSD data, obtaining results in good agreement with pre-test measurements, and which made us confident in the algorithms and techniques developed for the radar data analysis and for the extraction of information from the processed SAR images.

SIGNIFICANT RESULTS

The main results of our investigations on SIR-C/X-SAR data concern high-precision raw data processing and radiometric calibration by means of analysis on active point targets (ARC, Active Radar Calibrators) deployed on the Matera calibration supersite. This is the preliminary step necessary to the creation of consistent data sets containing information on biogeophysical information of the illuminated scene.

FUTURE PLANS

Further work on SIR-C/X-SAR data could be split into two main activities, namely, high-precision processing for radiometric and geometric calibration, and repeat-pass interferometry and polarimetric analysis. In the following a short description of the improvements envisaged for each activity will be given. The first activity is the most mature at this stage of research, and we will give short-term results, whereas the other two activities are considered in a medium-long-term fashion.

High-precision processing for radiometric and geometric calibration. Starting from the encouraging quantitative results obtained from the raw data compression through the simulation of the Shuttle mission, we intend to compare different data sets of the same scene (CB1) processed by JPL with the ones processed by means of the 2-D reference function provided by our SAR system simulator. Besides some minor improvements of the simulator, it will also be interesting to apply the procedure to focus all frequency bands and polarizations, and to evaluate a trade-off between the spatial range of validity of the reference function and the computational efficiency in updating it. Furthermore, more sophisticated interpolation techniques could be used to derive the satellite dynamics starting from ancillary data and including orbital and attitude propagators. This study could be connected to a theoretical analysis of the focusing errors induced by inaccurate orbital data, allowing us to evaluate the influence of the ephemeris inaccuracies on selection of Doppler parameters required for range-Doppler compression. The activities described in this section will be conducted, as well as the results so far attained, in the framework of the research program "Airborne and spaceborne interferometric SAR data corrections for topographic applications" approved by NASA within the Topography and Surface Change Program. The authors intend to apply the procedure to different data sets, frequencies and polarizations, in order to produce comparative tables of results and study the SAR system properties as a function of time, frequency and polarimetric state. Starting from the high-precision processed SAR images, radiometric calibration and cross-calibration between frequencies and polarizations will be performed with algorithms developed by the authors on the basis of existing methods. Emphasis will be given on applications of calibrated data: for example, the ARC's responses will be used to estimate polarimetric imbalances by applying suitable distortion models. Moreover, we will analyze and extract the in-flight azimuth antenna pattern by evaluating the ARCs' responses to the range-compressed images, obtained by correlating the raw data with a simple range matched filter, whose parameters will be derived from ancillary information. We also intend to exploit the different viewing geometries for different passes over the test site. The slight shift between successive orbits, providing images of the area under different illumination angles, would allow us to sample a portion of the in-flight range antenna pattern, and possibly achieve fine tuning of processing parameters. Another idea to be studied is the reconstruction of the spacecraft trajectory by using the Doppler history of the platform: encouraging results have been obtained by applying a coarse procedure to ERS-1 raw data, focused with a reference function obtained by the simulator using as input the ERS-1 Restituted Orbit Data and the ERS-1 Propagated State Vectors.

Repeat-pass interferometry and polarimetric analysis. Our group is primarily concerned with focusing spaceborne interferometric pairs. Therefore, our future activities will be devoted to verifying repeat-passes over Italian test sites with suitable values of the baseline, in order to evaluate the potential of SAR interferometry for topographic mapping, by means of processing procedures based on point targets of known RCS, geographic coordinates and phase behavior. We are planning to study and exploit the availability of different polarimetric information for interferometry, and its effect on the coherence of the output interferogram. An interesting by-product of the coherence analysis could be the study of the potential of SAR interferometry for classification of terrain, together with the development of semi-automatic and automatic procedures for 2-D phase unwrapping, in order to provide the end-user with consistent topographic information and eventually improve the existing methods for phase-preserving SAR processing. Data requests of possible interferometric passages over different test sites (for example, the three passages over Mount Etna, Sicily, Italy of October 9, 10, and 11, 1994) are planned.

PUBLICATIONS

Schena, V. D., F. Posa, S. Ponte, and G. De Carolis, "Development and Performance Validation of L-, C- and X-band Active Radar Calibrators (ARC) by Means of Laboratory Tests and SIR-C/X-SAR Experiments," presented at *IGARSS '95*, held at Florence (Italy), July 10-14, 1995.

Ponte, S. and A. Moccia, "Validating A Spaceborne SAR Simulator by Using SIR-C/X-SAR Data," presented at the *46th International Astronautical Congress*, held at Oslo (Norway), October 2-6, 1995.

Ponte, S. and S. Vetrella, "Multifrequency Analysis of the SIR-C/X-SAR Instrument: Preliminary results of the Italian Calibration Experiments," presented at the *XIII Congresso Nazionale AIDAA (Associazione Italiana di Aeronautica e Astronautica)*, held at Rome (Italy), September 11-15, 1995.

Dr. Daniel Vidal-Madjar
C.R.P.E.
U.V.S.Q.
10-12 Avenue de l'Europe
78140 Velizy
France

Co-Investigators:

M. Normand	CEMAGREF
O. Taconet	CETP/CNRS
S. Mascle	CETP/CNRS
M. Zribi	CETP/CNRS
C. Emblanch	CEMAGREF
C. Loumagne	CEMAGREF

Test of Roughness and Moisture Algorithms Using Multiparameter Spaceborne SAR and Application to Surface Hydrology

OBJECTIVES

Evaluate the usefulness of radar-derived parameters in surface hydrology.

Demonstrate the usefulness of the squint mode in the case of bare soil observations.

Compare various roughness/moisture algorithms in a real space imaging mode.

PROGRESS

The Orgeval SIR-C/X-SAR Experiment in April 1994

The area surveyed by SIR-C/X-SAR included two monitored watersheds, Mélarchez and Orgeval, covering 5x5 km^2 of intensive agricultural plains east of Paris (France). In April 94, the majority of fields were bare soils, except for wheat (20 cm high). During the 5 days of SAR passes, soil moisture remained high and constant ($0.35cm^3/cm^3$) over the watersheds and soil roughness and practices were the remaining variables.

A detailed survey was done and a crop map generated (70 fields of more of one ha) shown on Figure 1. Photography of soil surfaces was done over 50 bare fields. Ten fields (numbered one to 10) were intensively characterized and were representative of the region's cultures (four of wheat, two of peas, three of corn, one ploughed field): soil moisture and density data (gravimetric and neutronic), height profiles by pin-profilers, penetrometer. A SPOT image (from June 1994) was used to assess the field boundaries. The 70 fields were classified by roughness aspects (Table 1).

The SAR images' incidence angles range from 44° to 57°. Simultaneously, several flights of the copolar scatterometer ERASME of the CETP (C- and X-bands) were done in SAR site direction and over the tested region, keeping flights perpendicular and parallel to the row directions over test fields. The ERASME incidence angles were from 25° to 50°.

Intercomparison of SIR-C/X-SAR cross-sections was done over natural targets, on fields seen on the same incidence angle and the same view azimuthal angle. The intercalibration of the three radars was within 2 dB at maximum (Figures 2 and 3).

SIGNIFICANT RESULTS

Polarimetric signatures in multiconfiguration conditions (three frequencies, L, C, X, multi-incidence, and polarization) were studied, following two approaches:

- a global analysis of the ability of L- and C-band to discriminate (thanks to unsupervised classification algorithms) the polarimetric signatures of different land cover types, for crop map elaboration in an early stage of plant growth.

- the test of existing models of backscattering over agricultural surfaces and the appropriateness of surface descriptions.

Mono-Band and Multi-Band Classification

First, unsupervised mono-band mono-incidence classifications were performed on HH and HV SIR-C images. Cluster characteristics were determined using the fuzzy c-means algorithm and then images were classified according to the Maximum A Posterior criterion. The numbers of clusters were four for C-band classification and six for L-band classification. Then identification rates of the main cover land types were computed. For each of the four land cover types: forest, wheat, ploughed land and seedling, figure 4 shows the C-band and figure 5 shows the L-band identification rates versus incidence angle, and the classification algorithm used: supervised (called "svs") or unsupervised (called "nsvs"), blind (subscript "0") or MAP (subscript "1"). The main results are:

a- regularization step (MAP classification) reduces classification errors;
b- L-band performs better in soil cover type discrimination than C-band;
c- identification rates in C-band increase with incidence angle (between 44° and 57°);
d- ploughed land identification in L-band decreases with incidence angle.

Then, complementarity and redundancy between L- and C-bands were studied in a quantitative way. Figure 6 shows the redundancy rate (mutual information normalized by the image entropy) between L- and C-band unsupervised classification results, versus incidence angle. We found that redundancy increases when incidence angle increases between 44° and 57°. However at an incidence angle of 57°, redundancy between L- and C-band is only about 30%.

Recalling that, in C-band, land cover identification rates are not as good as in L-band, but increase with incidence angle, we may assume that the increase of redundancy between L- and C-band versus incidence angle is mainly due to the increase of "useful" information (which is probably due to increase of contrast or reduction of speckle noise) in C-band images.

FInally, data fusion between L- and C-band was performed to improve identification rates. The aim of data fusion is to use redundancy between images to reduce classification errors and to use complementarity to put in evidence new classes. The unsupervised multi-source classification algorithm used is based on Dempster-Shafer evidence theory. Figure 7 shows the identification rates obtained after data fusion, and improvement in identification of land cover types clearly appears.

The conclusion is that multi-band L and C can be successfully used to discriminate the different land cover types. Similar results were obtained with AIRSAR data for discrimination of the different culture types in Summer 1991.

Backscattering modeling and surface description

The main results are:

- There is a systematic azimuthal dependence of copolar radar cross sections (HH, VV) over the same field with the view angle towards the row direction in C- and X-bands, as well for smooth fields of peas eroded by rains and for rough ploughed fields. It is obtained by complementary view angles of targets with ERASME and SIR-C/X-SAR or

with fields of very similar roughness seen by SIR-C/X-SAR for smooth fields. The mean difference between perpendicular and parallel direction is about 2 dB, which is large compared to dielectric constant variations occurring between dry and moist soils (Figure 8). Points are from fields with incidence angles between 25 to 57°. In L-band the restricted number of cases prevents any conclusions.

- The complementary use of the ERASME scatterometer and SIR-C/X-SAR allows study in copolarization of the variation of radar cross sections with incidence angle. Over the 10 test fields, the surface roughness parameters are deduced from pin profiler data, parallel and perpendicular to rows and using the Shin and Kong's 1984 quasi periodic description of agricultural soils. Small spatial scale (clods) and large (rows) parameters are summed in Table 2 and localized in ks/kl space (k the wave number, s the r.m.s. h eights, l the length of correlation at small scale) on Figure 9. In L-band, all test fields are within IEM validity range. In C-band, only smooth ones (peas) are within. Most other ploughed fields are out of range. Field W3 is taken for eroded smooth soil, W2 for smooth ones, and C9 for ploughed ones, remaining within IEM limits.

Results of the comparison between IEM simulations and ERASME, SIR-C/X-SAR data are shown on Figures 10 and 11:

- There is in L-band a good agreement for smooth fields and a 5-dB gap underestimation by the model for the rough one.

- The agreement in C-band remains good for smooth fields between 25 to 40°. For larger incidence angles (40° to 57°), there is a systematic overestimation of the model. It is more pronounced in X-band where cross sections keep decreasing with incidence angle, even on the rougher C9 surface (-15 dB from 25° to 57°), as the model gives a flat response.

To explain these differences, they must be analyzed in two directions, the physical hypothesis of backscattering model, and also the adequacy of the surface used in them. For smooth ones, the surface remains a randomly quasi-sinusoidal surface, with a short range of spatial frequencies to describe it. For very rough soils, surfaces become discontinuous and other scattering models have to be considered, and soil-description parameters to be defined.

FUTURE PLANS

Unsupervised polarimetric SAR image classification

The following activities are proposed.

- A study of the complementarity of polarimetric components and comparison of classification results using different combinations of polarimetric information has begun. The aim is to provide a quantitative measurement of the increase of information provided by each polarimetric component (HH,HV,VV, amplitude and phase), versus land cover type.

- We aim at studying the influence of speckle filtering on classification results, and to derive a new speckle filter using unsupervised classification results, in an iterative way.

Surface Scattering Process

The following activities are proposed.

- Over rough surfaces, a PHD has begun in 1995 to define a new description of discontinuous surfaces and modeling in intensity in co- and cross-polarizations. This work gathers at CETP the remote sensing team of Dr. D. Vidal-Madjar and the team of Pr Lavergnat on Theoretical Electromagnetism. Various ground surfaces are studied and analyzed by geometrical image algorithms in collaboration with Dr. P. Boissard of NRA/Grignon (Institut National de Recherche Agronomique) and with Dr. M. Chapron of ENSEA (Ecole Nationale Superieure de l'Electronique et de ses Applications).

- The quantification of azimuthal dependence of cross sections with rows. Two approaches are foreseen. The first one by analysis of surface description with a larger frequency spectrum. The second one by analysis of different databases, obtained over "Pays de Caux" in 1995 with a large multiplicity of radar configurations and completed by the SIR-C/X-SAR Orgeval campaign. A polarimetric campaign over bare soils is forecasted in 1997 with the two scatterometers of CETP in the mentioned frame (EU proposal RESEDA in the south of France).

TABLE I: Classification of the Orgeval fields by soil cover and roughnesses

CLASS	FIELDS	DIRECTION TOWARDS ROWS FOR SIR-C/X-SAR
WHEAT	2,3,71,78	Perpendicular
	4,5,62	Parallel
	67,83,85,68	Between
ERODED SMOOTH BARE SOILS	10,12	Perpendicular
	40	Parallel
	23,18,31,42	Between
SMOOTH BARE SOILS	35	Perpendicular
	11,46	Parallel
	16,47,53	Between
PLOUGHED FIELDS	6, 8	Perpendicular
	1,9,7,49	Parallel

TABLE 2: Roughness parameters

Field	s	l	S	L	P	ks (L)	kl (L)	ks (C)	kl (C)	ks (X)	kl (X)
C1	2.66	6.1	0	0	0	0.70	1.6	2.95	6.77	5.28	12.1
W 2	0.70	5.97	0.97	34.69	99.58	0.18	1.57	0.78	6.63	1.40	11.9
W 3	0.55	12.68	0.73	143.38	197.31	0.14	3.33	0.61	14.08	1.09	25.2
W 4	0.92	2.51	0.83	42.37	104.56	0.24	0.66	1.02	2.79	1.82	4.8
L6	3.77	7.35	0.94	128.87	94.35	0.99	1.93	4.19	8.16	7.5	14.6
C7	2.49	8.1	1.73	147	45.2	0.65	2.12	2.76	8.99	4.94	16.9
P8	1.31	3.52	1.44	93.67	43.0	0.34	0.92	1.45	3.9	2.59	6.9
C9	0.97	8.07	1.63	115.26	40.22	0.25	2.12	1.07	8.96	1.91	16.2
P10	0.62	5.66	0.3	172.08	120.68	0.16	1.48	0.68	6.28	1.21	11.2

W:Wheat, C: Corn, P: Peas, L: Ploughed field

Echelle:1/31434

FIGURE 1

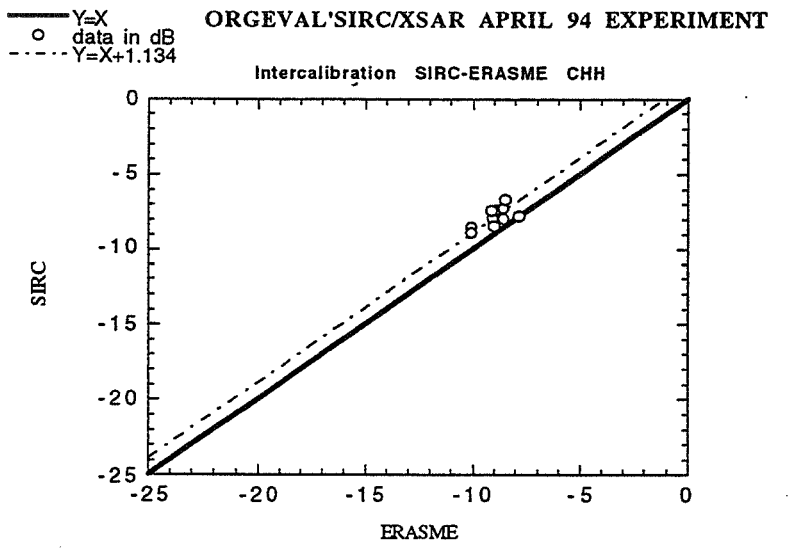

FIGURE 2-a

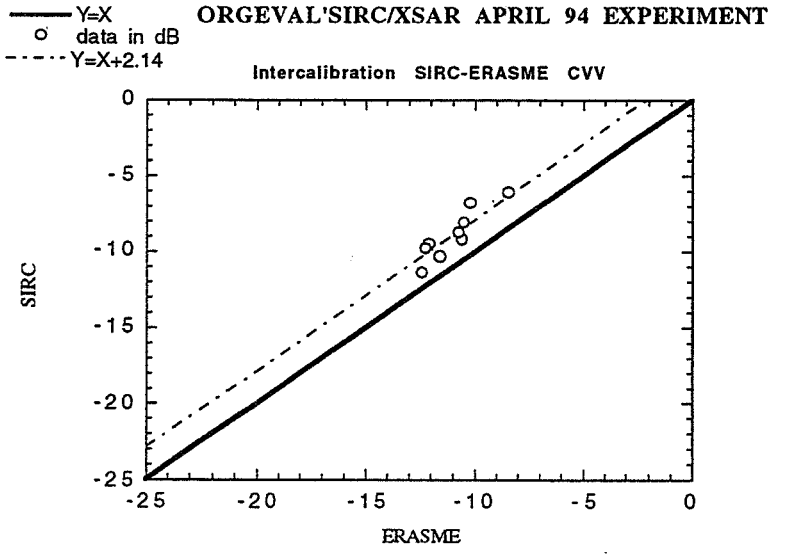

FIGURE 2-b

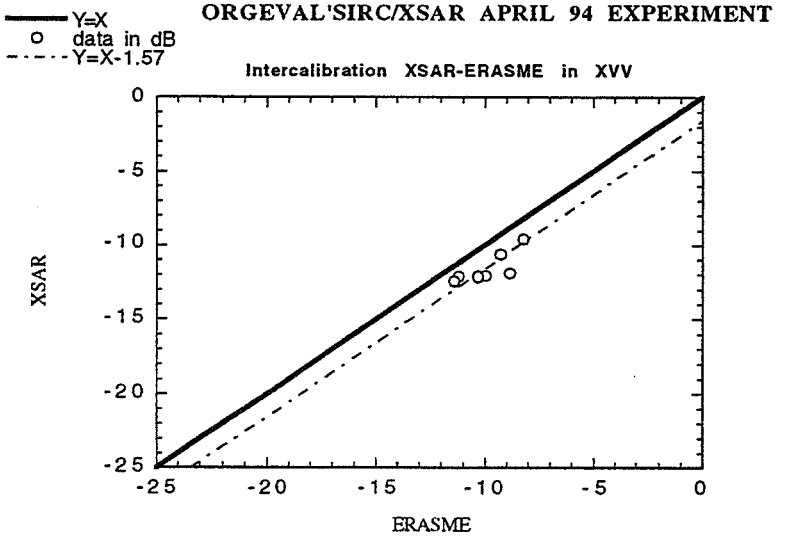

FIGURE 3

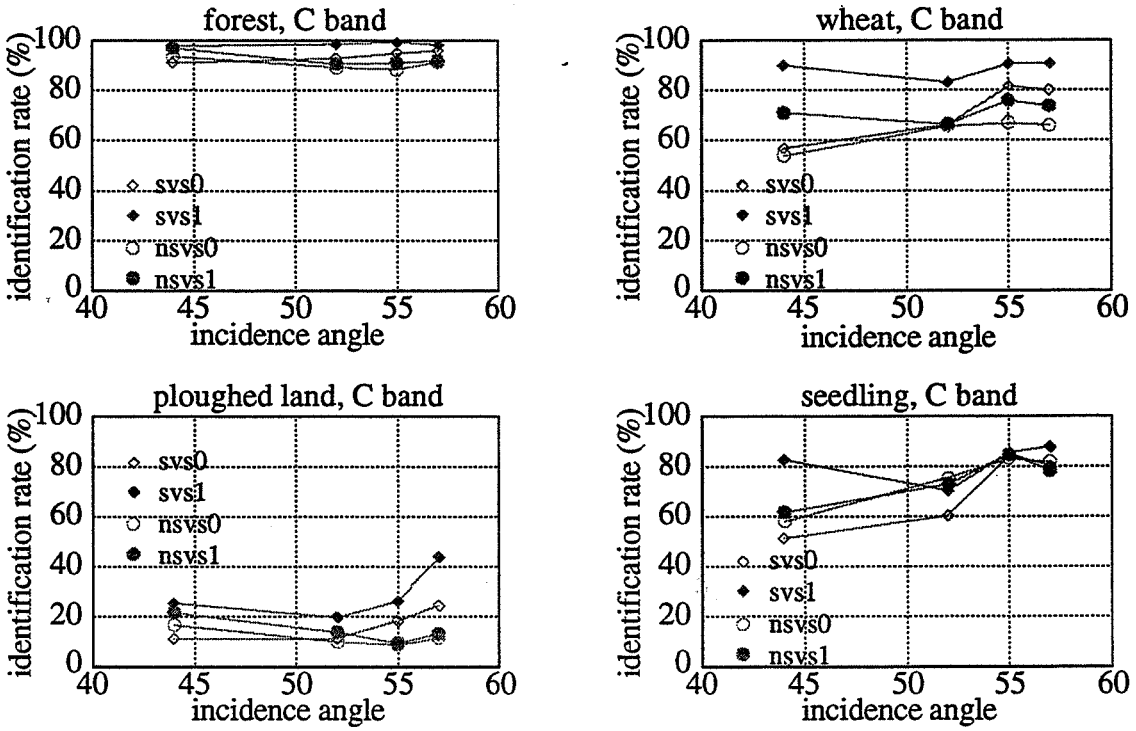

FIGURE 4

Identification rates of (a) forest, (b) wheat, (c) ploughed land, (d), seedling, versus incidence angle, provided by C band classification.

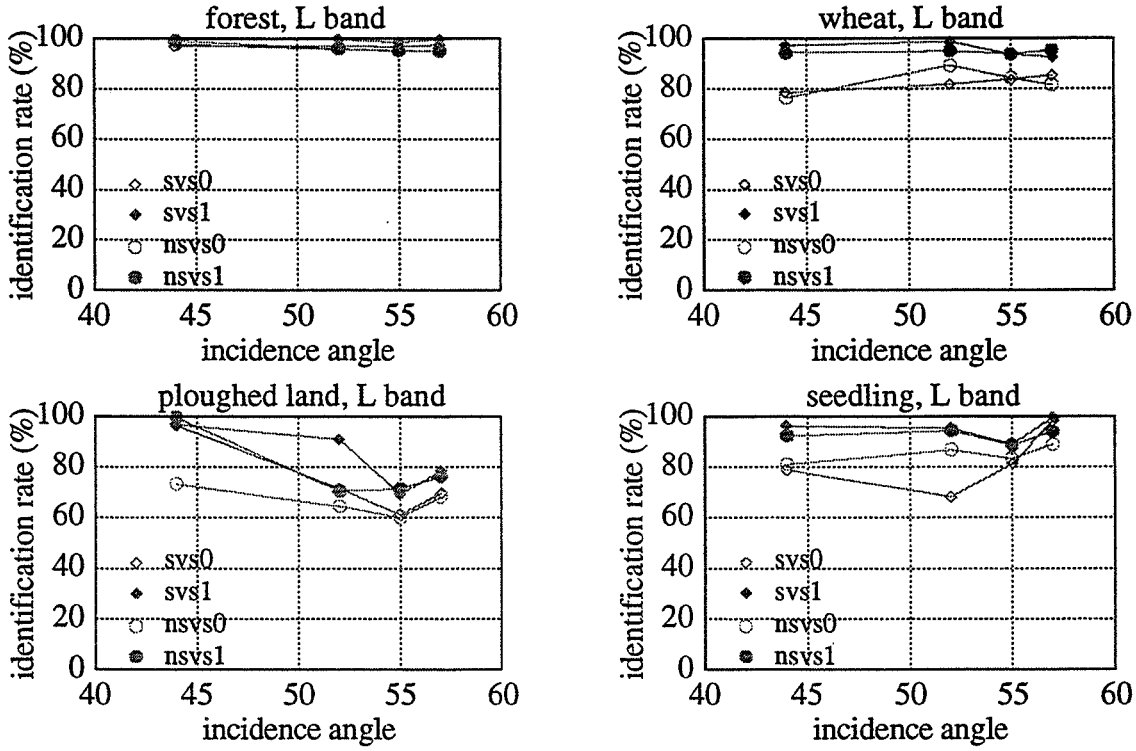

FIGURE 5

Identification rates of (a) forest, (b) wheat, (c) ploughed land, (d), seedling, versus incidence angle, provided by L band classification.

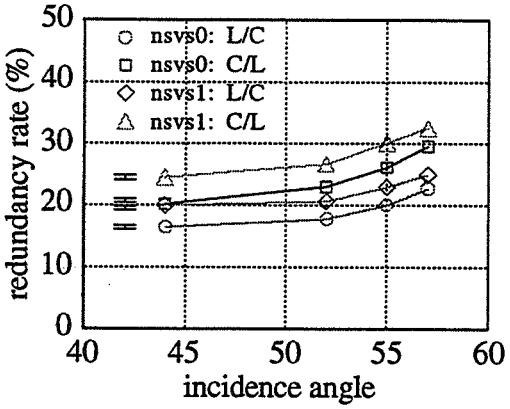

FIGURE 6

Redundancy rate between L and C band classification results vs incidence angle, case of unsupervised classification.

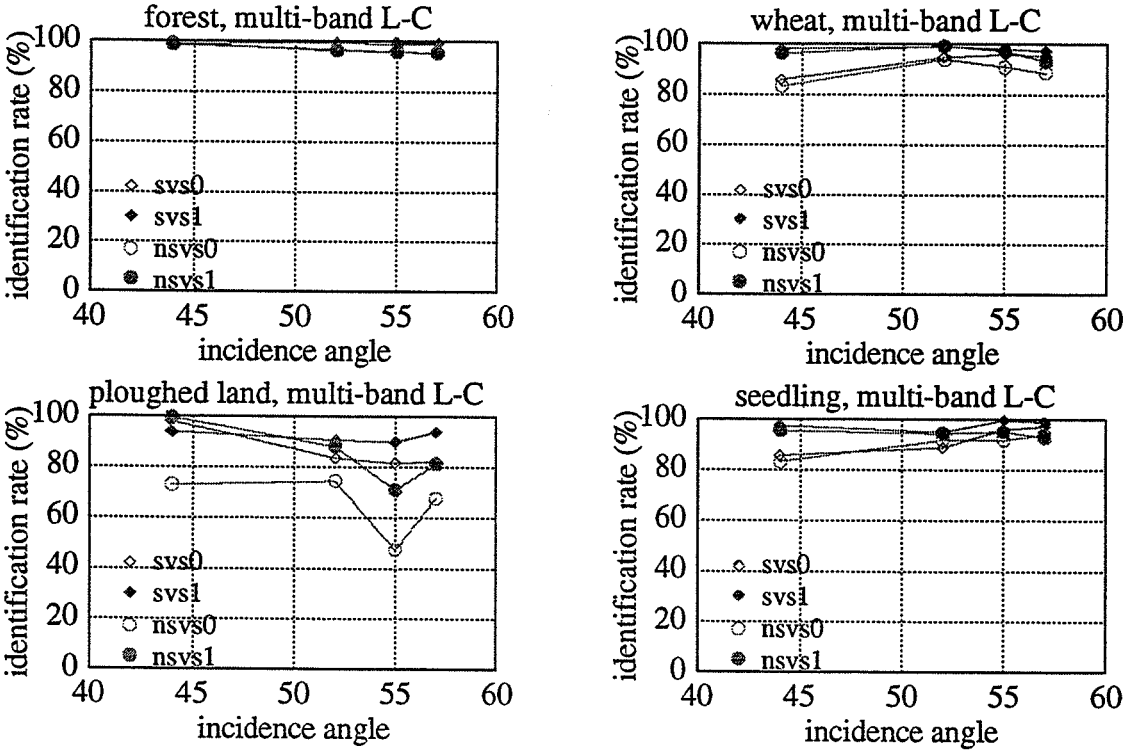

FIGURE 7

Identification rates of (a) forest, (b) wheat, (c) ploughed land, (d), seedling, versus incidence angle, provided by mulit-band L-C band classification.

ORGEVAL'SIRC/XSAR APRIL 94 EXPERIMENT

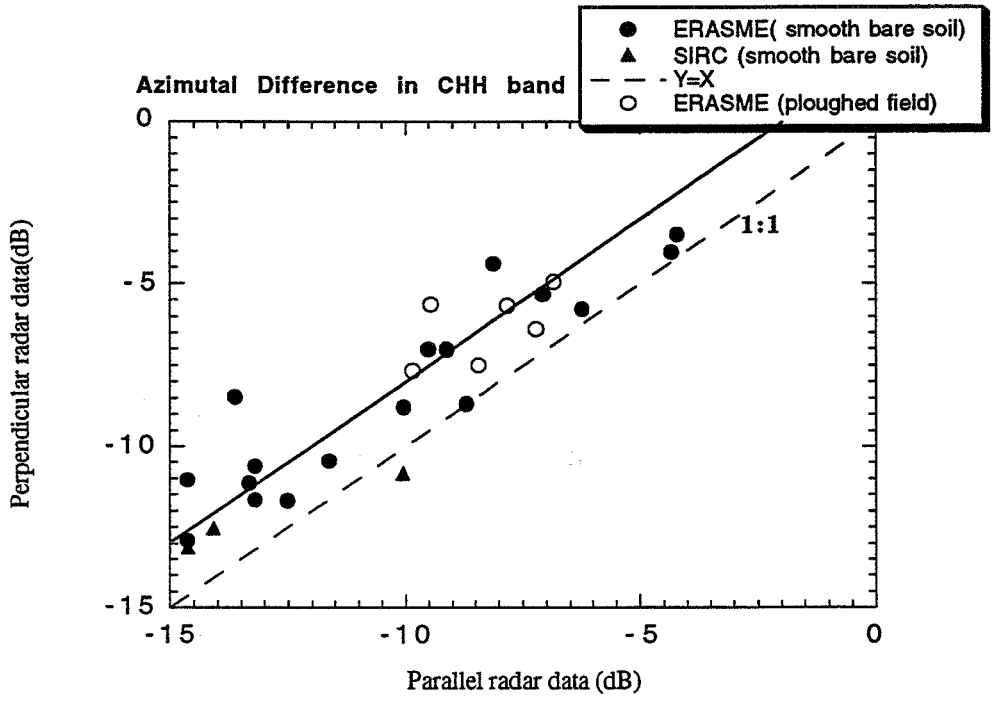

(a)

ORGEVAL'SIRC/XSAR APRIL 94 EXPERIMENT

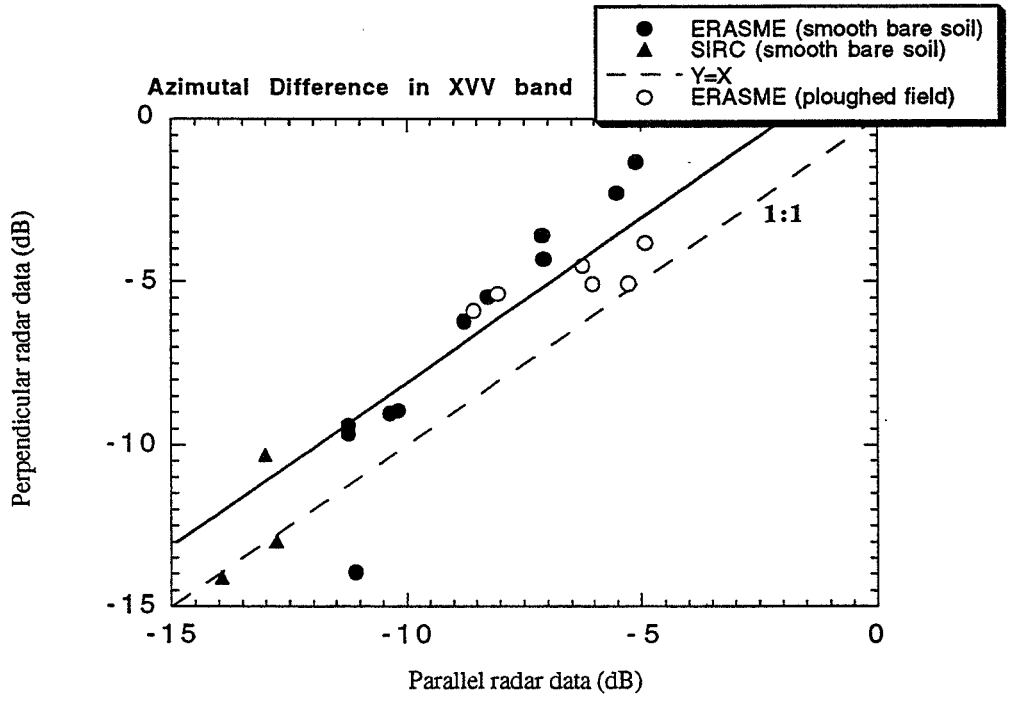

(b)

FIGURE 8

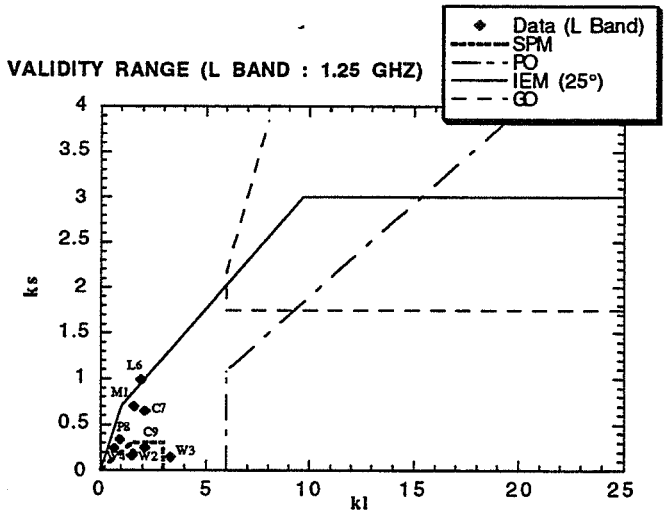
VALIDITY RANGE (L BAND : 1.25 GHZ)
Data (L Band)
SPM
PO
IEM (25°)
GO
ks
kl
L6
M1
C7
P8
C9
W4
W2
W3

(a)

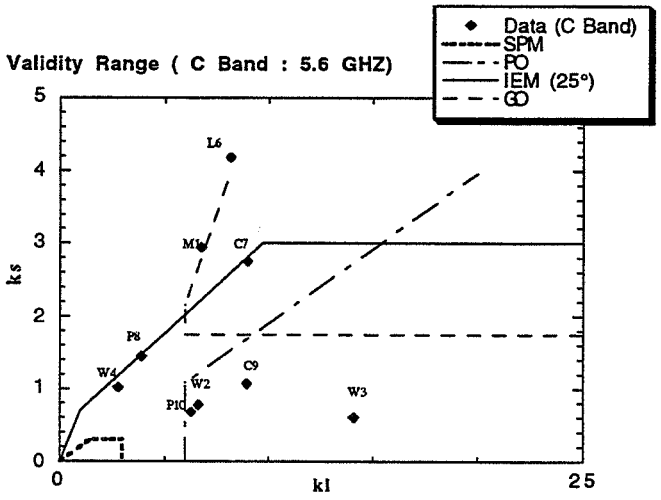
Validity Range (C Band : 5.6 GHZ)
Data (C Band)
SPM
PO
IEM (25°)
GO
ks
kl
L6
M1
C7
P8
W4
W2
C9
P10
W3

(b)

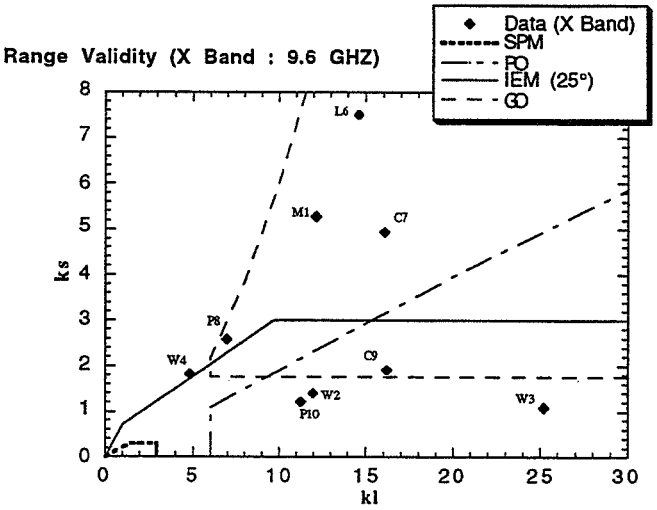
Range Validity (X Band : 9.6 GHZ)
Data (X Band)
SPM
PO
IEM (25°)
GO
ks
kl
L6
M1
C7
P8
W4
C9
W2
P10
W3

(c)

FIGURE 9

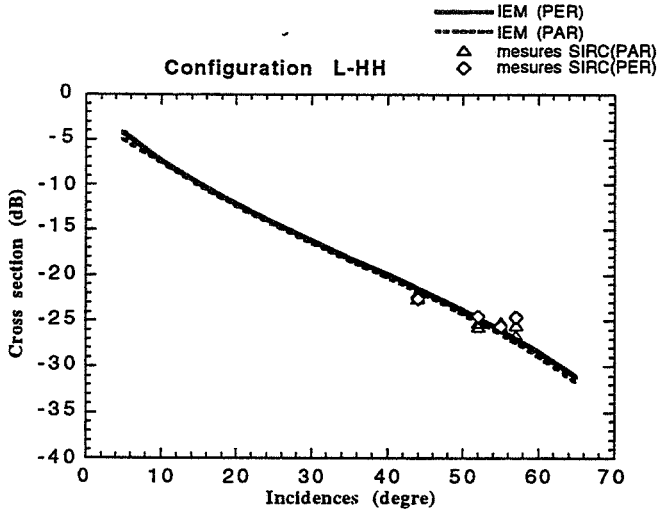

(a) very smooth soil

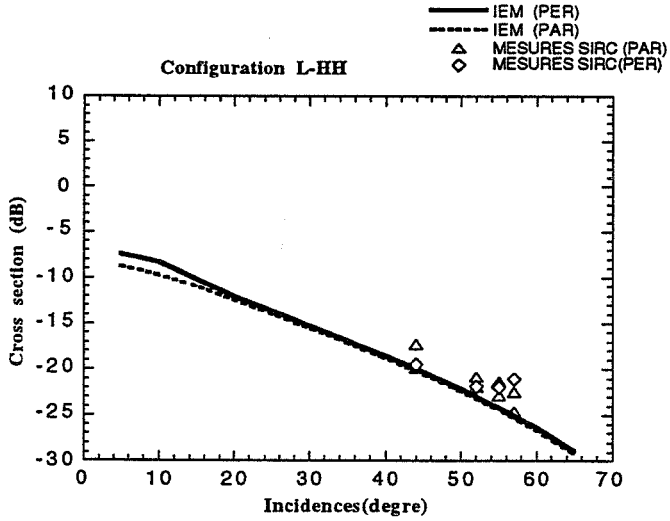

(b) smooth soils with clods

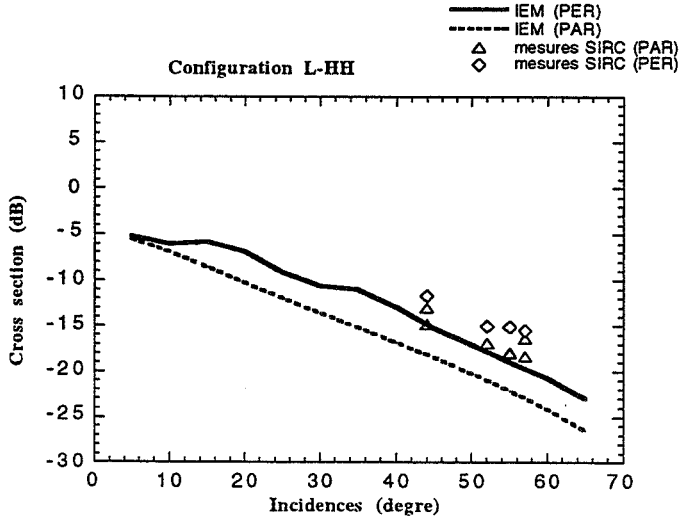

(c) ploughed field

FIGURE 10

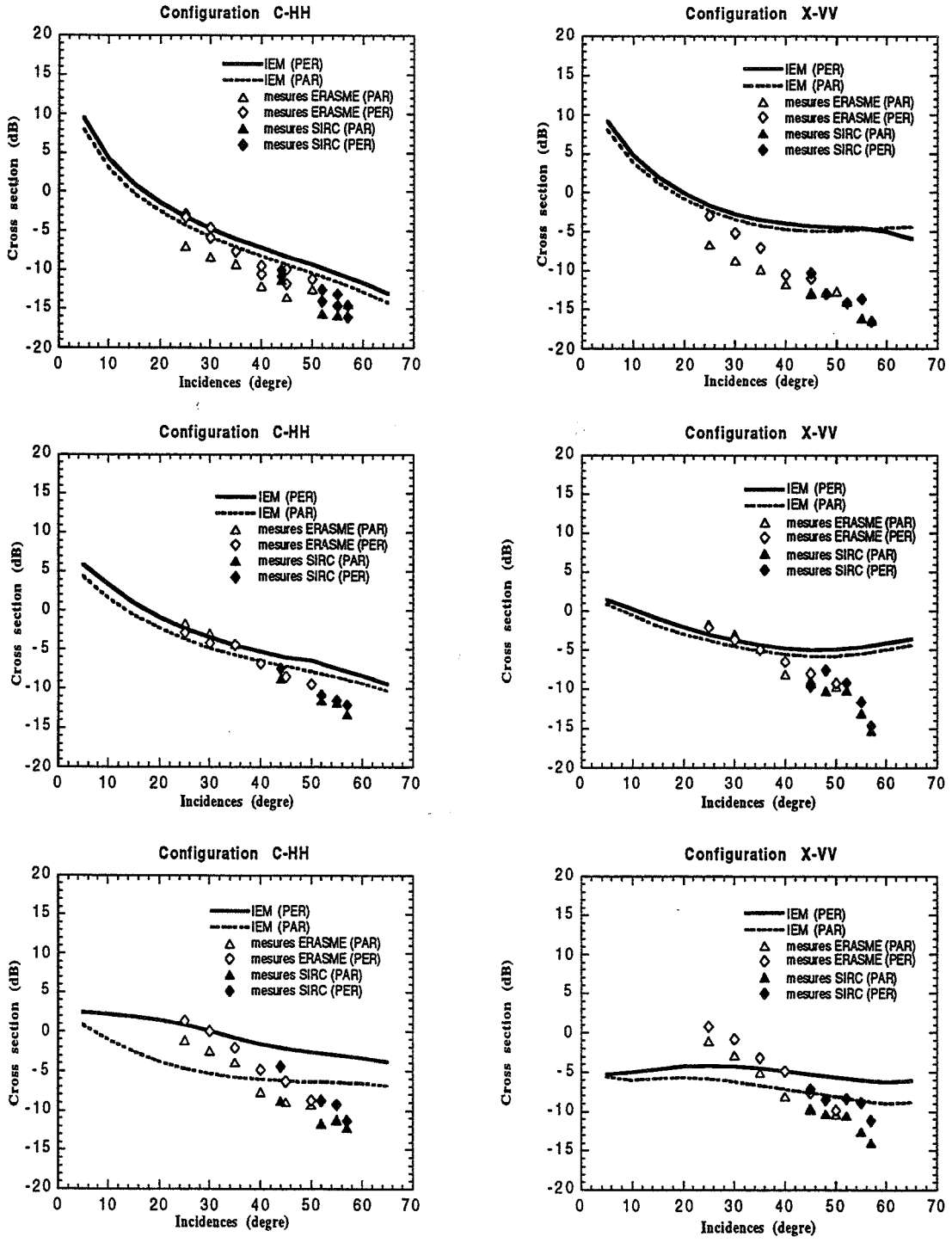

The first line figures are for very smooth soil, the second line ones for smooth surface with clods and the third line ones for ploughed field

FIGURE 11

PUBLICATIONS

1 TECHNICAL REPORT

[TR.1] EMBLANCH, C., Stage de DEA en Hydrologie, Premiers résultats de la campagne de Télédétection Radar Orgeval 94 pour la détermination de l'humidité de surface des sols, University Orsay-Paris XI, September 1994.

[TR.2] ZRIBI, M., Interpretation de l'imagerie radar polarimetrique pour l'hydrologie (Campagnes de la Nasa: Mac Europe'1991 et SIR-C/X-SAR'1994), Stage d'Ecole d'Ingénieurs, ENSICA-Toulouse, 22 June 1995.

2 CONGRESS COMMUNICATIONS

[AC.1] Mascle, S., D. Vidal-Madjar, M. Zribi, and O. Taconet, Comparison between L- and C- bands SIR-C polarimetric data versus incidence angle, *in Proceedings of International Symposium: "Retrieval of bio- and geophysical parameters from SAR data for land applications"*, in Toulouse, France, on October 10-13 1995.

[AC.2] Zribi, M., O. Taconet, D. Vidal-Madjar, S. Mascle, C. Loumagne and M. Normand, Backscattering response of bare soils with roughness from combination of SIR-C/X-SAR imagery and ERASME airborne scatterometer data (Orgeval'94 site), *PIERS96*, University of Innsbrück, Institute for Meteorology and Geophysics, Innsbrück, Austria, 8-12 July 1996.

[AC.3] Taconet, O., D. Vidal-Madjar, C. King, Y. Le Bissonnais, M. Zribi, S. Mascle, C. Loumagne and M. Normand, Soil backscattering behaviour with roughness from combination of SIR-C/X-SAR imagery and airborne scatterometer data (ERASME and RENE), *IGARSS'96*, Burnham Yates Conference Center, Lincoln, Nebraska, USA, 27-31 May 1996.

3 ARTICLE

[AR.1] Zribi, M., O. Taconet, D. Vidal-Madjar, S. Mascle, C.Loumagne and M.Normand, Backscattering response with direction angle relative with soil practices from combination of SIR-C/X-SAR imagery and ERASME airborne scatterometer data (Orgeval'94), in preparation for *Remote Sens. of Environment.*

Dr. James R. Wang
Laboratory for Oceans
Code 975
Goddard Space Flight Center
Greenbelt, MD 20771

SIR-C Measurements of Soil Moisture, Vegetation and Surface Roughness, and Their Hydrological Application

OBJECTIVES

Analysis of SIR-C/X-SAR response to soil moisture, vegetation and surface roughness and development of an algorithm to retrieve these parameters.

Combination of the visible and near-infrared data and the SIR-C/X-SAR data to improve the range and accuracy of vegetation classification.

Testing of theoretical models for microwave propagation with SIR-C/X-SAR and microwave radiometric measurements over rough surfaces.

Evaluation of a water balance model using SIR-C/X-SAR derived soil moisture values and other ancillary data.

PROGRESS

Data Acquisition and Analysis

Our test site is at the Little Washita watershed near Chickasha, Oklahoma, about 60 km southwest of Oklahoma City, Oklahoma. During the first mission, a total of eleven passes over the test site were made between April 11-17, 1994. In the second mission, only nine passes over the test site were made between October 2-7, 1994, because the SIR-C operation was switched to the interferometry mode in the last three days of the mission. All the data acquired from the first mission have been processed by JPL, and delivered to us for analysis. There are a total of 11 passes, 5 ascending and 6 descending passes. One of the passes was acquired in the wrong mode, and four others belong to passes with high incidence angles of 50 degrees, which are not optimal for soil moisture estimation. Data from the remaining six passes with incidence angles between 28-50 degrees have been used for studying the temporal variations of soil moisture in the watershed. We have also begun to receive the processed data from the second mission in October 1994. The X-SAR data from the first mission were also requested and we have received most of them. These data will help classify vegetation cover and improve soil moisture estimation from SIR-C L-band data.

During both missions, ground truth data of soil moisture and surface roughness were collected for a number of selected fields in the watershed. All the soil samples have been processed and ready for SIR-C/X-SAR data analysis. Survey of the vegetation cover was also made on about 70% of the entire test site - this information could be combined with the SPOT image to validate classification of vegetation from SIR-C/X-SAR data. In addition, there were 43 rain gauges distributed quite uniformly over the entire watershed roughly about 20 km by 40 km in area, which might be useful for comparing with the soil moisture distribution estimated from the SIR-C data.

We emphasize analysis of the data acquired from the first mission, because there was a moderate rainfall of about 2 cm over the entire watershed at the beginning of the mission on April 10-11 and no rain throughout the rest of the mission. The scenario provides a chance to look at the SIR-C response to the drying-down at the watershed. During the second mission there was no significant rainfall in the test area, and most of the region was dry to begin with; so we do not expect to see the change in the SIR-C signatures due to soil moisture.

Retrieval Algorithms

Most of previous studies on radar measurements of soil moisture dealt with the forward problem, i.e., the examination of correlation between radar backscattter and soil moisture. Only in recent years were there attempts to invert the measured radar parameters to soil moisture. Currently, there are three different algorithms reported in the literature for inversion of L-band SAR measurements to surface soil moisture, all of them dealing with bare soils with surface roughness and soil moisture as retrieved parameters. The first of them is developed by the University of Michigan group (Oh et al., 1992) based on the ground-based scatterometer measurements over bare fields with different surface roughness. The algorithm makes use of the ratios of measured backscattering coefficients σ° vv, σ° hh, and σ° hv at L-band to estimate both soil moisture and surface roughness. The second algorithm is also empirical and developed by Pascale et al. (1995). It is based on the same scatterometer data set acquired by Oh et at. (1992) and uses only the measured σ° vv, and σ° hh at L-band for the estimation of soil moisture and surface roughness. The third algorithm, developed by Shi et al. (1995), is based on a theoretical model for radar backscattering from bare soils. It can select any pair of quad-polarization measurements from AIRSAR or SIR-C measurements at L-band and make estimation of soil moisture and surface roughness. All three algorithms have been tested with the SIR-C data and the results are summarized in the next section.

SIGNIFICANT RESULTS

When the algorithm of Oh et al. was applied to the SIR-C L-band data for estimation of soil moisture and surface roughness, difficulty arose because of the incomparability between the measured ratios σ° hh/σ° vv and σ° hv/σ° vv. This is due to the fact that the SIR-C measured s∞hv values are generally about 3-4 db higher than those measured by the University of Michigan ground-based scatterometer system. As a consequence, only a few percent of SIR-C pixels fall in the category that the algorithm could provide a normal solution. This difficulty is not shared by the other two algorithms. These results have been reported recently (Wang et al., 1995). In general, the soil moisture distribution estimated from either Dubois et al.'s (1994) or Shi et al.'s algorithm over the period of April 11-17 shows a drying down sequence as expected. A comparison between the estimated soil moisture values and those concurrently measured on the ground, however, shows that the algorithm of Shi et al. gives very good estimation of soil moisture only for bare soils, while the algorithm of Dubois et al. appears to be applicable to fields with short vegetation cover as well. The main reason for this difference is most likely due to the fact that the algorithm of Dubois et al. deals strictly with σ°'s, while the algorithm of Shi et al. makes use of the phase information too; the contribution from vegetation may have overshadowed that from soil moisture.

When applying both algorithms of Dubois et al. and Shi et al. to the SIR-C L-band data for soil moisture estimation, it was found that a substantial number of pixels could not have a normal solution, and this number appeared to be higher on drier days. These pixels are typically characterized by σ° vv$\leq$ σ° hh. To avoid this from happening some averaging procedure would

have to be applied to the data and the spatial resolution of the SIR-C measurements would suffer as a result. We are in the process of writing up an article for journal publication. The article will present the first SIR-C results of soil moisture estimation over the Little Washita Watershed and discuss the problems associated with the retrieval algorithms.

FUTURE PLANS

We will attempt to perform a classification of vegetation cover, using the SIR-C/X-SAR data, for the Little Washita Watershed. This step is needed for soil moisture work, because more than 80% of the watershed is covered with vegetation. In addition, the problem encountered in the estimation of soil moisture discussed above could also be associated with the presence of vegetation. For fields covered with vegetation or wooded areas, σ° vv values could be close to or even smaller than those of σ° hh.

We will modify the currently available algorithms for estimation of soil moisture over vegetated areas. Most likely, this will be done empirically because the theoretical models for different vegetation types are too complicated and may not be practical for our main objective. We hope to come up with a soil moisture map to cover more than 80% of the watershed.

PUBLICATIONS

Shi, J. C., J. Wang, A. Hsu, P. O'Neill, and E. T. Engman, "Estimation of soil moisture and surface roughness parameters using L-band SAR measurements," *IGARSS '95*, Vol. I, 507-509, 1995.

Wang, J., P. O'Neill, E. Engman, R. Pardipuram, J. Shi, and A. Hsu, "Estimating surface soil moisture from SIR-C measurements over the Little Washita Watershed," *IGARSS '95*, Vol. III, 1982-1984, 1995.

References Cited

Dubois, P. C., J. Van Zyl, and E. T. Engman, "measuring soil moisture with imaging radars," submitted to *IEEE Trans. Geosci. Remote Sens.*, 1994.

Oh, Y., K. Sarabandi, and F. T. Ulaby, "An empirical model and inversion technique for radar scattering from bare soil surface," *IEEE Trans. Geosci. Remote Sens.*, 30(2), 370-381, 1992.

Drs. Rudolf Winter*, Manfred Keil
DLR Oberpfaffenhofen,
DFD, D-82230 Wessling
Germany

Co-Investigators:
U. Ammer, B. Foerster, A. Haas, Univ. of Munich, Institute of Landscape Planning and Nature Conservation
W. Kuehbauch, M. Davidson, Univ. of Bonn, Institut fuer Pflanzenbau
W. Mauser, M. Rombach, Univ. of Munich, Inst. f. Geography
B. Koch, Univ. of Freiburg, Abt. Luftbildmessung und Fernerkundung
Dr. S. Mohan, RSA, Ahmedabad, Gujarat, India

* now: JRC Ispra/Varese, Italy

Information Extraction from Shuttle Radar Images for Forest and Agricultural Applications

OBJECTIVES

The experiment will attempt to extract suitable polarimetric information for objectives of forest mapping and vegetation monitoring as well as for agricultural purposes.

In forest areas in Bavaria (e.g., near the Oberpfaffenhofen supersite and in the Bavarian Forest) and in the Harz Mountains, shuttle data are to be evaluated for different forest formations, age classes and other forest parameters and for the forest situation, e.g., concerning storm damages.

In the rainforest study areas in Brazil, especially in the states of Acre and Rondonia, SIR-C and X-SAR data are to be analyzed for differentiation of land cover classes like primary rainforest, initial and intermediate regrowth, clean pastures and overgrown pastures. By comparison of April and October data, information is to be gained on the dynamics of deforestation by clearing and burning and on other land use changes.

In the supersite Oberpfaffenhofen, the potential for crop classification is to be investigated, in comparison to other test sites like Montespertoli and Matera. The effect on polarimetric backscatter responses is to be studied in relation to biomass and biophysical parameters of vegetation, especially for agricultural purposes. The assessment of soil moisture conditions is another aspect under study in the Oberpfaffenhofen/Weilheim area and in a test site in Gujarat/India.

PROGRESS

Forest investigations in the test site Oberpfaffenhofen

Four data takes of April and October 94 have been investigated for the multipolarimetric and multifrequency information content of different land use classes, especially for forest areas and storm damage areas near the lake "Ammersee" and a region NE of Oberpfaffenhofen. Signature analysis of different polarization states has been performed in preparation of land use classification. In the region West of Ammersee a land cover classification has been performed using combined SIR-C/X-SAR data.

The X-SAR data takes have been studied for time variation effects, e.g., for different moisture conditions during the first and the second mission. Also interferometric datasets have been studied from the October mission.

Forest investigations in the test sites of Harz Mountains and Bavarian Forest

First investigations have been performed on the SIR-C/X-SAR data in the mountainous terrain of the Harz Mountains and the Bavarian Forest. Both forest areas are partly severely affected by forest damages, e.g., by storm damages and bark beetle calamities. In order to be able to combine the data with geocoded reference data, e.g., in a GIS environment, geocoded terrain corrected SIR-C data are necessary (besides available GTC products of the X-SAR component) in these areas of high relief. Terrain corrected multiband/ multiseasonal data are planned to be available in May/June 1996, within an initiative of DLR and DARA.

Investigations for rainforest monitoring in Acre and Rondonia, Brazil

In the area of Sena Madureira and Rio Branco in the state of Acre, Brazil, two SIR-C/X-SAR data takes of April 1994 and one of October have been studied for rainforest monitoring tasks, in cooperation with the National Brasilian Space Research Institute. Objectives are the differentiation within the rainforest and within the deforested areas (different states of pasture land and regeneration areas). By comparing X-SAR datasets of the April and the October mission, the dynamics in deforestation have been shown in an area NW of Rio Branco. Based on the field work in June/July 1994, analysis of backscatter responses in L-, C- and X-Band have been performed for forest, pasture and regrowth areas. In a region of 40 km by 40 km NW of Rio Branco, a landcover classification has been performed using the textural classifier EBIS, mainly based on different polarizations of L-Band data.

In the state of Rondonia, a region near the town Ji Parana has been investigated by several SIR-C / X-SAR datasets of April and October 1994. These datasets have been registered within the Amazon calibration experiment and as part of the "Pantanal" data take. In November 1995, a first ground campaign has been performed in cooperation with INPE and other Brasilian institutions. Different states of land use are under study, showing different land use intensities as well as different degradation and regeneration states.

Investigation of agricultural areas in the study sites of Oberpfaffenhofen, Montespertoli and Matera

In the Oberpfaffenhofen supersite, investigations for early crop identification have been performed by sets of April data, based on ground truth assessment during the overflights. Methodological studies show the different information content of different polarization/ band combinations. On a field-based approach (field limits coming from other sources), crop classifications have been performed by methods of polarimetric contrast and maximum likelihood classification.

The potential for the assessment of different growth states of winter wheat is under study by comparing the backscatter responses of winter wheat in the different climatic regions of Oberpfaffenhofen, Montespertoli and Matera.

In the test site Weilheim, Southwest of Oberpfaffenhofen, parallel registered airborne E-SAR data are investigated in comparison to SIR-C/X-SAR data. In this area, the study of soil moisture conditions is the main objective.

Investigation of soil moisture and vegetation cover in Gujarat/India

By the Indian Co-Investigator, several SIR-C and X-SAR datasets, mainly from April 1994, are under study for soil moisture and vegetation cover in a region of Gujarat in India.

SIGNIFICANT PRESENT RESULTS

Forest investigations in the test site Oberpfaffenhofen

In the forest area West of the lake Ammersee, ten landcover classes including five forest types could be classified with an overall classification accuracy of about 63 %, in an area which has a quite inhomogeneous distribution of land cover. Storm damaged areas could be separated by about 70% accuracy, the forest / nonforest separation accuracy is around 95 %. C-Band HV polarization seems to be important for structure identification between deciduous and coniferous forest. L-Band HV has a high correlation to natural forest age classes and biomass. Interesting is the result of using a three-date multitemporal complex X-SAR data set of the October mission. By an interferometric processing, the interferometric coherence of a one-day repeat cycle can be successfully be used to improve the classification of five main land cover classes, in addition to the three-date multitemporal X-SAR data set.

Investigations for rainforest monitoring in Acre and Rondonia, Brazil

Investigations of different polarimetric states of L- and C-band showed a better forest / non-forest separation in the L-band data, especially in the regeneration states. L-band HH-Polarization allowed the separation of alluvial rainforest areas along rivers. Integration of C-band and X-band data delivered a better differentiation of pasture land. For land use classification, the EBIS texture tool was successful which allows the integration of texture parameters for classification besides the evaluation of local histograms.

Investigation of agricultural areas in the study sites of Oberpfaffenhofen

Astonishing positive results have been reached in the Oberpfaffenhofen test site for early crop identification, using a five-band combination of all three frequencies. L-HV has proven to be an important layer also for this mapping, based on field-wise classification.

FUTURE PLANS

Forest Monitoring Investigations in the Harz Mountains and in the Bavarian Forest are planned to be performed, based on terrain-corrected, combined SIR-C/X-SAR products from the April and October missions. Storm damages and insect calamities are a heavy problem in those areas, e.g., the bark beetle damages in the area of the Bavarian Forest National Park.

Rainforest and Deforestation Monitoring Investigations will be continued, the results of the study sites of Acre (Sena Madureira) and Rondonia (Pantanal data takes) are to be compared with results from other projects in the Manaus test site. Different approaches are planned to get information for biomass estimates especially for forest regrowth, in cooperation with INPE, Brazil.

Investigations for crop identification will be continued, including October data takes.

PUBLICATIONS

Davidson, M. W., R. Steingiesser, W. Kuehbauch: Exploiting multifrequency multi-polarization radar images for mapping crop types early during the growing season, Int. Symposium "Retrieval of bio- and geophysical parameters from SAR data for land applications," Toulouse, Oct. 10-14, 1995, in press.

Davidson, M. W., R. Steingiesser, W. Kuehbauch: Assessing Agricultural Land Use early During the Growing Season Using Multi-frequency and Multi-Polarisation SIR-C Backscatter Features, EUSAR '96, Koenigswinter, Germany, 1996, in press.

Dos Santos, J. R., M. Keil, H. Kux, M. S. P. Lacruz, D. Scales: Interactive Analysis of polarimetric SIR-C and Landsat TM data for the spectral-textural characterization of the land cover in SW Amazon, Brazil. Paper for presentation at ISPRSS '96 conference, July 1996, Vienna/Austria, planned.

Haas, A., B. Foerster, U. Ammer, The suitability of multifrequency, multipolarimetric and multitemporal radar data for forest monitoring, *IGARSS '96*, May 1996, Nebraska, planned.

Keil, M., D. Scales, R. Winter: Investigation of Forest Areas in Germany and Brazil using SAR Data of the SIR-C/X-SAR and other SAR Missions, *IGARSS '95*, 10-14 July 1995, Vol. II, p. 997 - 999, Florence.

Keil, M., M. Schmidt, D. Scales, H. Kux, J. R. dos Santos: Investigation of polarimetric SIR-C / X-SAR data for characterization of land cover in Acre and Rondonia, Southwest Amazon, Brazil.

Paper for presentation at PIERS-96 Conference, July 1996, Innsbruck/Austria, planned.

Stolz, R., W. Mauser: First Evaluations of Shuttle SIR-C and X-SAR Data for Landcover Classification. *IGARSS '95*, 10-14 July 1995, Vol. II, p. 1058-1060, Florence.

Dr. Charles A. Wood
Space Studies
University of South Dakota
Fargo, ND

Co-Investigators:
Anthony England — Univ. of Michigan
Minard Hall — Escuela Pol. Nacl., Ecuador
Stanley Williams — Arizona State University

SIR-C Radar Investigations of Volcanism and Tectonism of the Northern Andes

OBJECTIVES

Increase understanding of the volcano-tectonic history of the Northern Andes of Colombia and Ecuador by testing and extending the volcano-tectonic segmentation model proposed by Hall and Wood (1985).

Develop radar models for detecting and mapping pyroclastic and mudflow deposits at Ruiz and other dangerous volcanoes of the Northern Andes.

SIR-C Radar Investigations of Volcanism and Tectonism of the Northern Andes was selected for participation in the SIR-C mission in 1988. We proposed a series of inter-related multi-disciplinary investigations to generate new information to (a) characterize radar roughness, (b) determine the relation of volcanism and tectonism in a poorly known volcanic arc, and (c) study hazards related to Ruiz volcano, Colombia and other potentially active volcanoes of the Northern Andes. Significant progress was made on each of these tasks, and the eventual arrival of actual SIR-C data has accelerated our research efforts, with the first results now being presented at national meetings.

PROGRESS

Discoveries came within minutes of examining the first SIR-C images provided to the team. Examination of the first browse image of DT-80.10 from SRL-1 resulted in the recognition of a very young volcano that was unknown to the international volcanological community. Within minutes, two older possible calderas were found in other parts of the first swath. These discoveries resulted in NASA JPL issuing a press release image and caption of San Diego volcano in northern Colombia, and these first results also were presented at the Geologic Society of America meeting in Seattle in fall, 1994 (Wood et al, 1994). Now that the easy results have been announced, the hard work of detailed analysis and interpretation is well underway.

Our team includes the PI and Co-Is listed above and the students we are working with. We are very proud that SIR-C funding has partially supported a number of graduate students, one of whom is now a post-doctoral fellow (Austin); two more are completing (Wessels) and starting (Gorman) PhD theses based on SIR-C data; and two others are undertaking masters degree projects (Borysewicz and K. Williams).

Radar Roughness Studies

Theoretical and experimental study to improve modeling of the mechanisms of radar scattering have been completed; application to SIR-C data is just beginning. Field measurements of the roughness spectrum at radar wavelength scales of millimeters to meters were obtained at Mt. St. Helens using normal surveying and a specially-designed computer-controlled 2-D laser profilometer (Austin and England, 1993). Specific conclusions include:

The surface profile measurements at Mt. St. Helens and the resulting spectral estimates show that some, but not all, volcanic debris flow terrains have a power-law roughness spectrum over some

range of spatial frequencies. Low and high-frequency spectral estimates from the primary debris flow surfaces seemed to conform to a single power law from about 0.05 to 25 or 50 m-1. It is expected that the intermediate-frequency region (roughly 0.25 to 2 m-1) follows the same power law, but this cannot be verified without additional surface profiles with a sampling interval in the 12.5-cm range. The flow surfaces that did not exhibit a power-law spectrum appeared to be part of a fluvial plain; i.e. they were not volcanic.

The one- and two-dimensional power-law fits to the spectral estimates derived from the volcanic debris flow profiles yield spectral slopes between -2.31 and -2.51, corresponding to surface fractal dimensions of 2.245 and 2.345. Fractal dimensions near 2.2 were cited by Mandelbrot and others as producing naturally realistic profiles. We found that spectra with slopes less than -2.0 could not have been measured using spectral estimators like the periodogram that are sensitive to low-frequency, spectral leakage. The leakage problem may be responsible for the fixed values of -2.0 reported in the literature.

Three power-law surfaces were manufactured in a plastic dielectric to have fractal dimensions of 2.100, 2.228, and 2.355. The polarized radar backscatter cross-sections were measured as a function of incidence angle for the three surfaces. In all cases, the scattering cross-sections decrease with incidence angle. Greatest sensitivity to spectral slope occurred for like-polarized cross-sections between 40 and 50 degrees and for cross-polarized cross-sections between 45 and 50 degrees.

None of the current theoretical models did a great job of explaining the backscatter observations. We explored a new theory, the Phased Wiener-Hermite model, but it was no better than average among the models. The best of the current theories was the Small Perturbation (SP) model. The shape of the responses were correct though absolute amplitudes were often offset by as much as 5 dB.

A major purpose of developing the new theoretical and field understanding of radar roughness is to apply it to SIR-C data of volcanic regions in the Andes. During the summer of 1995 we began to develop a roughness classification scheme for full-resolution, SIR-C radar images of the Colombian Ruiz volcano. Our candidate algorithms were based upon combinations of SP theory and our experimental observations. The early versions appear to have worked in some areas, but not others. We are now investigating those cases where they failed.

We expect the final classifier to be an empirical algorithm guided by SP theory and our experiments. Dr. Richard Austin, who is now a post-doctoral scientist in Australia, is guiding the development of the algorithm through e-mail. A senior-level engineering student spends a few hours per week testing algorithms on the SIR-C data. We expect to have a best estimate of a classifier by early 1996 and to have produced a report by May 1996. The classified image will then be provided to the volcanologist members of the team for geologic interpretation.

Volcanic Geology and Tectonics Study: Stan Williams, Rick Wessels and Caitlin Gorman

The Arizona component of our SIR-C team is focusing on studies of the tectonic controls of volcanism and the detailed mapping of hazardous volcanoes. Their main geographic area of interest is Colombia. Their initial interpretation of regional tectonics of Northern Andes using SRL-1 SIR-C survey data began in July of 1994, and since March 1995 new work has started on the full resolution data sets of specific areas.

A major accomplishment by Wessels has been the assembly of a geo-referenced on-line mosaic of twenty survey images over the active volcanic arc (covering 900 x 130 km). This giant mosaic provides the absolutely best data set for regional volcano-tectonic investigations of the Northern Andes. We are investigating how such a mammoth photo image might be published. This is a case

where looking at a compressed version or a series of individual sections on a computer monitor is vastly inferior to having the entire nearly 3 meter long hard copy rolled out on a table!

Wessels has also compiled a mosaic of three high-resolution subscenes from two data takes (computer processed, geo-referenced and mosaicked) for structure/geomorphology interpretation. More scenes will be added to expand the mosaic and the analysis. Both the large survey mosaic and the high resolution one are base layers for geographic information system (GIS) studies to aid regional interpretations. Additional layers include structural field data, seismicity, published faults, geochemistry, geochronology and eruptive activity. Experiments are starting to merge SIR-C data with Landsat TM, scanned shuttle photographs and AIRSAR/TOPSAR data for detailed analyses. Early results from this work will be presented at the fall 1995 American Geophysical Union meeting by Wessels. The SIR-C images are being used for geologic field research by Caitlin Gorman and Wessels.

Wessels will use subscenes of MLC products to document variations in active volcano morphology related to regional fault geometry. The data will be used to precisely measure orientations, areas, and vent locations. MLC data will also be used to better define previously unrecognized or poorly known volcanoes related to the faults. Wessels will also combine the regional information with individual volcano DEM data from the 1993 AIRSAR/TOPSAR flights. The SIR-C and X-SAR data received so far is very good. X-SAR scenes will be requested of Galeras and Cumbal volcanoes to combine with our 96.10 SIR-C data. Full resolution SIR-C/X-SAR data will also be requested for areas south of the Ruiz-Tolima scene to carefully examine poorly known volcanoes along the Palistina Fault.

Wessels and collaborators plan several possible papers which will comprise part of his dissertation:

The interaction of transcurrent tectonics and continental arc volcanism in Colombia and Ecuador. Overview for submission to Geology Summer 1996. Modeling the role of active faults in volcanic activity of southern Colombia. JGR Sum-Fall 1996 (possibly with Dr. Ramon Arrowsmith). Volcano-tectonic interactions from Ruiz to Galeras using high resolution SIR-C data (with Dario Mosqera). SIR-C and TOPSAR analysis of the geology and volcanic hazards of Volcan Cumbal (with Caitlin Gorman).

Volcanic Geology and Tectonics Study: Chuck Wood, Pete Hall, Henry Borysewicz and Kymbra Williams

To gain experience in working with radar we acquired a Russian Almaz radar image of part of the Northern Andes. The image was disappointing in resolution and signal to noise. We also were fortunate in acquiring significant AIRSAR images of Colombian volcanoes during a NASA flight to South America. Those images are being analyzed in association with SIR-C data.

In preparation for analyzing SIR-C data, Hall continued field studies of Ecuadorian volcanoes, providing a grounded framework for interpreting the future satellite images. This work has culminated in major studies of the Plio-Quaternary volcanism in Ecuador (Hall and Beate, 1991) and the tephrochronology of Holocene volcanoes in Ecuador (Hall and Mothes, 1994a). Hall has also coordinated the monitoring and evaluation of hazardous volcanoes in Ecuador (e.g. Hall and Mothes, 1994b) and established programs to mitigate future eruptions. SIR-C images are now being integrated into these types of studies, and will be a major source of data for future investigations of volcanism, tectonics and hazards by Hall and his colleagues. For example, an ongoing project to map the geology and potential hazards of Cayambe volcano will now incorporate information from high resolution SIR-C images.

In 1993 Wood and Hall participated in a symposium on Galeras volcano which was organized by Williams. Galeras is a good example of a volcano which is a great potential hazard, for the city of

Pasto (population 600,000) sits directly on the volcano's flanks. At the meeting, Wood presented a paper on the use of remote sensing to monitor active volcanoes, and Hall is now planning on adding SIR-C images to the arsenal of data used to evaluate threats from Ecuador's volcanoes.

One of the original reasons for proposing to participate in SIR-C was the frustration that we experienced when trying to assemble Landsat images of the Northern Andes for our original synthesis of volcanism and tectonics (Hall and Wood, 1985). Because of the tropical, equatorial setting, frequent clouds made it impossible to acquire useful Landsat images over more than about 30-40% of the area of interest. SIR-C has spectacularly penetrated the cloud barrier, allowing a compilation of a new regional synthesis of the tectonic controls on volcanism in Ecuador and Colombia. Thus our first task, during Woods' recent three-week visit to Ecuador, was to closely examine the SIR-C/X-SAR images and Wessels mosaic, searching for additional unknown and little known volcanoes and tectonic features. The directions of this new research - which will continue for the next two years and will lead ultimately to a major revision of Hall and Wood (1985) - include:

1. Recognition of new volcanic structures in the northern Andes (many possible volcanoes located in southern Colombia),

2. Improved interpretation of the major fault distribution in Ecuador,

3. Reconsideration of the major change in volcanism at the Galeras segmentation boundary, from the multi-row, varied chemistry of the southern volcanoes to the single line of Colombian volcanoes to the north.

FUTURE PLANS

The acquisition of SIR-C data for nearly the entire 2000-km-long Northern Andes volcanic arc provides an unique opportunity to examine how volcano distributions, sizes, and types change through time. Wood, Hall and their students intend to catalog and characterize each major volcano in the arc, based on its morphology as displayed in the radar images and available ancillary information. In particular, we wish to investigate changes in the dip of the subducted Nazca slab (estimated from potassium values (K60) in volcanic rocks) with time. We will infer ages of volcanoes from their morphology as seen on SIR-C images, calibrated by known radiometric dates. The inferred resulting history of volcanic evolution will then be tied to changes in plate movements in the central Pacific.

In order to clearly understand what SIR-C/X-SAR images show, Borysewicz has initiated a M.S. thesis comparing variations in radar brightness with known volcanic units for a few Andean volcanoes that have been adequately mapped on the ground. Chimborazo, Galeras and Cotopaxi volcanoes serve as ground truth and Borysewicz will examine the effects of different polarizations, bands and look angles in identifying volcanic lava flows, tephra deposits and debris avalanche deposits.

One significant but intangible result of studying SIR-C images is that the new perspectives raise numerous questions which initiate new directions for investigation. One major such refocusing is due to the remarkable appearance of a suspected caldera beyond the southern extension of known Quaternary volcanism in Ecuador. The 5-km-wide Quimsacocha caldera is surrounded by a ~25-km- wide dark patch on the SIR-C images, and the caldera rim is remarkably sharp. These features suggest that the caldera and its associated andesitic ejecta may be much younger than the proposed age of 11-15 million years. If so, the Northern Andes volcanic arc extends further south than anyone knew, and there is a real problem explaining why, tectonically. We are planning field

work to collect samples for radiometric dating, and also are re-examining earthquake data to better understand subduction in this region.

SIR-C images provide the first consistent view of volcanoes throughout the entire Northern Andes island arc. In order to make this valuable resource available to a wider scientific and educational community Wood, Hall and K. Williams are preparing a digital atlas of the best available SIR-C, Landsat, SPOT and ground images of each volcano in Ecuador and Colombia. This annotated collection will also include existing geological and chemical information as well as the images. This SIR-C based database will completely replace the 30-year-old Catalog of Active Volcanoes of the World volume on Ecuador and Colombia. Currently this compilation is part of Wood's NASA-funded Internet homepage, VolcanoWorld. The URL to go directly to the Northern Andes is

http://volcano.und.nodak.edu/cgi-bin/imagemap/volc_ image?385,114

VolcanoWorld also includes other SIR-C images to illustrate volcanoes around the world; a goal is that VW will ultimately include all SIR-C volcano images.

PUBLICATIONS

Austin, R. T. and A. W. England (1991) Surface characterization of volcanic debris flows at multiple scales, *Proc. of IGARSS '91*, pp. 1675-1678, Espoo, Finland, June 3-6, 1991.

Austin, R. T. and A. W. England (1991) Radar scattering from volcanic debris flows, Progress in Electromagnetic Research Symposium, 1991, Cambridge, MA, July 1-5, 1991.

Austin, R. T. and A. W. England (1992) Multi-scale roughness spectra of volcanic debris flows, Lunar and Planetary Science Conf. XXIII, Houston, Texas, March 16-20, 1992.

Austin, R. T. and A. W. England (1993) Multi-scale roughness spectra of Mount St. Helens debris flows, *Geophys. Res. Let.* 20, pp. 1603-1606.

Austin, R. T. (1994) Electromagnetic Wave Scattering by Power-Law Surfaces, a dissertation submitted in partial fulfillment of the requirements for the degree of Doctor of Philosophy at the University of Michigan.

Austin, R. T. and A. W. England (1994) Radar scattering by volcanic debris flow surface analogues, *Proc. of IGARSS '94*, Pasadena, CA, August 8-12, 1994.

Austin, R. T., A. W. England and G. H. Wakefield (1994) Special problems in the estimation of power-law spectra as applied to topographical modeling, *IEEE Trans. Geosci. Remote Sensing* 32, pp. 928-939, 1994.

Austin, R. T. and A. W. England (1995) Electromagnetic scattering by power-law surfaces, submitted to *IEEE Trans. Geosci. Remote Sensing*, July 7, 1995.

Hall, M. L. and Beate, B. (1991) El volcanismo Plio-Cuaternario en los Andes del Ecuador. In El Paisaje Volcanico de la Sierra Ecuatoriana. Estudios de Geografica 6, Colegio de Geografos del Ecuador, Quito; 5-17.

Hall, M. L. and Mothes, P. (1994a) Tefroestratigrafia Holocenica de los volcanes principales del Valle Interandino, Ecuador. In El Contexto Geologico del espacio Fisico Ecuatoriano. Estudios de Geografica 6, Colegio de Geografos del Ecuador, Quito; 46-67.

Hall, M. L. and Mothes, P. (1994b) Evaluaeion de los Peligros Volcanicos Potenciales Asociados con el Pryecto Quijos. Informe Final Inedito, Convenio EPN-EMELEC-Quito, 73 p.

Hall, M. L. and Wood, C. A. (1985) Volcano-tectonic segmentation of the northern Andes. *Geology* 13, 203-207.

Wessels, R. L. (1995) The interaction of transcurrent tectonics and continental arc volcanism in Colombia and Ecuador: Preliminary results from SIR-C radar analysis, fall Am. Geophys. Un. annual meeting, San Francisco, Dec. 1995.

Wood, C. A., R. L. Wessels, Williams, S. N. and M. C. Calvache V.(1994) SIR-C images of little known Colombian calderas, fall annual Geol. Soc. Am. meeting, Seattle, Oct. 1994.

Wood, C.A. (1995) Earth's environment from space. Invited talk, fall annual Geol. Soc. Am. meeting, New Orleans, Oct. 1995.

Wood, C.A. and S.R. Mattox (195) VolcanoWorld: World Wide Web volcano resource for education and science, fall Am. Geophys. Un. annual meeting San Francisco, Dec. 1995.

Dr. Howard A. Zebker
Stanford University
STAR Lab
232 Durand
Stanford, CA 94305-4055

Co-Investigators:
Charles Elachi JPL/Caltech
Jakob van Zyl JPL/Caltech

Radar Interferometric and Penetration Investigations using SIR-C Data

OBJECTIVES

To model, experimentally characterize, and verify penetration phenomena in hyperarid and vegetated regions using the SIR-C/X-SAR multiparameter radar system and groundbased receivers.

To invert measured radar backscatter as a function of frequency and polarization in terms of geophysical parameters of the surface, subsurface and vegetation canopy such as surface roughness, subsurface geomorphology, or tree height and density.

To display subsurface and within-canopy features in an image format, thus easing the interpretability of the results.

PROGRESS

We are currently involved in two study areas associated with SIR-C. The first is the study of penetration phenomena that relate radar backscatter data in vegetated and hyperarid regions to geophysical factors of the surface cover. The second involves development of radar interferometry as a technique and is important for the future of NASA's radar program, which is likely to contain a significant radar interferometry component.

Interferometric data are requested in raw signal sample format, which we process to interferograms and subsequent topographic and deformation products. We developed a SIR-C interferometric data processor which we run on workstation computers-- the software includes the SAR processing algorithms, interferogram generation software, baseline estimation algorithms, and product generation code.

The data for the penetration experiment are also obtained from the raw signal samples. They are extracted using Fourier spectrum techniques and times series of amplitude and phase fluctuations are produced. These times series are then cross correlated to infer the impulse response of sub-canopy radar reflectors as well as the attenuation of the canopy. These results must be related to parameters of the canopy to derive the ability of the system to "see" under the trees. This will be of significant note in future topographic and other interferometric systems aimed at obtaining under-canopy heights.

Significant Results and Publications

During the past year and one half, the most significant results have been those related to radar interferometry. We have quantified the performance of repeat pass spaceborne interferometric topographic maps, and verified the results by comparison with existing maps. We have also developed the three-pass surface deformation technique, verified it against GPS and field survey approaches, and compared results of two-pass and three-pass analyses of earthquakes.

We have also used SIR-C correlation measurements to track active lava flows at Kilauea, and obtained the most precise estimates of flow volume and mass rates to date.

For this work we developed a theory for the effects of atmospheric variability on repeat-pass interferometric observations. These are likely the limiting factors in any practical deformation or repeat-pass topographic system.

FUTURE PLANS

The approach to completing the science studies as identified in the original proposal, as well as the interferometric experiments that were added to the project science plan, is a two-fold strategy. Both sets of activities are in the data analysis phase, that is, the mission and field deployment component of the studies is essentially complete with the end of the planned flights of the SIR-C hardware. The remaining work concerns data processing, interferometric analysis, penetration analysis, verification with field measurements, and publication and reporting.

Penetration study. During the first and second SIR-C flights, special purpose portable transmitters and receivers were deployed at SIR-C supersites. For flight 1, the site was located at Raco, Michigan, and consisted of temperate forest trees. For flight 2, the site was located at Kilauea, Hawaii, and consisted of a rain forest region. During shuttle overflights, ground receivers recorded the absolute level of radar signals as they were propagated through and attenuated by the vegetation canopy. In addition, coherent tone generators transmitted narrowband signals back up to the shuttle. These signals are to be extracted from radar received echo waveforms. In each instance equipment was simultaneously placed under the canopy and also in an open area to provide a reference signal.

For each overpass, the receiver measurements will be compared between equipment in the open and in the canopy. The resulting fluctuating power measurements will then be related to models of scatter by the vegetation. The transmitter measurements will be extracted from the radar echoes and separated by frequency transform techniques. A cross-correlation of the open and canopy transmitter signals then yields an effective impulse response of the radar to targets hidden in the canopy independent of shuttle motion. This again will be related to scattering models of the canopy for both the temperate and rain forest terrain types.

Interferometer investigations. SIR-C collected two types of interferometric data. These were data with a six-month temporal baseline collected during both flight 1 and flight 2, and data with a one-, two-, or three-day temporal baseline collected wholly during flight 2. We propose to investigate this data set using two types of analysis: i) generation of topographic maps and ii) measurement of surface deformation.

Since SIR-C is a multifrequency instrument, it offers the unique opportunity to compare results at different frequencies. Phenomenological differences in the scattering behavior at 24 cm and 6 cm wavelength will comprise a major part of this investigation.

We will process these data from the raw signal sample format, as delivered by the SIR-C ground data processing facility. We will generate topographic maps of several of the supersite areas at both frequencies, and compare them to conventionally derived digital elevation models to assess their accuracy. These will then be made available to the science team to aid in other investigations.

We also will examine the potential of SIR-C to determine surface deformation. The principal data set here will be the six-month data as the centimeter-level motion we are sensitive to will be much more apparent over six months than three days.

A significant part of the latter study is to understand the effects of the atmosphere on the received signals. This will involve processing some of the 1, 2, and 3 day data to look for apparent motion caused by atmospheric irregularities. These interfering signals will be quantified and assessed for their impact in future space-based radar systems.

The benefits from these investigations will accrue from both sets of activities. The penetration studies will aid in design of radar systems capable of imaging beneath canopies, important for ecological studies as well as for target detection systems. They also will provide new insights into the physics behind scattering from dense canopies.

It has now been demonstrated that interferometric radar techniques benefit a wide variety of Earth science investigations, including production of digital elevation models of the Earth's surface, centimeter-scale surface deformation measurements of coseismic displacement fields, and centimeter-per-day velocity maps of ice sheets and glaciers. The SIR-C experiments will give us the first quality set of multifrequency data that can be used to examine phenomenological changes dependent on radar wavelength. It also will permit the first full examination of the artifacts induced by atmospheric interference. This approach will enable the fastest and most thorough means to realize the full potential of radar interferometry for geoscience applications.

PUBLICATIONS

Zebker, H. A., P. Rosen, S. Hensley, and P. Mouginis-Mark, Analysis of active lava flows on Kilauea Volcano, Hawaii, using SIR-C radar correlation measurements, submitted to Nature, August 1995.

Zebker, H. A., R. Goldstein, P. Rosen, and S. Hensley, Effect of atmospheric variability on interferometric deformation and topography measurements, in preparation, August 1995.

Farr, T. G., D. Evans, H. A. Zebker, D. Harding, J. Bufton, T. Dixon, S. Vetrella, and D. Gesch, Mission in the works promises precise global topographic data, *EOS Transactions*, Vol. 76, No. 22, pp.225-228, May 30, 1995.

Zebker, H. A., T. G.Farr, R. P. Salazar, and T. H. Dixon, Mapping the world's topography using radar interferometry: the TOPSAT mission, *IEEE Proceedings,* Vol. 82, No. 12, pp 1774-1786, December 1994.

Zebker, H. A., P. A. Rosen, R. M. Goldstein, A. Gabriel, and C. Werner, On the derivation of coseismic displacement fields using differential radar interferometry: the Landers earthquake, *Journal of Geophysical Research* - Solid Earth, Vol. 99, No. B10, pp 19617-19634, October 10, 1994.

Zebker, H. A., C. L. Werner, P. Rosen, and S. Hensley, Accuracy of topographic maps derived from ERS-1 radar interferometry, *IEEE Transactions on Geoscience and Remote Sensing*, Vol. 32, No. 4, pp 823-836, July 1994.

ADDITIONAL REPORTS

Dr. Ornella Bombaci
Dr. Fabrizio Impagnatiello
Dr. Andrea Torre
Alenia Spazio S.p.A.
Via Saccomuro 24, 00131
Rome, Italy

1. Introduction

Alenia Spazio has developed, on internal funds, a complete set of processing tools to produce three-dimensional images of the observed area using two complex images coming from SAR sensors like ERS-1 and SIR-C/X-SAR. This paper describes the whole processing of the complex SAR data to obtain the 3-D representation of the image.

In the frame of interferometric processing some steps have been pointed out: the evaluation of range and azimuth shifts between the two images; the filtering of the complex data in order to improve the coherence between the images; the extraction and filtering of the interferogram; the phase unwrapping; the phase-to-height conversion.

The whole processing has been tested and applied to images coming from SIR-C/X-SAR (and ERS-1) on Monte Etna in Sicily, in order to evaluate the eventual differences between the two kinds of sensors in terms of radar wavelength, baseline, and repetition time of the images.

2. Shift evaluation and images registration

The registration of the two SLC images is done using the following procedures, after the removal of the coarse misregistration carried out by estimating the pixel shift with the cross-correlation on the amplitude images. For the fine (sub-pixel) registration we use the technique proposed in Lin, et al., 1991.

$$\zeta(\underline{a}) = \sum_{i,j} \frac{\left|P(i+1,j) - P(i,j)\right| + \left|P(i,j+1) - P(i,j)\right|}{2} \quad (1)$$

The fringe fluctuation function (1) has been improved with respect to the original algorithm by introducing pixel by pixel a weight factor derived from the correlation matrix between the two images. Fig. 1 shows the results obtained with the fringe fluctuation algorithm applied to X-SAR images coming from Monte Etna in Sicily, during the SRL-2 mission.

3. Complex images filtering

The objective is to improve the correlation coefficient and so to reduce the phase and height noise observing that one of the causes of phase noise is the relative shift of the reflectivity spectra of the two images. This is principally due to baseline decorrelation.

3.1 Baseline decorrelation

It is well known (Rodriguez and Martin, 1991) that the spectra of the received signals represent different terrain reflectivity bands. This is due to the different angle of view of each pixel on the ground with respect to the two points of observation. Calling q_1 the view angle of a pixel for the first antenna (platform pass) and q_2 the view angle of a pixel for the other antenna (platform

pass) it has been noted that the same spectral components of the signal coming from one acquisition is shifted by a frequency f_W with respect to the other, being:

$$f_\Omega \cong f_0 \frac{\Delta\vartheta}{\tan(\vartheta - \alpha)} \qquad (2)$$

with $\Delta\vartheta = \vartheta_1 - \vartheta_2$, f_0 the radar frequency, and a the local mean terrain slope. Observing that $\Delta\vartheta \cong \frac{n_s}{\rho_0}$, the spectral shift becomes

$$f_\Omega \cong f_0 \frac{n_s}{\rho_0 \tan(\vartheta - \alpha)} \qquad (3)$$

The behavior of frequency shift versus local slope is plotted in Fig. 2 for X-SAR images. One can observe that f_Ω increases with increasing terrain local slope. Let us call "blind angles" those angles which cause an infinite shift. Moreover if the terrain slope exceeds the off-nadir angle (layover) the absolute value of f_Ω decreases and it becomes negative.

As seen this spectral shift depends on baseline and local slope and it causes that part of each image spectrum, exactly f_Ω width, that is not common in the two images. When, extracting the interferogram, the spectra correlation is performed, the result is noisy because of the correlation of these not-common parts: hence the cross-correlation presents the following three contributions: a peak at the frequency of perfect alignment of the spectra, a sequence due to a common band in adifferent position, and a sequence due to the cross-correlation between the not- common bands.

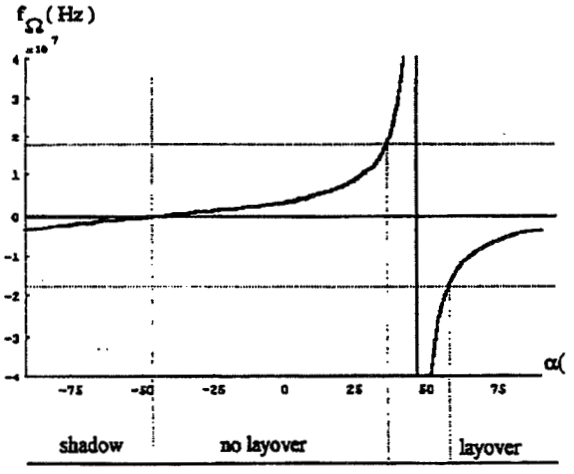

Fig. 2. Spectral shift vs local slope (X-SAR)

It is important to remember (Prati and Rocca, 1993) that this spectral shift is the cause of the fringe generation. The interferogram, hence is described by

$$\Delta\varphi = \frac{2\pi R_y}{c} f_\Omega \qquad (4)$$

with R_y range resolution. So we do not have to remove this shift, but only to filter the not common parts of the spectra.

To do this, because of the dependency from terrain slope, it is necessary to estimate the shift in a sufficiently small portion of image in which a constant slope is supposed. In the following the processing of one subimage is described.

3.2 Range Filtering

It is necessary to design two filters with the same bandwidth and different central frequency. These will be obtained by realizing a real high-pass filter H(f) with $f_{pass} = \frac{1}{2} f_\Omega$ and shifting the filter once on $f_1 = \frac{\mu}{2} - f_{pass}$ and once on $f_2 = -\left(\frac{\mu}{2} - f_{pass}\right)$.
After having estimated the spectral shift the project of filters is performed: the high pass FIR filter is realized with the Parks McClellan technique.

To determine the optimum filter the Golden Section algorithm has been used: it seeks the maximum of a function to find, varying the stopband from zero to the stopband at -31 dB, the optimum stopband that maximizes the correlation coefficient γ. It is interesting to note that if the scene is supposed to be white and uniform, the correlation coefficient between the two images correspond to the correlation coefficient between the transmitted signal and the f_Ω shifted one.
So, the maximum detection algorithm can determine the optimum stopband that maximizes the correlation between the transmitted signal filtered with the centre on f_1 filter and the same signal filtered with the centre on f_2 and shifted by f_Ω filter.

3.3 Azimuth Filtering

The results obtained applying the processing described before to X-SAR and ERS-1 images lead to some observations.

The azimuth spectra of the X-SAR present two different Doppler centroids. In this case there is a common and a not-common part of the azimuth spectra and so in X-SAR images also an azimuth filtering is necessary.

In this case the Doppler centroids have been estimated and with the Parks McClellan method a high pass filter has been projected with N=127, $f_{pass} = \frac{(CD_1 - CD_2)}{2}$, and $f_1 = CD_1 - \frac{\mu}{2} + f_{pass}$, $f_2 = CD_2 + \frac{\mu}{2} - f_{pass}$.

4. Phase unwrapping

4.1 Bidimensional analytical approach

The phase unwrapping is based on the well known weighted least-mean square estimation of the phase from the phase differences. It has been implemented on a general purpose computer for testing (maps of up to 4096x4096 pixels have been processed and unwrapped), and as a basis for a next implementation on a parallel computer.

Another very promising technique is based on direct integration of the Poisson equation coming from the derivation (second derivative) of the complex logarithm of the interferogram. With the second derivative operation we have reduced the problem to a well known one. Now, we have to solve the Neumann problem with non-homogeneous boundary conditions: the first derivative along the boundary has been previously calculated. Techniques and s/w programs to solve the above problem are widely described in the literature. We use the Fourier method to solve the homogeneous problem and then add the particular solution for the boundary conditions.

Two major practical points are: i) the calculation of derivatives; ii) the presence of noise (i.e. corrupted samples). In our implementation we use the Savitzky-Golay (S-G) smoothing filters for both computing the derivatives and smoothing noise. The characteristic of the S-G filter is to use c_n coefficients that preserve higher moments: for each point f_i, the least square fitted polynomial to all n_L+n_R+1 points is computed, and g_i is the value of that polynomial at position i..

The S-G filter allows us to compute directly the filtered derivative, simply taking the n^{th} derivative of the fitted polynomial and dividing g_i by Δ^n (Δ is the stepsize).

4.2 Global classification approach

Why do some algorithms find a lot of difficulties in doing what the human brain-eye system does in a very easy way? A try to understand the interpretation mechanism of human visual inspection of interferometric fringes leads to a new method for phase unwrapping.

The fringes, after their generation, are examined by a continuity tester which performs a segmentation of the 2-D fringe map into homogeneous areas. These bidimensional segments are then grouped into classes, the result of which is defined as connected sets of pixels having the same phase ambiguity.

Finally the discrete ambiguity problem is solved against classes which are mapped into a ambiguity matrix.

This algorithm has been implemented on a conventional HP Apollo RISC machine and results are 10 times faster than others if applied to L-band interferometric data (SIR-C). The only drawback is that non-contiguous regions (e.g. islands within the sea) cannot be uniquely assigned to an ambiguity map, but this is a common problem in the phase unwrapping matter.

5. Phase to height conversion

Most of the methods suggested in the literature need the knowledge of at least three points on the ground of which height, position in image, and absolute phase is known. In order to demonstrate the feasibility of a global interferometric mission to produce DEM of the whole Earth surface and especially of those areas about which the topographic data are unknown, a method that reduces the a priori information is developed. Fig.3 shows the typical geometry, where h(i,j) is the height of the pixel in the object, ρ(i,j) its slant range distance, q(i,j) the off-nadir angle from which it is observed, H the platform height and Re the Earth radius at the observed point. The idea is to refer the analysis to the interferometer axis: to this the off-nadir angle is equal to the tilt angle, that is the baseline attitude with respect to cross-track direction. Along this axis the interferometric phase should be zero: the interferogram phases are referred to

this zero point in terms of variation with respect to different off-nadir angles. So, the interferometric absolute phase can be written as

$$\varphi = \frac{4\pi}{\lambda} \cdot B \cdot (\sin \vartheta' - \sin \vartheta_{axis}) . \qquad (5)$$

with $\vartheta' = \vartheta - \vartheta_{tilt}$.

Deriving (5) with respect to off-nadir angle

$$\partial\vartheta = \frac{\lambda}{4\pi B \cdot \cos\vartheta'} \cdot \Delta\varphi . \qquad (6)$$

$$\rho(i,j)^2 + (H + \mathrm{Re})^2 - 2\rho(i,j)(H + \mathrm{Re}) \cdot \cos(\vartheta(i,j)) = (h(i,j) + \mathrm{Re})^2 \qquad (7)$$

$$\Delta h_{i,j} = \frac{H' \cdot \rho(i_m, j_m) \cdot \sin\vartheta(i_m, j_m)}{h(i_m, j_m) + \mathrm{Re}} \cdot \frac{\lambda}{4\pi B \cdot \cos(\vartheta(i_m, j_m) - \vartheta_{tilt})} \Delta\varphi_{i,j}$$

$$- \frac{H' \cdot \cos\vartheta(i_m, j_m) - \rho(i_m, j_m)}{h(i_m, j_m) + \mathrm{Re}} \Delta\rho_{i,j} . \qquad (8)$$

Deriving (7) with respect to ρ, θ and h with H'=H+Re and substituting (6) we obtain every image pixel (i,j) slope behavior toward the interferometric phase and slant range increasing distance (as function of off-nadir angle), where $\Delta\rho_{i,j} = j \cdot f_r$ (j is the range coordinate and f_r is the range sampling rate) and (i_m, j_m) is the only ground reference point about which we should know both its position in the image toward the interferometer system ($\theta(i_m, j_m)$, $\rho(i_m, j_m)$) and the absolute height ($h(i_m, j_m)$). In this way it is possible to reconstruct the height in the whole image knowing information of just one ground control point and the unwrapped phases, with the simple implementation of a linear equation in which the constant term is given by the attitude of the interferometric system and by the reference point height. Moreover implementing the same procedure to the wrapped phase one can obtain the phase behavior without a flat terrain contribution, so that it is possible to know the level contour lines on the image. Fig. 4 shows the level contour lines referred to in Fig. 1. Fig. 5 shows the corresponding 3-D reconstruction.

6. Multifrequency (and Multibaseline) Interferometry.

The multifrequency capability of the SIR-C/X-SAR system has been used to improve the achievable performances of the final interferometric product. Two techniques have been used: the first one to help the processing of the low correlated X-band data; the second to improve the final sensitivity by the fusion of the L- and X-band DEM's.

The unwrapping of the X-band interferogram is difficult due to: i) the low level of correlation affecting large areas of the examined scene; ii) the quite large baseline which results in very narrow fringes where the slope is steeper. To help the unwrapping process the L-band

interferogram is first unwrapped, then it is scaled (according to the wavelength ratio), registered, and subtracted from the X-band fringes. The result (delta fringes) is an interferogran at X-band with a few wide fringes which are easily unwrapped; the result is then added to the previously subtracted interferogram giving the final X-band product. The processing can be improved by weighting the "delta fringes" with the correlation map before unwrapping; obviously the result is a merging of the L-band (where the correlation is low) and X-band unwrapped phases.

The second technique (only partially tested) uses the multiresolution analysis (via the wavelet decomposition) to perform the fusion between the L- and X-band. The X-band and the scaled L-band unwrapped phases are firstly decomposed using the wavelet decomposition, then a final image is composed using the HF components of the X-band and the LF components of the L-band.

7. Conclusions

All the processing has been developed in order to realize a massive parallel technique for a following implementation on a parallel computer. The results are very interesting especially as far as the coherence improvement and phase unwrapping are concerned. The trend is that of a greater use of the interferometric technique to classify radar images using low noise coherence images and to use the low noise fringes to develop a differential Interferometry to detect small changes in the earth's surface.

References

[1] Bombaci, O., F. Rubertone, and A. Torre "Alenia Spazio Activities on SAR Interferometry: application on scientific mission," *IGARSS '95*, Florence, 1995.

[2] Bombaci, O. and A. Torre, "Alenia Spazio Research Activities on SAR Interferometry," EUROPTO '95, Paris, Sept. 1995.

[3] Bombaci, O., F. Impagnatiello, and A. Torre, "New features for on-line processing in interferometric applications" EUSAR '96, March 1996.

[4] Lin, Q., J. F.Vesecky, and H. A. Zebker, "New Approaches in Interferometric SAR Data Processing," *IEEE Trans. on Geoscience and Renote Sensing,* vol. 30, no. 3, May 1992.

[5] Rodriguez, E. and J. Martin, "Theory and design of interferometric SAR's," *Proceedings of IEEE*, 1991.

[6] Prati, C. and F. Rocca,"Improving slant-range resolution with multiple SAR surveys," *IEEE Transaction on Aerospace and Electronic Systems*, vol. 29, no. 1, January 1993.

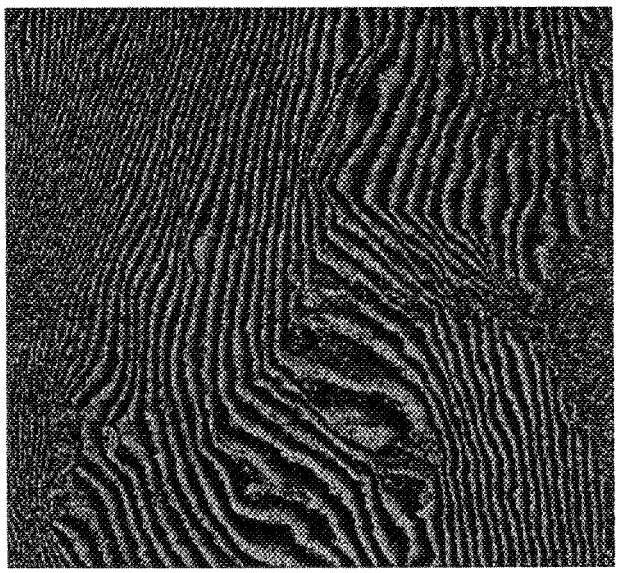

Fig.1. X-SAR fringes over Monte Etna, Sicily, obtained with fringe fluctuation algorithm

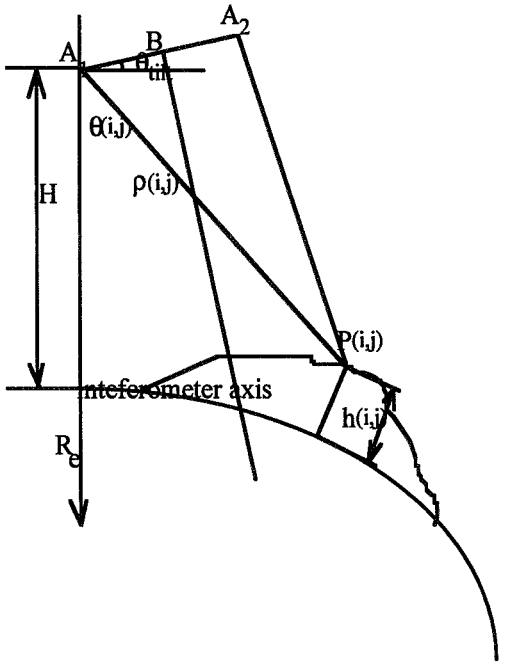

Fig.3. Phase to Height projection geometry

Figure 4 Mt. Etna Flat Terrain subtracted interferogram (SIR-C L band)

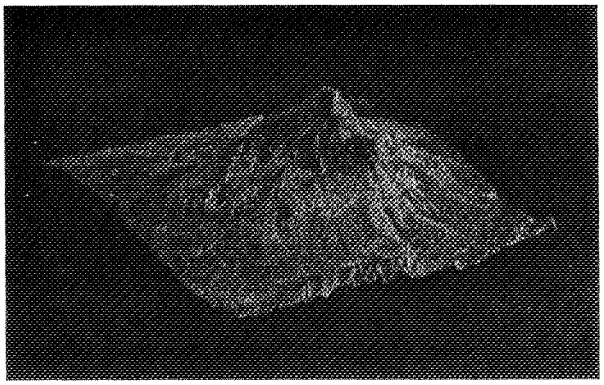

Figure 5 Mt. Etna DEM

Malcolm Davidson
Roland Steingießer
Institut für Pflanzenbau
University of Bonn
Tel: 0228-733186
Fax: 0228-732870
email: ulp107@ibm.rhrz.uni-bonn.de

1. Introduction

Remote sensing in agriculture has a number of inherent advantages with respect to conventional data gathering methods since it can:

- Image a large area in a very short time. Thus the data possess a high degree of actuality and have a high economic value.
- Provide area-wise information as compared to the traditional point-wise sampling techniques. The ability to produce crop maps as well as statistics is considered particularly important for crop studies at regional and local levels.
- Advance the distribution and timeliness of the thematic information that is essential for the planning, policy making and management of agriculture.
- Act as a stratifier in that it can help stratify large regions according to land-use or agroclimatological conditions.

While active radar systems have demonstrated considerable potential in collecting information over agricultural lands, the full-potential of SAR systems has not yet been realized due to the low dimensionality of the data recorded by existing earth-orbiting SAR systems such as ERS-1 and JERS-1. These operate at a single frequency and polarization, which limits their sensitivity to crop geometry and hence crop type, and condition.

The two SIR-C/S-SAR shuttle missions provided the first opportunity to collect multi-frequency multi-polarization images over a number of sites worldwide. While the missions took place at non-optimal times during the growing season (i.e. early and late) for agricultural applications in Europe, a number of images were taken over agricultural areas characterized by distinct climatic conditions and soil types, different crop types or similar crops but at different development stages and subject to varying crop management practices. The research at the Institut für Pflanzenbau has focused so far on using this wealth of data in terms of the two basic aspects of agricultural remote sensing; *the recognition of crop types* over a large area on the basis of self-similar but distinct backscatter characteristics for each crop of agricultural land-cover type and, *the mapping of the biophysical status* of certain crop types. Ground truth data was collected in three very different test sites (Oberpfaffenhofen in southern Germany, Oltrepo Pavese in northern Italy, and Matera in southern Italy) during the first mission and in two sites (Oberpfaffenhofen again and Flevoland, Holland) during the second mission. The general aim was therefore to judge the sensitivity of the multi-dimensional SIR-C/X-SAR radar data to the biophysical condition of crops and their utility for large scale agricultural inventories.

2. Work in Crop Classification

So far classification work has focused mainly on data acquired during the April 1994 mission over the Oberpfaffenhofen test site, partially because better crop maps could be compiled for this test site and partially because, until recently, data were lacking for the other test sites. Two supervised classification methodologies have been tested on a single full-polarimetric scene for the area; the maximum likelihood method using the amplitude at the standard linear polarizations (X-VV, C-HH, -HV, -VV and L-HH, -HV, VV) and the maximum contrast method which uses

the complex covariance matrices at C- and L-band. Also the information content of each frequency/polarization feature was evaluated by comparing the observed classification accuracy as a function of features used in the classification process. The following list summarizes the main results so far.

- Classification accuracies achieved for agricultural plots only (i.e. general land cover categories such as urban areas, forested areas, water and road systems were not considered) were quite high. The main agricultural land cover types at this time were ploughed and seedbed bare soil fields, winter barley, winter wheat, oilseed rape, meadows and set-aside (fallow). While there was some confusion between barley and wheat fields due to their almost identical appearance at this time, average classification accuracies, using the maximum likelihood classifier for the above categories, reached 80 to 90% in a number of cases — depending on the frequency/polarization features used and the minimum field size considered.

- By comparing the classification accuracies as a function of frequency/polarization features used it was possible to derive a figure of merit for each feature and thus assess which instrument configuration was most sensitive to agricultural features. In general cross-pol polarizations contained more information than like-pol features and L-band, with a higher between category dynamic range, was more useful than C-band. Adding X-VV information to an L-band only and C-band only classification also improved classification accuracies by 10.9 and 19.2% respectively.

- The maximum likelihood classification methodology, using amplitude only images, proved to be more robust than the maximum polarimetric contrast method, which uses both amplitude images and information provided by the complex correlation coefficient between HH and VV polarizations. A plot of the complex correlation coefficient showed that the latter contains little information on agricultural land cover type, except perhaps to distinguish seedbed from the other categories. This can be explained by the fact that crops at this time have little structure — they are all more or less at a grasslike stage — and lack a distinct geometry. It is expected that the HH-VV complex correlation coefficient will play a more significant role when data taken during the second shuttle flight is analyzed since crops with significant structure such as corn, sugar beet and potatoes were fully developed at that time.

- The benefits of the added dimensionality of SIR-C/X-SAR data were demonstrated by comparing the average classification accuracies as a function of the number of polarimetric features used for the classification. N.B. that these classification results (from a single image early during the growing season) compare favorably with multi-temporal ERS-1 results, using images taken throughout the growing season.

Number of Pol./Freq. Features	Maximum Likelihood Avg. Class, Accuracy (%)
2	64,3
3	78,2
4	85,4
5	88,4
6	89,3
7	89,3

3. Mapping Crop Status

Much of the recent research has focused on quantifying the sensitivity of various polarimetric features to the biophysical status of certain crop types. A large database was collected during the

first and second missions containing the biophysical plant parameters—biomass, height, water content, leaf area index, etc.—and soil parameters—density and humidity—for a selected number of fields in each test area. The suitability of multi-parameter radar instruments such as SIR C/X-SAR was then judged by comparing ground measurements with the backscatter signatures for each field. Initial results are:

- No clear correlation between single channel backscatter features (single frequency, single polarization) and crop biophysical parameters was observed.

- The use of ratios, especially the L-HH/L-VV ratio, appear to be more promising. The L-HH/L-VV index appears to be sensitive to the presence of vegetation scattering with respect to soil scattering.

  For relatively smooth seedbed fields, L-VV is greater than L-HH, as predicted by the small perturbation model. However as more vegetation is added on top (e.g., barely early during the growing season) the interaction component which favors L-HH becomes more important and the L-HH/L-VV ratio tends towards values greater than 1. This is illustrated at the end of this report.

4. Future Work

Over the last few months a nearly complete data set of reach test site has been delivered by JPL and the DLR, posing a tremendous challenge to process and evaluate such large data sets before the end of our project (December 1996). However only a limited number of SIR-C scenes were taken in the full-polarimetric mode and since these allow for a complete analysis of backscatter features, we will concentrate on using these first, and move on to the other ones later. Specific goals for next year are

- Inter-test site comparisons of classification results and backscatter signatures for certain crop types.

- Analysis of data collected during the second shuttle mission.

- Classification of crop and land cover types in an unknown region (i.e., for which no ground truth was collected by our institute). Two candidate areas imaged during the SIR-C/X-SAR mission are:

  1. Erdingen (west of Munich) where classification results can be compared to the official agricultural statistics for the region.

  2. Straßbourg (France) in collaboration with SERTIT, who would provide us with the crop maps after a classification of the area was carried out.

5. Publications/Proceedings

Docter, K., M. W. J. Davidson, R. Steingießer, and W. Kühbauch, "Multitemporale Pernerkundunglandwirtschaftlicher Nutzflächen," *Proceedings of the 1st German-French Colloquium for Remote Sensing*, Bonn, January 1995.

Kühbauch, W., M. W. J. Davidson, R. Steingießer, and K. Dockter, "Investigation of the agricultural land use in Italy and Germany by means of the multi-band/multi-frequency SIR-C/X-SAR system," *Proceedings of the 1995 International Geoscience and Remote Sensing Symposium (IGARSS)*, Florence, Italy, July 1995, pp. 1061–1063.

Davidson, M. W. J., R. Steingießer, and W. Kühbauch, "Exploiting multi-frequency multi-polarization radar images for mapping crop types early during the growing season," *Proceedings for the 1st International Symposium of the Retrieval of Bio and Geophysical Parameters from SAR Data for Land Applications*, Toulouse, France, October 1995, (in press).

Davidson, M. W. J., R. Steingießer, and W. Kühbauch, "A comparison of two classification methods for mapping crop types early during the growing season using SIR-C/X-SAR data," *IEEE Transactions on Geoscience* (Special Issue), (in preparation).

In addition, papers are being prepared for IGARSS '96 (USA) and EUSAR '96 (Germany). Other activities have included an information seminar with the regional agricultural office of Fürstenfeldbruck, near Munich, where results from the first mission were presented to staff and those farmers involved with our project. In the future we hope to publish three peer-reviewed papers; one on classification methodology for multi-parameter SAR, one on the analysis of backscattered signatures as a function of crop condition and a final one on inter-test site comparisons and the classification of an unknown agricultural area.

The Ratio L-HH/L-VV as an Indicator of Vegetation Levels

Oberpfaffenhofen Germany
SIR-C/X-SAR data from April 11th, 1994

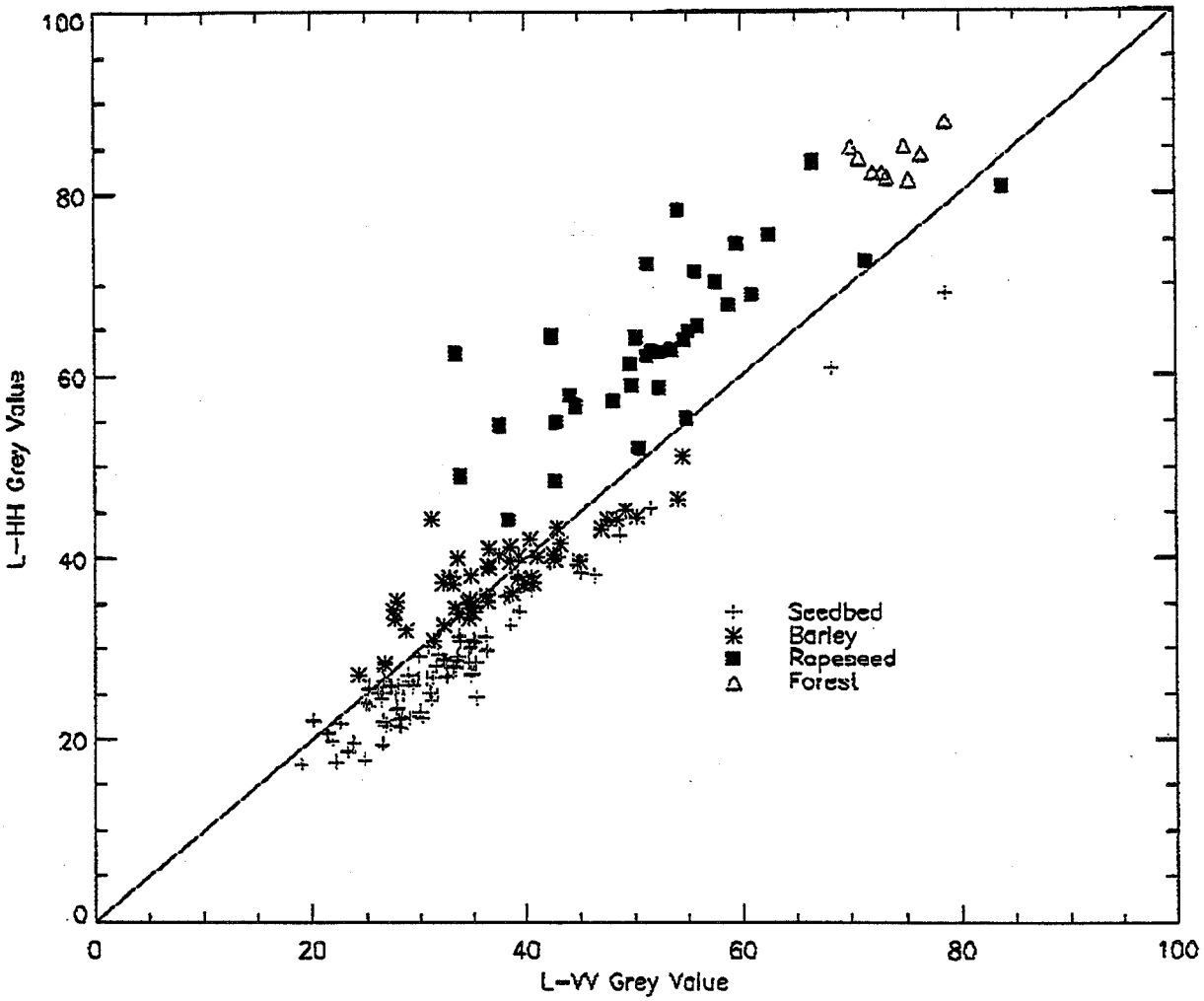

The ratio of L-band HH over VV returns is an indicator of the amount of vegetation scattering with respect to soil scattering. For bare soils the vertically polarised returns are higher so that the ratio values lie below the L-HH/L-VV=1 line. When vegetation is present, the higher interaction at HH polarisation with respect to VV polarisation between vegetation and the illuminating radiation, causes the ratio of the HH and VV returns to move above the L-HH/L-VV=1 line. The shifts in the case of barley fields were small since very little biomass was present this early during the growing season.

Dr. G. Franceschetti
IRECE-CNR and the
University of Napoli, Italy

Research activity has been developed in the following areas:

- Development of innovative processing codes for Interferometric SAR (IFSAR) image generation
- Development of innovative architectures for real-time SAR data processing

The research activity is briefly summarized and appropriate references provided.

1. Innovative IFSAR processing codes.

Two problems have been studied: IFSAR image registration and phase unwrapping.

As far as image registration is concerned, an innovative procedure has been developed and implemented: the raw data couple is processed with respect to a common reference point, thus assuming accurate automatic registration with no need of image interpolation procedures. However, the two images are deformed: one is stretched and the other is compressed; but these deformations are efficiently accounted for with a scaling procedure. Experiments on real data validated the procedure.

References:

[1] Fornaro, G. and G. Franceschetti, "Image registration in interferometric SAR processing," in print on *Proc. IEEE on Radar, Sonar and Navigation*, December 1995.
[2] Fornaro, G. and G. Franceschetti, "A new approach for image registration in interferometric processing," *IGARSS '94*, pp. 1983-1985, Pasadena, CA, (USA), 1994.
[3] Fornaro, G. and G. Franceschetti, "Image registration in interferometric SAR," EUROPTO, Parigi, (Francia), September 1995.

Coming to the phase unwrapping, an innovative procedure has been developed and implemented. The procedure is based on the first Green's identity, is robust as far as noise is concerned, and limits the spread of DEM errors due to phase undersampling or low signal to noise ratio. Experiments on real data validated the procedure. In addition, new innovative procedures based on a variational formulation of phase retrieval is under investigation.

References:

[1] Fornaro, G. and G. Franceschetti, R. Lanari, J. Moreira, et al. "X-SAR interferometry, first results," *IEEE Trans. Geosci. Remote Sensing*, 33, pp. 950-956, 1995.
[2] Fornaro, G. and G. Franceschetti, R. Lanari "Interferometric SAR phase unwrapping using Green's formulation," accepted by *IEEE Trans. Geosci. Remote Sensing.*

[3] Isernia, T, V. Pascazio, R. Pierri, and G. Schirinzi, "Image reconstruction from Fourier transform magnitude with applications to SAR imaging," accepted by *J. Opt. Soc. Am. A.*
[4] Isernia, T., V. Pascazio, R. Pierri, and G. Schirinzi, "Synthetic Aperture Radar imaging from phase corrupted data," submitted to *IEEE Proc Radar, Sonar and Navigation.*
[5] Isernia, T., G. Leone, V. Pascazio, R. Pierri, G. Schirinzi, and F. Soldovieri, "Phase retrieval in antennas and remote sensing," *3rd EMC & CEM ESA Workshop*, Pisa (Italy), 1993.
[6] Isernia, T., G. Leone, V. Pascazio, R. Pierri, and G. Schirinzi, "Application of phase retrieval techniques in Synthetic Aperture Radar data processing," *PIERS '93*, Pasadena (USA), 1993.
[7] Isernia, T., G. Leone, V. Pascazio, R. Pierri, G. Schirinzi, and F. Soldovieri, "Non linear inversion in E. M. imaging, *PIERS '94*, pp. 768-772, Noordwijk (The Nederlands), 1994.
[8] Isernia, T., M. Materazzi, V. Pascazio, G. Schirinzi, and F. Soldovieri, "Non linear inversion in SAR imaging, *PIERS '95*, Seattle, WA, (USA), 1995.
[9] Fornaro, G., G. Franceschetti, and R. Lanari "Two dimensional phase unwrapping based on the Laplace Eikonal equations," *IGARSS '95*, Firenze (Italy), 3, pp. 1828-1830, 1995.

2. Innovative real-time architectures for SAR processing

An innovative architecture for real-time processing of a one-bit coded SAR signal has been designed. The architecture makes use of only phase shifters and adders; the elementary cell has been already realized, thus validating the original idea.

It is intended to realize a full prototype, to be using during the third SIR-C/X-SAR mission for a real-time processing demonstration. It is planned to realize the hardware in cooperation with CGS (Matera), under the ASI sponsorship. Obviously, ASI funding of the project is a critical point.

References:

[1] Cappuccino, G., G. Cocorullo, P. Corsonello, and G. Schirinzi, "Design and demonstration of a real time processor for one bit coded SAR signals," submitted to *IEEE Proc. Radar, Sonar and Navigat.*
[2] Isernia, T., V. Pascazio, and G. Schirinzi, "Synthetic Aperture Radar interferometry using one bit coded raw and reference signals," submitted to *IEEE Trans. Geosci. Remote Sensing.*
[3] Cocorullo, G., G. Franceschetti, M. Magliulo, V. Pascazio, and G. Schirinzi, "A novel architecture for real time one bit coded SAR data processing," *Proc. of SPIE - The International Society for Optical Engineering*, 19941, pp. 182-188, Orlando, FL, (USA), 1993.
[4] Fornaro, G., G. Franceschetti, V. Pascazio, and G. Schirinzi, "Signum coded SAR interferometry," *IGARSS '95*, Firenze (Italy), pp. 778-780, 1995.

Prof. Giuliano Manara
Department of Information Engineering
University of Pisa, Italy

1. State of the activity

The research activity at the Department of Information Engineering of the University of Pisa (Italy) has been mainly concerned with the definition of suitable processing procedures for estimating the two-dimensional sea wave spectrum from Synthetic Aperture Radar (SAR) images [1].

Classical methods proposed in the literature rely on the definition of a suitable analytical relationship between the sea-wave spectrum and the corresponding SAR image spectrum. This relationship accounts for the main effects contributing to the image formation process, as for instance velocity bunching, hydrodynamic phenomena, tilting of the local sea surface normal. In the most general case, the function relating the two-dimensional sea wave spectrum to SAR image spectrum is non-linear, rendering the inversion procedure a very complicated task. A solution to this latter problem can be obtained by resorting to an iterative technique, based on the minimization of a suitable functional. To this end, a sea wave first guess spectrum is assumed; then, this estimate is upgraded at each iteration till convergence is obtained. It is important to note that the convergence of the algorithm strongly depends on the first guess choice, which, in order to guarantee the effectiveness of the procedure, must be not too far from the actual sea wave spectrum. This guess is usually determined through hydrodynamic models or buoy measurements.

The availability of experimental data, contemporaneously recorded with in situ measurements, is of fundamental importance for testing and validating the aforementioned techniques. Moreover, this comparative analysis may also suggest optimization and extensions of these spectral estimation methods.

2. Significant results

At a first stage, these techniques are being applied to areas of the Mediterranean Sea. The attention is mainly devoted to the tuscan and ligurian coasts and in particular to La Spezia and Genoa Gulfs, where *in situ* measurements are available for our research group. These two gulfs represented a test-site during the last two SIR-C/X-SAR missions, but unfortunately no data relevant to this test-site were recorded during the missions. However, comparisons between experimental and numerical results have been performed using images recorded by the European satellite ERS-1.

A considerable part of the activity is devoted to the definition of efficient inversion algorithms making use of a numerical simulator previously implemented. This latter numerical code allows reconstruction of the SAR raw signal received by the spaceborne radar sensor in the presence of specific values of physical parameters as, for instance, local wind direction and intensity, and possible presence of swell. It can be used in the framework of an iterative inversion algorithm to provide a more accurate estimate of the SAR image spectrum generated from an assigned sea wave spectrum [2]. This evaluation is needed at each iteration step and is usually performed by an analytical transform. The introduction of this numerical tool may allow us to gain a deeper physical insight into several phenomena contributing to the SAR image formation process. It is important to note

that this can be obtained at the expense of an increased computational cost which is essentially due to the time-varying character of the sea surface. This latter aspect makes numerical modelling very cumbersome. The simulation code implemented is capable of describing the case of a Real Aperture Radar (RAR) system as well. Consequently, to the end of validating the simulator, numerical tests have been carried out, comparing their outputs with experimental data presented in the literature [3], [4].

3. Future developments and data request

Concerning the next SIR-C/X-SAR mission, the acquisition of images of the sea surface by a two-antenna SAR system is of remarkable interest for the applications under consideration. Significant improvements in the above estimation procedures could be obtained with such a system [5]. By extending the numerical simulator implemented, the experiment could be simulated *a priori* to analyze the advantages of this operating configuration and to test the effectiveness of processing techniques. Later on, during the next mission, an *in situ* measurement campaign could be performed for validating both processing and numerical simulation. For these reasons, we are strongly interested, for the future developments of this research activity, in the acquisition of data relevant to the La Spezia and Genoa Gulf test sites during the next SIR-C/X-SAR mission in a two-antenna SAR configuration.

4. References

[1] Corsini, G., E. Ferretti, G. Manara, and G. Milillo, A. Monorchio, "Methods for directional sea wave spectrum retrieval from SAR images," to be published in AIT Italian Journal on Remote Sensing (in Italian).

[2] Corsini, G., G. Manara, and A. Monorchio, "Sea wave spectrum estimation from SAR images: a simulation based approach," *1995 International Geoscience and Remote Sensing Symposium (IGARSS '95)*, Florence, Italy, July 10-14, 1995.

[3] Berizzi, F., G. Corsini, G. Manara, and A. Monorchio, "Simulation of electromagnetic backscattering data for sea clutter analysis," NATO AC243 Panel 3 RSG21 Conference on "Sea Surface Characteristics and Interaction with cm and mm Waves", Pisa, April 5-6, 1995.

[4] Corsini, G., G. Manara, and A. Monorchio, "Simulation of RAR reflectivity maps of the sea surface for remote sensing applications," *1996 International Geoscience and Remote Sensing Symposium (IGARSS '96)*, Lincoln, Nebraska, May 27-31, 1996.

[5] Milman, A. S., A. O. Scheffler, and J. R. Bennett, "Ocean imaging with two-antenna radars," *IEEE Trans. on Antennas Propagat.*, Vol. AP-40, No. 6, June 1992.

Dr. S. Paloscia
CNR/IROE
Firenze

SIR-C/X-SAR Experiment on Montespertoli test site

1. Data Acquisition

1.1 Data takes

a) April: 7 data takes at incidence angles between 24° and 55°- weather conditions: scattered rains.
b) October: 5 data takes at incidence angles between 24° and 55° (35° was missing) - weather conditions: clouds and showers.

SIR-C data at incidence angles lower than 45 degrees were full polarimetric.

1.2 Delivering/Processing

All SIR-C data collected in April and October have been delivered and processed. Only X-SAR data collected in April have been delivered and processed.

1.3 Calibration

A check, carried out with external Calibrators (Corner reflectors), has shown a good calibration of SIR-C data, whereas X-SAR data had to be calibrated.

2. Results

- A comparison with ERS-1, JERS-1 and AIRSAR data has shown a very good consistency of L- and C-band data.

- The sensitivity of L-band HV pol to both arboreous and herbaceous vegetation biomass has been confirmed.

- A good separation between bare and vegetated fields has been obtained from the ratio RL/RR at C band.

3. Publications:

Journals:

[1] Baronti, S., F. Del Frate, S. Paloscia, P. Pampaloni and D. Solimini, 1995 "SAR polarimetric features of agricultural areas," *Int. J. Remote Sensing*, vol. 16, no. 14, pp. 2639-2656.
[2] Ferrazzoli, P., S. Paloscia, P. Pampaloni, G. Schiavon, S. Sigismondi and D. Solimini, 1996, "The potential of multifrequency polarimetric SAR in assessing agricultural and arboreous biomass," submitted to *IEEE Trans. Geosci.Remote*

Sensing Special Issue, "Symposium on Retrieval of Geo-and Bio-Physical Parameters from SAR data for Land Application."

Conference Digests:

[1] Pampaloni, P. , S. Paloscia and S. Sigismondi, 1995, "The Microwave Backscattering of Vineyards," *Proc.International Geoscience and Remote Sensing Symposium, IGARSS '95*, Firenze (Italy), T. Stein Editor, pp. 222-223, IEEE N 95CH 35770, ISBN 0-7803-2567-2.

[2] Baronti, S., G. Macelloni, S. Paloscia, P. Pampaloni and S. Sigismondi, 1995, "An Automatic Method for Land Surface Classification using Multi-frequency Polarimetric SAR Data", *Proc. International Geoscience and Remote Sensing Symposium, IGARSS'95,* Firenze (Italy), T. Stein Editor, pp. 973-975, IEEE N 95CH 35770, ISBN 0-7803-2567-2.

[3] Ballerini, P., F. Catani, S. Moretti, S. Paloscia, P. Pampaloni and S. Sigismondi, 1995,"Hydrological modeling integrated with multifrequency SAR data on the Pesa and Virginio basins of Montespertoli site," *Proc. International Geoscience and Remote Sensing Symposium, IGARSS '95*, Firenze (Italy), T. Stein Editor, pp. 1055-1057, IEEE N 95CH 35770, ISBN 7803-2567-2.

[4] Amodeo, G., P. de Matthaeis , P. Ferrazzoli, S. Paloscia, P. Pampaloni, G. Schiavon, S. Sigismondi and D. Solimini, 1995, "The potential of multifrequency polarimetric SAR in assessing agricultural and arboreous biomass," *Proc. Int. Symp. Retrieval of Geophysical Parameters from SAR Data for Land Application*, Toulouse (France) 10-13 October 1995.

[5] Ferrazzoli, P., S. Luciani, G.Schiavon, D. Solimini, P. Pampaloni, S. Paloscia and S. Sigismondi 1995, "Correlating Polarimetric SAR data with vegetation biomass", Progress in Electromagnetic Research Symposium (*PIERS '95*), 24-28 July 1995, Seattle, Washington, USA.

[6] Coppo, P., G. Macelloni, P. Pampaloni, S. Paloscia and S. Sigismondi, 1996, "The SIR-C /X-SAR experiment: the sensitivity of microwave backscattering to surface roughness of bare soils," *Proc. Int. Geosci. Remote Sensing Symp. (IGARSS '96)*, Lincoln, Nebraska.

[7] Amodeo, G., P. de Matthaeis, P.Ferrazzoli, S. Paloscia, P. Pampaloni, G.Schiavon, S. Sigismondi and D. Solimini, 1996, "Monitoring vegetation features with multi-temporal SAR data," *Proc. Int. Geosci. Remote Sensing Symp. (IGARSS '96),* Lincoln, Nebraska.

4. Future plans

4.1 Planned investigations

a) Sensitivity to soil moisture and surface roughness parameters
b) Comparison of experimental data with theoretical models of surface roughness (IEM, GO, SPM)
c) Assimilation of SAR data in Hydrological models
d) Interferometry of hilly areas

4.2 Publications:

Accepted conference communications and Invited Papers:

[1] Coppo, P., S. Lolli, G. Nesti, P.Pampaloni and D. Tarchi, 1996, "Microwave surface scattering models validation on artificial dielectric surfaces at the EMSL," Invited paper Progress in Electromagnetic Research Symposium (PIERS '96), Innsbruck 8-12/7/96,

session: "Experimental studies on microwave emission and scattering from rough surfaces," organized by P. Pampaloni.

[2] Coppo, P., G. Macelloni , P. Pampaloni, S. Paloscia and S. Sigismondi, 1996, "The sensitivity of microwave backscattering to surface roughness of bare soils," Invited paper Progress in Electromagnetic Research Symposium (PIERS '96), Innsbruck 8-12/7/96, session: "Experimental studies on microwave emission and scattering from rough surfaces", organized by P. Pampaloni.

[3] Pampalon, P., G. Macelloni, S. Paloscia and S. Sigismondi , 1996, "Multifrequency SAR sensitivity to hydrological parameters: the SIR-C/X-SAR experiment on Montespertoli supersite", Invited Paper at URSI General Assembly, Lille 28.8-5.9 1996, session : SIR-C/X-SAR results.

[4] Pampaloni, P., G. Macelloni, S. Paloscia, R. Ruisi and C. Susini, 1996, "Estimating Crop Biomass with Microwave Sensors", Invited Paper at URSI General Assembly, Lille 28.8-5.9 1996, session : Remote Sensing for ecology.

[5] Pampaloni, P., 1996, "Microwave remote sensing of soil and vegetation parameters, Invited Paper at the International Congress on Environment Climate, ICEC-96. Roma (Italy), March 4-8, 1996.

Research Papers on subjects a, b, c will be submitted to International Journals.

C. Prati, F. Rocca, A. Monti Guarnieri
Dipartimento di Elettronica del Politecnico
Piazza L. da Vinci 32, 20133
Milano, Italy

SAR Interferometry: Summary of the Research Activities at POLIMI

From 1987, the research activities on SAR data processing at POLIMI have been mainly devoted to problem solving for specific SAR missions. Many problems stem from the fact that the available satellite missions (e.g., SEASAT, ERS-1, ERS-2, Radarsat) have not been designed for interferometrical applications.

Here is a summary of the POLIMI activities on SAR data processing with *present activities* in italics and **most recent research** in bold.

- 1 - Phase preserving focusing. A focusing technique (w-k) that preserves the phase of the scatterers has been introduced in 1987 and tested on SEASAT data [1, 2, 3]. It is now the basic processing used at POLIMI and many other sites to focus satellite and airborne SAR images to be exploited for interferometric applications [4]. A phase preserving test suggested by ESA shows that the phase dispersion and the phase constant term introduced by the ω–κ focusing are less than 0.1 and 10^{-4} degrees respectively.

- 2 - Doppler Centroid ambiguity estimation. A blind deconvolution technique for DC ambiguity estimation in the case of the {\bf SIR-C/X-SAR} data [5] has been developed as well as a technique for efficient focusing of SAR data with time and space varying DC [6].

- 3 - Interferogram generation. A software code made in POLIMI for interferogram generation [11,10] from ERS-1 and ERS-2 images has been extensively tested at ESA-ESRIN and then distributed via Internet. Its features include:

- image registration within the limit imposed by coherence (e.g., 1/50th of a pixel for coherence better than 0.4),
- coherence map generation;
- azimuth and range local frequencies (linked to terrain slopes) estimation;
- local spectral shift filtering [7,8];
- fringe generation and filtering.

Recent and ongoing research activities:

(3 a) - Quick-look interferometric processing for ERS data (i.e., generation of interferograms and coherence maps of a 30 x 100 km area with a 100 x 100 m resolution in about 8 minutes on a typical low-cost workstation).

(3 b) - Optimization of the *tradeoff between local spatial resolution and phase noise* of the interferogram.

(3 c) - Study of efficient and *phase preserving interpolators* for image registration in case of single pass interferometry (e.g., the envisaged 3rd SIR-C/X-SAR mission) where the theoretical coherence is close to 1.

- 4 - Phase unwrapping. Both local (i.e., ghost lines) and global (i.e. Least Mean Squares) techniques have been developed, compared, and combined to get the unwrapped phase with the minimum interaction with the operator [11].

Recent and ongoing research activities:

(4 a) - Phase unwrapping using **multibaseline interferometric SAR images.**

(4 b) - 3-D target reconstruction (e.g., getting resolution in foreshortening and layover areas) using multibaseline images [13, 14, 16, 18].

- **5 - Phase preserving ScanSAR focusing**. A technique has been developed for efficient phase preserving ScanSAR focusing [15, 17]. The technique has been tested on Radarsat data simulated using ERS-1 data. Repeat-pass ScanSAR interferometry has also been analyzed and simulated using ERS-1 data.

Recent and ongoing research activities:

(5 a) - *Use of Radarsat data.*

(5 b) - Phase consistent *block mosaicking* both in azimuth and in range (subswaths).

- **6 - Combination of ascending and descending satellite passes**. Ascending and descending interferometric ERS-1 passes have been exploited to overcome the problem of foreshortening and layover due to the steep off-nadir angle [12]. Foreshortening areas in one pass are well imaged in the other if not in shadow.

- 7 - Differential interferometry. Differential interferometry for centimetric terrain motion estimation has been tested in different situations: a landslide in St. Etienne de Tinee, subsidence along the Adriatic coast in Italy and in the area of Pozzuoli (Naples) [19]. From a methodological point of view a criterion for image selection and methods for differential phase generation that do not need phase unwrapping have been identified.

Recent and ongoing research activities:

(7 a) Use of the interferometric quick look for image browsing.

- **8 - Interference cancellation**. A technique for e.m. interference cancellation has been successfully tested on SAR P-band airborne images.

- 9 - Future activity: *X-SAR boom motion compensation*. One of the main problems envisaged for the next SIR-C/X-SAR mission is the effect of the 60m boom oscillations on the single pass interferogram generation (especially in X-band). We plan to develop techniques for estimating and compensating these effects from the data themselves.

REFERENCES

[1] Cafforio, C. Prati, and F. Rocca, 1991, "SAR data focusing using seismic migration techniques," *IEEE Transactions on AES*, vol. 27-2, pp. 194-207.

[2] Cafforio, C. Prati, F. Rocca, 1989, "Synthetic Aperture Radar: a new application for wave-equation techniques," Geophysical Prospecting, vol. 37, pp. 809-830.

[3] Cafforio, C. Prati, F. Rocca, 1991, "Full resolution focusing of SEASAT SAR images in the frequency-wave number domain," *International Journal of Remote Sensing*, vol. 12, no. 3, pp. 491-510.

[4] Prati, F. Rocca, A. Monti Guarnieri, E. Damonti, 1990, "Seismic migration for SAR focusing: Interferometrical applications," *IEEE Transactions on Geoscience and Remote Sensing*, vol. 28, no. 4, pp. 627-640.

[5] Prati, C., F. Rocca, Y. Kost, and E. Damonti, 1991, "Blind deconvolution for Doppler centroid estimation in high frequencies SAR," IEEE Transactions on Geoscience and Remote Sensing, vol. 29, no. 6, pp. 934-941.

[6] Prati, F. Rocca, 1992, "Focusing SAR data with time-varying Doppler centroid," *IEEE Transactions on Geoscience and Remote Sensing*, vol.30, no. 3, pp. 550-559.

[7] Prati, C. and F. Rocca, 1993, "Improving slant range resolution of stationary objects with multiple SAR surveys," *IEEE Transactions on AES*, vol. 29, no. 1, pp. 135-144.

[8] Gatelli, A. Monti Guarnieri, F. Parizzi, P. Pasquali, C. Prati, F. Rocca, 1994, "The wavenumber Shift in SAR Interferometry," *IEEE Transactions on Geoscience and Remote Sensing*, vol. 32, no. 4, July 1994.

[9] Prati, C., F. Rocca, and A. Monti Guarnieri, 1994, "Topographic Capabilities of SAR exemplified with ERS-1," Geo-Information-Systems, vol. 7, no. 1, February 1994, pp. 17-22.

[10] Prati, C., and F. Rocca, "Process for generating Synthetic Aperture Radar Interferograms," U.S. Patent N.5, pp. 332, 999, July 26, 1994.

[11] Prati, C., F. Rocca, A. Monti Guarnieri, and P. Pasquali, "ERS-1 SAR interferometric techniques and applications," ESRIN, Frascati, June 1994.

[12] Pasquali, P., R. Pellegrini, C. Prati, and F. Rocca, "Combination of interferograms from ascending and descending orbits," *IGARSS '94*, Pasadena, CA, pp. 733-735.

[13] Fortuny, E. Holmer, A. J. Sieber, Pasquali, C. Prati, and F. Rocca, "Validating SAR interferomertry applications by using EMSL," *IGARSS '94*, Pasadena, CA, pp. 736-738.

[14] Prati, C., F. Rocca, and Monti Guarnieri, "Measuring volumetric scattering effects with SAR interferometry," *PIERS '94*, Noordwjik.

[15] Guarnieri, Monti, C. Prati, and F. Rocca, "Interferometry with SCANSAR," *PIERS '95*, Seattle, WA, (USA), p. 158.

[16] Pasquali, P., C. Prati, C., F. Rocca, M. Seymour, J. Fortuny, E. Ohlmer, and A. Sieber, "A 3-D SAR experiment with EMSL data," *PIERS '95*, Seattle, WA, (USA), p.362.

[17] Guarnieri, Monti, C. Prati, and F. Rocca, "Interferometry with SCANSAR," *IGARSS '95*, Firenze, pp. 550-552.

[18] Pasquali, P., C. Prati, F. Rocca, M. Seymour, J. Fortuny, E. Ohlmer, and A. Sieber, "A 3-D SAR experiment with EMSL data," *IGARSS '95*, Firenze, pp. 784-786.

[19] Prati, C., F. Rocca, and Monti Guarnieri, "Monitoring surface deformations with SAR interferometry," *Int. Symp. on Retieval of bio and geophysical parameters from SAR data for land applications*, Toulouse, October 1995.

Domenico Solimini
Paolo Ferrazzoli
Giovanni Schiavon
Paolo de Matthaei
Marco Cappelli
Dipartimento di Informatica,
Sistemi e Produzione Universita`
Tor Vergata, Roma, Italy

Analysis of SIR-C/X-SAR Data on Montespertoli Test Site

Introduction

Our analysis refers to Multi Look Complex (MLC) data, which have been multilooked and usually resampled to a ground range projection. Two different data products, depending on the polarization mode, have been provided by NASA/JPL: quad-pol data, with 10 bytes per pixel, containing the information on all polarization combinations and phase differences between polarizations; dual-pol data, with 5 bytes per pixel, containing information only on two polarization combinations and phase differences between them. From the software development point of view, it is important to point out that there are many differences between AIRSAR format data and SIR-C format data, even if the set of data by itself is very similar. For X-SAR, the standard Multilook Ground-range Detected (MGD) data products have been selected and were provided by I-PAF.

Status of data analysis

The Montespertoli test site

The Montespertoli test site is located in Tuscany (Italy), a few kilometers South East of Florence and has been selected as a SIR-C/X-SAR super-site. It is a representative example of those Thyrrenian-Appennine slopes where bedrock is made up of Plio-Pleistocene marine deposits and fluvial/lacustrine soft sediments, which were intensively affected by geomorphological processes of erosion and mass movements. More than half of the site is hilly (the average height is 250 m above the sea level), with some small forest areas, vineyards, olive groves, agricultural fields, pastures, and small urban areas. The remaining part is flat with alluvial wetlands of Pesa river, agricultural fields and urbanization. Two areas have been selected for ground truth measurements: a relatively flat area along the Pesa river, including agricultural fields, which, depending on the season, may grow different crops (mainly wheat, barley, alfalfa, colza, sorghum, sunflower and corn), bare soils, and a small sub-basin of Virginio river. The average field size is about 4-5 ha. The Montespertoli super-site was imaged on seven different days with different incidence angles during both the April and October 1994 missions. Due to system limitations and compatibility with data takes over other sites, fully polarimetric SIR-C data were available only for four data takes, i.e., 12, 13, 14, and 15 April, whereas dual-polarization data have been provided for the remaining three. A list of these data take segments is given in Table 1.

Data Take	Scene Center Time (GMT)	Incidence Angle (deg)
50.30	12 April 1994, 12:06	26.7
66.41	13 April 1994, 11:46	35.2
82.30	14 April 1994, 11:27	44.2
98.20	15 April 1994, 11:07	48.5
114.31	16 April 1994, 10:46	52.6
130.30	17 April 1994, 10:25	55.6
146.30	18 April 1994, 10:03	57.5

Table 1

The X-SAR data corresponding to the same data take segments are also available.

Software development

The software developed and used for analyzing the AIRSAR data taken in the course of the MAESTRO-1 and MAC-EUROPE '91 campaigns has formed the basis for the SIR-C/X-SAR data analysis. However, the mentioned differences between the AIRSAR and the SIR-C/X-SAR data formats and the fact that the previous software had been developed under VMS and basic in a VAX environment, resulted in a major effort to implement the adjourned algorithms in the recently available UNIX/X-window Hp environment. The main features of the developed software include:

I. SAR data reading and image visualization;
II. polygonal area selection with shifting capabilities;
III. computation of average values of
    A. backscattering coefficients at each needed polarization state,
    B. phase differences between polarizations,
    C. correlation coefficients at relevant polarization states within a chosen polygonal area;
IV. visualization of single or combined average values;
V. creation of auxiliary input files.

A total of 98 polygonal areas (77 in the Pesa river sub-site and 21 in the Virginio sub-site) have been constructed within the Montespertoli site. Both extensive and intensive ground truth data have been collected in correspondence of the April and October periods of the Shuttle mission. Data collections have taken place on 7, 11, 13, 14 and 19 April and on 5 October, 1994. Ground data regard the soil and vegetation parameters which have a major effect on the radar response of the surface, i.e.:

I. vegetation parameters:
    A. type of crop or grass
    B. phenological state
    C. fresh and dry weights
    D. water content of leaves
    E. water content of stalks and stems
    F. leaf area index
    G. cultivation geometry
    H. dimensions of leaves
    I. dimensions of stalks and stems;

II. soil parameters:
   A. soil moisture profile (between 0 and 2.5 cm, 0 and 5 cm, and 5 and 15 cm)
   B. soil density
   C. soil surface rms roughness
   D. soil roughness correlation length.

Data calibration and validation

A first step consisted in the comparison of SIR-C data with those taken by the AIRSAR on the same Montespertoli area in 1991 (MAC-Europe campaign), which underwent calibration by means of corner reflectors and extensive validation. At this stage of data analysis, backscattering values measured by SIR-C L- and C-band radar appear to be consistent with those of the MAC-Europe campaign.

Data analysis

At present, the following quantities have been computed from the April SIR-C data for each of the 98 polygonal areas selected within the Montespertoli site:

I. backscattering coefficients at hh, hv, vv, rr, rl, 45 degree co-pol, 45 deg cross-pol;
II. phase differences between hh and vv and hh and hv returns;
III. conventional and new (circular polarizations and "scalar") correlation coefficients for the fully polarimetric L- and C-band data.

In the case of dual-polarized data, the computed quantities are consequently and substantially reduced. As far as SAR-X data are concerned, only a single quantity can be computed from the radar data, i.e., the mean vv backscattering coefficient. The computation of the X-band average values for the same surface parcels for which the above L- and C-band quantities were obtained has been carried out. The request for the October mission data has been forwarded.

Obtained results

The aforementioned large preparatory activity needed for the extensive and systematic analysis of the SIR-C/X-SAR data has absorbed a substantial fraction of the manpower available for the SIR-C/X-SAR project. At this stage, only preliminary scientifically significant results have been obtained. The L- and C-band backscattering coefficients have been employed in a vegetation discrimination scheme, and their link with arboreous and crop biomass has been determined, thus establishing a further step towards the monitoring of vegetation by SAR sensors [1], [2]. It should be noted, however, that the season of the flights was not favorable from this point of view, since only few types of crops in spring and almost only bare soil in autumn were present. A study on the correlation with soil moisture content has also been undertaken and results are now being obtained [5]. Inclusion of the April SIR-C/X-SAR and October measurements into our backscattering database is planned to obtain additional important multi-temporal information on the radar response to vegetation and soil moisture [3], [4].

Future activities and data requests

As said, the October data have been requested and their analysis is planned to follow the present April data study, adding relevant pieces of multi-temporal information. However, a real breakthrough in this field would be produced by the availability of SIR-C/X-SAR data covering an extended period of time, ideally one year, which would provide coverage of the whole cycle of growth of vegetation and would span the entire hydrological cycle. The possible launch of a free-flier multifrequency radar, as already discussed by NASA, could provide such a useful wealth of data of high interest for practical applications of remote sensing technology. Year-round systematic overflies of the AIRSAR could partially replace the free-flier.

BIBLIOGRAPHY

[1] Amodeo, G., P. de Matthaeis, P. Ferrazzoli, S. Paloscia, P. Pampaloni, G. Schiavon, S. Sigismondi, and D. Solimini, "The potential of multifrequency polarimetric SAR in assessing agricultural and arboreous biomass," *Proc. International Symposium on Retrieval of Bio- and Geophysical Parameters from SAR Data for Land Applications*, Toulouse (France), Oct. 1995, in press.

[2] Ferrazzoli, P., S. Paloscia, P. Pampaloni, S. Sigismondi, G. Schiavon, and D. Solimini, "The potential of multifrequency polarimetric SAR in assessing agricultural and arboreous biomass," submitted to the *IEEE Trans. Geosci. Remote Sensing*, Special Issue on the above Toulouse symposium.

[3] Amodeo, G., P. de Matthaeis, P. Ferrazzoli, S. Paloscia, P. Pampaloni, G. Schiavon, S. Sigismondi, and D. Solimini, "Monitoring vegetation features with multitemporal SAR data," submitted to 1996 *International Geoscience and Remote Sensing Symposium*, Lincoln, Nebraska (USA), May 1996.

[4] Amodeo, G., M. Cappelli, P. Ferrazzoli, S. Paloscia, P. Pampaloni, G. Schiavon, S. Sigismondi, and D. Solimini, "Monitoring seasonal land changes with polarimetric SAR," submitted to *Progress in Electromagnetics Research Symposium*, Innsbruck (Austria), Jul. 1996.

[5] A paper is being planned for submission to Remote Sensing of the Environment (due February 1996).

P. Trivero
Università di Torino

1. State of the activity.

Our activity is mainly concerned with the detection and characterization of marine surface films by means of multifrequency SAR. The activity outline was contained in the Proposal "Marine SAR images at three frequencies" for the SIR-C missions. This study represents the extension to the remote sensing of the methodology we developed to characterize sea surface films by means of in situ measurements. The methodology requires: wave height measurements inside and outside the film covered area, derivation of the their power spectra to obtain the spectral ratio, the best fitting of the latter with the theoretical damping ratio [1] for the extraction of the rheological parameters. In the remote sensing based methodology the first two steps are substituted with a suitable analysis of multifrequency SAR data.

As far as the SIR-C/X-SAR data are concerned we considered the quick looks of the SAR data of the April and October '94 missions. We selected some scenes of the Northern Sea containing some slicks. We are waiting for the digital data of the same images in the L-, C- and X-bands in order to refine the model for the detection and characterization of slicks we developed using SAR-580 and AIRSAR images.

During the flights of SAR-580 (October 1990) and AIRSAR (June 1991) we collected sea truth data. We measured: time series of wind and temperature, of sigma zero by using L, S, C platform based scatterometers, and of instant wave height (up to 26 Hz) by using a microwave gauge [2] installed on platform or on board of a small boat.

In the above mentioned proposal we inserted another objective regarding the derivation, from SAR images, of the spatial structure of the wind stress over the sea surface for different meteorological conditions. Wind stress produces the sea surface roughness which, interacting with the incoming e.m. waves via the Bragg resonance, is responsible for the radar backscattering. A study carried out so far on the data of the SAR-580 campaign [3] provided evidence of the capabilities of this kind of analysis and the wealth of information about the surface boundary layer that may be extracted by the SAR images.

2. Results and publications

The data processing of the SAR-580 campaign allowed us:

a) to affirm that the SAR signal attenuation in presence of sea surface films is in tight connection to the measured damping of the wave components in Bragg condition [4, 5, 6, 7] and then, that the presence of sea surface films can be detected by means of SAR imagery.

b) to obtain wind stress spatial distributions. It has been possible, by studying the radar backscattering structures, to infer the wind direction and evaluate the lifetime of the wind stress bursts that create them. Furthermore, by analyzing the tail of the backscattering structures (connected to the Bragg wave damping), we derived the translation velocity of

the wind stress structures. Finally we désigned a model for the wind vector extraction from SAR imagery. This model is an improvement of a previous one [8].

The AIRSAR campaign data processing demonstrated that the role of the backscattering due to Bragg resonance in the SAR signal is prevalent over other backscattering mechanisms for incidence angles between 16 and 61 degrees with VV polarization. From the P, L, C bands images of this campaign, by extracting the corresponding Bragg components for each incidence angle, we obtained a wide portion of the high frequency sea spectra inside and outside the film covered areas. We observed the same spectral trends obtained with the wave gauge. Spectral ratios obtained from remote sensing and by means of sea truth measurements are almost coincident. This demonstrates the possibility of detection and characterization of surface films by means of multifrequency SAR images [9].

These results are reported in the references 3, 7, and 9.

3. Future activity

Our aim is the application of the described methodologies to some 1994 SIR-C/X-SAR data in order to tune models and methodologies we developed using the data of the preparatory flights.

While waiting for the 1997 SIR-C mission we plan to perform a preliminary measurement campaign in the Mediterranean Sea.

Aims of the campaign are the following:
a) evaluation of the amount of wind energy transferred to the sea inside and outside the film;
b) investigation of the aspects of the energy transfer from shorter waves, directly wind coupled, to longer ones (in Bragg condition) which are responsible for the SAR backscattering.
c) investigation about the damping effects in the marine environment caused by concentration and breaking for adsorption and spreading films respectively. We also plan to make some artificial slick and surface measurements with ground based scatterometers, high frequency wave meters and to collect surface water samples for physico-chemical analysis.
d) improving of the performances of the L, S, C scatterometer with a new single multiband antenna and testing of the new Ku band scatterometer. Tune-up of the new multi wire interferential microwave probe (10 GHz) for the measurement of bi-dimensional sea spectra in the gravito-capillary region useful for the understanding of the relation between backscattering and wave azimuth and possible spectral frequency shifts due to sea currents.

Such a campaign will be conducted in collaboration with several research institutions (Univ. Torino, Univ. Firenze, CNR-Torino, CNR-Venezia).

Finally we plan a second campaign in the Mediterranean Sea during the SIR-C flight with collection of all the needed sea truth data.

The use of the three-band images will also permit us to extend the research on the wind stress. It will be possible to extract the wind speed from the comparison between the backscattering intensities, and, thanks to the Bragg condition, to retrieve the pattern of the high frequency part of the wave spectrum. A study about the tail of the backscattering structures at the three bands will permit the evaluation of the translation velocity of the

atmospheric structures. The planned experimental campaign will be useful in order to match the information of the time structure with that of the spatial structure. This study will permit us to obtain from SAR data the spatial picture of the marine surface layer as well as an estimate of the fraction of area covered by the wind stress structures at different atmospheric regimes.

References

[1] Fiscella, B., P. P. Lombardini, P. Trivero, and R., "Ripple damping on water surface covered by a spreading film: theory and experiment," Il Nuovo Cimento, vol. 8C, no. 5, p. 491 (1985) .

[2] Lombardini, P. P., B.Fiscella, P. Trivero, C.Cappa, and W. D.Garrett, "Modulation of the spectra of short gravity waves by sea surface films: slick detection and characterization with a microwave probe," Journal of Atmospheric and Oceanic Technology, vol. 6, no.6, p. 882, (1989).

[3] Zecchetto, S., P. Trivero, B.Fiscella, and P.Pavese, "The turbulent structures in the unstable marine surface layer detected by SAR," submitted to Boundary Layer Meteorology.

[4] S.Zecchetto, P.Trivero, "Experiment and results of the italian activity in the field of ocean microwave backscattering", Pacific Ocean Remote Sensing, Okinawa Japan, Vol. I, 347, (1992).

[5] Zecchetto, S., P. Trivero, "Experimental ocean active microwave remote sensing," Satellite Remote Sensing of the Oceanic Environment, Ed. by I.S.F.Jones, Y. Sugimori and R. W. Stewart, Publ.by Seibutsu Kenkyusha Co Ltd, Tokyo Japan, Chap. 4, p. 115, (1993).

[6] Fiscella, B., F. Gomez, P. Pavese, P. Trivero, S.Curiotto, G. Umlieber, and S. Zecchetto, "The Venice SAR-580 Experiment," Rapp. Int. ICG-CNR, 242/91, (1991).

[7] Trivero, P., B.Fiscella, F. Gomez, P. Pavese, and S. Zecchetto, "Microwave Remote Sensing of Marine Surface Films from Multiband Radar," in progress.

[8] Trivero, P., B. Fiscella, F. Gomez, and P. Pavese, "Wind field deduced from marine SAR images," Il Nuovo Cimento C, vol. 17, no. 5, p. 689, (1994).

[9] Trivero, P., B.Fiscella, F. Gomez, and P. Pavese, "Detection and characterization of sea surface films by means of multi-frequency SAR," in progress.

N. Veneziani
G. Guerriero

Progress Report on SAR Data Processing at IESI-CNR and Physics Department of the University of Bari, Bari, Italy

The research activity of the two coordinate units at IESI-CNR and Physics Deptartment of the University of Bari, Bari, Italy, is mainly addressed to SAR Interferometry (INSAR).

In the last year, the following actions have been developed:

- implementation of software modules for INSAR techniques, and their test on real and simulated SAR data (in this phase, the ESRIN ERS-1 INSAR Reference Data Set on Gennargentu (Sardinia, Italy) has been used);

- verification of phase preserving performance of the Italian Space Agency (ASI) X-SAR processor, by interferogram extraction from X-band data taken at the Mt. Etna interferometric test site during the second SIR-C/X-SAR mission.

- sub-aperture Doppler rate estimation by analysis of Wigner-Ville joint time-frequency distributions of automatically selected azimuth lines.

The following data sets from the second SIR-C/X-SAR mission have been required through ASI, and received on the last December:

- single look complex interferometric pairs of images on Mt. Etna, Sicily (Italy), in L-band, C-band, and X-band (new ASI processing), for a multifrequency INSAR experiment;

- X-SAR raw data on Oberpfaffenhofen (Germany), and related Shuttle PATH product, for a motion and attitude compensation experiment.

A presentation has been submitted to IGARSS '96 Int. Symp., concerning the phase unwrapping problem in the presence of phase inconsistencies due to noise and topography. A single spectral band of the available SIR-C/X-SAR data on Mt. Etna will be exploited in order to produce experimental results of our unwrapping technique.

Authors and title of this presentation should be: M. T. Chiaradia, L. Guerriero, G. Pasquariello, A. Refice, and N. Veneziani, "Absolute Phase Determination in SAR Interferometry."

Moreover, a technical note is in preparation, concerning a preliminary analysis and the characterization of a pseudo-differential approach to the multifrequency INSAR. The aim of this note is to define the outlines of an experiment based on the SIR-C/X-SAR multiple frequency data of Mt. Etna, such that the whole data set may be exploited in an integrated way during the phase unwrapping and the elevation map computation.

With regard to the SIR-C/X-SAR system, in the near future the following activities will be developed. In order of priority:

- experimentation on single and multifrequency INSAR techniques, aimed to optimize the phase unwrapping procedure;

- analysis and compensation of different motion conditions, induced by platform attitude changes, between the two radar antennas of a spaceborne bistatic INSAR instrument (in reference to the interferometric SIR-C/X-SAR mission foreseen).

ACRONYMS

2-D	two-dimensional
3-D	three-dimensional
ADRO	Application Development and Remote Sensing Opportunity
AGARD	Advisory Group for Aerospace Research and Development
AGU	American Geophysical Union
AIDAA	Associazione Italiana di Aeronautica e Astronautica
AIG	Applied Intelligence Group
AIRSAR	Airborne Synthetic Aperture Radar
APL	Applied Physics Lab
ARC	active radar calibrators
ARMAR	Airborne Rain Mapping Radar
ASU	Arizona State University
AVHRR	Advanced Very High Resolution Radiometer
AVIRIS	Airborne Visible/Infrared Imaging Spectrometer
BOREAS	Boreal Eco System-Atmosphere Studies
BRGM	Bureau de Recherches Géologiques et Minières (Orléans, France)
C	C-band
Co-I	co-investigator
CCD	charged coupled device
CD-ROM	compact disk read only memory
CEOS	Committee on Earth Observations Satellites
CESBIO	Centre d'Etudes Spatiales de la Biosphère
CETP	Centre d'Etudes des Environnements Terrestre et Planétaires
CMOD-3, -4	C-band scatterometer model functions
CNN	Cable News Network
CNRS-IMAGEO	Centre National de la Recherche Scientifique-Imaging
CPD	C-band phase difference
CSAP	Critical Size Area Project
CSI	Canopy Structure Index
CSOWM	Canadian Spectral Ocean Wave model
CSUF	California State University, Fresno
CTD	conductivity temperature depth
D-PAF	German Processing and Archive Facility
DARA	Deutsche Agentur für Raumfahrtangelegenheiten (German Space Agency)
DC-8	Douglas Commercial aircraft - model 8
DEM	digital elevation map
DLR	Deutsche Forschungsanstalt für Luft- und Raumfahrt
DMSP	Defense Meteorological Satellite Program
DT	data take
DTM	digital terrain model
EARSeL	European Association of Remote Sensing Laboratories
ECMWF	European Center for Medium Range Weather Forecast
ECU	East Carolina University
EECS	Electrical Engineering and Computer Science
ELA	equilibrium line altitude
EM	electromagnetic

ENSEA	Ecole Nationale Şupérieure de l'Electronique et de ses Applications
EOS	Earth Observing System
EPA	Environmental Protection Agency
ERASME	Electronically Steerable Antenna Copolar Scatterometer
ERIM	Environmental Research Institute of Michigan
ERS-1, ERS-2	European Remote Sensing Satellite, 1 and 2
ESA	European Space Agency
ESTAR	Electronically Steered Thinned Array Radiometer
EUROPTO	Europto Joint Venture European Optical Society and International Society for Optical Engineering (EOS/SPIE)
EUSAR	European Synthetic Aperture Radar
FEL-TNO	TNO - Physics and Electronics Laboratory
FIR	finite impulse response
FNMOC	Fleet Numerical Meteorology and Oceanography Center
FY	fiscal year
GCIP	Global Change Research Program, also referred to as GCP and GCRP
GCM	general circulation model
GCP	ground control point
GIS	geographic information system
GOM	Geometrical Optics Model
GPS	Geophysical Processor System, or Global Positioning System
GRS	Grid Reference System (SPOT)
GSFC	Goddard Space Flight Center
GTC	geocoded terrain corrected
HF	high frequency
HH	horizontal polarized transmission, horizontally polarized reception
HV	horizontal polarized transmission, vertically polarized reception
ICESS	Institute for Computational Earth System Science
IDS	Image Display System Ionosphere Detection System Information Display System
IEEE	Institute of Electrical and Electronics Engineers
IEM	integral equation method
IF	intermediate frequency
IGARSS	International Geoscience And Remote Sensing Symposium
IGCP	International Global Change Program
IJRS	International Journal of Remote Sensing
INPA	Instituto de Pesquisas Amazonas (Brazilian Institute for Amazonion Research)
INPE	Instituto Nacional de Pesquisas Espaciais (Brazilian Space Agency)
INRA	Institut National de Recherche Agronomique
IR	infrared
IRSA	Institute for Remote Sensing Applications
ISLC	interferometric single look complex
ISPRSS'96	International Society for Photogrammetry and Remote Sensing Symposium 1996
ITCZ	Intertropical Convergence Zone
ITI	Interaction Type Index
JERS-1	Japanese Earth Remote-Sensing Satellite
JGR	Journal of Geophysical Research
JPL	Jet Propulsion Laboratory

JSC	Johnson Space Center
KEYT	television station located in Santa Barbara, California, USA
L	L-band
LAI	Leaf Area Index
LANDSAT	Land Satellite
LDR	linear depolarization ratio
LLNL	Lawrence Livermore National Laboratory
LPD	L-band phase difference
LTER	Long Term Ecological Research (Program) (U.S. National Science Foundation)
MAC	Multsensor Aircraft Campaign
MGD	multi-look ground-range detected
MIT	Massachusetts Institute of Technology
MLD	multi-look detected
MSS	Multispectral Scanner
MTF	modular transfer function
MTPE	Mission to Planet Earth
NAS	Numerical Aerodynamic Simulation
NASA	National Aeronautics and Space Administration
NASDA	National Space Development Agency (Japan)
NCAR	National Center for Atmospheric Research
NDVI	Normalized Difference Vegetation Index
NESDIS	National Environmental Satellite Data and Information Services
NOAA	National Oceanic and Atmospheric Administration
NRC	National Research Council
NS001	Airborne LANDSAT simulator
NSF	National Science Foundation
OCF	Orbiter Computational Facilities
P	P-band
PARC	polarimetric active radar calibrator
PD	phase difference
PI	principal investigator proportion-based indices
PIERS	Progress In Electromagnetic Research Symposium
POM	Physical Optics Model
RADAR	radio detection and ranging
RADARSAT	Radar Satellite
RAR	real aperture radar
RAVEN	Radar Analysis and Visualization Environment
RCS	radar cross section
RDC	Radar Data Center
RESEDA	Remote Sensor Data Analysis
RMS	root mean square
RSADU	Remote Sensing Application Development Unit
RSD	reformatted signal data
SALT	Savanas in the Long Term
SAPARC	single antenna polarimetric active radar calibrator
SAR	synthetic aperture radar

SAREX	South American Radar Experiment (ESA)
SCANSAR	scanning synthetic aperture radar
SIR-A, SIR-B	Shuttle Imaging Radar, -A , -B
SIR-C/X-SAR	Spaceborne Imaging Radar-C/X-Band Synthetic Aperture Radar
SLC	single look complex
SMMR	Scanning Multichannel (or Multifrequency) Microwave Radiometer
SP	small perturbation
SPI	South Patagonian Icefield
SPM	small perturbation model
SPOT	Système Probatoire d'Observation de la Terre
SRG	surface roughness gauge
SRL-1, SRL-2	Space Radar Laboratory flight 1 and flight 2
SRL-3	Proposed Future Mission Space Radar Laboratory flight 3
SSC	single look slant range complex
SSM/I	Special Sensor Microwave/Imager (DMSP) (U.S. Air Force)
STS 59 and STS 68	Space Transportation System, flights 59 and 68
SWH	significant wave height
TGARS	Transactions on Geoscience and Remote Sensing
TIMS	Thermal Infrared Multispectral Scanner
TIR	thermal infrared
TM	Thematic Mapper
TNTmips	map image processing system
TOPSAR	Topographic Synthetic Aperture Radar
TV	television
UC	University of California
UCSB	University of California, Santa Barbara
UK	United Kingdom
US	United States
USDA	United States Department of Agriculture
UTD	University of Texas, Dallas
VH	vertically polarized transmission, horizontally polarized reception
VNIR	visible/near-infrared
VSI	volume scattering index
VV	vertically polarized transmission, vertically polarized reception
WAM	wave analysis model
WAMODEL	A third-generation wave prediction model
WHOI	Woods Hole Oceanographic Institution